

# Leak, Purge, and Gas Permeability Testing to Support Active Soil Gas Sampling

REPORT

# **Leak, Purge, and Gas Permeability Testing to Support Active Soil Gas Sampling**

Dominic C. DiGiulio  
PSE Healthy Energy  
Oakland, CA 94612

Kristie D. Rue and Richard T. Wilkin  
U.S. Environmental Protection Agency  
Office of Research and Development  
National Risk Management Research Laboratory  
Groundwater, Watershed, and Ecosystems Restoration Division  
Ada, OK 74820

Christopher J. Ruybal  
Department of Civil and Environmental Engineering  
Colorado School of Mines  
Golden, CO 80401

Project Officer: David S. Burden  
U.S. Environmental Protection Agency  
Office of Research and Development  
National Risk Management Research Laboratory  
Groundwater, Watershed, and Ecosystems Restoration Division  
Ada, OK 74820

Project Manager: Daniel F. Pope  
CSS  
10301 Democracy Lane, Suite 300  
Fairfax, Virginia 22030

U.S. ENVIRONMENTAL PROTECTION AGENCY  
OFFICE OF RESEARCH AND DEVELOPMENT  
NATIONAL RISK MANAGEMENT RESEARCH LABORATORY  
CINCINNATI, OH 45268

## **NOTICE**

The U.S. Environmental Protection Agency (US EPA) through its Office of Research and Development (ORD) funded and managed the research described here through in-house efforts and under Contract No. EP-W-12-026 to CSS. It has been subjected to the Agency's peer and administrative reviews and has been approved for publication as an US EPA document.

Results of field-based studies and recommendations provided in this document have been subjected to external and internal peer and administrative reviews. This report provides technical recommendations, not policy guidance. It is not issued as an US EPA Directive, and the recommendations of this report are not binding on enforcement actions carried out by the US EPA or by the individual States of the United States of America. Neither the United States Government nor the authors accept any liability or responsibility resulting from the use of this document. Implementation of the recommendations of the document and the interpretation of the results provided through that implementation are the sole responsibility of the user.

Research in this report was performed by the US EPA. This report was prepared under the Consolidated Safety Services (CSS) Decontamination Analytical and Technical Service (DATS) II contract with US EPA under Contract Number: EP-W-12-026.

## **FOREWORD**

The U.S. Environmental Protection Agency (US EPA) is charged by Congress with protecting the Nation's land, air, and water resources. Under a mandate of national environmental laws, the US EPA strives to formulate and implement actions leading to a compatible balance between human activities and the ability of natural systems to support and nurture life. To meet these mandates, US EPA's research program is providing data and technical support for solving environmental problems today and building a science knowledge base necessary to manage our ecological resources wisely, understand how pollutants affect our health, and prevent or reduce environmental risks in the future.

The National Risk Management Research Laboratory (NRMRL) is the US EPA's center for investigation of technological and management approaches for reducing risks from threats to human health and the environment. The focus of the NRMRL's research program is on methods for the prevention and control of pollution of air, land, water, and subsurface resources; protection of water quality in public water systems; remediation of contaminated sites and groundwater; and prevention and control of indoor air pollution. The goal of this research is to catalyze development and implementation of innovative, cost-effective environmental technologies; develop scientific and engineering information needed by US EPA to support regulatory and policy decisions; and provide technical support and information transfer to ensure effective implementation of environmental regulations and strategies.

## **ABSTRACT**

Active soil-gas sampling has been used as a reconnaissance method in support of soil and groundwater sampling of volatile and biodegradable organic compounds for over 30 years. More recently, soil gas sampling has been used directly to evaluate risk posed by vapor migration from groundwater and soil to indoor air (vapor intrusion). This has prompted development of improved quality assurance and quality control measures. To supplement improvement in this area, four aspects of active soil gas sampling were investigated: (1) continuing calibration and flow testing of portable gas analyzers; (2) leak testing of above ground components of the soil gas sampling train and the borehole of vapor probes (including leakage between screened intervals of a vapor probe cluster) and groundwater monitoring wells used for soil gas sampling; (3) selection of vapor probe construction materials and equations suitable for gas permeability testing; and (4) purge testing to evaluate stabilization of fixed gases and hydrocarbon concentrations prior to collection of a soil gas sample for fixed-laboratory analysis. Findings from this investigation should be useful to environmental practitioners and regulatory agencies in improving the state-of-the-art of active soil gas sampling collection.

## TABLE OF CONTENTS

|  |      |
|--|------|
| Notice.....  | ii   |
| Foreword.....  | iii  |
| Abstract.....  | iv   |
| List of Acronyms and Abbreviations.....  | viii |
| List of Figures.....   | x    |
| List of Tables.....  | xv   |
| Acknowledgements.....  | xvi  |
| Executive Summary.....   | xvii |
| Project Data Quality Assurance and Quality Control.....                                    | xxix |
| 1.0 INTRODUCTION.....  | 1    |
| 2.0 MATERIALS AND METHODS.....   | 4    |
| 2.1 Probe Cluster and Monitoring Well Installation.....                                    | 4    |
| 2.2 Soil-Gas Sample Train Configuration.....   | 10   |
| 2.3 Calculation of Purge Volume.....   | 13   |
| 2.4 Leak Testing of Above Ground Fittings.....   | 14   |
| 2.5 Selection of Tracers for Leak Testing Boreholes.....                                   | 18   |
| 2.6 Methods for Leak Testing Boreholes.....  | 21   |
| 2.7 Methods of Calibration and Flow Testing of Portable Gas Analyzers.....                 | 25   |
| 2.8 Collection of Equipment Blanks.....  | 31   |
| 2.9 Methods of Gas Permeability Testing.....   | 31   |
| 2.10 Methods of Purge Testing.....   | 39   |
| 3.0 RESULTS and DISCUSSION.....  | 42   |
| 3.1 Testing of Continuing Calibration Checks (Bump Testing) on Portable Gas Analyzers..... | 42   |

**TABLE OF CONTENTS continued**

3.1a Bump Test Results for Oxygen (O<sub>2</sub>) .....42

3.1b Bump Test Results for Carbon Dioxide (CO<sub>2</sub>).....44

3.1c Bump Test Results for Methane .....45

3.1d Bump Test Results for 2,2 dichloro-1,1,1-trifluoroethane (R-123).....47

3.1e Bump Test Results for Carbon Monoxide (CO).....48

3.1f Bump Test Results for Hydrogen Sulfide (H<sub>2</sub>S) .....48

3.1g Bump Test Results for Flame Ionization Detector (FID) Using Methane in Air .....49

3.1h Bump Test Results for Photo Ionization Detector (PID) Using Isobutylene in Air .....50

3.2 Testing the Effect of Flow Rate on Measurement of Hydrocarbons Using the Thermo-Scientific TVA-1000B FID and PID and R-123 Using the Bacharach H-25IR Portable Gas Analyzers .....52

3.3 Testing of Flow Rate on Gas Measurement During Soil-Gas Purging.....53

3.4 Comparison O<sub>2</sub>, CO<sub>2</sub>, and CH<sub>4</sub> Concentrations Measured Using a GEM2000 Plus Gas Analyzer During Purging with Fixed-Laboratory Analysis.....55

3.5 Results of Equipment Blanks.....57

3.6 Results of Shut-in Testing.....59

3.7 Variation of Tracer Concentration in the Leak Detection Chamber Used for Vapor Probe .....61

3.8 Results of Leak Testing of Probe and Quick-Connect Compression Fittings Clusters .....61

3.9 Results of Leak Testing Between Surface and Upper Probe in Probe Clusters.....64

3.10 Results of Leak Testing Between Upper and Intermediate Probes in Probe Clusters .....66

3.11 Results of Leak Testing Between an Intermediate and Lower Probe in a Probe Cluster .....69

3.12 Results of Leak Testing Between the Surface and Sandpack of Monitoring Wells .....69

3.13 Development of a Heuristic Model of Leakage .....70

**TABLE OF CONTENTS continued**

3.14 Estimation of Vacuum Loss in Tubing and Fittings .....73

3.15 Comparison of Prolate-Spheroidal and Axisymmetric-Cylindrical Domains for  
Permeability Estimation.....75

3.16 Evaluation of Temporal Variability in Gas Permeability Estimation.....81

3.17 Results of Transient Gas Permeability Estimation .....83

3.18 Stabilization of O<sub>2</sub> and CO<sub>2</sub> Concentrations During Purging .....83

3.19 Purging Simulations.....85

Summary.....98

References.....107

## LIST OF ACRONYMS AND ABBREVIATIONS

|                  |   |
|------------------|---|
| Ar               | argon   |
| atm              | atmosphere  |
| calib            | calibration   |
| CH <sub>4</sub>  | methane   |
| cm               | centimeter  |
| CO <sub>2</sub>  | carbon dioxide  |
| CO               | carbon monoxide   |
| DESO             | double-end shutoff  |
| EC               | electrochemical cell  |
| US EPA           | Environmental Protection Agency                             |
| FID              | flame ionization detector                                   |
| g                | gram  |
| GAC              | granular activated carbon                                   |
| GC               | gas chromatograph   |
| GC-MS            | gas chromatography-mass spectrometry                        |
| GWERD            | Groundwater, Watershed, and Ecosystems Restoration Division |
| H <sub>2</sub> S | hydrogen sulfide  |
| He               | helium  |
| HDPE             | high density polyethylene                                   |
| ID               | internal diameter   |
| IR               | infrared cell   |
| IUPAC            | International Union of Pure and Applied Chemistry           |
| K                | Kelvin  |
| kPa              | kilopascal  |
| L                | liter   |
| LDPE             | low density polyethylene                                    |
| m                | meter   |

## LIST OF ACRONYMS AND ABBREVIATIONS *continued*

|                |   |
|----------------|---|
| m <sup>3</sup> | cubic meters                                    |
| mg             | milligram                                       |
| mm             | millimeter                                      |
| NIST           | National Institute for Standards and Technology |
| N <sub>2</sub> | nitrogen  |
| NRMRL          | National Risk Management Research Laboratory    |
| OD             | outside diameter                                |
| QA             | quality assurance                               |
| QC             | quality control                                 |
| Pa             | Pascal  |
| PID            | photoionization detector                        |
| ppbv           | parts per billion by volume                     |
| ppmv           | parts per million by volume                     |
| PRT            | post-run-tubing                                 |
| PVC            | polyvinylchloride                               |
| R-123          | 1,1-dichloro-2,2,2-trifluoroethane              |
| RSKSOP         | Robert S. Kerr Standard Operating Procedure     |
| SCCM           | standard cubic centimeter per minute            |
| SESO           | single-end shutoff                              |
| SLPM           | standard liter per minute                       |
| SGC            | soil gas cap                                    |
| Std            | standard  |
| STP            | standard temperature and pressure               |
| SVE            | soil vapor extraction                           |
| TCD            | thermal conductivity detector                   |
| µg             | microgram                                       |
| VOC            | volatile organic compound                       |

## LIST OF FIGURES

**Figure 1.** States and Canadian Provinces (light blue) where guidelines to support soil-gas sampling were reviewed. The area in dark blue denotes Atlantic Partners in Risk-Based Corrective Action Implementation consisting of New Brunswick, Newfoundland and Labrador, Nova Scotia, and Prince Edward Island.....2

**Figure 2.** Photograph of track-mounted Geoprobe™ rig adjacent to a house in Valley Center, Kansas .....4

**Figure 3.** Photograph of removal of a PVC liner containing soil and a PVC core catcher.....5

**Figure 4.** Photograph of soil core removed from clear PVC liner .....5

**Figure 5.** Photograph of thin-walled 7.6 cm tube used to enlarge boreholes.....6

**Figure 6.** Photograph of black clay. Hole in center of clay is from previous push with steel rods containing PVC liners .....6

**Figure 7.** Schematic illustrating typical probe cluster construction at Valley Center, KS .....7

**Figure 8.** Photograph of stainless-screen and tubing used for probe construction .....8

**Figure 9.** Schematic of three-monitoring well cluster of PVC wells used for groundwater sampling and soil-gas sampling across the water table .....9

**Figure 10.** Photograph of rubber fitting with brass quick-connect fitting to seal PVC wells .....10

**Figure 11.** Schematic for leak detection chamber and soil-gas sample train for soil-gas probe clusters .....11

**Figure 12.** Photograph illustrating vacuum testing of fittings associated with leak detection chamber.....18

**Figure 13.** Estimated gas viscosity of O<sub>2</sub>, N<sub>2</sub> CO<sub>2</sub> and Air from Gas Viscosity Calculator from LMNO Engineering, Research, and Software, Ltd.....34

**Figure 14.** Results of bump tests for oxygen (O<sub>2</sub>) using a Landtec GEM2000 Plus portable gas analyzer. (a) Measurement of gas standards (Std) at calibration (Calib) concentrations in 5-L Flex Foil™ gas sampling bags. (b) Deviation from standard concentrations with stipulated quality control criteria (±1% of standard) illustrated with magenta lines. Quartiles, median (line), mean (+), minimum (whisker), and maximum (whisker) values illustrated in box plots with values to right of box plots.....42

**LIST OF FIGURES continued**

**Figure 15.** Results of bump tests for carbon dioxide (CO<sub>2</sub>) using a LandTec GEM2000 Plus portable gas analyzer. (a) Measurement of gas standards (Std) at calibration (Calib) concentrations in 5-L Flex-Foil™ gas sampling bags. (b) Deviation from standard concentrations with stipulated quality control criteria: ± 0.3% (0 - <5.0%), ± 1.0% (5.0 - <15%), and ± 3.0% (15 - 60%) illustrated with magenta lines. Quartiles, median (line), mean (+), minimum (whisker), and maximum (whisker) values illustrated in box plots with values to right of box plots.....45

**Figure 16.** Results of bump tests for methane (CH<sub>4</sub>) using a LandTec GEM2000 Plus portable gas analyzer. (a) Measurement of gas standards (Std) at calibration (Calib) concentrations in 5 L Flex Foil gas sampling bags. (b) Deviation from standard concentrations with stipulated quality control criteria: ± 0.3% (0 - <5.0%), ± 1.0% (5.0 - <15%), and ± 3.0% (15 - 100%) illustrated with dashed magenta lines. Quartiles, median (line), mean (+), minimum (whisker), and maximum (whisker) values illustrated in box plots with values to right of box plots.....46

**Figure 17.** Results of bump tests for 2,2 dichloro-1,1,1-trifluoroethane (R-123) using a Bacharach H-25-IR Industrial Refrigerant Leak Detector. (a) Measurement using a gas standard (Std) after instrument calibration (Calib) at the same concentrations in 5-L Flex Foil™ gas sampling bags. (b) Fractional deviation from a standard concentration (%) with stipulated quality control criterion (90 – 110%) illustrated with magenta lines. Quartiles, median (line), mean (+), minimum (whisker), and maximum (whisker) values illustrated in box plots with values to right of box plots.....47

**Figure 18.** Results of bump tests for carbon monoxide (CO) in air using Landtec GEM2000 Plus portable gas analyzer: (a) Measurement of gas standards (Std) at calibration (Calib) concentrations in 5 L Flex Foil gas sampling bags. (b) Deviation from standard concentration with stipulated quality control criterion (90 – 110% of standard concentration) illustrated with magenta lines. Quartiles, median (line), mean (+), minimum (whisker), and maximum (whisker) values illustrated in box plots with values to right of box plots.....48

**Figure 19.** Results of bump tests for hydrogen sulfide (H<sub>2</sub>S) using the Landtec GEM2000 Plus portable gas analyzer: (a) Measurement of gas standards (Std) at calibration (Calib) concentrations in 5-L Flex Foil™ gas sampling bags. (b) Deviation from standard concentration with stipulated quality control criteria (90 – 110% of standard concentration) illustrated with magenta lines. Quartiles, median (line), mean (+), minimum (whisker), and maximum (whisker) values illustrated in box plots with values to right of box plots.....49

**Figure 20.** Results of bump tests for flame ionization detector (FID) for methane in air using the Thermo Scientific TVA 1000B portable gas analyzer. (a) Measurement of gas standards (Std) at calibration (Calib) concentrations in 5-L Flex Foil™ gas sampling bags. (b) Deviation from standard concentration with stipulated quality control criterion ± 2.5 ppmv at ≤ 10 ppmv and within 90 – 110% of standard concentration > 10 ppmv illustrated with a red circle (13.9 ppmv) for the former and magenta lines for the latter. Quartiles, median (line), mean (+), minimum (whisker), and maximum (whisker) values illustrated in box plots with values to right of box plots.....50

**LIST OF FIGURES continued**

**Figure 21.** Results of bump tests for photo ionization detector (PID) in the Thermo Scientific TVA 1000B portable gas analyzer. (a) Measurement of PID response at gas standard (Std) and calibration (Calib) concentrations in 5-L Flex-Foil™ gas sampling bags. (b) Deviation from standard concentration with the stipulated quality control criterion of 80 – 120% of standard concentration illustrated with magenta lines. Quartiles, median (line), mean (+), minimum (whisker), and maximum (whisker) values illustrated in box plots with values to right of box plots.....51

**Figure 22.** Response of Thermo Scientific TVA-1000B to measurement of CH<sub>4</sub> using the FID and isobutylene using the PID to flow rate using gas standards .....52

**Figure 23.** Response of Bacharach H-25-IR to measurement of R-123 to flow rate using gas standards .....53

**Figure 24.** Change in O<sub>2</sub> and CO<sub>2</sub> concentration with flow rate during purging (a) Probe PB1S, (b) Probe PB2D, (c) Probe PA1D, (d) Probe WA1S .....54

**Figure 25.** The magnitude of change of O<sub>2</sub> and CO<sub>2</sub> concentration with change in flow rate. Data points for PA1D are illustrated on the plot.....57

**Figure 26.** Comparison of measured O<sub>2</sub> and CO<sub>2</sub> concentrations using a GEM2000 Plus gas analyzer and fixed-laboratory analysis .....58

**Figure 27.** Vacuum loss and calculated leakage through vapor well caps.....59

**Figure 28.** Applied vacuum (in steps) and calculated leakage in fittings used for leak chamber construction while testing at WB2S on 8/11/2009 .....60

**Figure 29.** Calculated leakage from fittings used for leak chamber construction from one-minute vacuum tests (n=141).....61

**Figure 30.** Leak testing of probe connection at surface at PA3I. 1 purge volume = 0.534 L.....62

**Figure 31.** Testing of leakage from the surface at PA1S on 9/30/2010. Tracer mixture containing R-123 introduced at 3.6 L. Concentration of R-123 in chamber measured at 10,200 ppmv at 9.5 L of soil-gas extraction. 1 purge volume = 0.622 L.....65

**Figure 32.** Results of leak testing between PA1S and PA1I on 9/16/2009 - soil-gas extraction from PA1S, 1 purge volume = 0.534 L: (a) Introduction of R-123 in chamber at the surface – no leakage from the surface observed, (b) introduction of 20,100 ppmv CO in PA1I, (c) repeat testing of (b).....67

## LIST OF FIGURES continued

|  |    |
|--|----|
| <b>Figure 33.</b> Leak testing between PA1S and PA1I on 11/14/2006. Soil-gas extraction from PA1S at 0.74 SLPM and 16.9 kPa vacuum. CO introduced in PA1I at 20,100 ppmv. 1 purge volume = 0.534 L.....  | 68 |
| <b>Figure 34.</b> Results of leak testing at PC1 on 9/14/2009. 1 purge volume = 3.46 L.....  | 70 |
| <b>Figure 35.</b> Schematic of heuristic model used to evaluate leakage .....  | 71 |
| <b>Figure 36.</b> Simulation of gas flow at 0.900 SLPM to a screen interval between 0.46 – 0.60 m with a well diameter of 2.5 cm. Blue dashed lines are vacuum (Pa), red solid lines are travel time to the probe (min), arrows denote velocity (cm/s), (a) gas porosity = 0.1, $k_r/k_z = 1.0$ , $k_r = 1.4e-07 \text{ cm}^2$ ; (b) gas porosity = 0.05, $k_r/k_z = 0.1$ , $k_r = 1.4e-07 \text{ cm}^2$ .....                       | 74 |
| <b>Figure 37.</b> Vacuum loss (Pa) as a function of flow (SLPM)at the surface due to fittings associated with the leak detection chamber.....  | 76 |
| <b>Figure 38.</b> Stacked column plot of vacuum induced from soil, fittings at the surface, and subsurface tubing during gas permeability testing. Plots illustrated at 3 scales to facilitate comparison of vacuum loss from frictional headloss and soil: (a) scale from 0 to 65,000 Pa, (b)scale from 0 to 1000 Pa, (c) scale from 0 to 200 Pa.....   | 79 |
| <b>Figure 39.</b> Pressure loss as a function of internal diameter of tubing and flow rate.....  | 80 |
| <b>Figure 40.</b> Comparison of radial permeability estimation (n=121) using equations for a prolate-spheroidal domain and a radial axisymmetric cylindrical domain. The $L/r_w$ value for the blue-circled data point was 2.1.....  | 82 |
| <b>Figure 41.</b> Temporal variability in gas permeability estimation at dedicated vapor probes. Green, orange, and blue colors indicate probes at shallow, intermediate, and deeper depths in probe clusters at two residential areas (A, B). Probes in black indicate 1” PVC wells screened across the water table at two residential areas (B, C) .....   | 84 |
| <b>Figure 42.</b> Transient gas permeability estimation at (a) WB3s and (b) WC1S August 2009: $k_r$ = radial permeability ( $\text{cm}^2$ ), $k_r/k_z$ = ratio of radial to vertical gas permeability (-), $\theta_g$ = gas filled porosity (-), $V_b$ = borehole storage ( $\text{cm}^3$ ).....   | 85 |
| <b>Figure 43.</b> Purge test results monitoring wells. (a) WB1S installed 8/6/2009, open borehole 16 hours, closed borehole 149 hours prior to purging, 1 purge volume = 2.46 L. (b) WB2S installed 8/7/2009, open borehole 3 hours, closed borehole 94.5 hours before purging, 1 purge volume = 2.62 L, (c) WB3S installed 8/11/2009, open borehole 5 hours, closed borehole 47 hours before purging, 1 purge volume = 2.64 L ..... | 87 |
| <b>Figure 44.</b> Purge testing at PC1 at Valley Center, KS completed on 8/12/2009, open borehole 2.5 hours, closed borehole 2 hours prior to purging. 1 purge volume ~ 3.46 L .....   | 88 |

**LIST OF FIGURES continued**

**Figure 45.** Purge test results at soil-gas probe cluster PB1 installed on 8/6/2009. Open borehole time = 3.5 hr. Closed borehole time on 8/7/2009 prior to purging = 19.1, 21.8, and 21.3 hours at PB1S, PB1I, and PB1D, respectively. 1 purge volume = ~ 0.45, 0.52, and 0.93 L at PB1S, PB1I, and PB1D, respectively. O<sub>2</sub> and CO<sub>2</sub> measurements for PB1D affected by variation of flow rate on 8/7/2009 .....90

**Figure 46.** Purge test results at soil-gas probe cluster PB2 installed on 8/6/2009. Open borehole time = 4.5 hr. Closed borehole time on 8/7/2009 prior to purging = 93.5, 94.5, and 94.0 hours at PB1S, PB1I, and PB1D, respectively. 1 purge volume = ~ 0.44, 0.46, and 1.27 L at PB2S, PB2I, and PB2D, respectively. O<sub>2</sub> and CO<sub>2</sub> measurements for PB2S and PB2D impacted by flow rate on 8/11/2009 and 9/19/2010, respectively .....91

**Figure 47.** Purge test results at soil-gas probe cluster PA4 installed on 8/5/2009. Open borehole time = 5.7 hr. Closed borehole time prior to initial purging = 208, 209, and 209 hours at PA4S, PA4I, and PA4D, respectively. 1 purge volume = ~ 0.44, 0.45, and 0.52 L at PA3S, PA3I, and PA3D, respectively .....92

**Figure 48.** Purge test results at soil-gas probe cluster PA2 installed on 8/4/2009. Open borehole time = 23 hr. Closed borehole time prior to initial purging = 207, 208, and 211 hours at PA2S, PA2I, and PA2D, respectively. 1 purge volume = ~ 0.28, 0.91, and 0.62 L at PA2S, PA2I, and PA2D, respectively .....93

**Figure 49.** Purge test results at soil-gas probe cluster PA3 installed on 8/5/2009. Open borehole time = 8.2 hr. Closed borehole time prior to purging = 208.2, 208.8, and 209.0 hours at PA3S, PA3I, and PA3D, respectively. 1 purge volume = ~ 0.45, 0.47, and 0.58 L at PA3S, PA3I, and PA3D, respectively .....94

**Figure 50.** Hypothetical purging scenarios for O<sub>2</sub> and CO<sub>2</sub> concentrations in soil-gas at 0% and 21%, respectively, and initial soil-gas concentrations in soil-gas probes for O<sub>2</sub> and CO<sub>2</sub> at 21%, 15%, 10%, 5%, and 0% for (a) no leakage, (b) 10% leakage, (c) 40% leakage, and (d) 90% leakage .....95

## LIST OF TABLES

|   |    |
|---|----|
| <b>Table 1.</b> Portable gas analyzer calibration and check standard requirements.....  | 29 |
| <b>Table 2.</b> Summary of bump test results, frequency of attainment of manufacturer’s quality control criteria, statistical analysis of bias. Significant deviations are highlighted in bold.....   | 43 |
| <b>Table 3.</b> Results of change in O <sub>2</sub> and CO <sub>2</sub> concentration measured with a GEM2000 Plus portable gas analyzer as a result of change in flow rate during purging (entries in bold reflect significant variation)..... | 56 |
| <b>Table 4.</b> Comparison O <sub>2</sub> and CO <sub>2</sub> concentrations measured using a GEM2000 Plus gas analyzer during purging with fixed-laboratory analysis.....  | 58 |
| <b>Table 5.</b> Analytical Results of Travel and Equipment Blanks.....  | 59 |
| <b>Table 6.</b> Results of Leak Testing.....  | 63 |
| <b>Table 7.</b> Input parameters and results of gas permeability estimation.....  | 77 |

## **ACKNOWLEDGEMENTS**

The authors would like to acknowledge Mr. Ken Jewell and Mr. Russell Neill of the US EPA Office of Research and Development, National Risk Management Research Laboratory (NRMRL) in Ada, Oklahoma and Mr. Tim Lankford, formerly of NRMRL-Ada for their effort in collecting data in this investigation.

## **EXECUTIVE SUMMARY**

Active soil-gas sampling refers to vacuum-based extraction of a gas sample from unsaturated unconsolidated (e.g. soil) or consolidated (e.g., fractured rock) subsurface media for subsequent field or fixed-laboratory analysis. Passive soil-gas sampling refers to placement of an adsorbent media directly in soil or in a monitoring well for later withdrawal and fixed-laboratory analysis.

Active soil-gas sampling has been used to support a variety of commercial and environmental activities. For instance, commercial applications include use of soil-gas sampling to locate sulfide ore deposits and oil and gas deposits. Environmental applications include evaluation of transport of carbon dioxide in the vadose zone due to volcanic degassing. Soil-gas studies at volcanic degassing locations have been used as natural analogues for evaluating the potential release of gaseous carbon dioxide to the atmosphere during geologic sequestration of supercritical carbon dioxide. Soil-gas studies have also been conducted during carbon dioxide based enhanced oil recovery to support research on geologic sequestration. Soil-gas sampling has also been used to trace seismically active faults and fracture systems and to detect gas migration due to subsurface nuclear testing.

Soil-gas sampling is commonly used to assess the effectiveness of subsurface gas flow-based remediation technologies such as soil vapor extraction. Soil-gas sampling has been widely used to support reconnaissance of groundwater contamination by organic compounds. Soil-gas sampling has been used to locate petroleum contamination in soil by detection of degradation products (e.g., carbon dioxide, hydrogen sulfide, methane) and depressed levels of oxygen.

Relatively recent concern regarding migration of vapors from contaminated soil and groundwater into indoor air (i.e., vapor intrusion) and direct-use of soil-gas concentrations to assess risk posed by volatile organic compounds in soil gas in the parts per billion by volume range has prompted development of guidance documents by regulatory agencies and trade organizations (e.g., American Petroleum Institute) to improve the quality assurance and quality control aspects of soil-gas sampling.

To support this investigation, guidance documents on soil-gas sampling from 22 state regulatory agencies, six Canadian Provinces, and five professional organizations in the United States were reviewed. Many of these documents were developed to support assessment of vapor intrusion.

We could find only one institutional document providing guidance on soil-gas sampling outside of North America (France).

The U.S. Environmental Protection Agency has published several documents describing soil-gas sampling but these documents lack specific recommendations to support quality assurance and quality control aspects of soil-gas sampling. Similarly, the U.S. Air Force Center, U.S. Navy, and U.S. Army have published documents describing soil-gas sampling but these documents lack specific recommendations to support soil-gas sampling.

The purpose of this investigation was to conduct research to improve quality assurance/quality control procedures related to soil-gas sampling, especially those associated with leak, purge, and gas permeability testing. Testing was performed on the properties of three homes in a residential development in Valley Center, Kansas to support assessment of stray gas (carbon dioxide) into homes. During a period of heavy precipitation on September 13, 2008, the City of Wichita Health Department measured oxygen concentrations in basements of homes as low as 10% and carbon dioxide concentrations as high as 7%. The homes lie in a topographically flat area where extensive flooding had occurred during a heavy precipitation event. The working conceptual model is that a rapid rise in the water table induced advective transport of naturally occurring carbon dioxide rich soil-gas into tile drains surrounding domestic foundation walls with subsequent entry into basements.

The following discussion is a brief description of results pertaining to quality assurance and control aspects of soil-gas sampling in this investigation.

#### Testing of Portable Gas Analyzers

Portable gas analyzers are widely used to support active soil-gas sampling, including leak testing and evaluation of attainment of gas or vapor stabilization prior to sample collection for fixed laboratory analysis. Portable gas analyzers used in this investigation included: (1) a Landtec GEM 2000 Plus equipped with electrochemical cells for measurement of oxygen, carbon monoxide, and hydrogen sulfide and infrared cells for measurement of methane and carbon dioxide; (2) a Bacharach H25-IR equipped with an infrared cell for measurement of 1,1-dichloro-2,2,2-trifluoroethane (a gas tracer used for leak testing); and a Thermo Scientific TVA-1000B

equipped with a flame ionization detector and a photoionization detector for measurement of hydrocarbons.

Portable gas analyzers were calibrated at the beginning of each workday using certified gas standards. Calibration was checked (bump tests) throughout the workday using gas standards at concentrations used for calibration and at other concentrations not used for calibration. In this investigation, quality control criteria for maintaining instrument calibration were based on the manufacturer's recommendations which depending on the instrument and gas were either absolute deviation from a standard concentration or measurement within a fractional percent of a standard.

During bump testing of the GEM2000 Plus portable gas analyzer, there were a significant number of measurements outside the stipulated quality control criterion of  $\pm 1\%$  for oxygen at standard concentrations of 10.0% and 20.9% and outside the quality control criterion of  $\pm 0.3\%$  for methane at a standard concentration of 2.5% necessitating frequent re-calibration. While reasons for exceedance of the quality control criterion are unknown, these observations reinforce the need for frequent bump tests throughout a workday. Depending on use of measurements from portable gas analyzers, it may be desirable to conduct bump tests prior to and after soil-gas measurement at individual probes.

In many instances, the stipulated quality control criterion was achieved but a minor negative or positive bias in measurement was observed. In one case though, a significant negative bias was observed during measurement of carbon dioxide at a standard concentration of 20.0% (the mean observed value was 18.8% carbon dioxide) with calibration at 5.0% even though the quality control criterion of  $\pm 3.0\%$  carbon dioxide was attained for 6 of 6 measurements.

Bias was absent during measurement of carbon dioxide at a standard concentration of 20.0% with calibration at 20.0% (7 measurements with mean=20.0%) suggesting improvement in measurement with calibration and measurement at the same concentration. However, a comparison of gas measurement at concentrations of calibration and at other concentrations using gas standards provided mixed results. For instance, measurement of carbon dioxide at a standard concentration of 5.0% did not improve measurement when calibrated at 5.0% compared to calibration at 20.0% and 35.0%. Thus, in this investigation, the benefit of using calibration

standards with concentrations close to expected concentrations of measurement was not apparent.

Requirements for calibration and bump testing of portable gas analyzers were absent in guidance documents reviewed from state regulatory agencies, Canadian Provinces, and professional organization. It would appear that this is an area requiring reconsideration.

Since portable gas analyzers were used in the soil-gas sampling train, the effect of flow rate on gas measurement was investigated using two methods. The first method of evaluation involved restricting the flow rate of gas standards from 5-liter gas sampling bags using gas standards for the Thermo Scientific TVA-1000B flame ionization detector (methane) and photoionization detector (isobutylene), and the Bacharach H-25 IR (1,1-dichloro-2,2,2-trifluoroethane). There was a slight increase in measurement of 1,1-dichloro-2,2,2-trifluoroethane with increasing flow. The magnitude of increase though did not necessitate correction or compensation during leak testing. Similarly, there was little change in response of the photoionization detector with flow rate.

There was however a strong linear increase in detector response of the flame ionization detector with increased flow. Thus, measurements using the flame ionization must be corrected for flow. Since the upper limit of measurement of the flame ionization detector was 10,000 parts per million by volume or 1.0% by volume and methane was detected at only one location in percent concentrations during testing within one meter of a leaking natural gas line, correction of flame ionization measurements was unnecessary in this investigation.

The second method of evaluating restriction of flow on the portable gas analyzer (GEM 2000 Plus) measurement was to restrict flow in the soil-gas sampling train during purging. During purging, concentrations of carbon dioxide increased with flow rate while concentrations of oxygen decreased with flow rate. The magnitude of change with increasing flow rate in oxygen and carbon dioxide measurement was greatest at lower flow rates. At flow rates above approximately 0.65 standard liters per minute there was little effect of flow rate on measurement of oxygen and carbon dioxide. Thus, in this investigation, a minimum flow rate of 0.65 standard liters per minute was necessary for use of the GEM2000 Plus portable gas analyzer in the soil-gas sampling train during purging.

If in-line portable gas analyzers are used to evaluate stabilization of gas concentrations prior to soil-gas sample collection, flow testing is necessary to evaluate the potential effect of flow rate on instrument readings. To our knowledge, flow testing of portable gas analyzers for in-line use during soil-gas purging has not been evaluated elsewhere.

Field measurements of oxygen and carbon dioxide using the GEM2000 Plus portable gas analyzer at flow rates in excess of 0.65 standard liters per minute were compared with fixed-laboratory analyses. There was a slight negative bias in field measurement of oxygen and a slight positive bias in field measurement of carbon dioxide compared to fixed-laboratory measurement. However, this bias was well within the stipulated quality control criterion for both gases.

### Shut-In and Leak Testing

Shut-in testing refers to leak testing of above ground components of a vapor probe. This testing is typically conducted by applying a vacuum at 25 kilopascal (~ 100 inches of water vacuum) to a closed system and monitoring for “noticeable” vacuum loss over a period of time, typically one minute. This testing is qualitative in nature providing little insight into the magnitude of leakage. In this investigation, the internal volume of above ground components was calculated, a vacuum was applied to a closed system, and a pressure transducer was used to continuously (every second) measure vacuum in the system. The Ideal Gas Law was then used to quantitate the leakage rate as a function of vacuum. Since flow rates during purging and sampling were typically in excess of 900 standard cubic centimeters per minute, leakage at less than 1 standard cubic centimeters per minute (< 0.1% leakage) at high vacuum (e.g. 90 kilopascals) was regarded as insignificant and hence acceptable.

In this investigation, 2.54-centimeter diameter rubber well plugs with brass quick-connect fittings were used for soil-gas sampling 2.54-centimeter internal diameter polyvinylchloride (PVC) monitoring wells. At 90 kilopascals vacuum (nearly one atmosphere), leakage was less than 1 standard cubic centimeter per minute and declined to less than 0.01 standard cubic centimeter per minute below 40 kilopascals of vacuum. Since vacuum during soil-gas sampling was typically less than 0.5 kilopascals and the flow rate during purging and sampling was typically between 900 – 1000 standard cubic centimeters per minute, leakage through well plugs was virtually nonexistent.

The leak detection chamber and sampling train used in this investigation had numerous fittings. Use of fittings in a soil-gas sampling train is typically minimized to avoid leakage. A vacuum was applied to the closed system soil-gas sampling train and monitored continuously with a pressure transducer. Since the leakage rate was very low, a stainless-steel toggle valve was used to periodically introduce air in steps to effectively monitor leakage as a function of vacuum.

While effective, this procedure was time consuming. To better enable rapid leak testing in the field, the leak testing procedure was modified to include three one-minute tests at high (e.g. 90 kilopascals), medium (e.g. 40 kilopascals), and low (e.g. 10 kilopascals) vacuum. Fittings were tested prior to each purge and sampling event. At high vacuum, leakage exceeded 1 standard cubic centimeter per minute in only 5 out of 141 tests. When leakage exceeded 1 standard cubic centimeter per minute, fittings were tightened and shut-in tests at high vacuum were repeated until leakage was below 1 standard cubic centimeter per minute. Thus, leakage through fittings used for the leak detection chamber and soil-gas sampling train were inconsequential in this investigation. This testing demonstrates that given adequate shut-in testing, use of a fairly complicated soil-gas sampling train with numerous fittings, as was the case in this investigation, is not a limiting factor for soil-gas sampling.

Unlike fittings used for a leak detection chamber for a soil-gas sampling train, compression fittings on soil vapor probes, O-rings on PVC pipe, and bentonite in the borehole generally cannot be modified after installation. Thus, a leak detection chamber and gas tracers must be used to evaluate leakage in the borehole. In this investigation, a leak detection chamber was designed to enable simultaneous leak, purge, and gas permeability testing prior to soil-gas sample collection. Leak testing in probe clusters consisting of three probes was conducted to discern: (1) leakage from the surface through compression fittings connected to subsurface tubing, (2) leakage from the surface to the screened interval of an upper probe through compromised bentonite, (3) leakage between the screened interval of an upper probe to the screened interval of an intermediate probe through compromised bentonite, and (4) leakage from the screened interval of an intermediate probe to the screened interval of a lower probe through compromised bentonite.

To our knowledge, use of gas tracers to quantitate leakage between screened intervals of a vapor probe cluster has not been documented elsewhere. Hence, this testing approach is novel.

Pure phase helium is commonly used, and in several cases required by state agencies, in chambers for leak detection. However, helium is a buoyant gas necessitating the presence of sufficient vacuum in a leakage pathway to a screened interval to overcome buoyancy. In this investigation, gas mixture containing tracers were formulated to have gas densities similar to expected soil-gas densities to eliminate the potential for negative bias in leak detection.

A tracer gas mixture containing 1% 1,1-dichloro-2,2,2-trifluoroethane and 99% argon was used to determine leakage between the surface and stainless-steel quick-connect compression fittings attached to stainless-steel tubing and from the surface to the screened interval of an upper probe in a probe cluster. A tracer gas mixture containing 1 – 2% carbon monoxide in air in 5-liter gas sampling bags was passively introduced into the screened intervals of intermediate probes to determine leakage between the screened interval of an intermediate probe and the screened interval of an upper probe and between the screened interval of an intermediate probe and a screened interval of a lower probe.

Leakage between stainless-steel tubing and stainless-steel quick-connect compression fittings attached to tubing was evaluated at 4 probe cluster locations. This type of leak testing was relevant only to quick-connect fittings for intermediate and lower probes in a soil-gas probe cluster since leakage through the quick-connect fittings at the upper probe cannot be distinguished from leakage down the borehole from a poor bentonite seal. Leakage was detected at one location at 2.1%. Detection of leakage was unexpected since quick-connect compression fittings were carefully tightened to stainless-steel tubing prior to deployment in boreholes since manual working space in boreholes was limited.

Leakage down the annular bentonite seal between the surface and the screened interval of the upper probe was tested 15 times at 6 probe clusters. During testing at 3-time periods, leakage occurred to some degree at all 6 upper probes tested. Leakage in 5 of the 6 shallow probes varied from 0.1% to 1.3%. Most state regulatory agencies stipulate a maximum leakage between 5% and 10%.

Leakage at one shallow probe in September 2010 was in excess of 94%. During two previous tests in September and November 2009, leakage was detected between the upper and intermediate probe, but not from the surface in this probe cluster indicating that a leakage

pathway from the surface developed sometime after November 2009. This result indicates that the absence of leak detection in a previous soil-gas sampling event does not preclude the development of leak pathways prior to later soil-gas sampling events. Thus, depending on intended use of data, leak testing prior to every soil-gas sampling event should be considered.

Leakage between screened intervals of upper and intermediate probes was tested 19 times at 7 probe clusters. During one of three testing periods, leakage was detected between an upper and intermediate probe at one probe cluster at 2.0%. However, leakage between an upper probe and an intermediate probe was detected at 59% in September 2009 at the same probe cluster where leakage from the surface to the upper probe was measured at 94% in September 2010. To evaluate reproducibility, leak testing was repeated with leakage measured at 36%. Thus, while both tests indicated significant leakage, there was considerable variability between results. Interestingly, leakage between the upper and intermediate probe was not detected in this probe cluster in September 2010 indicating a highly variable bentonite seal in this borehole.

Leakage between screened intervals of intermediate and lower probes was tested 12 times at 6 probe clusters. No leakage was observed in 10 tests at 5 probe clusters. Leakage at 0.6% was measured at one probe cluster. The ability to evaluate leakage between probes in a probe cluster by extracting soil-gas from one probe while passively introducing tracer in an overlying or underlying probe was demonstrated in this investigation. This procedure should be applicable to probe cluster configurations elsewhere.

Leakage between the surface and an unsaturated portion of a screened interval in monitoring wells was tested 8 times at 6 monitoring wells with leakage at 0.8% and 2.6% observed at two monitoring wells. These rates of leakage were similar to leakage associated with probe clusters. Probe clusters provide an economic means, especially in consolidated media, to repeatedly sample soil-gas over multiple intervals. If probe clusters are properly installed and leak tested, probe cluster provide comparable data to single probe or single monitoring well soil-gas sampling configurations.

While common in stray gas and soil-atmosphere greenhouse gas exchange investigations, shallow (< 1 meter) soil-gas sampling is generally discouraged at vapor intrusion investigations due to concern regarding entry of atmospheric air during sampling. However, when consolidated

media or cobbles are at or near the surface, direct-push sampling below 1 meter is often infeasible.

Gas flow simulations were conducted to determine whether leakage down a borehole could be distinguished from atmospheric recharge in soil having preferential vertical pathways (e.g., desiccation cracks). In a simulation assuming isotropic (radial permeability = vertical permeability) conditions, travel time of atmospheric air to a probe far exceeded the typical time of leak testing (minutes). However, when anisotropic conditions were simulated (vertical permeability = 10X radial permeability at the same radial permeability), gas tracer arrived in the soil-gas sampling train in less than 3 minutes – the time in which leakage was observed in most probes in this investigation. These results indicate that sealing of the surface using bentonite or some other means near a vapor probe should be considered if leakage is detected during leak testing when soil-gas sampling is shallow (e.g. < 1 meter) to distinguish leakage from atmospheric recharge.

A heuristic model was developed as part of this study to provide a conceptual model of leakage in a borehole during soil-gas sampling. For a given borehole radius, as the length of the bentonite seal increases, leakage decreases. When the ratio of radial permeability in the sampled formation to vertical permeability of a borehole sealant is greater than 100X, leakage will be less than 1.0% regardless of geometric factors. Thus, leakage is less likely when a probe is screened in high permeability media such as sand and more likely when a probe is screened in low permeability media such as silt or clay as one would expect. Thus, leak testing is of considerable importance when collecting soil-gas samples from lower permeability media.

### Gas Permeability Testing

Gas permeability testing is sometimes performed during soil-gas purging to better document soil conditions (e.g., presence of a wetting front) at the time of soil-gas sampling. Since vacuum measurement at the surface is not equivalent to vacuum in the screened interval due to frictional head loss, vacuum loss in tubing or well casing must be estimated in addition to vacuum loss in fittings at the surface used for the leak detection chamber and soil-gas sampling train.

Surprisingly, state guidance documents requiring gas permeability testing during soil-gas sampling do not require evaluation of frictional head loss associated with tubing and fittings.

In this investigation, a non-linear equation was used to estimate vacuum loss as function of flow rate in surface fittings using data from a field experiment conducted with the leak detection chamber and surface fittings. Vacuum loss in straight tubing and pipe was estimated using theoretical equations for laminar flow which was maintained during all gas permeability determinations.

In general, vacuum loss due to surface fittings, tubing, and pipe was relatively minor compared to high induced vacuum in lower permeability soils. However, in higher permeability soils, there were several instances using 0.617-centimeter (cm) internal diameter (ID) stainless-steel tubing where vacuum induced by soils was equivalent to or less than vacuum loss induced by fittings and tubing. In this situation, estimation of gas permeability was constrained by potential error in estimation of vacuum loss from surface fittings and tubing.

To aid future gas permeability estimation efforts for others, theoretical vacuum or pressure loss as a function of tube length and flow rate were evaluated for 6 internal diameters for tubing or pipe commonly used for soil-gas probe construction. In small diameter tubing such as 0.158-cm internal diameter stainless-steel tubing, expected vacuum loss during testing would be excessive and hence is not suitable for gas permeability testing.

Estimated vacuum loss in 0.617-centimeter internal diameter stainless-steel tubing used for soil-gas probe cluster construction in this investigation and 0.635-centimeter internal diameter low density polyethylene (LDPE) tubing typically used for the Geoprobe Post-Run-Tubing direct-push soil-gas sampling system exceeded 100 Pascals at 1.0 standard liter per minute at tubing lengths of 10 to 15 meters. Use of tubing with comparable small internal diameters is undesirable for gas permeability testing at depths exceeding 10 meters.

Estimated vacuum loss was insignificant regardless of depth at flow rates used for soil-gas sampling at less than 1 standard liter per minute for 1.59-cm ID steel drive pipe used for the Geoprobe soil-gas cap sampling system or for 1.53-cm ID schedule 40 PVC pipe. Hence, the Geoprobe soil-gas cap system is preferable to the Geoprobe Post-Run-Tubing system for gas permeability estimation during direct-push soil-gas sampling. PVC pipe having an ID of 1.52-cm or larger is preferable for gas permeability estimation in deeper soil gas probes.

The pseudo-steady-state radial gas flow equation is typically used for gas permeability estimation to support active soil-gas sampling. Since vacuum propagates to infinity in a closed radial domain, use of this equation necessitates stipulation of a pressure boundary at some arbitrary distance from a vapor probe. To overcome this limitation, the California Environmental Protection Agency recommends use of a modified equation for a prolate-spheroidal domain. Estimates of radial permeability using this simple algebraic equation were compared with use of a more geometrically correct, but computationally more difficult (requiring use of a Fortran code) solution for an axisymmetric-cylindrical domain. Estimates of radial permeability using the modified equation for a prolate-spheroidal domain were consistently lower than the latter by a factor of 1.03 to 1.43 compared to estimates of radial permeability using a solution in an axisymmetric-cylindrical domain. The reason for a minor negative bias in permeability estimation is unclear.

Comparison of gas permeability measurements conducted during the same time period at two and three different flow rates indicated random variability between a factor of 1.01 to 1.63. Thus, random variation in radial gas permeability estimation was greater than the choice of model for gas permeability estimation. Also, the difference in use of equations for permeability estimation is minor when considering variation in orders of magnitude in permeability of various soil types. Hence, use of the modified equation for a prolate-spheroidal domain to estimate radial permeability is appropriate for reporting gas permeability where required. However, use of more sophisticated analytical solutions is necessary for gas flow simulation and particle tracking or time of travel to a screened interval during purging.

The presence of lower permeability at two monitoring wells allowed transient gas permeability testing. Transient gas permeability was estimated using an analytical solution for an axisymmetric-cylindrical domain incorporating the effect of borehole storage. This solution enables the use of 4 fitting parameters (radial permeability, the ratio of radial to vertical permeability or anisotropy, gas-filled porosity, and borehole storage). Estimates of borehole storage were constrained by realistic estimates of gas-filled porosity in sandpacks (e.g., 10 – 40%). Estimates of radial permeability were constrained by steady-state gas permeability estimation. Curve fitting was relatively insensitive to anisotropy. Curve fitting however was very sensitive to formation gas-filled porosity estimation which was relatively low (e.g., 1 – 9%) as

would be expected in lower permeability media. Gas-filled porosity is an important parameter in particle tracking or estimation of time of travel during gas flow simulation. Thus, if gas flow simulations in lower permeability media are desirable to support active soil-gas sampling, transient gas permeability estimation should be considered.

### Purging

Vapor probes and monitoring wells are typically purged prior to soil-gas sample collection. The often-stated purpose of purging is to remove atmospheric air remaining in the borehole after probe or well installation. Recommended initial (after probe installation) purge volumes vary from 2 to 5 internal volumes (including the gas-filled porosity of sandpacks). In some instances, fixed gases (typically oxygen and carbon dioxide) are monitored to evaluate attainment of stabilization.

During this investigation, purging experiments were conducted to determine the number of purge volumes required for stabilization ( $\pm 0.1\%$  random variation on a portable gas analyzer) of oxygen and carbon dioxide concentrations in vapor probes and monitoring wells as affected by equilibration time (time since soil-gas probe and monitoring well completion or setting of bentonite seal). Purging simulations were conducted using a mass-balance mixing model to compare observed versus expected results.

Extraction of 2 to 4 purge volumes was typically required for stabilization of oxygen and carbon dioxide concentrations during the first purge event regardless of time of purging (0.3 – 211 hours) after probe or monitoring well installation. However, the rate of change in oxygen and carbon dioxide concentration appeared more rapid in probes having lesser equilibration time, especially in probes with low oxygen and high carbon dioxide concentrations (i.e. distinct contrast with atmospheric air). During subsequent purge events, stabilization oxygen and carbon dioxide was often achieved in less than 1 purge volume. These observations were consistent with purging simulations.

In some instances, more than 10 purge volumes was required for stabilization of oxygen and carbon dioxide concentrations during the first purge event in the upper probe while only 2 to 4 purge volumes were required for stabilization of oxygen and carbon dioxide concentrations in intermediate and lower probes. The reason for this anomalous behavior was unclear. However,

based on simulation results, gas removal in excess of 10 purge volumes indicates a perturbation of oxygen or carbon dioxide concentration outside the borehole either naturally present or induced during probe installation. For instance, at one probe in a soil-gas probe cluster, a significant change in soil-gas concentration over two sampling periods resulted in the need for purging more than 10 purge volumes for stabilization oxygen and carbon dioxide concentrations.

Finally, it is often assumed that leakage is indicated by increasing oxygen and decreasing carbon dioxide concentrations during purging. This assumption appears to be generally valid. However, a corollary assumption that a decrease in oxygen concentration and an increase in carbon dioxide concentration during purging indicates little or no leakage is not valid. Simulations conducted here indicate that a decrease in oxygen concentration and an increase in carbon dioxide concentration could be observed even at 90% leakage when the initial oxygen concentration in a vapor probe is 21% and the initial carbon dioxide concentration is 0%. Simulations indicated that there are numerous initial oxygen and carbon dioxide concentration conditions in which a decrease in oxygen concentration and an increase in carbon dioxide concentration could be observed at lesser values of leakage.

### **Project Data Quality Assurance and Quality Control**

As required by EPA policy, a Quality Assurance Project Plan (QAPP) was prepared and approved in November 2008, prior to data collection, entitled “The Use of Soil Gas, Gas Flux, and Groundwater Sampling to Evaluate Potential Leakage from Well Penetrations during Geological Sequestration of CO<sub>2</sub>”. A QAPP integrates the technical and quality activities to support a research effort, describes the type and quality of data needed, and the methods for collecting and assessing the data. A Technical System Audit was conducted at the field site on August 11, 2009, by the EPA QA Manager using the QAPP as the audit standard. As a result of the audit, even though the QAPP described the methods for sampling and collecting data, it was determined that a new QAPP should be written to specifically address this site and objectives. This QAPP, entitled, “Evaluation of Gas Intrusion in Homes in Valley Center, Kansas: QA ID No. G-13480” was approved in March 2010. As described in this report, standard operating procedures were implemented for sampling and analysis of soil gas. All on-site instruments were calibrated daily prior to use and checked periodically throughout the day with gas standards of known concentrations. The purpose of this research effort was to improve the QA/QC procedures

for soil gas sampling, in particular, leak, purge, and gas permeability testing. Throughout this report the quality of the data and any limitations with the use of the data are presented and discussed.

## 1.0 INTRODUCTION

Active soil-gas sampling has been used to widely to support a number of commercial and environmental activities. For instance, commercial applications include use of soil-gas sampling to locate sulfide ore deposits (Alpers et al. 1990) and oil and gas deposits (Jones and Drozd 1983). Soil-gas sampling has also used to evaluate transport of carbon dioxide (CO<sub>2</sub>) in the vadose zone as a result of volcanic degassing (D'Alessandro and Parello 1997). Soil-gas studies at volcanic degassing locations have been used as natural analogues for evaluating potential release of CO<sub>2</sub> to the atmosphere during geologic sequestration (Annunziatellis et al. 2008, Bateson et al. 2008, Beaubien et al. 2008). Soil-gas studies have also been conducted during CO<sub>2</sub> enhanced oil recovery to support research on geologic sequestration (Beaubien et al. 2013).

Soil-gas sampling has been widely used to trace seismically active faults and fracture systems (Azzaro et al. 1998, Baubron et al. 2002, Ciotoli et al. 1998, 1999, 2004, 2005, 2007, Fountain and Jacobi 2000, Fridman 1990, King et al. 1996, Lewicki and Brantley 2000, Lewicki et al. 2003) and to detect gas migration as a result of subsurface nuclear testing (Carrigan et al. 1996).

Soil-gas sampling is commonly used to assess the effectiveness of subsurface gas flow-based remediation systems such as soil vapor extraction (Aelion et al 1996). Soil-gas sampling has been widely used to support reconnaissance of groundwater contamination by organic compounds (Barber et al. 1990, Marrin, 1988, Marrin and Kerfoot 1988) and the extent of degradation of petroleum hydrocarbons in soil (Amos et al. 2005, Bouchard et al. 2008).

Observation of elevated levels of degradation products CO<sub>2</sub>, methane (CH<sub>4</sub>) and hydrogen sulfide (H<sub>2</sub>S) and depressed levels of oxygen (O<sub>2</sub>) (Robbins et al. 1990b, Robbins et al. 1995, Kerfoot 1988, Deyo et al. 1993) in soil gas have also been used to detect the presence of parent organic compounds in soil and groundwater.

Relatively recent concern regarding migration of vapors from contaminated soil and groundwater into indoor air (i.e., vapor intrusion) and direct use of soil-gas concentrations for risk assessment has necessitated analysis of volatile organic compounds (VOCs) in soil gas in the parts per billion by volume (ppbv) range and prompted discussion of methods to improve quality assurance (QA)/quality control (QC) protocols for soil-gas sampling (DiGiulio et al. 2006a, b;

DiGiulio 2007a, b, 2009, Hartman 2002, 2004, 2007, Hers et al. 2004, McAlary et al. 2009, 2010).

The need for improved quality assurance/quality control protocols and consistency in soil-gas sampling has prompted development of guidance documents in States and Canadian Provinces illustrated in **Figure 1**. In Canada, the Canadian Council of Ministers of Environment (CCME 2009) and Health Canada (2007) have also developed guidelines to support soil-gas sampling.

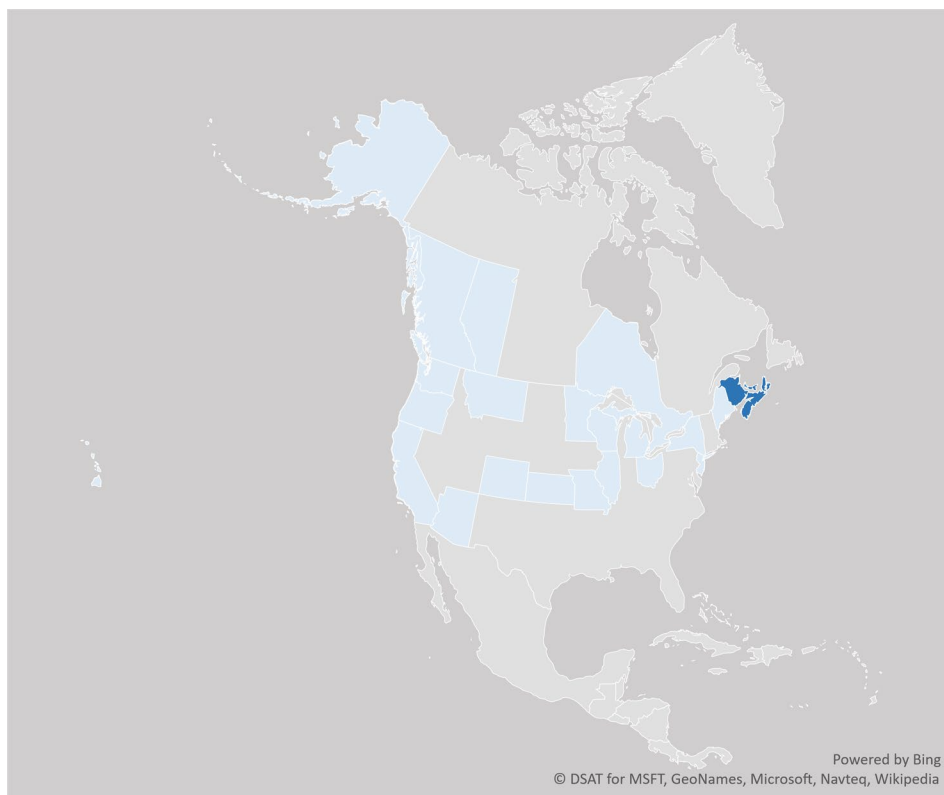


**Figure 1.** States and Canadian Provinces (light blue) where guidelines to support soil-gas sampling were reviewed. The area in dark blue denotes Atlantic Partners in Risk-Based Corrective Action Implementation consisting of New Brunswick, Newfoundland and Labrador, Nova Scotia, and Prince Edward Island

In the United States, the U.S. Environmental Protection Agency (US EPA) has published documents describing soil gas sampling (US EPA 1987, 1996, 1997, 2003, 2009, 2015) but these documents lack specific recommendations to support soil-gas sampling. Similarly, the U.S. Department of Defense (DOD 2009), the U.S. Air Force Center of Environmental Excellence (AFCEE 1994), the U.S. Navy (2008), and the U.S. Air Force, Navy, and Army (2008) have

published documents describing soil gas sampling but these documents lack specific recommendations to support soil-gas sampling.

In the United States, professional and industry organizations have issued guidance documents on soil-gas sampling. These organization include the American Society of Testing Materials (ASTM 2012), the Interstate Technology and Regulatory Council (IRTC 2007), the American Petroleum Institute (API 2005), the Electric Power Research Institute (EPRI 2005), and the Atlantic Richfield Company 2006). Many of these documents were developed to support assessment of vapor intrusion. We could find only one institutional document providing guidance on soil-gas sampling outside of North America in France (City Chlor 2013).

The purpose of this investigation was to improve QA/QC protocols related to soil-gas sampling, especially those associated with leak, purge, and gas permeability testing. Leak detection chambers were designed to enable simultaneous leak, purge, and gas permeability testing prior to soil-gas sample collection. Multiple tracers were deployed in probe clusters to discern leakage between screened intervals rather than just from the surface as is typically done.

## 2.0 MATERIALS AND METHODS

### 2.1 Probe Cluster and Monitoring Well Installation

Soil-gas sampling was performed to support assessment of stray gas (carbon dioxide) into homes in Valley Center, Kansas (KS). During a period of heavy precipitation on September 13, 2008, the City of Wichita, KS Health Department measured O<sub>2</sub> concentrations in homes as low as 10% and carbon dioxide CO<sub>2</sub> concentrations as high as 7%. The homes lie in a topographically flat area where extensive flooding had occurred during a precipitation event. The working conceptual model is that a rapid rise in the water table induced advective transport of naturally occurring CO<sub>2</sub> rich gas into tile drains surrounding domestic foundation walls with subsequent entry into basements.

A track-mounted Geoprobe™ rig was deployed in the Valley Center neighborhood to install soil-gas probes within 1 meter (m) of homes (**Figure 2**). To create boreholes for probe cluster and monitoring well installation, 5.72-centimeter (cm) (2.25 inch) outside diameter (OD) pipe steel drive rods containing 122 cm (4 feet) long transparent polyvinylchloride (PVC) liners (**Figure 3**) were pushed to target depths. A PVC core catcher was used with each liner to avoid loss of soil during retrieval.



**Figure 2.** Photograph of track-mounted Geoprobe™ rig adjacent to a house in Valley Center, Kansas.



**Figure 3.** Photograph of removal of a PVC liner containing soil and a PVC core catcher.

Liners were sliced open for manual inspection and categorization of soil texture (**Figure 4**). The Geoprobe™ rig was then used to push 7.62 cm (3 inch) diameter thin-walled tubes through existing holes to enlarge the borehole for probe installation (**Figure 5**) and to reduce compression of black clay (**Figure 6**) present within the first 1 – 2 m of the surface. This procedure also minimized smearing the clay in sand below the black clay.



**Figure 4.** Photograph of soil core removed from clear PVC liner.



**Figure 5.** Photograph of thin-walled 7.6 cm tube used to enlarge boreholes.



**Figure 6.** Photograph of black clay. Hole in center of clay is from previous push with steel rods containing PVC liners.

Probe clusters consisting of three separate probes (**Figure 7**) were installed to allow a vertical profile of soil-gas concentration and repeated sampling over several time intervals at the same location.

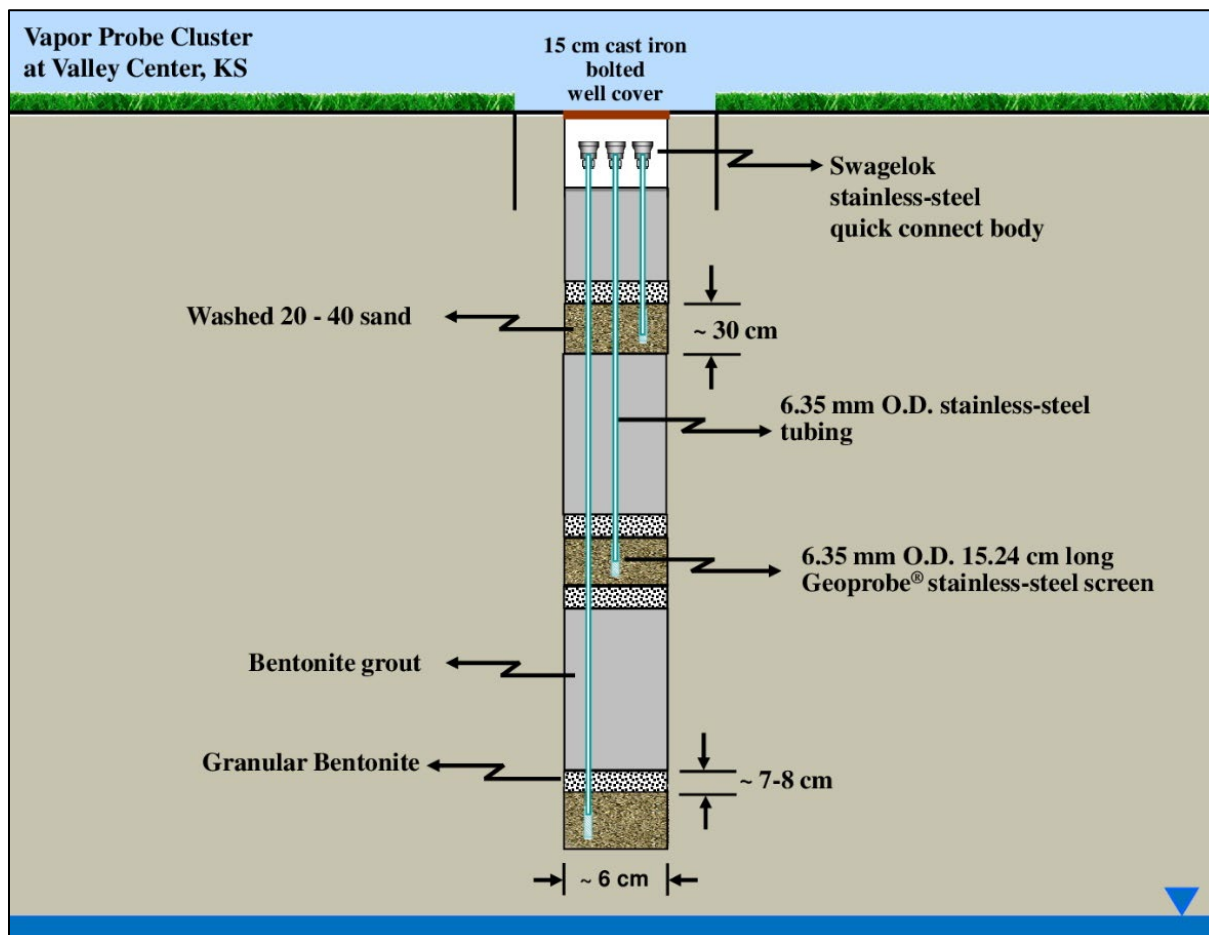


**Figure 7.** Schematic illustrating typical probe cluster construction at Valley Center, KS.

Probe clusters were installed near three homes designated as ‘A’, ‘B’, and ‘C’. “Shallow” (e.g., 2 m) “intermediate” (e.g., 3 m) and “deep” (e.g., 4 m) probes were designated with the letters ‘S’, ‘I’, and ‘D’. The first letter of each probe was identified with a ‘P’, followed by the home location, the probe cluster number, and the probe cluster interval. For example, the uppermost probe in the first probe cluster at home A was designated as PA1S. There were 4 probe clusters installed at location A, 3 probe clusters at location B. No probe clusters were installed at location C.

Each probe consisted of a 6.35-millimeter (mm) (0.25 inch) OD 15.2 cm (6 inch) long stainless-steel Geoprobe™ screen, 6.35 mm (0.25 inch) OD x 6.17 mm ID (0.09 mm wall thickness)

thermocouple-cleaned 316 stainless-steel Swagelok™ tubing (**Figure 8**), and a stainless-steel Swagelok™ tube fitting quick-connect body at the surface. Screens and tubing were transported in air-tight packages and separated from other equipment and materials used for field testing to eliminate the potential for cross-contamination during transport.



**Figure 8.** Photograph of stainless-steel screen and tubing used for probe construction.

Stainless-steel fittings and thermocouple cleaned stainless-steel tubing were used to minimize potential material artifacts. For instance, toluene and benzene have been detected off-gassing from nylon tubing and 1,1-difluoroethane has been detected from off-gassing of Teflon™ tubing (Hayes et al. 2006). Probes were constructed at the surface prior to placement in a borehole to avoid difficulty with clearance in a borehole when hand-tightening compression fittings.

Prior to manual placement of the lower probe, 20-40 grade washed sand was poured down the open borehole using a graduated cylinder to form an approximate 7 – 8 cm (3 inch) base. After probe placement, additional sand was poured down the borehole until approximately 7 – 8 cm of sand was present above the probe to form a 30.5 cm (1 foot) soil-gas monitoring interval. A tremie tube consisting of 9.53 mm (3/8”) internal diameter (ID) high density polyethylene (HDPE) tubing was used to place 7 - 8 cm of dry granular bentonite above the sandpack to prevent infiltration of grout slurry. Dry granular bentonite has a texture similar to sand enabling easy manual placement above a sandpack and rapid hydration. Use of dry granular bentonite above a sandpack is recommended in a number of guidance documents, especially during installation of multiple probes in a probe cluster (e.g., British Columbia 2011, California

Environmental Protection Agency 2012, City Chlor 2013, Missouri Department of Natural Resources 2013).

A grout tremie tube consisting of 9.53 mm (3/8 inch) ID HDPE tubing was used to pump a bentonite slurry (formulated using domestic tap water) in the borehole to within 7 - 8 cm of the base of the next screened interval where an additional 7 - 8 cm layer of granular bentonite was placed. The intermediate and upper probes were then installed in a similar manner to the deepest probe. Bentonite grout was extended to within 15 cm (6 inch) of the surface. Probes were encased in a 15 cm (6 inch) OD steel box.

Shallow groundwater monitoring wells were used for both groundwater and soil-gas sampling at the water-table interface. Depending on the location, 2 additional monitoring wells were installed next to shallow monitoring wells to enable groundwater sampling at deeper intervals as illustrated in **Figure 9**.

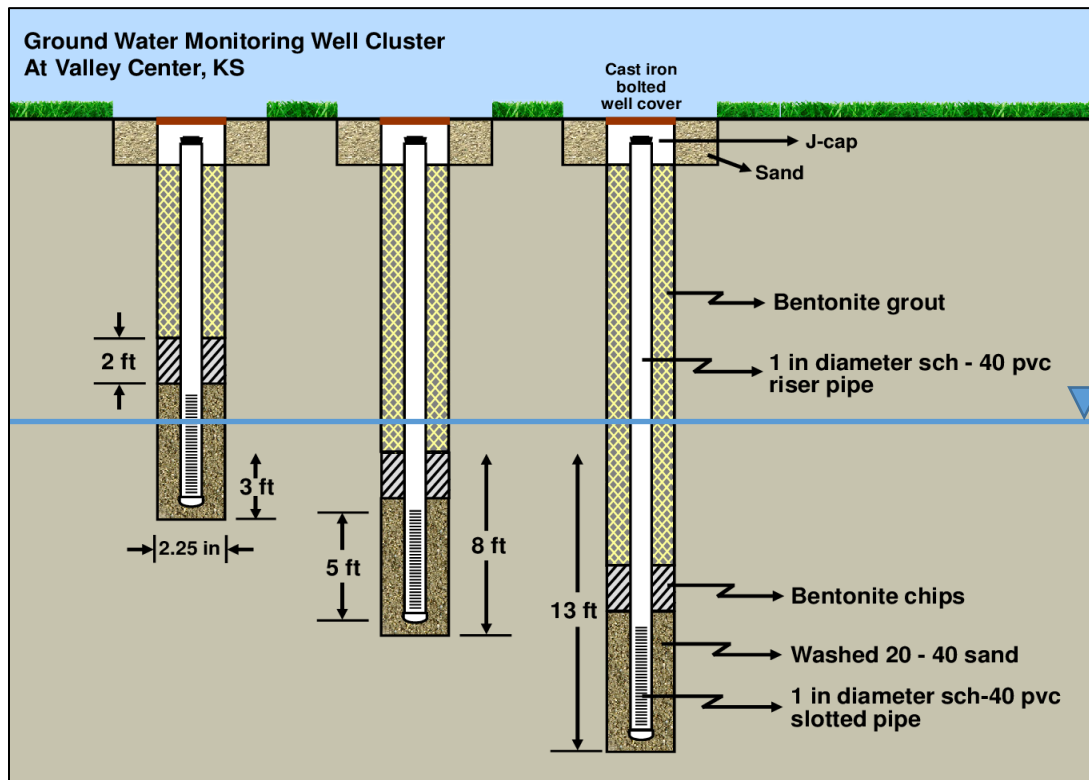


**Figure 9.** Schematic of three-monitoring well cluster of PVC wells used for groundwater sampling and soil-gas sampling across the water table.

Boreholes for monitoring wells were created in the same manner as that for probe clusters. Monitoring wells were constructed using sections of 152 cm (5 feet) long 2.54 cm (1 inch) ID schedule-40 PVC slotted screen and 2.54 cm ID PVC riser pipe. All casing materials were connected without use of solvents or glues. O-rings were placed between sections of riser pipe to ensure gas-tight connections. The wells were sealed and locked using commercially available caps. Wells were shut in with rubber compression fittings containing a quick-connect fitting (**Figure 10**).



**Figure 10.** Photograph of rubber fitting with brass quick-connect fitting to seal PVC wells.

Monitoring wells were designated with a ‘W’ as the first letter, the home location as the second letter, the well number, and then as shallow (S), intermediate (I), or deep (D) depth. For example, the first upper monitoring well at home A was designated as WA1S. At home location ‘C’, two monitoring wells were installed above the water table and were designated as ‘PC1’ and ‘PC2’.

## 2.2 Soil-Gas Sample Train Configuration

For vapor probe clusters, a sample train was configured to enable leak testing between probes within a cluster and to enable simultaneous purge and gas permeability testing. The sample train for a three-probe soil-gas cluster is illustrated in **Figure 11**.

A 36 cm (14 inch) diameter 25 cm high (10 inch) stainless-steel leak detection chamber was fabricated from sheet metal. The weight of the unit ensured stable (did not move during testing) contact with the ground surface during testing. Within the chamber, soil-gas was extracted from each probe through 0.635 cm (1/4 inch) OD Swagelok™ flexible stainless-steel tubing connected

to a stainless-steel Swagelok™ double-end shutoff (DESO) stem via a stainless-steel compression. This fitting snapped into a stainless-steel Swagelok™ quick connect body connected to a stainless-steel soil-gas probe via a compression fitting. The DESO stem is designed to have a gas-tight seal which when disconnected allowed leak testing of connections used for the sampling train.

A “bypass” using the same materials was created to enable sample collection for fixed laboratory analysis using an evacuated canister while bypassing connections and tubing required for purging. This bypass eliminates issues associated with sample material effects (e.g., off-gassing of volatile organic compounds from synthetic tubing or plastic). This design feature was created for future sampling efforts. Gas samples in this investigation were collected using gas sample bags.

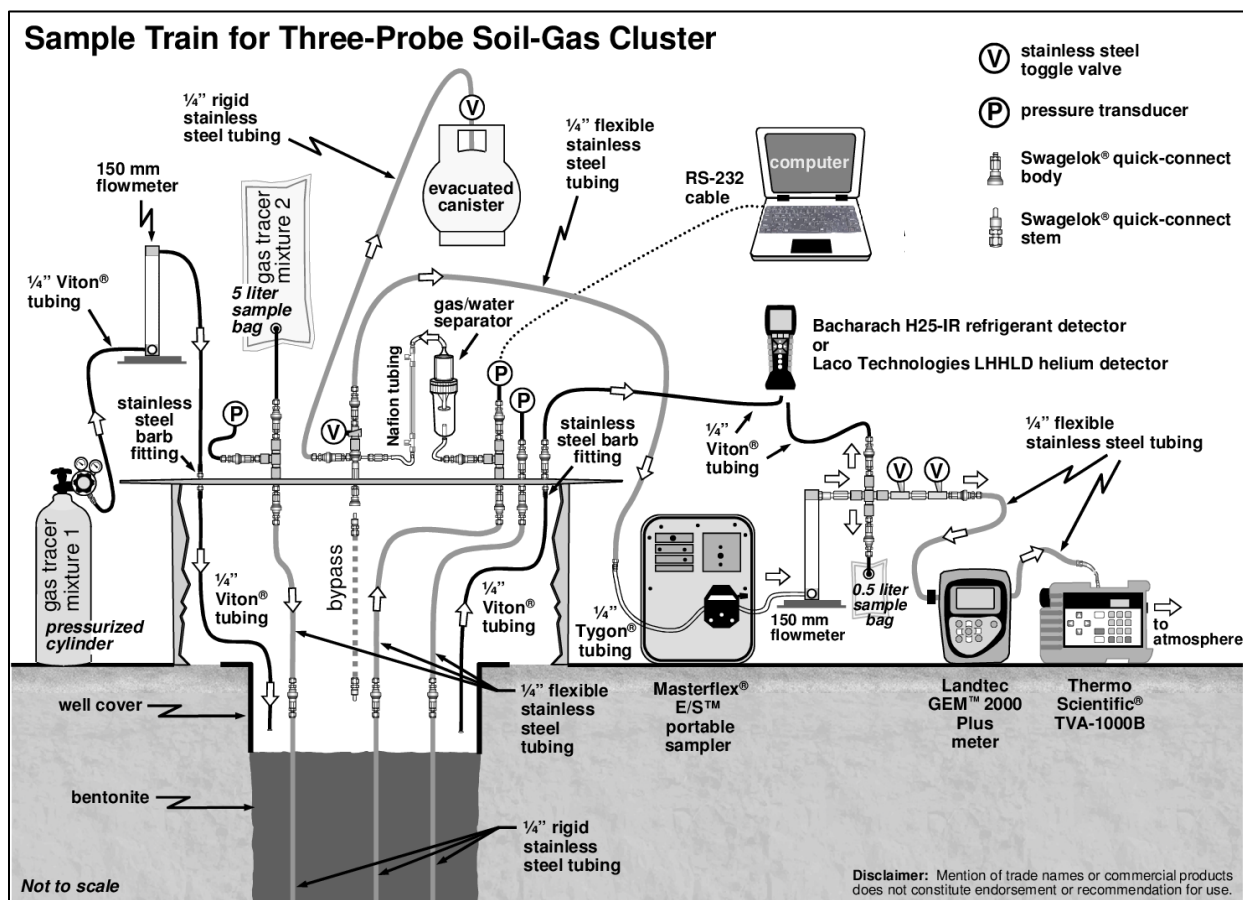


**Figure 11.** Schematic for leak detection chamber and soil-gas sample train for soil-gas probe clusters

To introduce and monitor tracer concentration, stainless-steel 6.35 mm (1/4 inch) barbed fittings were threaded on the interior and exterior of the chamber and attached to Masterflex™ Viton L/S

6.35 mm ID tubing. Viton tubing was placed directly above probes in the cast iron well cover to inject and monitor tracer concentration directly above soil-gas probes to ensure maximum tracer concentrations at locations of potential leakage. The flow rate of the gas tracer mixture was monitored during leak testing with a 150-mm Cole-Parmer variable area flow meter with a capacity to 29 standard liters per minute (SLPM) equipped with a needle valve. Viton tubing was used to connect the flowmeter to a pressurized canister of the tracer gas mixture.

To evaluate leakage between screened intervals in a probe cluster, a second gas tracer mixture was passively introduced from a 5-liter (L) Flex Foil gas sampling bag to a soil-gas probe above or below the soil-gas probe in which gas extraction was occurring. Entry of the second tracer into a screened interval was reliant upon vacuum induced as a result of leakage. A Swagelok<sup>TM</sup> stainless-steel tee and Swagelok<sup>TM</sup> stainless-steel quick-connect body was used to manually monitor vacuum between probe clusters. Vacuum was also manually monitored at the third probe in which tracer gas was not introduced or in which gas was extracted.

During purging, upon exiting the chamber, soil-gas flow was directed to a plastic gas/water separator using 0.635 cm (1/4 inch) ID Masterflex<sup>TM</sup> Tygon tubing in the event of water flow due to vacuum induced water table upwelling. This occurred several times while purging lower probes necessitating replacement of gas/water separators. A 1.0 micrometer (um) polypropylene Whatman<sup>TM</sup> disposable filter was initially planned for use for gas-water separation, but filters caused a response to the TVA-1000B flame ionization detector (FID) and photoionization detector (PID). The reason for this response was unclear but use of Whatman<sup>TM</sup> filters was abandoned.

The gas stream was then directed through Nafion<sup>TM</sup> tubing to reduce the relative humidity of the gas stream and to ensure a non-condensing atmosphere in portable gas analyzers. Nafion<sup>TM</sup> tubing consists of tubing within tubing in which gas flow in the inner tubing is directed further downstream while moisture passes through the inner tubing to the outer tubing. Dry gas flow in the outer tubing removes moisture to the atmosphere through countercurrent gas flow. Nafion<sup>TM</sup> is a copolymer of perfluoro-3,6-dioxo-4-methyl-7-octene-sulfonic acid and tetrafluoroethylene (Teflon). Only three compounds or classes of compounds are normally removed directly by Nafion<sup>TM</sup> tubes: water, ammonia, and alcohols.

Masterflex™ Tygon tubing was then used to direct the soil-gas gas stream to a Masterflex™ E/S portable peristaltic pump at pumping rates varying from 0.35 to 1.0 SLPM and to a 150 mm Gilmont™ Accucal flowmeter. The outlet of the flowmeter was connected to a Swagelok™ stainless-steel cross equipped with two Swagelok™ stainless-steel quick-connect bodies to allow duplicate collection of soil-gas samples using Cali-5 Bond gas sample bags for submittal to a commercial laboratory. The cross was connected to a Swagelok™ stainless-steel toggle valve to allow gas flow through the flowmeter to be shut-in while bypass gas flow from the leak chamber flowed through another in-line Swagelok™ stainless-steel toggle valve in route to portable gas analyzers. This toggle valve allows the use of one gas analyzer to measure gas tracer concentration in the sample train and chamber during leak testing. Swagelok™ stainless-steel single-end shutoff stems (SESO) were used to connect the port used for sampling (two external quick-connects) to the centrally located port. SESO stems remain open when uncoupled.

The gas stream was then directed to a LandTec GEM2000 Plus portable gas analyzer (LandTec North America, Colton, CA) for continuous measurement of O<sub>2</sub>, CO<sub>2</sub>, CH<sub>4</sub>, carbon monoxide (CO), and H<sub>2</sub>S in the soil-gas stream during purge testing in accordance with NRMRL-GWERD standard operating procedure Robert S. Kerr Standard Operating Procedure (RSKSOP)-314v1.

The outlet of GEM2000 Plus LandTec Gas Analyzer was fed into a Thermo Scientific Toxic Vapor Analyzer (TVA-1000B) (Thermo Electron Corp, address) to measure FID and PID response to total hydrocarbons in accordance with NRMRL-GWERD standard operating procedure RSKSOP-320v0. A Bacharach H25-IR Industrial Refrigerant Leak Detector (Bacharach, New Kensington, PA) was used to measure 2,2 dichloro-1,1,1-trifluoroethane (R-123) in both soil gas and a leak detection chamber in accordance with NRMRL-GWERD standard operating procedure RSKSOP-313v1. A second GEM2000Plus was used to periodically monitor CO concentration in the workspace. CO was not detected in the working space at a detection limit of 1 part per million volume (ppmv).

### 2.3 Calculation of Purge Volume

A purge volume for a lower probe in a probe cluster, monitoring well, or soil-gas well was calculated by:

$$V_{PV} = \frac{\pi}{4} \left[ D_T^2 L_T + D_P^2 L_P + (D_B^2 - D_P^2) L'_S \theta_g + D_B^2 (L_S - L'_S) \theta_g \right] \quad (1)$$

$D_T$  = internal diameter of tubing at the surface (cm),

$D_B$  = diameter of borehole (cm),

$D_P$  = internal diameter of probe (cm),

$L_T$  = length of tubing at the surface (cm),

$L_P$  = length of probe (cm),

$L_S$  = length of sandpack,

$L'_S$  = length of probe into sandpack below bentonite (cm),

$\theta_g$  = gas filled porosity of sandpack (-).

In intermediate probes, calculation of a purge volume was adjusted by subtracting out the volume of tubing present in the sandpack from the lower tubing. Similarly, in upper probes, calculation of a purge volume was adjusted by subtracting out the volume of tubing present in the sandpack from both the intermediate and lower tubing. Internal volume associated with a gas/water separator and flowmeters was added in calculation of the purge volume.

#### 2.4 Leak Testing of Above Ground Fittings

Leak testing of above ground fittings and a borehole are often combined. One method of combined leak testing fittings is to place “clean” towels or rags soaked with a liquid around above ground fittings and soil-gas probes (California Environmental Protection Agency 2012). Recommended liquid tracers include difluoroethane, alcohols (e.g., ethanol, isopropanol), solvents (e.g., hexane, pentane), and consumer products (e.g., butane in shaving foam) (California Environmental Protection Agency 2012).

The California Environmental Protection Agency (2012) states that if the leak detection compound is  $\geq 10 X$  the reporting limit for target analytes, then “corrective action” must be taken. The Missouri Department of Natural Resources (2013) stipulates sample rejection if the leak detection compound in sample results is  $> 100$  micrograms per liter ( $\mu\text{g/L}$ ). This procedure

was used in an US EPA investigation (US EPA 2009) where a cloth rag saturated with 1,1-difluoroethane was placed in a plastic bag over a probe.

There are a number of concerns with using liquid tracers for leak testing (DiGiulio 2007a, Canadian Council of Ministers of the Environment 2009) briefly summarized here. (1) There is a potential for cross-contamination when handling concentrated liquid solvents during soil-gas sampling. When collecting soil-gas samples to support a vapor intrusion investigation, soil-gas concentrations at the parts-per-billion-volume (ppbv) range are of concern. (2) Solvents may be flammable thereby posing a safety hazard during testing. (3) Detection of the vapor used for leak testing may result in elevated detection and reporting limits of target analytes. For instance, the vapor concentration of isopropanol at 25 °C is 143,000 µg/L. The concentration of isopropanol in a soil-gas sample at just 0.1% leakage would likely be significantly greater than concentrations of target analytes. (4) In the absence of previous soil-gas sampling or reliable background information, the tracer compound used for leak detection may be a target analyte. Also, if there is a desire to quantitate leakage using liquid tracers, the concentration of compounds or propellants such as pentane, propane, and butane in consumer products such as shaving cream foam are unknown.

If an enclosure is used during leak testing, the concentration of the leak detection in the enclosure must be determined using gas chromatography (GC) with a suitable detector or with gas chromatography-mass spectrometry (GC-MS). Otherwise, to calculate vapor concentration in the chamber, it must be assumed that the liquid solvent has not evaporated, sufficient time has elapsed since placement of the liquid solvent to assume liquid-vapor equilibration time, and there is no air exchange between the chamber and atmosphere. If these assumptions are valid, vapor concentration can be estimated from the product of vapor pressure (corrected for temperature) and the mole fraction of the compound in the solvent mixture. For these reasons outlined above, liquid solvents were not used for shut-in or leak testing in this investigation.

Liquid solvents may be useful for leak testing during soil-gas sampling in very low permeability soils. For instance, McAlary et al. (2009) applied a vacuum in soils and allowed vacuum dissipation to occur in the sandpack of vapor probes over hours or days during soil-gas sampling. They injected helium in a shroud over a short period of time relative to time of sampling and did not adjust estimates of leakage based on the ratio of time for leak testing and sampling. In this

instance, sensitivity of leak detection could have significantly improved through use of a liquid tracer over the entire sampling period.

A second method is to flood a shroud covering the sampling train and soil-gas probe with gas or air containing a gas tracer such as helium (American Petroleum Institute 2005, California Environmental Protection Agency 2012). A portable thermal conductivity detector (TCD) is used to measure helium from a gas sampling bag collected during soil gas sampling (American Petroleum Institute 2005). This method of leak testing of fittings was not used in this investigation because leakage in above ground fittings cannot be differentiated from leakage in a borehole. It could be argued that if helium is detected in a soil-gas sample, fittings could be tightened and the test conducted again to determine if fittings were partially or fully the causative factor of leakage. However, when separate leak testing is conducted for both above ground fittings and a borehole, a combined method of testing, while conservative, is redundant.

The most common method of leak testing above ground fittings is to apply vacuum or pressure to a closed sample train and monitor pressure differential with time. This procedure is commonly referred to as “shut-in testing.” The Alaska Department of Conservation (2012), California Environmental Protection Agency (2012) and the Canadian Council of Ministers of Environment (2009) recommend testing at a vacuum of 25 kilopascals (kPa) (100 inches water) with no observable vacuum loss over a period of at least one minute. The Wisconsin Department of Natural Resources (2012, 2014) recommends testing at a vacuum of 12.5-25 kPa (50-100 inches water) with no observable vacuum loss over a period of at least one minute. The American Society of Testing Materials (2012) recommends testing at a vacuum of 15 inches mercury or 50.7 kPa (203 inches water) with < 0.5 inches Hg or 1.7 kPa (7 inches water) vacuum loss. The California Environmental Protection Agency (2012) recommends using a calibrated gauge sensitive enough to detect pressure change of 0.1 kPa (0.5 inches water).

Using this method, leakage in fittings can easily be quantified using the Ideal Gas Law where:

$$Q_S^{STP} = \frac{V_S \Delta P T^S}{\Delta t P^S T} \quad (2)$$

$Q_S^{STP}$  = flow (SCCM) into sampling train at standard temperature and pressure (STP),

$V_S$  = internal volume of sample train components (cubic centimeters or  $\text{cm}^3$ ),

$\Delta P$  = change in pressure (P) over  $\Delta t$  (kPa),

$P^S$  = standard pressure (101.325 kPa),

T = temperature of gas in sample train (Kelvin or K),

$T^S$  = standard temperature (293.15 K),

$\Delta t$  = change in time (min).

The most commonly used standards for STP are those of the International Union of Pure and Applied Chemistry (IUPAC) and the National Institute of Standards and Technology (NIST). The IUPAC STP is 273.15 K (0 °C, 32°F) and 100.000 kPa. The NIST STP is 293.15 K (20°C, 68°F) and 101.325 kPa (14.696 psi, 1 atm). The NIST definition of STP was used throughout this document.

Guzman and Lohrstorfer (1994) used the Ideal Gas Law during shut-in testing to quantify leakage from straddle packers during gas permeability testing in fractured rock. The British Columbia Ministry of Environment (2011) recommends using the Ideal Gas Law to quantify leakage in fittings with acceptable leakage  $\leq 1\%$ .

Leakage through monitoring well plugs and the associated brass quick-connect fitting used in this investigation was determined by applying a vacuum in excess of 90 kPa induced by a peristaltic pump to a 0.91 m (3 foot) long section of 2.54 cm (1 inch) ID PVC pipe sealed on both ends with vapor well caps. Vacuum loss was measured at one well plug every second over a 34-hour period using a Sper Scientific manometer (resolution of 0.1 kPa) and a RS-232 cable connected to a laptop computer.

To test leakage in above ground fittings associated with the leak detection chamber and the soil-gas sampling train, a peristaltic pump was used to create vacuum in the sample train in excess of 90 kPa. Vacuum was then measured every second using a Sper Scientific manometer, recorded, and downloaded to a laptop computer (**Figure 12**).

To determine leakage as a function of applied vacuum, a stainless-steel toggle valve was used to allow atmospheric air to enter the sample train in discrete steps. Leakage into the sample train was then calculated when a drop of 0.1 kPa in vacuum occurred. However, routine application of this procedure proved to be too time consuming and was subsequently modified to include three

one-minute tests at high (e.g., 90 kPa), medium (e.g., 40 kPa), and low (e.g., 10 kPa) vacuum. A maximum (without tightening fittings) leakage rate of 1 standard cubic centimeter per minute (SCCM) was deemed acceptable. Leakage of 1 SCCM at a sample flow rate of 500 to 1000 SCCM is equivalent to 0.1 to 0.2% and hence inconsequential. When leakage exceeded 1 SCCM, fittings were disassembled and units individually tested to determine the point of leakage. This stringent criterion is appropriate since leakage in above ground fittings can be largely controlled in the field.



**Figure 12.** Photograph illustrating vacuum testing of fittings associated with leak detection chamber

## 2.5 Selection of Tracers for Leak Testing Boreholes

Helium is often used as a tracer for leak testing because of lack of toxicity, lack of flammability, negligible sorption to solids, non-reactivity (no degradation), high Henry's Law Constant, low cost, widespread availability, and ability to be monitored with a handheld thermal conductivity detector (TCD) (CCME 2009). Since helium is often used a carrier gas in a GC, there is no potential for interference during analysis of volatile organic compounds (VOCs) (Canadian Council of Ministers of Environment 2009). Portable TCDs respond primarily to helium and hydrogen ( $H_2$ ) in a gas stream because their thermal conductivities are significantly higher than other gases typically found in soil gas such as nitrogen ( $N_2$ ),  $O_2$ ,  $CO_2$ , and  $CH_4$ .

Use of pure phase helium for leak testing boreholes is recommended or explicitly required by the Hawaii Department of Health (2014), Michigan Department of Environmental Quality (2013), the Wisconsin Department of Natural Resources (2012, 2014), Alberta Environment (2007), Atlantic Partnership in Risk-Based Corrective Action (RBCA) Implementation (2006) and the Ontario Ministry of Environment (2007).

However, pure phase helium is a buoyant gas necessitating sufficient vacuum in a leakage pathway to overcome gas buoyancy. At low pressure differential (<50 kPa) where gas compressibility can be neglected, Darcy's Law can be used to estimate vacuum necessary to overcome buoyancy by:

$$\Delta P > \frac{\Delta \rho_g g H}{10^4} \quad (3)$$

$\Delta P$  = pressure differential or vacuum between sandpack and surface (Pa),

$\Delta \rho_g$  = difference in gas density between tracer mixture and soil gas ( $\text{g L}^{-1}$ ),

$g$  = gravitational constant  $980 \text{ cm s}^{-2}$ ,

$H$  = distance from the surface to sandpack (cm).

Given that total gas pressure is the sum of water vapor and dry gas pressure, gas density using the Ideal Gas Law can be calculated by:

$$\rho_g = \frac{1}{ZRT} \left[ M_w \frac{f}{100} e_s + \left( P_g - \frac{f}{100} e_s \right) \sum_{i=1}^n \chi_i M_i \right] \quad (4)$$

$\rho_g$  = gas density ( $\text{g L}^{-1}$ ),

$R$  = Ideal Gas constant ( $0.0821 \text{ L atm mol}^{-1} \text{ K}^{-1}$ ),

$T$  = temperature (K),

$f$  = relative humidity (%),

$e_s$  = saturated vapor pressure (atm) of water at reference temperature,

$M_w$  = molecular weight of water ( $18.02 \text{ g mol}^{-1}$ ),

$M_i$  = molecular weight of gas component ( $\text{g mol}^{-1}$ ),

$P_g$  = gas pressure (atm),

$\chi_i$  = mole fraction of gas component (-),

$Z$  = gas compressibility factor (-).

Saturated vapor pressure as a function of temperature can be estimated using the Antoine Equation:

$$\text{Log}_{10} P_w = A - \frac{B}{C + T} \quad (5)$$

$P_w$  = vapor pressure (mm Hg or torr),

$T$  = temperature ( $^{\circ}\text{C}$ ),

$A = 8.07131$ ,

$B = 1730.63$ ,

$C = 233.426$ .

For instance, the gas densities of pure phase helium and a soil-gas mixture containing 10%  $\text{O}_2$ , 65%  $\text{N}_2$  and 25%  $\text{CO}_2$  at  $20^{\circ}\text{C}$  and 100% relative humidity are 0.119 and 0.980 grams per liter (g/L), respectively – a factor of 8 difference or almost an order of magnitude. If a sandpack is 5 m below surface, a minimum vacuum of 42 Pa ( $\sim 0.2$  inches of water) is necessary to overcome buoyancy.

At flow rates typically used for soil-gas sampling and purging ( $< 1$  SLPM), this pressure differential is within the expected range for sandy soils and in less permeable soils when a leakage pathway to the surface is present. Insufficient vacuum in a leakage pathway will cause underestimation of leakage which will increase in magnitude with depth. This was demonstrated by Banikowski et al. (2009). They measured leakage at 22% and 0.2% using helium in an open borehole at depths of 4 feet and 8 feet. Leakage in an open borehole should be 100%. If pure phase helium is used for leak testing, attainment of a minimum calculated vacuum in the screened interval of a soil-gas probe is necessary to ensure overcoming buoyancy.

In this investigation, leak detection gas mixtures were formulated to avoid potential buoyancy effects. A chlorofluorocarbon, R-123, was selected as a tracer because of its non-reactivity, moderately high dimensionless Henry's Law Constant (1.4), low global warming potential of 90 ( $\text{CO}_2 = 1.0$ ), and low ozone depletion factor of 0.02. A 1% R-123, 99% argon gas mixture has a density at 20°C of 1.220 g/L thereby having a higher density than soil-gas composition under most conditions.

CO was selected for use as the second tracer because of the availability of portable gas analyzers to detect this gas and its high dimensionless Henry's Law Constant (43). Gas mixtures containing 18,000 ppmv CO in air and 10,100 ppmv R-123 in argon were purchased in 103 L gas cylinders from Air Liquide. A 1% CO, 99% air gas mixture has a density at 20°C of 0.856 g/L thereby having a density slightly less than soil-gas composition under most conditions. At Valley Center, a residential area, CO was used in 5-L Flex-Foil™ gas sampling bags for passive introduction into probes presenting no risk to residents or workers. Nevertheless, CO was monitored without detection in the workspace.

## 2.6 Methods for Leak Testing Boreholes

Leak testing of 2.54 cm (1 inch) diameter monitoring wells was conducted by extracting soil gas from wells while injecting a gas mixture containing a tracer at a flow rate 5 to 10 SLPM into a chamber surrounding the wellhead. Gas flow in the chamber was directed below ground surface inside the well cover. This ensured a maximum tracer concentration in the proximity of the well in the event of variable tracer concentration within the chamber due to a poor seal between the base of the chamber and ground surface and subsequent ventilation from the atmosphere. Tracer concentration was monitored at a flow rate of 1 SLPM using separate tubing at the same location as injection. Tracer injection continued until a maximum concentration or fluctuation around a maximum concentration was achieved. This method tested leakage at both the fitting attached to the PVC well at the surface and the borehole containing the PVC well.

Leak testing of three-probe clusters typically started with injection of R-123 into a chamber and extraction of soil-gas from the intermediate probe to determine leakage through quick-connect bodies used to seal the intermediate probe. Leakage from the surface to the uppermost probe and between the intermediate and uppermost probe was then evaluated by extracting soil gas from

the uppermost probe while simultaneously injecting a gas mixture containing R-123 into the well cover adjacent to the uppermost probe and passively introducing a gas mixture containing CO into the intermediate probe. Passive introduction of CO was accomplished by connecting a 5-liter Cali-Five Bond™ sample bag with a Leur-Lock™ fitting to the intermediate probe. CO entered the intermediate screened interval by advection if leakage from the upper interval incurred a vacuum in the intermediate interval.

R-123 concentration inside a chamber was measured at the point of injection. It was assumed that CO concentration in the intermediate interval was equivalent to sample bag concentration. Maximum CO concentration in the sample train was used to quantify leakage. Leakage between the intermediate and lower probe was evaluated by extracting soil gas from the lower probe while passively introducing CO into the intermediate probe or by extracting soil-gas from the intermediate probe while passively introducing CO in the lower probe.

This sequence of testing allowed determination of all relevant leak pathways. Purge testing was generally conducted prior to leak testing to avoid introduction of gas containing tracer into probes during leak testing. For instance, the CO mixture consisted of 2% CO and 98% air. Therefore, significant leakage from the intermediate probe to the shallow or deep probe would result in increasing O<sub>2</sub> concentrations during purging as a result of leak testing using a CO-air gas mixture rather than recharge from the atmosphere.

Calculations for leak detection are as follows. The concentration of a vapor or gas *i* in a soil-gas sample train from the uppermost probe as impacted by leakage from the surface enclosed by a chamber and by leakage from a lower intermediate probe can be described by:

$$V \frac{dC_s^i}{dt} = Q_{SG} C_{SG}^i + Q_C C_C^i + Q_I C_I^i - Q_T C_S^i \quad (6)$$

Where

*V* = internal volume of uppermost probe system (e.g., gas-filled porosity of the sandpack, tubing to the surface, tubing above surface, etc.) (cm<sup>3</sup>),

*C<sub>S</sub><sup>i</sup>* = concentration of a tracer *i* in sample train (ppmv)

$C_C^i$  = concentration of a tracer  $i$  in chamber (ppmv),

$C_I^i$  = concentration of a tracer  $i$  in intermediate probe (ppmv),

$C_{SG}^i$  = concentration of a tracer  $i$  in soil gas (ppmv),

$Q_{SG}$  = flow rate of soil gas into screened interval used for extraction ( $\text{cm}^3/\text{min}$ ),

$Q_C$  = flow rate from leakage in chamber ( $\text{cm}^3/\text{min}$ ),

$Q_I$  = flow rate from leakage at intermediate probe ( $\text{cm}^3/\text{min}$ ),

$Q_T$  = total flow rate into the sample train ( $Q_{SG} + Q_C + Q_I$ ) ( $\text{cm}^3/\text{min}$ ),

$t$  = time (min).

All parameters except the concentration of tracer  $i$  are assumed constant with time. If the initial concentration of tracer  $i$  in the sampling train at time zero is  $C_0$  in ppmv, then

$$C_S^i(t) = \left[ C_{SG}^i + \xi_C (C_C^i - C_{SG}^i) + \xi_I (C_I^i - C_{SG}^i) \right] (1 - e^{-PV}) + C_0 e^{-PV} \quad (7)$$

where:

$\xi_C = Q_C/Q_T$  (leakage coefficient from the chamber to the shallow probe),

$\xi_I = Q_I/Q_T$  (leakage coefficient between the upper probe and intermediate probe),

$PV = Q_T t/V$ .

PV is commonly referred to as purge volume. As time goes to infinity or steady-state conditions prevail

$$C_S^i - C_{SG}^i = (C_C^i - C_{SG}^i) \xi_C + (C_I^i - C_{SG}^i) \xi_I. \quad (8)$$

Similarly, for a tracer  $j$  introduced into the intermediate probe,

$$C_S^j - C_{SG}^j = (C_C^j - C_{SG}^j)\xi_C + (C_I^j - C_{SG}^j)\xi_I \quad (9)$$

where

$C_S^j$  = concentration of a tracer  $j$  in sample train (ppmv),

$C_C^j$  = concentration of a tracer  $j$  in chamber (ppmv),

$C_I^j$  = concentration of a tracer  $j$  in intermediate probe (ppmv),

$C_{SG}^j$  = concentration of a tracer  $j$  in soil gas (ppmv).

These two equations can then be solved to yield,

$$\xi_C = \frac{CD - AF}{CE - BF} \quad (10) \quad \xi_I = \frac{AE - BD}{CE - BF} \quad (11)$$

where:

$$A = C_S^i - C_{SG}^i \quad B = C_C^i - C_{SG}^i \quad C = C_I^i - C_{SG}^i$$

$$D = C_S^j - C_{SG}^j \quad E = C_C^j - C_{SG}^j \quad F = C_I^j - C_{SG}^j$$

If an experiment is designed to ensure that

$$C_{SG}^i = 0 \text{ (no tracer i in soil gas)}$$

$$C_{SG}^j = 0 \text{ (no tracer j in soil gas)}$$

$$C_I^i = 0 \text{ (no tracer i in intermediate interval)}$$

$$C_C^j = 0 \text{ (no tracer j in chamber)}$$

then

$$\xi_C = \frac{C_S^i}{C_C^i} \quad (12)$$

$$\xi_I = \frac{C_S^j}{C_I^j}. \quad (13)$$

Thus, for leak testing using a chamber, the leakage coefficient is simply the gas tracer concentration in the soil-gas sampling train divided by the gas tracer concentration in the chamber. For single probe configurations or for direct-push testing,  $\xi_I = 0$ , no simplifications are necessary and

$$\xi_C = \frac{C_S^i - C_{SG}^i}{C_C^i - C_{SG}^i}. \quad (14)$$

Thus, in this case, the initial concentration of tracer in soil-gas can be accounted for. However, it is preferable to select a gas tracer that does not occur naturally in soil gas. Similarly, when testing leakage from an intermediate probe to the deeper probe,  $L_C = 0$ , and

$$\xi_I = \frac{C_S^j - C_{SG}^j}{C_I^j - C_{SG}^j}. \quad (15)$$

Acceptable leakage varies from less than 1% (Health Canada 2007), less than 2% (British Columbia 2011), less than 5% (Electric Power Research Institute 2005, New Jersey Department of Environmental Protection 2005, Canadian Council of Ministers of Environment 2009), and less than 10% (New York Department of Health 2006).

## 2.7 Methods of Calibration and Flow Testing of Portable Gas Analyzers

An electrochemical cell with no stated influence from CO<sub>2</sub>, CO, H<sub>2</sub>S, SO<sub>2</sub>, or H<sub>2</sub> is used to measure O<sub>2</sub> in the GEM2000 Plus (LandTec 2007). Electrochemical sensors operate on a fuel-cell principle providing linear response between gas concentration and an electrical output (current or voltage) (Henderson 1999, Thompson and Goedert 2009).

A dual wavelength infrared cell with an absorption wavelength of 4.29 μm and a reference channel is used to measure CO<sub>2</sub> in the GEM2000 Plus (LandTec 2007). Chemical bonds absorb infrared energy and vibrate at precise frequencies enabling identification of gases or vapors

(Henderson 1999). Since this wavelength is specific to CO<sub>2</sub>, response is not impacted by the presence of other gases (LandTec 2007).

A dual wavelength infrared cell with reference channel is used for measurement of CH<sub>4</sub> in the GEM2000 Plus. The absorption wavelength used (3.41 μm) responds non-linearly to hydrocarbons other than CH<sub>4</sub> (LandTec 2007). Interference from other hydrocarbons can be minimized or eliminated by using a granular activated carbon (GAC) trap upstream of measurement and qualitatively tested by comparing instrument response during bypass of the GAC trap (Jewell and Wilson 2011).

Removal of individual hydrocarbons by a GAC trap can also be tested by “flashing” a liquid standard containing compounds butane and higher molecular weight in a closed vessel with subsequent displacement of a gas through a GAC trap to a portable gas analyzer (Jewell and Wilson 2011). Retention of gases, ethane, and propane, are not evaluated using this technique necessitating use of gas standards if the presence of these light hydrocarbons is suspected as would be the case in a stray gas investigation. A GAC trap was not used to monitor CH<sub>4</sub> using the GEM2000 Plus in this investigation because there was no instrument response to CH<sub>4</sub> during soil-gas purging except at a vapor probe less than 1 meter from a natural gas domestic pipeline leak at the latter location. Instrument response at this location was assumed to be primarily from CH<sub>4</sub> but was likely affected by ethane and propane.

Electrochemical cells are used for measurement of CO and H<sub>2</sub>S in the GEM2000 Plus (LandTec 2007). In the absence of “compensation”, electrochemical cells which measure CO are susceptible to cross-gas interference from hydrogen and H<sub>2</sub>S resulting in a biased high reading for CO if these gases are present (LandTec 2007). In the GEM2000 Plus, a “hydrogen compensated” CO cell is used to counteract the interference by H<sub>2</sub> (LandTec 2007). Interference from H<sub>2</sub>S is achieved through the use of an internal filter (LandTec 2007). The integrity of the filter can be tested by measurement of CO from a gas standard containing H<sub>2</sub>S but not CO, with detection indicating sensor malfunction and need for replacement (LandTec 2007). In this investigation, CO was not detected during calibration and calibration check testing (bump testing) with H<sub>2</sub>S indicating full functioning of the H<sub>2</sub>S filter.

An infrared sensor is used in the H25-IR for measurement of R-123. Information on absorption wavelength and potential inference from other gases was not provided in the user's manual (Bacharach 2006).

FID response is produced by destructive ionization of hydrocarbons in a hydrogen flame with subsequent capture of ions at a collector electrode with a polarizing voltage (Thermo Electron Corp 2003). Migration of ions produces a current directly proportional to hydrocarbon concentration which is amplified and sent to a microprocessor and/or analog readout device producing a linear response over a wide range (Thermo Electron Corp 2003).

Low O<sub>2</sub> (<16%) levels in the gas stream cause biased high readings prior to extinguishing of the flame (Thermo Electron Corp 2003). FID response is very sensitive to CH<sub>4</sub> and not affected by CO<sub>2</sub> concentration and water vapor (Thermo Electron Corp 2003). The primary disadvantage of a FID is that hydrogen must be transported, usually by land, to the field to recharge the pressurized cylinder containing hydrogen for flame combustion. In this investigation, we transported a hydrogen cylinder to the field via work vehicles.

PID response is produced by non-destructive ionization of hydrocarbons by an ultraviolet lamp of a specific energy (electron volts). Ions are attracted to a collecting electrode, producing a current proportional to the concentration of the compound (Thermo Electron Corp 2003). Detection is dependent on lamp energy. The standard lamp in the TVA-1000B, and used in this investigation, is 10.6 electron volts. PIDs are generally more sensitive than FIDs to aromatic hydrocarbons such as benzene, toluene, and xylenes (Nyquist et al. 1990). A PID can also detect some inorganic or organic compounds that the FID cannot (e.g., ammonia, carbon disulfide, carbon tetrachloride, chloroform, ethylamine, formaldehyde, and hydrogen sulfide) (Thermo Electron Corp 2003).

Although methane cannot be ionized by a PID, methane and other alkanes absorb UV light. Senum (1981) observed a significant reduction in PID response when methane was used as a carrier gas for a PID. Nyquist et al. (1990) noted an exponential decrease in PID response with increasing methane gas concentration. PID response decreased by 30% and 90% at methane concentrations of 0.5% and 5%, respectively.

Factors negatively impacting PID response are multiplicative (product of response factors) (Robbins et al. 1990a, b). PID response can be reduced up to 99% by the combined presence of water vapor (relative humidity), CO<sub>2</sub>, and alkanes (including CH<sub>4</sub>) (Robbins et al. 1990a, b). Robbins et al. (1990a, b) developed a serial dilution method where equal amounts of gas in a sample bag were removed and replaced with dry uncontaminated gas resulting in a log-linear concentration-dilution increment relationship (Robbins et al. 1990a, b).

In this investigation, Nafion™ tubing was used in the sample train to reduce relative humidity. However, relative humidity was not measured in the sample train. To address potential interference from relative humidity, CO<sub>2</sub> and hydrocarbons, the sample train was equipped with inlet valves to introduce dry compressed air or atmospheric air to dilute soil gas prior to measurement. Using this method, “true” concentration can be determined from simple linear dilution calculations. Since there was no PID response during soil-gas sampling, this method was not used during this investigation.

The GEM2000 Plus, H25-IR, and TVA-1000B were calibrated and operated in accordance with standard operating procedures developed at US EPA’s research laboratory in Ada, Oklahoma including RSKSOP-314v1, RSKSOP-313v1, and RSKSOP-320v0. Portable gas analyzers were calibrated at the beginning of each workday using a gas standard. Calibration was then bump tested prior to leak and purge testing using concentrations of calibration and at one or two other concentrations not used for calibration. Measurement at concentrations other than that used for calibration was conducted to determine whether or not accuracy and precision decreased during bump testing using concentrations not used for calibration.

If measured concentrations exceeded quality control (QC) criteria in **Table 1** at any standard concentration utilized, instruments were immediately re-calibrated at a standard concentration and checked again using the calibration concentration and one or two additional concentrations. Stipulation of QC criteria was based on the manufacturer’s recommendations. The QC criteria for CO<sub>2</sub> and CH<sub>4</sub> measurement using the GEM2000 Plus are a function of absolute gas concentration, while the QC criteria for the Thermo Scientific TVA-1000B are a function of both absolute concentration (below 10 ppmv) and percent response for the FID and percent response only for the PID (**Table 1**).

**Table 1. Portable gas analyzer calibration and check standard requirements**

| Analyte          | Instrument                  | Sensor | T90  | Range             | Resolution | Calibration Standard                                   | Check Standards                     | QC Criteria   |
|------------------|-----------------------------|--------|------|-------------------|------------|--|-------------------------------------|---|
| O <sub>2</sub>   | LandTec GEM2000 Plus        | EC     | <20s | 0 - 21%           | 0.1%       | 4.0%, 10.0%, 20.9%                                     | 4.0%, 10.0%, 20.9%                  | ± 1.0% (0 - 21%)  |
| CO <sub>2</sub>  | LandTec GEM2000 Plus        | IR     | <20s | 0 - 100%          | 0.1%       | 5.0%, 20.0%, 35.0%                                     | 0.25%, 20.0%, 5.0%, 35.0%           | ± 0.3% (0 - <5.0%)<br>± 1.0% (5.0 - <15%)<br>± 3.0% (15 - 60%)  |
| CH <sub>4</sub>  | LandTec GEM2000 Plus        | IR     | <20s | 0 - 100%          | 0.1%       | 2.5%, 50.0%  | 2.5%, 50.0%                         | ± 0.3% (0 - <5.0%)<br>± 1.0% (5.0 - <15%)<br>± 3.0% (15 - 100%) |
| CO               | LandTec GEM2000 Plus        | EC     | <60s | 0 – 2000 ppmv     | 1 ppmv     | 504, 1000 ppmv   | 504, 1000 ppmv                      | 90 - 110%   |
| H <sub>2</sub> S | LandTec GEM 2000 Plus       | EC     | <60s | 0 - 200 ppmv      | 1 ppmv     | 25, 100 ppmv   | 25, 100 ppmv                        | 90 - 110%   |
| VOCs             | Thermo Scientific TVA-1000B | FID    | <5s  | 1.0 - 10,000 ppmv | 1 ppmv     | 10, 100, 1000, ppmv CH <sub>4</sub>                    | 10, 100, 1000, ppmv CH <sub>4</sub> | ± 2.5 ppmv ≤ 10 ppmv, 90 - 110% otherwise                       |
| VOCs             | Thermo Scientific TVA-1000B | PID    | <5s  | 0.5 - 500 ppmv    | 1 ppmv     | 050, 100 ppmv Isobutylene                              | 50, 100 ppmv Isobutylene            | 80 - 120%   |
| R-123            | Bacharach H25-IR            | IR     | <1s  | 0 – 10,000 ppmv   | 1 ppmv     | Internal source (25.3 ppmv)<br>200, 1000 ppmv external | 200, 1000 ppmv                      | 90 - 110%   |

T90 = time to 90% response

Gas standards were introduced into 5-liter Flex Foil™ bags using Tygon tubing from pressurized canisters and then subsequently drawn into portable gas analyzers by internal pumps. Calibration and check standard gases for measurement of O<sub>2</sub>, CO<sub>2</sub>, and CH<sub>4</sub> for the GEM2000 Plus were obtained from LandTec, 850 S. Via Lata, Suite 112, Colton, CA 92324, James Welding Supply, P. O. Box 360 Pauls Valley, OK 73075, and Ideal Gases Inc. 14056 Fort St. Southgate, MI 48195. Calibration and check standard gas for CO were obtained from James Welding Supply and LandTec. CO used for leak testing was obtained from Air Liquide, 6141 Easton Road Building #1, Plumbsteadville, PA 18949.

Calibration and check standard gases for H<sub>2</sub>S for the GEM2000 Plus were obtained from Landtec and James Welding Supply. Leak testing, calibration, and check standard gas for 2,2 dichloro-1,1,1-trifluoroethane (R-123) were obtained from Scotty Specialty Gas. Calibration and

check standard gases for TVA-1000B FID and PID were obtained from Scotty Specialty Gas. Ultra-high purity nitrogen used for zero gas and equipment blanks was obtained from James Supply.

Statistical analysis of data sets for bump testing were conducted to evaluate positive or negative bias in measured values compared to known gas concentrations in gas standards. The Shapiro-Wilk Test was used to evaluate rejection of the null hypothesis of a normally distributed measured data set at a p-value of 0.05. For normally distributed data, a Student t-test was used to calculate p-values for rejection of the null hypothesis that the mean of measured values was equal to, less than, or greater than the known gas concentration in a gas standard. One-tailed tests were used when the calculated mean of measured values was less than or greater than the known gas concentration in a gas standard. When the null hypothesis for a normal distribution was rejected, the nonparametric Wilcoxon Signed Rank Test was used to calculate p-values for rejection of the null hypothesis that the median of measured values was equal to, less than, or greater than the known gas concentration in a gas standard. One-tailed tests were used when the calculated median of measured values was less than or greater than the known gas concentration in a gas standard.

To evaluate the potential effect of flow rate on measured concentration, 5-liter Flex Foil™ bags were filled with a gas standard and introduced into portable gas analyzers using Tygon tubing and a high precision Gilmont Flowmeter using the instrument's internal pump. When an apparent effect was observed, response was fitted to a linear relationship.

To compare O<sub>2</sub>, CO<sub>2</sub>, and CH<sub>4</sub> concentrations measured with the GEM2000 Plus during purging with fixed-laboratory samples, samples were collected in 0.5 liter Cali-5 Bond™ gas sampling bags equipped with a Leur-Fit Valve™. Aelion et al. (1996) reported poor correlation of measurement of O<sub>2</sub> using a portable gas analyzer with fixed laboratory analysis. Gas sampling bags were sent to Isotech Laboratories in Champaign, IL for analysis. All samples were analyzed for fixed gases (Ar, He, H<sub>2</sub>, O<sub>2</sub>, N<sub>2</sub>, CO<sub>2</sub>) and light hydrocarbons using gas chromatography and a combination of TCD and FID detectors based upon ASTM D1945-03 with stated accuracy within +/-15% of values in certified gas standards. Precision for duplicate analysis as measured by Relative Percent Difference (RPD) was defined by:

$$RPD = \frac{2(a-b)}{a+b} 100 \quad (16)$$

where a = sample analysis and b = duplicate analysis. Four duplicate samples were collected at 17 sample locations (approximately 1 in 4 duplicate to sample frequency).

Seven travel and 8 equipment blanks (approximately 1 to 1 frequency of blank to sample frequency) were collected using ultra high purity N<sub>2</sub> gas with the former collected in gas sampling bags only and the latter passing through the sample train prior to collection in gas sampling bags. Blanks were utilized to determine potential interference in fixed gas and hydrocarbon determination. Full data packages were provided by Isotech Laboratories for all sample analyses.

## 2.8 Collection of Equipment Blanks

Equipment blanks for Cali-Five Bond Sample bags were collected in addition to equipment blanks for the entire sample and purge train using ultra-pure nitrogen gas. Also prior to purging, atmospheric air was circulated through the sample train (atmospheric air blank) and O<sub>2</sub>, CO<sub>2</sub> and CH<sub>4</sub> and tracer concentrations were measured to ensure that the GEM2000 Plus portable gas analyzer was working properly and that tracer bleed off (diffusion of tracer off tubing from previous testing) was not occurring.

## 2.9 Methods of Gas Permeability Testing

Gas permeability testing is routinely performed to support gas-based subsurface remediation such as soil vapor extraction (SVE) and bioventing (DiGiulio and Varadhan 2001a). Guidelines for gas permeability testing for SVE and bioventing are provided by US EPA (DiGiulio and Varadhan 2001a) and the U.S. Army Corps of Engineers (USACE 2002). Radial and vertical components of gas permeability are determined by extracting or injecting gas from or into a SVE or bioventing well with vacuum or pressure monitoring in nearby multiple probe clusters with examples provided by Cho and DiGiulio (1992), DiGiulio and Varadhan (2000, 2001a) and USACE (2002). Gas permeability testing has also been conducted on sub-slab media to support assessment of vapor intrusion (DiGiulio et al. 2006a).

Steady-state, axisymmetric analytical solutions to solve the inverse (gas permeability estimation) and forward (gas flow simulation) problems have been developed for a line source/sink term with a domain open to the atmosphere (Shan et al. 1992), for a finite-radius well with a domain open to the atmosphere (Baehr and Hult 1991, Perina and Lee 2005) and for a finite-radius well with a domain separated from the atmosphere by a layer of lower permeability (Baehr and Joss 1995).

Transient, axisymmetric solutions have been developed for a line source/sink open to atmosphere (Falta 1996) for both a line source/sink and finite-radius (to incorporate borehole storage) well both open to the atmosphere and separated from the atmosphere by a layer of lower permeability (DiGiulio and Varadhan 2001a). User-friendly Fortran-based programs have been developed to solve partial differential equations associated with estimating radial and vertical components of gas permeability and the vertical component of gas permeability of the layer of lower permeability (Falta 1996, Joss and Baehr 1997, DiGiulio and Varadhan 2001a). User-friendly Fortran-based programs have also been developed to simulate gas flow, streamlines, and travel time (particle tracking) from one or more wells (DiGiulio and Varadhan 2001a).

Gas permeability testing during soil-gas sampling is necessary to evaluate subsurface gas flow patterns and associated travel times during purging and sampling. This is especially important when a soil-gas probe is located close to the surface resulting in a potential negative bias in sample results due to atmospheric recharge. While soil-gas sampling near the surface ( $< 1$  m) is discouraged during vapor intrusion investigations, soil-gas sampling near the surface is common during stray gas investigations. Gas flow modeling could also be conducted to determine the volume of soil around a soil-gas probe impacted by purging and sampling. Cumulative gas extraction volumes could be decreased or increased depending on whether it is desirable to know soil-gas concentration directly outside a soil-gas probe or whether it is desirable to know an integrated concentration over a larger volume of soil at some distance from the soil-gas probe.

In contrast to gas permeability testing for SVE and bioventing design, gas permeability testing in soil-gas probes involves gas flow and vacuum or pressure measurement in the same probe. Thus, isotropic conditions (at least for permeability estimation) must be assumed and only radial permeability can be estimated. While it is conceivable that vacuum or pressure could be detected in an overlying or underlying probe in a soil-gas probe cluster enabling estimation of the vertical

component of gas permeability, flow rates typical of soil gas sampling (0.2 – 1.0 SLPM) are usually too low to generate a sufficient vacuum or pressure for testing.

The California Environmental Protection Agency (2011), in a document to support evaluation of vapor intrusion, is the only State agency that provides guidance on gas permeability testing during soil-gas sampling. The California Environmental Protection Agency (2011) recommends the use of a modified equation originally developed to evaluate steady-state gas flow within a prolate-spheroidal domain (Bassett et al. 1994):

$$k_r = Q_s \frac{\mu \ln(L/r_w) TP_s Z}{\pi L (\phi - \phi_{atm}) T_s} \quad (17)$$

$k_r$  = gas permeability ( $m^2$ ),

$Q_s$  = volumetric gas flow at standard conditions ( $m^3 s^{-1}$ ),

$\mu$  = dynamic viscosity of gas at standard conditions (1.81E-05 Pa-s for air),

$L$  = length of screen or sandpack (m),

$r_w$  = radius of borehole (m),

$T$  = temperature of gas stream (K),

$T_s$  = standard temperature (273 K),

$P_s$  = air pressure at standard conditions (1.01E+05 Pa),

$Z$  = gas compressibility factor (-), assume 1.0,

$\phi$  = gas pressure squared at well screen or sandpack ( $Pa^2$ ),

$\phi_{atm}$  = ambient or atmospheric gas pressure squared ( $Pa^2$ ).

Use of this equation requires that  $L/r_w > 5$  (Bassett et al. 1994).

Dynamic gas viscosity (gas viscosity) varies with gas composition and temperature. Gas viscosity for air, and gas mixtures containing O<sub>2</sub>, N<sub>2</sub>, and CO<sub>2</sub> were estimated using mole fractions and a “Gas Viscosity Calculator” from LMNO Engineering, Research, and Software,

Ltd. accessed at <http://www.lmnoeng.com/Flow/GasViscosity.php>. Even in a gas mixture enriched with CO<sub>2</sub> (e.g., 35% CO<sub>2</sub> and 65% N<sub>2</sub>) (**Figure 13**) there is only an 11% difference compared to the viscosity of air.

This equation is identical to the pseudo-steady-state radial flow equation used by Johnson et al. (1990) for gas permeability estimation but avoids selection of an arbitrary “radius of influence” (ROI) at some distance from the soil gas probe (Bassett et al. 1994). In the pseudo-steady-state radial flow equation, the ROI is specified in the numerator of the natural logarithm and denotes an atmospheric or some other selected pressure boundary at the ROI. Use of the pseudo-steady-state radial flow equation and arbitrary selection of ROI values for SVE and bioventing design lead to poor design and monitoring practices for SVE and bioventing and hence its use has been discouraged (DiGiulio and Varadhan 2001b). British Columbia (2011) recommends use of the pseudo-steady-state radial flow equation, stating that as a rule of thumb, the ROI may be approximated by the depth of the probe. Due to the arbitrary nature of ROI selection, the pseudo-steady-state radial flow equation was not used for gas permeability estimation in this investigation.

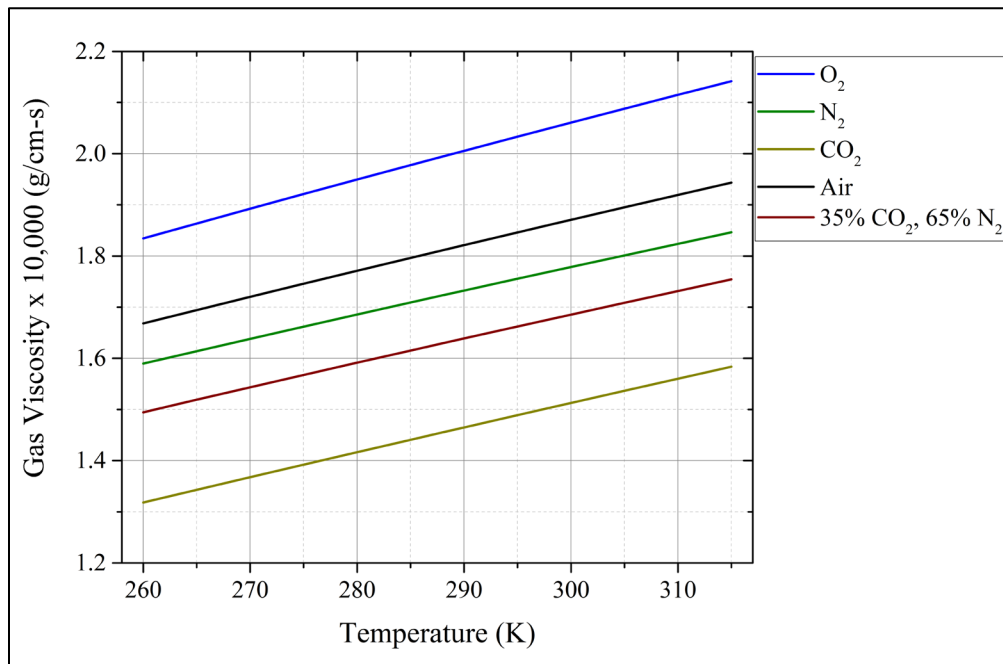


**Figure 13.** Estimated gas viscosity of O<sub>2</sub>, N<sub>2</sub> CO<sub>2</sub> and Air from Gas Viscosity Calculator from LMNO Engineering, Research, and Software, Ltd

For small length screened intervals compared to depth (criterion not specified), British Columbia (2011) also recommends the use of a spherical equation developed by Garbesi et al. (1996). However, if the length of monitoring wells and soil-gas wells extend over a significant portion of the modeled domain, it is inappropriate to assume a spherical domain. Thus, the spherical equation was not used in this investigation.

Since there is only one vacuum or pressure measurement and the vertical component of gas permeability cannot be determined, radial permeability estimation using an axisymmetric solution may be similar to that using the modified prolate-spheroidal equation enabling estimation of radial permeability using a simple algebraic equation. A comparison of radial permeability estimation using the modified prolate-spheroidal equation and the axisymmetric finite-radius equation with a domain separated from the atmosphere by a lower permeability layer was evaluated in this investigation to determine whether boundary effects associated with the latter solution significantly affect this comparison.

Use of equations for single-interval gas permeability testing requires measurement or estimation of vacuum or pressure at the sandpack or screened interval, not at surface, because of frictional headloss associated with gas flow in tubing. In recommending use of the modified prolate-spheroidal equation for gas permeability testing during soil-gas sampling, the California Environmental Protection Agency (2011) did not discuss vacuum or pressure loss in tubing or fittings during gas flow. Failure to incorporate vacuum or pressure loss from tubing will result in underestimation of radial gas permeability – the degree of which increases with increasing vacuum or pressure loss.

Vacuum or pressure loss due to friction can be determined experimentally or estimated using theoretically-based equations (Joss and Baehar 1997). Experimental determination requires that the entire soil-gas sampling train be laid out at the surface with vacuum or pressure measurement at the point of gas exit (atmospheric pressure assumed at the gas entry point for vacuum application) at flow rates to be used during soil-gas sampling. Determination of vacuum or pressure loss then is valid only for a specific configuration, length of tubing, and flow rate. This type of testing is impractical when various lengths of tubing and flow rates are to be used during sampling. In this investigation, a combined experimental and theoretical approach was used.

Since stainless-steel fittings and tubing associated with leak testing at the surface remained the same during soil-gas sampling and fittings and bends are less amenable to theoretical analysis compared to straight sections of tubing and pipe, vacuum loss in surface fittings as a function of flow rate was measured and fit to a nonlinear function. This function was then used to estimate vacuum loss associated with surface fittings at various flow rates used throughout this investigation.

Theoretical calculations modified by Joss and Baehr (1997) were used to estimate vacuum loss as a function of flow rate associated with straight sections of pipe and tubing. Vacuum or pressure loss can be expressed by:

$$\phi = \phi_1 \pm \left[ \frac{Cf/D}{C/\bar{\phi}-1} \right] y \quad (18)$$

$\pm$  = negative for gas extraction, positive for gas injection,

$\phi$  = pressure squared at screen or sandpack  $(\text{g cm}^{-1} \text{s}^{-2})^2$ ,

$\phi_1$  = pressure squared at the point of temperature and pressure measurement  $(\text{g/cm-s}^2)^2$ ,

$y$  = coordinate along the length of the tube or pipe (cm),

$f$  = friction factor (-),

$D$  = internal diameter of the tube or pipe (cm)

and

$$\bar{\phi} = \phi_1 \pm \frac{Cf\bar{y}}{D} \quad (19)$$

$\pm$  = positive for gas extraction, negative for gas injection,

$\bar{y}$  = half-length of tubing or a pipe (cm)

and

$$C = (v_1 \rho_1)^2 \frac{RT}{\omega} \quad (20)$$

$\rho_1$  = density of a gas at the point of temperature and pressure measurement  $(\text{g/cm}^3)$ ,

$v_1$  = velocity of a gas at the point of temperature and pressure measurement (cm/s),

$\omega$  = molecular weight of gas (g/mol),

R = Ideal Gas Law Constant ( $8.314E+07$  g cm<sup>2</sup> s<sup>-2</sup> mol<sup>-1</sup> K<sup>-1</sup>),

T = temperature of gas stream (K).

Similar to density calculations, the molecular weight of the gas is that of a multicomponent mixture including water vapor which was assumed at 100% relative humidity. Gas velocity was determined by dividing the actual flow rate ( $Q_A$ ) by the cross-sectional area of a pipe or tubing

$$v_1 = \frac{4Q_A}{\pi D^2} \quad (21)$$

The actual flow rate was calculated from the standard flow rate using the Ideal Gas Law by

$$Q_A = Q_S \frac{P_S T_A}{P_A T_S} \quad (22)$$

Estimation of a friction factor requires classification of flow as laminar, transitional, or turbulent.

The flow condition is defined by the non-dimensional Reynolds number (Re):

$$Re = \frac{\rho v_1 D}{\mu} \quad (23)$$

$\mu$  = dynamic gas viscosity (g cm<sup>-1</sup> s<sup>-1</sup>).

Component and temperature corrected viscosities of soil gas were used for calculation of Reynolds numbers. On the basis of the Reynolds number, the following flow conditions can be identified (Joss and Baehr 1997):

$0 \leq Re \leq 2,000$       laminar,

$2,000 < Re < 4,000$       transitional,

$4,000 \leq Re$       turbulent.

Under transitional and turbulent conditions, the friction factor is influenced by surface protrusions or wall roughness in addition to the Reynolds number. For laminar flow in a smooth tube or pipe with a circular cross section,  $f$  can be estimated using Hagen-Poiseuille equations by (Joss and Baehr 1997):

$$f = \frac{64}{\text{Re}} \quad (24)$$

During gas permeability measurement vacuum or pressure loss due to friction should be minimized to decrease potential error associated with estimation of gas permeability. The potential for error will be greatest when vacuum or pressure loss due to friction is similar to or greater than vacuum or pressure generated as a result of gas flow in soil. In addition to estimating vacuum loss due to tubing and pipe used in this investigation at various depths and flow rates, theoretical equations were used to gain insight into vacuum or pressure loss for tubing and pipe of various diameters and lengths typically used for soil-gas sampling.

Steady-state radial gas permeability estimates using the modified prolate-spheroidal equation and the analytical solution for axisymmetric flow for a finite-radius well with a domain separated from the atmosphere by a layer of lower permeability (Baehr and Joss 1995) were compared using a Fortran-based program provided in DiGiulio and Varadhan (2001a). In this program, mass gas flow is required which can be calculated using the Ideal Gas Law as:

$$Q_m = \frac{Q_s P_s M_g}{RT_s} \quad (25)$$

$Q_m$  = mass flow (g/min),

$Q_s$  = standard volumetric flow (SLPM),

$M_g$  = molecular weight of gas (g/mol),

$R$  = Ideal Gas Constant (0.0821 L atm mol<sup>-1</sup> K<sup>-1</sup>),

$T_s$  = standard temperature (273K),

$P_s$  = 1.0000 atm.

In this investigation, only extraction was used for gas permeability testing since gas injection would induce a compositional change in soil-gas. However, if soil-gas sampling is infeasible because a narrowly screened soil-gas probe is located directly above the water table and water upwelling into the probe occurs during gas extraction, gas permeability estimation using gas injection may be desirable.

Transient gas permeability testing was conducted at 2 locations using a finite-radius, axisymmetric solution incorporating borehole storage (DiGiulio and Varadhan 2001a). To fit observed vacuum as a function of time at a constant mass flow rate data, a Fortran-based program provided by DiGiulio and Varadhan (2001a) was used to fit radial permeability, vertical permeability, gas-filled porosity, and borehole storage. Borehole storage estimates were bound by estimates of gas-filled porosity in sandpacks between 10% to 40%.

#### 2.10 Methods of Purge Testing

During installation of vapor probes, tubing and other construction materials used for probe construction have direct contact with ambient air. Thus, the distribution of gases and vapors inside the tubing initially reflect atmospheric levels. Also, the process of borehole creation substantially decreases vapor concentration inside the open borehole and likely some radial distance in soil outside the borehole. Borehole installation methods which involve air injection, such as air rotary, would be expected to impact vapor concentrations a significant distance from a borehole. Direct-push sampling methods such as the Geoprobe PRT system likely result in the least disturbance.

Vapor diffusion modeling can be conducted to estimate a time period after probe installation for attainment of near equilibrium gas or vapor concentration at the probe. Concentration rebound would be a function of the chemical properties of a volatile organic compound (Henry's Law constant, organic carbon - water partition coefficient, aqueous diffusion coefficient, air diffusion coefficient), material properties of sub-surface media (water content, porosity, bulk density, and organic carbon content), and temperature. The diffusion path length would be a function of how long a borehole was left open and whether air injection occurred during borehole installation.

Wong et al. (2003) simulated equilibration time after soil-gas probe installation using an analytical solution for conservative (no soil-water or air-water partitioning) gas diffusion in an

isotropic homogeneous media having a gas-filled porosity of 0.281 within a symmetrical cylindrical geometry. The initial condition consisted of zero concentration from the center of the borehole to a radial distance of 7.62 cm (3 inch) and a boundary condition of constant concentration. Near (80%) steady-state concentration was achieved within 10 hours.

Attainment of vapor equilibration could be evaluated by collecting discrete samples over time. However, the process of active sample collection draws soil gas to a borehole thereby perturbing the system being monitored - in this case, increasing concentration in the sandpack and in the vicinity of the borehole. Thus, this procedure would likely underestimate equilibration time to some unknown degree. Also, a stable concentration or concentration range must be selected in the context of natural temporal variability.

Schumacher et al. (2016) estimated equilibration time from 0.32 cm (1/8") OD Nylaflow semi-permanent probes, the PRT system, and "micro-purge" direct-push probes consisting of 0.10 cm OD stainless-steel tubing. Near equilibration (80-90% of maximum level) of TCE was achieved with 24-48 hours for semi-permanent probes and within 2 hours (70% achieved within 30 minutes) for the PRT and min-purge systems.

A fundamental question is whether soil-gas probes can be "developed" or purged to more quickly achieve equilibrated concentrations. In this approach, a soil-gas probe is purged until primary (VOC concentrations) or secondary parameters (e.g., O<sub>2</sub>, CO<sub>2</sub>, CH<sub>4</sub>, FID, PID concentrations) "stabilize." There are few stipulated guidelines for attainment of stabilization. British Columbia (2011) recommends purging until readings are within 10% of each other. In an audit conducted for the Environmental Protection Authority in Victoria, Australia (US EPA Victoria 2007), stabilization using a GEM Portable Gas Analyzer was defined as attainment of  $\pm 0.1\%$  of O<sub>2</sub>, CO<sub>2</sub>, and CH<sub>4</sub> during consecutive measurements. The latter stabilization was used for this investigation since it is more stringent than the former (e.g. 10% of a 20% gas reading is  $\pm 2.0\%$ )

During soil-gas sampling, mass removed in the vicinity of a probe is replaced by mass drawn in by gas advection from surrounding soil and by partitioning from soil to water and water to air. If vapor nonequilibrium exists, vapor concentration will increase with gas extraction volume as less contaminated disturbed soil gas is replaced by more contaminated less disturbed soil gas.

Subsequent purging efforts then should result in achievement of steady-state concentrations at lower purge volumes.

When evaluating the potential impact of excessive purging, concentration reduction during gas extraction will not occur until significant mass removal occurs at and above a probe as relatively clean atmospheric air replaces contaminated soil gas or when rate-limited mass exchange occurs due to high pore-gas velocities. Thus, attainment of a near constant concentration during purging ensures attainment of equilibrium and the absence of excessive purging.

### 3.0 RESULTS and DISCUSSION

#### 3.1 Testing of Continuing Calibration Checks (Bump Testing) on Portable Gas Analyzers

##### 3.1a Bump Test Results for Oxygen (O<sub>2</sub>)

Results of O<sub>2</sub> measurement using the GEM2000 Plus portable gas analyzer and associated deviation from gas standards during continuing calibration tests (i.e. bump test) are illustrated in **Figures 14a, b**, respectively, and **Table 2**.

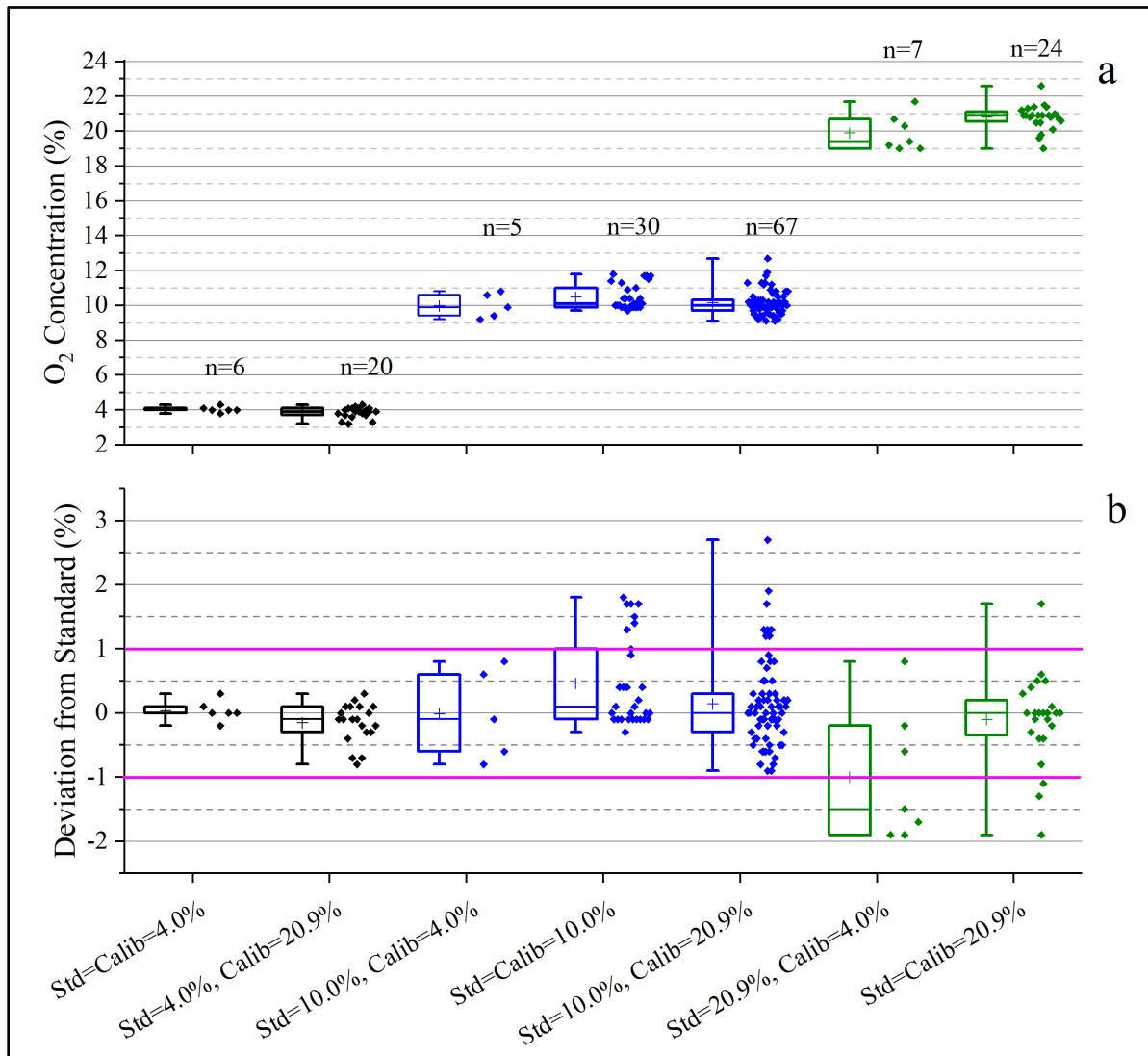


**Figure 14.** Results of bump tests for oxygen (O<sub>2</sub>) using a Landtec GEM2000 Plus portable gas analyzer. (a) Measurement of gas standards (Std) at calibration (Calib) concentrations in 5-L Flex Foil™ gas sampling bags. (b) Deviation from standard concentrations with stipulated quality control criteria ( $\pm 1\%$  of standard) illustrated with magenta lines. Quartiles, median (line), mean (+), minimum (whisker), and maximum (whisker) values illustrated in box plots with values to right of box plots.

**Table 2.** Summary of bump test results, frequency of attainment of manufacturer’s quality control criteria, statistical analysis of bias. Significant deviations are highlighted in bold.

| Standard Concentration   | Calibration Concentration | Quality Control Criteria | Frequency Outside Quality Control Criterion | Reject Null Hypothesis for Normal Distribution | Range                 | Mean         | Median     | p-Value | Reject Null Hypothesis for Mean or Median |
|--|---------------------------|--------------------------|---|--|-----------------------|--------------|------------|---------|---|
| <b>Oxygen (O<sub>2</sub>) using GEM 2000 Plus</b>                        |                           |                          |   |  |                       |              |            |         |   |
| 4.0%   | 4.0%                      | ±1.0%                    | 0/6 (0%)                                    | No   | 2.8%-4.3%             | 4.0%         | 4.0%       | 0.6383  | No  |
| 4.0%   | 20.9%                     | ±1.0%                    | 0/20 (0%)                                   | No   | 3.2%-4.3%             | 3.8%         | 3.9%       | 0.0098  | Yes                                       |
| 10.0%  | 4.0%                      | ±1.0%                    | 0/5 (0%)                                    | No   | 9.2%-10.7%            | 10.0%        | 9.9%       | 0.5000  | No  |
| 10.0%  | 10.0%                     | ±1.0%                    | <b>7/30 (23%)</b>                           | Yes  | 9.7%-11.8%            | 10.5%        | 10.1%      | 0.0005  | Yes                                       |
| 10.0%  | 20.9%                     | ±1.0%                    | <b>8/67 (12%)</b>                           | Yes  | 9.1%-11.3%            | 10.1%        | 10.0%      | 0.3327  | No  |
| 20.9%  | 4.0%                      | ±1.0%                    | <b>4/7 (57%)</b>                            | No   | 19.0%-21.7%           | <b>19.1%</b> | 19.4%      | 0.0214  | Yes                                       |
| 20.9%  | 20.9%                     | ±1.0%                    | <b>4/24 (17%)</b>                           | Yes  | 19.0%-21.5%           | 20.8%        | 20.9%      | 0.2376  | No  |
| <b>Carbon Dioxide (CO<sub>2</sub>) using GEM 2000 Plus</b>               |                           |                          |   |  |                       |              |            |         |   |
| 0.25%  | 20.0%                     | ± 0.3%                   | 0/7 (0%)                                    | Yes  | 0.3-0.4%              | -----        | -----      | -----   | -----                                     |
| 5.0%   | 5.0%                      | ±1.0%                    | 0/34 (0%)                                   | Yes  | 4.2%-5.1%             | 4.8%         | 4.9%       | <0.0001 | Yes                                       |
| 5.0%   | 20.0%                     | ±1.0%                    | 0/10 (0%)                                   | Yes  | 4.8%-5.2%             | 5.1%         | 5.0%       | 0.2310  | No  |
| 5.0%   | 35.0%                     | ±1.0%                    | 0/57 (0%)                                   | Yes  | 4.3%-5.2%             | 4.8%         | 4.9%       | <0.0001 | Yes                                       |
| 20.0%  | 5.0%                      | ±3.0%                    | 0/6 (0%)                                    | No   | 17.7%-21.0%           | <b>18.8%</b> | 18.2%      | 0.0349  | Yes                                       |
| 20.0%  | 20.0%                     | ±3.0%                    | 0/7 (0%)                                    | Yes  | 19.9%-20.2%           | 20.0%        | 19.9%      | 0.2843  | No  |
| 35.0%  | 35.0%                     | ±3.0%                    | 0/44 (0%)                                   | Yes  | 32.7%-35.5%           | 34.4%        | 34.7%      | <0.0001 | Yes                                       |
| <b>Methane (CH<sub>4</sub>) using GEM 2000 Plus</b>                      |                           |                          |   |  |                       |              |            |         |   |
| 2.5%   | 2.5%                      | ±0.3%                    | <b>19/53 (36%)</b>                          | Yes  | 1.9%-3.7%             | 2.6%         | 2.4%       | 0.1595  | No  |
| 2.5%   | 50.0%                     | ±0.3%                    | <b>7/59 (12%)</b>                           | Yes  | 2.1%-3.6%             | 2.4%         | 2.4%       | <0.0001 | Yes                                       |
| 50%  | 50.0%                     | ±3.0%                    | 0/37 (0%)                                   | No   | 47.8%-50.8%           | 49.5%        | 49.6%      | 0.0007  | Yes                                       |
| <b>2,2 dichloro-1,1,1-trifluoroethane (R-123) using Bacharach H25 IR</b> |                           |                          |   |  |                       |              |            |         |   |
| 200 ppmv   | 200 ppmv                  | ±10%                     | 1/32 (3%)                                   | No   | 185 ppmv-223 ppmv     | 204 ppmv     | 203 ppmv   | 0.0008  | Yes                                       |
| 1000 ppmv  | 1000 ppmv                 | ±10%                     | 0/59 (0%)                                   | Yes  | 900 ppmv-1080 ppmv    | 1011 ppmv    | 1019 ppmv  | 0.1152  | No  |
| <b>Carbon Monoxide (CO) using GEM 2000 Plus</b>                          |                           |                          |   |  |                       |              |            |         |   |
| 504 ppmv   | 504 ppmv                  | ±10%                     | 0/36 (0%)                                   | No   | 476 ppmv-538 ppmv     | 509 ppmv     | 507 ppmv   | <0.0083 | Yes                                       |
| 1000 ppmv  | 1000 ppmv                 | ±10%                     | 0/23 (0%)                                   | No   | 909 ppmv-1081 ppmv    | 1010 ppmv    | 1009 ppmv  | 0.0319  | Yes                                       |
| <b>Hydrogen Sulfide (H<sub>2</sub>S) using GEM 2000 Plus</b>             |                           |                          |   |  |                       |              |            |         |   |
| 25 ppmv  | 25 ppmv                   | ±10%                     | 0/57 (0%)                                   | Yes  | 23 ppmv-27 ppmv       | 25 ppmv      | 25 ppmv    | 0.1720  | No  |
| 100 ppmv   | 100 ppmv                  | ±10%                     | <b>2/5 (40%)</b>                            | No   | 102 ppmv-124 ppmv     | 112 ppmv     | 109 ppmv   | 0.0313  | Yes                                       |
| <b>Flame Ionization Detector (FID) using Thermo Scientific TVA 1000B</b> |                           |                          |   |  |                       |              |            |         |   |
| 10.0 ppmv  | 10.0 ppmv                 | ± 2.5 ppmv               | 1/32 (3%)                                   | No   | 8.0 ppmv-13.9 ppmv    | 10.7 ppmv    | 10.6 ppmv  | <0.0004 | Yes                                       |
| 100 ppmv   | 100 ppmv                  | ±10%                     | 2/31 (6%)                                   | Yes  | 92.4 ppmv – 126 ppmv  | 100.8 ppmv   | 99.6 ppmv  | 1.0000  | No  |
| 1000 ppmv  | 1000 ppmv                 | ±10%                     | 0/8 (0%)                                    | No   | 979 ppmv-1013 ppmv    | 993.5 ppmv   | 993.5 ppmv | 0.0656  | No  |
| <b>Photoionization detector (PID) using Thermo Scientific TVA 1000B</b>  |                           |                          |   |  |                       |              |            |         |   |
| 50.0 ppmv  | 50.0 ppmv                 | ±20%                     | 0/29 (0%)                                   | No   | 40.5 ppmv – 51.8 ppmv | 47.3 ppmv    | 47.8 ppmv  | <0.0001 | Yes                                       |
| 100 ppmv   | 100 ppmv                  | ±20%                     | 0/26 (6%)                                   | No   | 82.1 ppmv -99.4 ppmv  | 90.8 ppmv    | 90.7 ppmv  | <0.0001 | Yes                                       |

There were a significant number of measurements outside the manufacturer-stipulated quality control criterion of ± 1% O<sub>2</sub> at concentrations of 10.0% and 20.9% necessitating frequent re-calibration (**Table 2**). While the reason for this is unclear, these results reinforce the need to conduct frequent bump tests when using portable gas analyzers.

There was a slight negative bias for measurement of O<sub>2</sub> at a standard concentration of 4.0% at a calibration concentration of 20.9% (mean=3.8%, 20 measurements). There was a slight positive bias for measurement of O<sub>2</sub> at a standard concentration of 10.0% at a calibration concentration of

10.0% (median=10.1%, 30 measurements). However, there was a significant negative bias for measurement of O<sub>2</sub> at a standard concentration of 20.9% at a calibration concentration of 4.0% (mean=19.1%, 7 measurements) (**Table 2**). It is notable that 4 of 7 measurements (57%) were also outside the quality control criterion of  $\pm 1\%$  O<sub>2</sub> for this measurement series.

Calibration at 4.0% appeared to improve O<sub>2</sub> measurement at 4.0% compared to calibration at 20.9% in which a minor negative bias was observed. Calibration at 20.9% appeared to improve O<sub>2</sub> measurement at 20.9% compared to calibration at 4.0% in which a significant negative bias was observed (**Table 2**). Hence, at least for O<sub>2</sub>, there was merit in calibration close to measurement concentration in this investigation.

The evaluation of performance of portable gas analyzers is dependent on the specification of quality control criteria. For instance, Patterson and Davis (2008) placed an electrochemical cell in a gas-permeable silicon membrane to monitor in-situ groundwater dissolved oxygen concentration during an air sparging demonstration. They observed linearity ( $r^2=0.999$ ) over 8 measured partial pressures from a single-point calibration at 21% O<sub>2</sub> with bump tests within 95-105% of calibration over a 6-month placement period. Although not reported, based on this statement, O<sub>2</sub> measurements were also within  $\pm 1\%$  of 20.9% indicating good performance using both metrics. In this investigation, measurements at 20.9% O<sub>2</sub> with calibration at 4% O<sub>2</sub> varied from 19.0% - 21.7% with values exceeding the manufacturer's quality control criterion of  $\pm 1\%$  O<sub>2</sub> in 4 of 7 tests (57%) indicating poor performance. Yet, all values were within 91-104% of calibration indicating good performance if this metric had been used.

### 3.1b Bump Test Results for Carbon Dioxide (CO<sub>2</sub>)

Results of CO<sub>2</sub> measurement using the GEM2000 Plus portable analyzer and associated deviation from gas standards during bump tests are illustrated in **Figures 15a, b**, respectively and **Table (2)**.

All measurements were within the manufacturer-stipulated quality control criteria which varied with concentration range:  $\pm 0.3\%$  (0 - <5.0%),  $\pm 1.0\%$  (5.0 - <15%), and  $\pm 3.0\%$  (15 - 60%). There was a slight negative bias for measurement of CO<sub>2</sub> at a standard concentration of 5.0% at a calibration concentration of 5.0% (median=4.9%, 34 measurements), at a standard concentration of 5.0% at a calibration concentration of 35.0% (median=4.9%, 57 measurements), and at a

standard concentration of 35.0% at a calibration concentration of 35.0% (median=34.7%, 44 measurements) (**Table 2**).

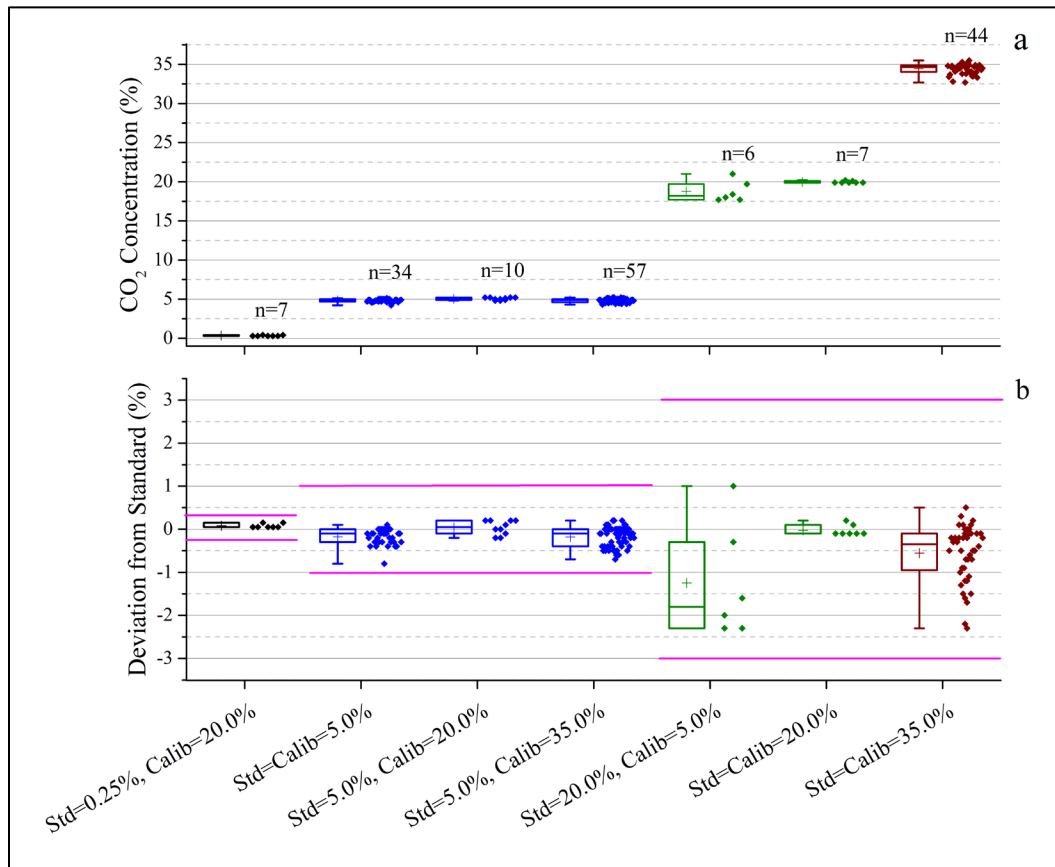


**Figure 15.** Results of bump tests for carbon dioxide (CO<sub>2</sub>) using a LandTec GEM2000 Plus portable gas analyzer. (a) Measurement of gas standards (Std) at calibration (Calib) concentrations in 5-L Flex-Foil™ gas sampling bags. (b) Deviation from standard concentrations with stipulated quality control criteria:  $\pm 0.3\%$  (0 - <5.0%),  $\pm 1.0\%$  (5.0 - <15%), and  $\pm 3.0\%$  (15 - 60%) illustrated with magenta lines. Quartiles, median (line), mean (+), minimum (whisker), and maximum (whisker) values illustrated in box plots with values to right of box plots.

A significant negative bias was observed for measurement of CO<sub>2</sub> at a standard concentration of 20.0% at calibration concentration of 5.0% (mean=18.8%, 6 measurements) (**Table 2**). There was not a bias for measurement of CO<sub>2</sub> at a standard concentration of 20.0% at calibration concentration of 20.0% (median=19.9%, 7 measurements) again indicating merit in calibration close to measurement concentration. Bias could not be evaluated at a CO<sub>2</sub> concentration of 0.25% CO<sub>2</sub> since the GEM 2000 Plus portable gas analyzer provided readings at increments of 0.1% (e.g., 0.2%, 0.3%, etc.)

### 3.1c Bump Test Results for Methane

Results of CH<sub>4</sub> measurement using the GEM2000 Plus portable gas analyzer and associated deviation from gas standards during bump tests are illustrated in **Figures 16a, b**, respectively and **Table 2**.

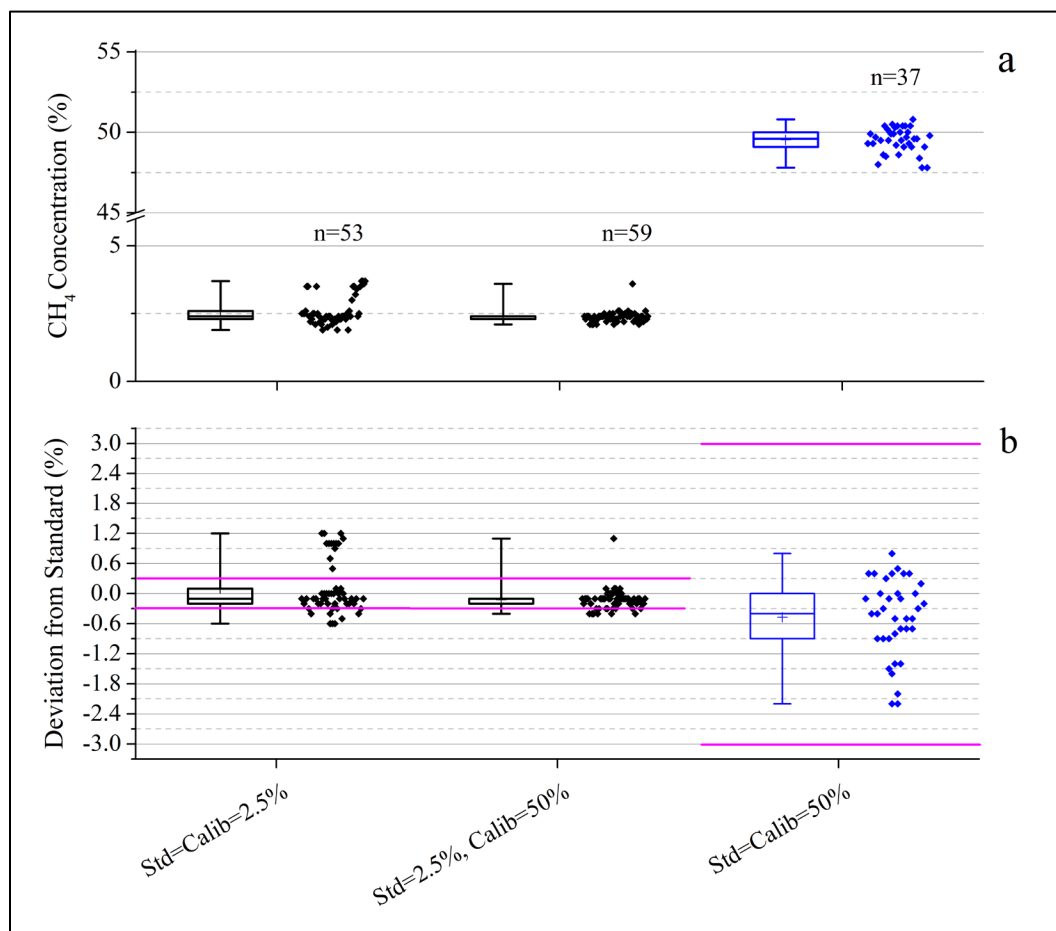


**Figure 16.** Results of bump tests for methane (CH<sub>4</sub>) using a LandTec GEM2000 Plus portable gas analyzer. (a) Measurement of gas standards (Std) at calibration (Calib) concentrations in 5 L Flex Foil gas sampling bags. (b) Deviation from standard concentrations with stipulated quality control criteria:  $\pm 0.3\%$  (0 - <5.0%),  $\pm 1.0\%$  (5.0 - <15%), and  $\pm 3.0\%$  (15 - 100%) illustrated with dashed magenta lines. Quartiles, median (line), mean (+), minimum (whisker), and maximum (whisker) values illustrated in box plots with values to right of box plots.

For measurement at a standard concentration of 2.5% and calibration at 50% CH<sub>4</sub>, 7 of 59 (12%) measurements were outside the QC criterion of  $\pm 0.3\%$ . There was a slight negative bias for this data set (median=2.4%, 59 measurements). For both measurement and calibration of CH<sub>4</sub> at 2.5%, 19 of 53 (36%) measurements were outside the quality control criterion of  $\pm 0.3\%$  with no apparent bias (median=2.4% with p-value=0.1595, 53 measurements). Measurement and calibration at 2.5% did not improve attainment of the quality control criterion of  $\pm 0.3\%$ . For both measurement and calibration of CH<sub>4</sub> at 50%, all measurements were within the QC

criterion of  $\pm 3.0\%$ . There was a slight negative bias for this data set (mean=49.5%, 37 measurements) (**Table 2**).

### 3.1d Bump Test Results for 2,2 dichloro-1,1,1-trifluoroethane (R-123)

Results of bump tests for R-123 in air using the Bacharach H-25-IR portable gas analyzer are illustrated in **Figures 17a, b**, respectively and **Table 2**.

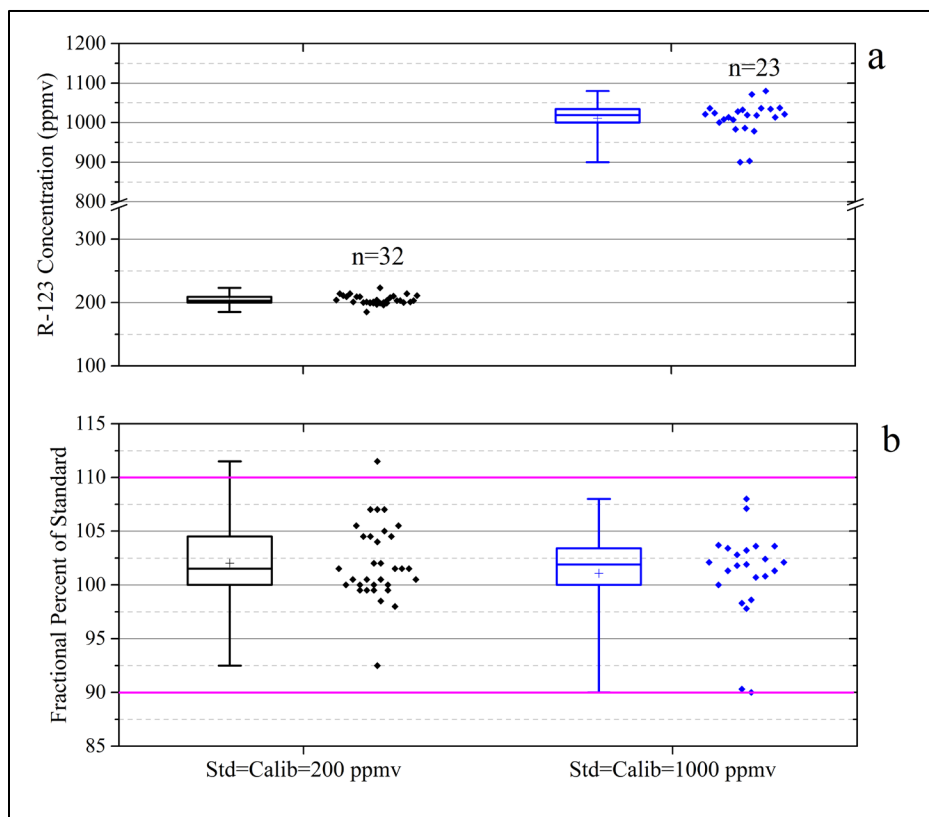


**Figure 17.** Results of bump tests for 2,2 dichloro-1,1,1-trifluoroethane (R-123) using a Bacharach H-25-IR Industrial Refrigerant Leak Detector. (a) Measurement using a gas standard (Std) after instrument calibration (Calib) at the same concentrations in 5-L Flex Foil™ gas sampling bags. (b) Fractional deviation from a standard concentration (%) with stipulated quality control criterion (90 – 110%) illustrated with magenta lines. Quartiles, median (line), mean (+), minimum (whisker), and maximum (whisker) values illustrated in box plots with values to right of box plots.

The stipulated QC criterion for measurement of R-123 was attainment of 90-110% of R-123 concentration in the gas standard. With the exception of 1 of 32 measurements, this QC criterion was attained at 200 ppmv with a slight positive bias (mean=204 ppmv). Similarly, the QC criterion was attained for all measurements at 1,000 ppmv R-123 in the absence of bias (**Table 2**).

### 3.1e Bump Test Results for Carbon Monoxide (CO)

Results of bump tests for CO in air using Landtec GEM2000 Plus portable gas analyzer are illustrated in **Figures 18a, b**, respectively and **Table 2**.

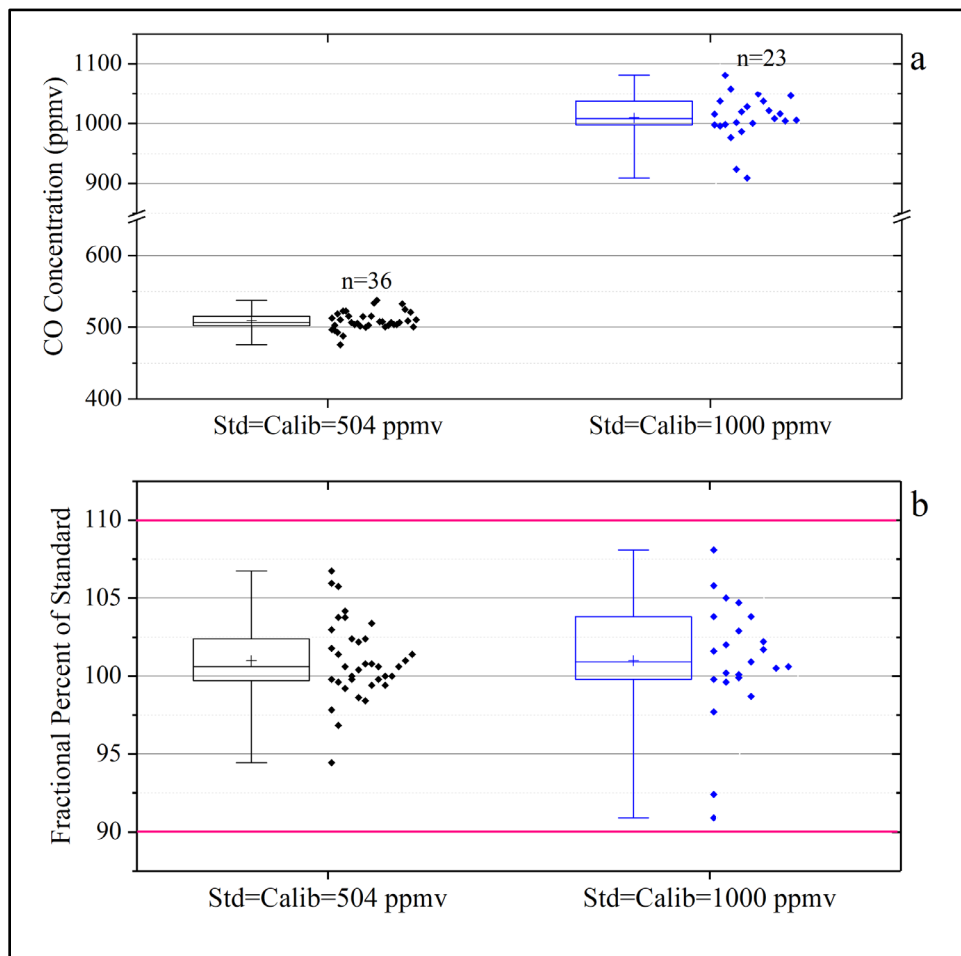


**Figure 18.** Results of bump tests for carbon monoxide (CO) in air using Landtec GEM2000 Plus portable gas analyzer: (a) Measurement of gas standards (Std) at calibration (Calib) concentrations in 5 L Flex Foil gas sampling bags. (b) Deviation from standard concentration with stipulated quality control criterion (90 – 110% of standard concentration) illustrated with magenta lines. Quartiles, median (line), mean (+), minimum (whisker), and maximum (whisker) values illustrated in box plots with values to right of box plots.

The stipulated QC criterion was CO measurement within 90-110% of CO concentration in gas standards. There was consistent attainment of the QC criterion at both 504 and 1,000 ppmv CO. There was a slight positive bias for CO measurement at a standard concentration of 1000 ppmv (mean=1010 ppmv, 23 measurements) (**Table 2**).

### 3.1f Bump Test Results for Hydrogen Sulfide (H<sub>2</sub>S)

Results of H<sub>2</sub>S measurement using the Landtec GEM2000 Plus portable gas analyzer and associated deviation from gas standards during bump tests are illustrated in **Figures 19a, b**, respectively and **Table 2**.

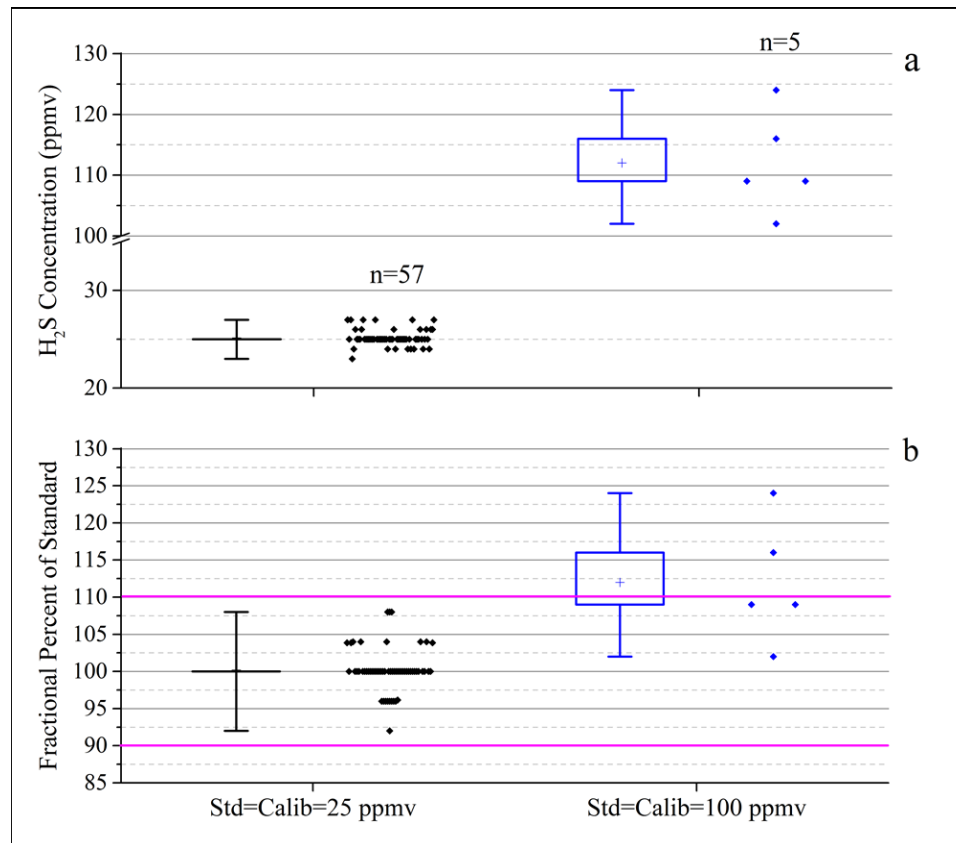


**Figure 19.** Results of bump tests for hydrogen sulfide (H<sub>2</sub>S) using the Landtec GEM2000 Plus portable gas analyzer: (a) Measurement of gas standards (Std) at calibration (Calib) concentrations in 5-L Flex Foil™ gas sampling bags. (b) Deviation from standard concentration with stipulated quality control criteria (90 – 110% of standard concentration) illustrated with magenta lines. Quartiles, median (line), mean (+), minimum (whisker), and maximum (whisker) values illustrated in box plots with values to right of box plots.

The QC criterion of measurement of H<sub>2</sub>S within 90-110% of H<sub>2</sub>S concentration in gas standards was consistently attained at 25 ppmv (57 measurements) but not at 100 ppmv at 2 of 5 (40%) measurements with a positive bias (mean=112 ppmv) (**Table 2**). The reason for poor performance of H<sub>2</sub>S measurement at 100 ppmv is unclear.

### 3.1g Bump Test Results for Flame Ionization Detector (FID) Using Methane in Air

Results of bump tests for FID in the Thermo Scientific TVA-1000B portable gas analyzer for CH<sub>4</sub> in air are illustrated in **Figures 20a, b**, respectively and **Table 2**.

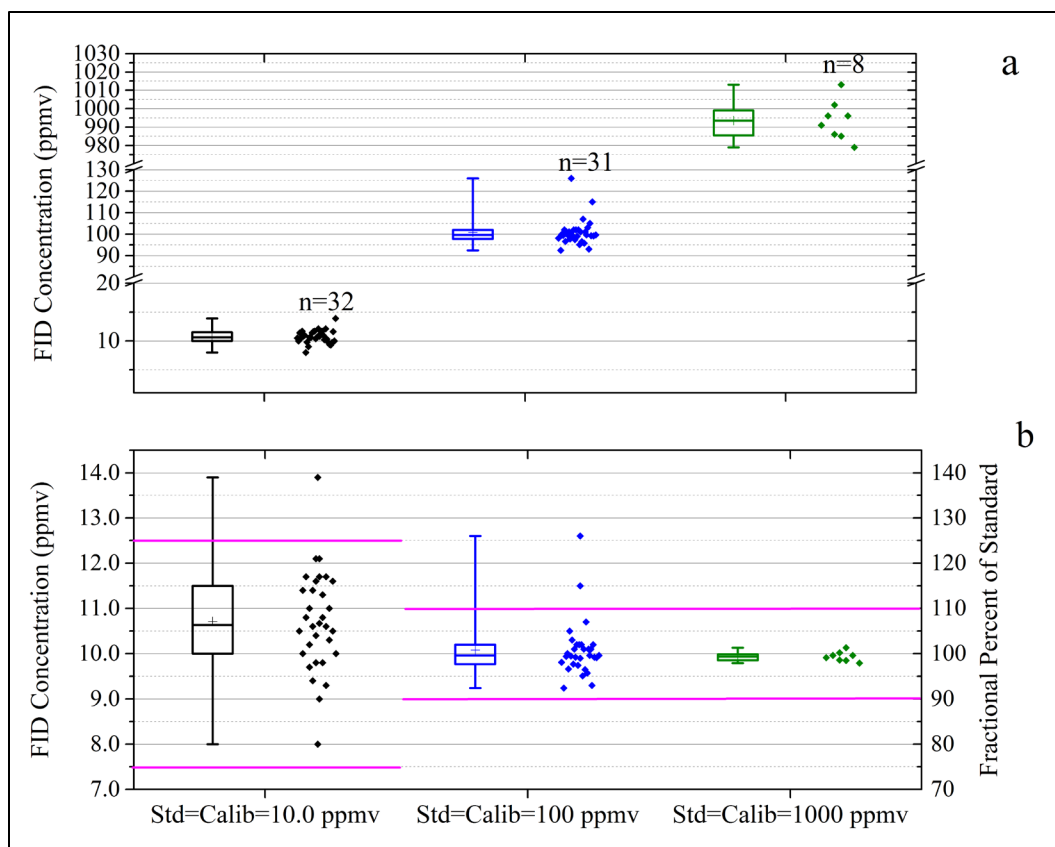


**Figure 20.** Results of bump tests for flame ionization detector (FID) for methane in air using the Thermo Scientific TVA 1000B portable gas analyzer. (a) Measurement of gas standards (Std) at calibration (Calib) concentrations in 5-L Flex Foil™ gas sampling bags. (b) Deviation from standard concentration with stipulated quality control criterion  $\pm 2.5$  ppmv at  $\leq 10$  ppmv and within 90 – 110% of standard concentration  $> 10$  ppmv illustrated with a red circle (13.9 ppmv) for the former and magenta lines for the latter. Quartiles, median (line), mean (+), minimum (whisker), and maximum (whisker) values illustrated in box plots with values to right of box plots.

The QC criterion for FID response at  $\text{CH}_4$  concentration  $\leq 10$  ppmv was  $\pm 2.5$  ppmv of  $\text{CH}_4$  concentration in a gas standard. Above this  $\text{CH}_4$  concentration, the QC criterion was  $\text{CH}_4$  measurement within 90 – 110% of  $\text{CH}_4$  concentration in gas standards. With the exception of 1 of 32 (3%) measurements, there was consistent attainment of the specified quality control criterion at a standard and calibrated concentration of 10 ppmv. However, there was a slight positive bias at this concentration (mean=10.7 ppmv). With the exception of 2 of 31 (6%) measurements, there was consistent attainment of the specified quality control criterion of measurement within 90-100% of  $\text{CH}_4$  in a gas standard at 100 ppmv and 1,000 with calibration at these concentrations without an apparent bias (**Table 2**).

### 3.1h Bump Test Results for Photo Ionization Detector (PID) Using isobutylene in Air

Results of bump tests for PID in the Thermo Scientific TVA-1000B portable gas analyzer for isobutylene in air are illustrated in **Figures 21a, b**, respectively and **Table 2**.

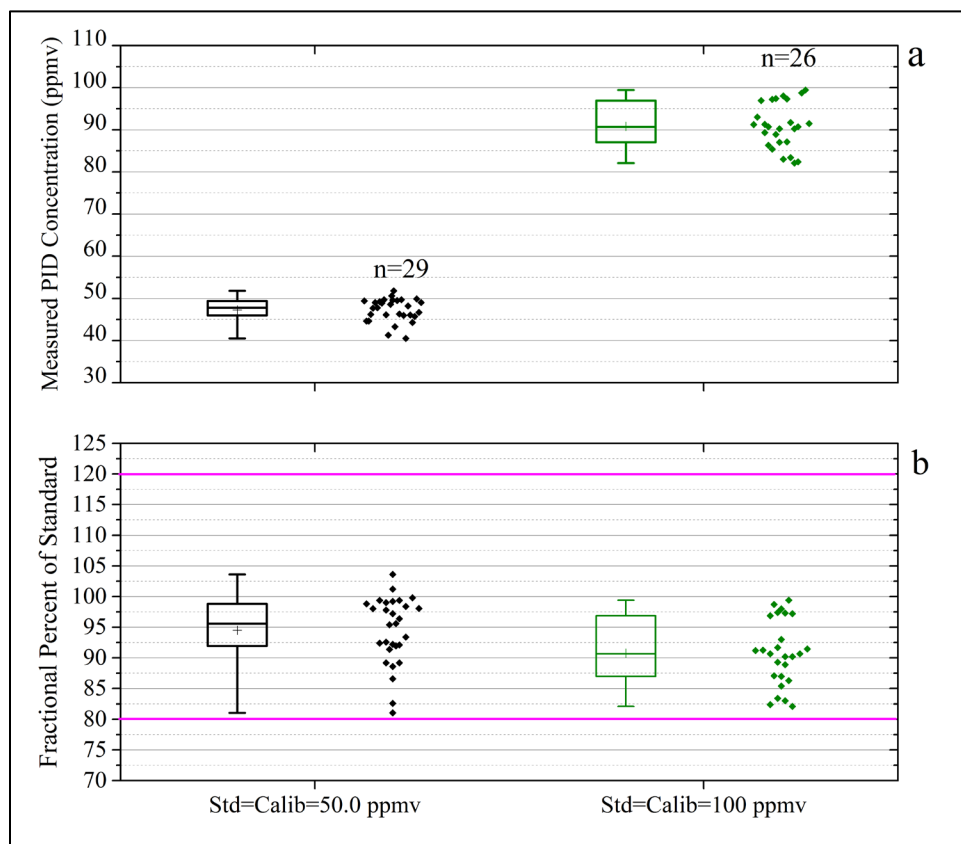


**Figure 21.** Results of bump tests for photo ionization detector (PID) in the Thermo Scientific TVA 1000B portable gas analyzer. (a) Measurement of PID response at gas standard (Std) and calibration (Calib) concentrations in 5-L Flex-Foil™ gas sampling bags. (b) Deviation from standard concentration with the stipulated quality control criterion of 80 – 120% of standard concentration illustrated with magenta lines. Quartiles, median (line), mean (+), minimum (whisker), and maximum (whisker) values illustrated in box plots with values to right of box plots.

There was consistent attainment of the specified QC criterion of measurement within 80-120% of isobutylene in air in gas standards at 50 and 100 ppmv with calibration at these same concentrations. However, there was a negative bias at 50 ppmv (mean=47.3 ppmv, 29 measurements) and at 100 ppmv (mean=90.8 ppmv, 26 measurements) (**Table 2**). The less rigorous stipulated QC criterion for the PID (80-120% of concentration of gas standard) compared to the FID (90-110% of concentration > 10 ppmv and within  $\pm 2.5$  ppmv  $\leq 10$  ppmv of a gas standard) is notable.

### 3.2 Testing the Effect of Flow Rate on Measurement of Hydrocarbons Using the Thermo-Scientific TVA-1000B FID and PID and R-123 Using the Bacharach H-25IR Portable Gas Analyzers

There was little effect of flow rate on measurement using the TVA-1000B PID but a strong linear flow effect on measurement of CH<sub>4</sub> using the TVA-1000B FID while extracting gas standards from 5-liter Flex-Foil™ gas sampling bags (**Figure 22**).

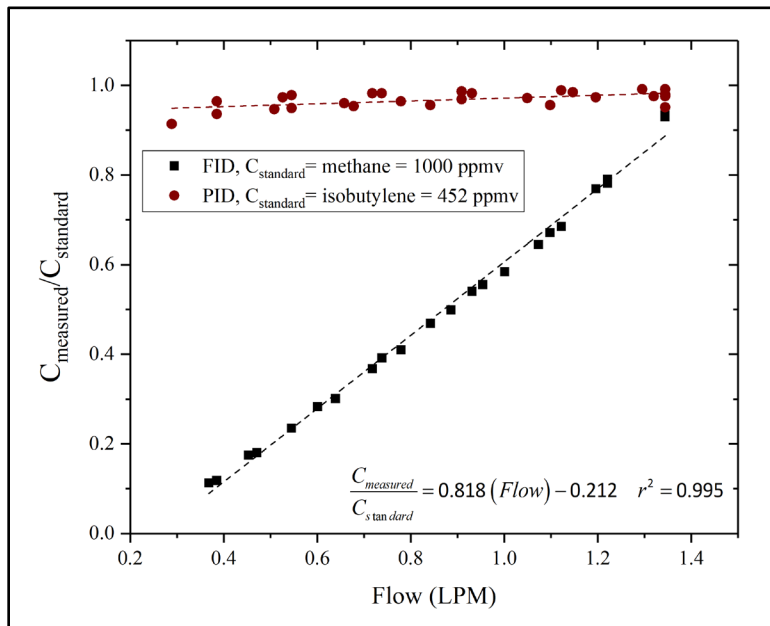


**Figure 22.** Response of Thermo Scientific TVA-1000B to measurement of CH<sub>4</sub> using the FID and isobutylene using the PID to flow rate using gas standards

The linear increase in response of the FID with flow rate indicates that in-line FID measurement in a soil-gas sampling train must be corrected for flow rate. This correction is not necessary if samples are extracted into 5-L gas sampling bags and FID measurement is conducted in the same manner as calibration for the FID. Since CH<sub>4</sub> was only detected in a soil-gas probe at percent concentrations near a leaking gas line, adjustment of measured CH<sub>4</sub> concentration using TVA-1000 B FID during soil-gas purging was unnecessary in this investigation.

Measurement of R-123 increased with flow rate (**Figure 23**). Since the flow of tracer gas mixture containing R-123 coming from the leak detection chamber was not restricted and soil-gas flow during leak testing using R-123 was at flow rates generally exceeding 0.65 SLPM,

concentrations of measured R-123 were not adjusted in this investigation. The effect of flow rate on CO and H<sub>2</sub>S concentration using the GEM 2000 Plus gas analyzer was not evaluated.

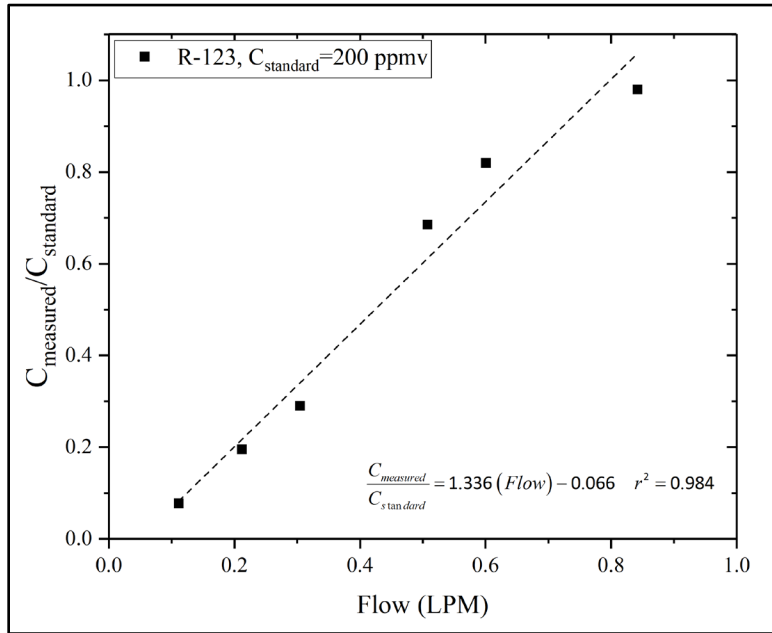


**Figure 23.** Response of Bacharach H-25-IR to measurement of R-123 to flow rate using gas standards

### 3.3 Testing of Flow Rate on Gas Measurement During Soil-Gas Purging

During purging, flow rate was varied to evaluate the effect of flow rate on O<sub>2</sub> and CO<sub>2</sub> measurement using the GEM2000 Plus portable gas analyzer. O<sub>2</sub> concentrations decreased and CO<sub>2</sub> concentrations increased with flow rate.

Measured concentrations of O<sub>2</sub> and CO<sub>2</sub> as a function of cumulative gas extraction volume (with calculated purge volume) and flow rate in 4 vapor probes are illustrated in **Figures 24a-d**. At PB1S, during an approach to stabilization of O<sub>2</sub> and CO<sub>2</sub> concentration, there was no apparent impact on O<sub>2</sub> and CO<sub>2</sub> concentrations with variable flow rate from 0.522 to 1.031 SLPM. However, after extraction of approximately 16 liters of gas, a decrease in flow rate from 0.646 to 0.368 SLPM caused an increase in O<sub>2</sub> concentration from 1.6 to 2.1% and a decrease in CO<sub>2</sub> concentration from 21.9 to 20.9% (**Figure 24a**). Concentrations of O<sub>2</sub> and CO<sub>2</sub> reverted to 1.8 and 21.2%, respectively after increasing flow rate to 0.544 SLPM.

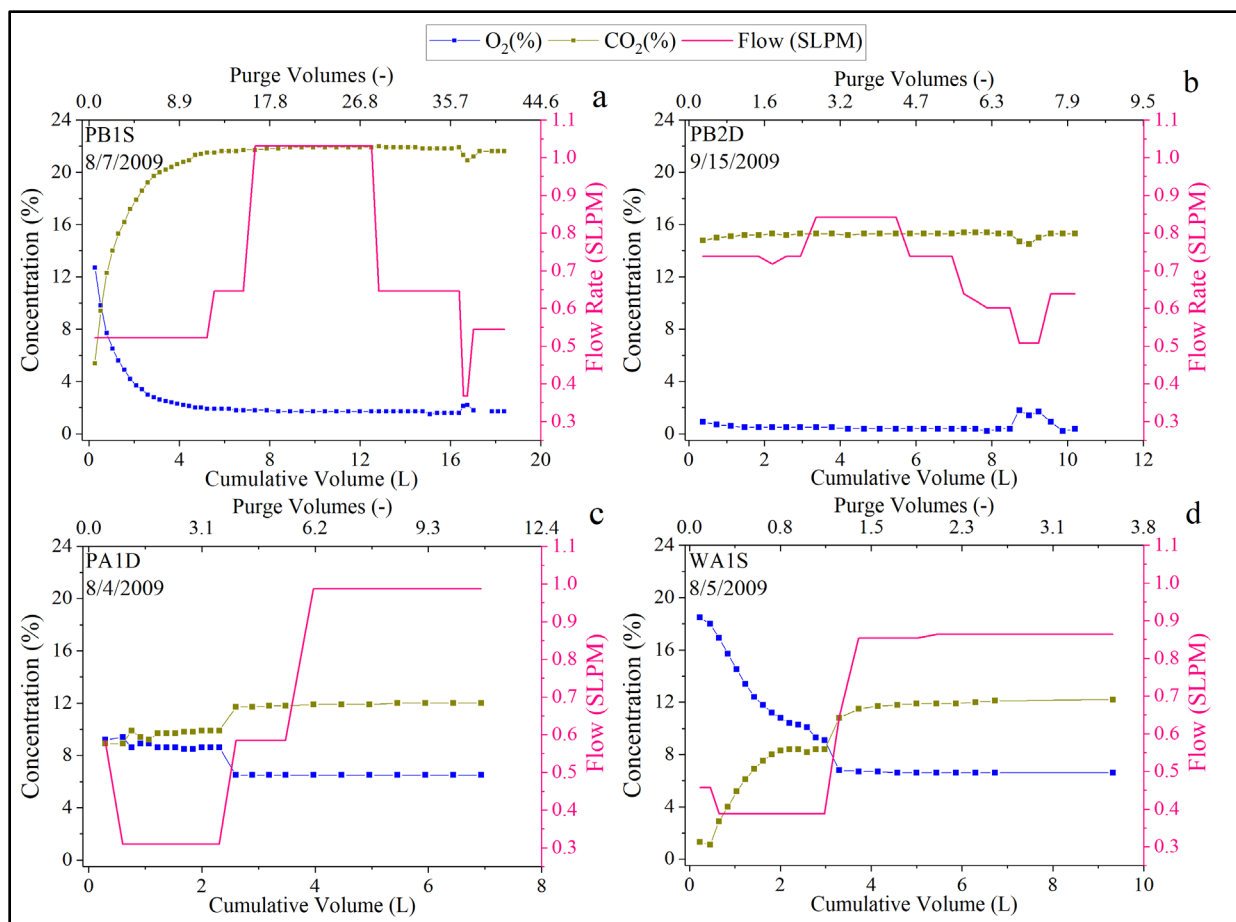


**Figure 24.** Change in O<sub>2</sub> and CO<sub>2</sub> concentration with flow rate during purging (a) Probe PB1S, (b) Probe PB2D, (c) Probe PA1D, (d) Probe WA1S

At PB2D, there was no apparent variation of O<sub>2</sub> and CO<sub>2</sub> concentration with variable flow rate from 0.601 to 0.842 SLPM. However, when flow was decreased to 0.508 SLPM after approximately 9 liters of soil-gas extraction, O<sub>2</sub> increased from 0.4 to 1.8% and CO<sub>2</sub> decreased from 15.3 to 14.7% (**Figure 24b**). Concentrations of O<sub>2</sub> and CO<sub>2</sub> reverted to 0.4 and 15.3%, respectively when flow increased to 0.639 SLPM.

At PA1D, an increase in flow rate from 0.310 to 0.585 SLPM after approximately 2 liters of soil-gas extraction caused a decrease in O<sub>2</sub> concentration from 8.6 to 6.5% and an increase in CO<sub>2</sub> concentration from 9.9 to 11.7% which remained constant throughout the remainder of purging (**Figure 24c**).

At WA1S, an increase in flow rate from 0.387 to 0.853 SLPM after approximately 3 liters of soil-gas extraction caused a more rapid decrease in O<sub>2</sub> concentration from 9.1 to 6.7% and a more rapid increase in CO<sub>2</sub> concentration from 8.4 to 11.5% (**Figure 24d**).

Abrupt changes in O<sub>2</sub> and CO<sub>2</sub> concentrations as a result of increased or decreased flow rate are highlighted in bold in **Table 3**. To graphically illustrate the change in magnitude of O<sub>2</sub> decrease and CO<sub>2</sub> increase in concentration with increase in flow rate (change is greater at lower flow rates), change in concentration (from a lower to a higher flow rate) was normalized by the absolute value of flow rate change and plotted as a function of the lower flow rate (**Figure 25**).

For instance, at PA1D, O<sub>2</sub> concentration measured with the GEM2000 Plus decreased from 8.6 to 6.5% (-2.1% change) when flow rate increased from 0.321 to 0.585 SLPM (0.264 SLPM change) resulting in a negative change of -7.95%/SLPM (**Figure 25**). At the same flow rate change, CO<sub>2</sub> concentration increased from 9.9 to 11.7% (+1.8%) resulting in a positive change of 6.8%/SLPM.

Oxygen concentrations measured with the GEM 2000 Plus consistently decreased (negative values) with increased flow rate and CO<sub>2</sub> concentrations generally (not always) increased (positive values) with increased flow rate. The magnitude of change decreased with increasing flow rate. At flow rates above of approximately 0.65 SLPM there was little impact on O<sub>2</sub> and CO<sub>2</sub> measurement. Thus, in this investigation, purging at a flow rate in excess of 0.65 SLPM was necessary for stable (and assumed more accurate) measurement of O<sub>2</sub> and CO<sub>2</sub> concentration using the GEM2000 Plus portable gas analyzer for real-time in-line sample train measurement.

#### 3.4 Comparison O<sub>2</sub>, CO<sub>2</sub>, and CH<sub>4</sub> Concentrations Measured Using a GEM2000 Plus Gas Analyzer During Purging with Fixed-Laboratory Analysis

A comparison of O<sub>2</sub>, CO<sub>2</sub>, and CH<sub>4</sub> concentrations measured using a GEM2000 Plus gas analyzer during purging at flow rates above 0.74 SLPM with fixed-laboratory analysis (**Table 4**) indicates general agreement with field- and laboratory-measured values. RPD values varied from -15.8% to -2.0% for O<sub>2</sub> and -0.5% to 9.6% for CO<sub>2</sub>. Hence, there was only one value outside the stipulated requirements of  $\pm 15\%$ . There was only one data set available for CH<sub>4</sub> with a RPD of -5.3%.

**Table 3.** Results of change in O<sub>2</sub> and CO<sub>2</sub> concentration measured with a GEM2000 Plus portable gas analyzer as a result of change in flow rate during purging (entries in bold reflect significant variation)

| Probe | Date      | Flow 1 (SLPM) | Flow 2 (SLPM) | O <sub>2</sub> at Flow 1 (%) | O <sub>2</sub> at Flow 2 (%) | CO <sub>2</sub> at Flow 1 (%) | CO <sub>2</sub> at Flow 2 (%) |
|-------|-----------|---------------|---------------|------------------------------|------------------------------|-------------------------------|-------------------------------|
| PA1S  | 9/16/2009 | 0.718         | 0.718         | 4.8                          | 4.2                          | 12.4                          | 12.9                          |
| PA1I  | 8/4/2009  | 0.585         | 0.875         | 5.7                          | 5.7                          | 13.2                          | 13.3                          |
|       | 9/16/2009 | 0.718         | 0.909         | 4.1                          | 4.1                          | 13.2                          | 13.2                          |
| PA1D  | 8/4/2009  | <b>0.310</b>  | <b>0.585</b>  | <b>8.6</b>                   | <b>6.5</b>                   | <b>9.9</b>                    | <b>11.7</b>                   |
|       | 9/16/2009 | 0.738         | 0.931         | 4.4                          | 4.4                          | 13.0                          | 13.1                          |
| WA1S  | 8/4/2009  | 0.585         | 0.853         | 7.2                          | 7.1                          | 11.0                          | 11.1                          |
|       | 8/5/2009  | <b>0.387</b>  | <b>0.853</b>  | <b>9.1</b>                   | <b>6.7</b>                   | <b>8.4</b>                    | <b>11.5</b>                   |
| PA2S  | 9/15/2009 | 0.738         | 0.909         | 1.4                          | 1.4                          | 15.4                          | 15.5                          |
| PA3S  | 8/14/2009 | 0.779         | 0.909         | 8.4                          | 8.3                          | 11.1                          | 11.1                          |
|       | 9/15/2009 | 0.738         | 0.909         | 6.8                          | 6.8                          | 11.8                          | 11.9                          |
| PA3I  | 9/15/2009 | 0.738         | 0.909         | 7.8                          | 7.7                          | 11.0                          | 11.0                          |
| PA3D  | 9/15/2009 | 0.738         | 0.909         | 7.7                          | 7.7                          | 11.2                          | 11.1                          |
| PA4S  | 8/14/2009 | 0.738         | 0.909         | 9.5                          | 9.5                          | 11.2                          | 11.1                          |
|       | 9/16/2009 | 0.738         | 0.931         | 6.4                          | 6.4                          | 12.2                          | 12.2                          |
| PA4I  | 9/16/2009 | 0.738         | 0.909         | 6.7                          | 6.7                          | 11.8                          | 11.8                          |
| PB1D  | 8/7/2009  | <b>0.522</b>  | <b>0.763</b>  | <b>2.4</b>                   | <b>1.5</b>                   | <b>19.4</b>                   | <b>20.2</b>                   |
|       |           | 0.762         | 1.096         | 1.4                          | 1.4                          | 20.3                          | 20.2                          |
|       |           | 1.096         | 0.875         | 1.4                          | 1.4                          | 20.4                          | 20.5                          |
|       |           | 0.875         | 0.646         | 1.4                          | 1.4                          | 20.6                          | 20.6                          |
|       |           | 0.646         | 0.522         | 1.4                          | 1.4                          | 20.6                          | 20.6                          |
| PB1S  | 8/7/2009  | 0.522         | 0.646         | 1.9                          | 1.9                          | 21.5                          | 21.5                          |
|       |           | 0.646         | 1.031         | 1.8                          | 1.8                          | 21.7                          | 21.7                          |
|       |           | 1.031         | 0.646         | 1.7                          | 1.7                          | 21.9                          | 22.0                          |
|       |           | 1.031         | 0.646         | 1.7                          | 1.7                          | 21.9                          | 22.0                          |
|       |           | <b>0.646</b>  | <b>0.368</b>  | <b>1.6</b>                   | <b>2.1</b>                   | <b>21.9</b>                   | <b>21.3</b>                   |
|       |           | <b>0.368</b>  | <b>0.544</b>  | <b>2.1</b>                   | <b>1.8</b>                   | <b>20.9</b>                   | <b>21.2</b>                   |
|       | 9/15/2009 | 0.646         | 0.762         | 0.5                          | 0.4                          | 21.1                          | 21.1                          |
|       |           | 0.762         | 0.646         | 0.4                          | 0.4                          | 21.1                          | 21.1                          |
|       |           | 0.622         | 0.522         | 0.3                          | 0.3                          | 21.1                          | 21.1                          |
|       |           | 0.522         | 0.739         | 0.3                          | 0.3                          | 21.1                          | 21.1                          |
|       | 9/29/2010 | 0.739         | 0.652         | 12.4                         | 12.4                         | 10.6                          | 10.6                          |
|       |           | 0.652         | 0.739         | 11.8                         | 11.8                         | 10.7                          | 10.7                          |
| PB1I  | 8/7/2009  | 0.522         | 0.762         | 1.6                          | 1.6                          | 19.8                          | 19.8                          |
|       | 9/15/2009 | 0.646         | 0.747         | 0.8                          | 0.7                          | 20.8                          | 20.9                          |
| PB2S  | 8/11/2009 | <b>0.522</b>  | <b>0.693</b>  | <b>2.6</b>                   | <b>2.0</b>                   | <b>16.1</b>                   | <b>15.8</b>                   |
|       |           | 0.669         | 1.009         | 2.0                          | 2.0                          | 15.7                          | 15.9                          |
|       | 9/15/2009 | 0.779         | 0.909         | 0.4                          | 0.4                          | 16.0                          | 16.0                          |
|       |           | 0.909         | 0.738         | 0.3                          | 0.3                          | 16.0                          | 16.0                          |
|       |           | 0.639         | 0.545         | 0.3                          | 0.3                          | 16.0                          | 16.0                          |
|       |           | 0.678         | 0.909         | 0.3                          | 0.3                          | 16.0                          | 16.0                          |
| PB2I  | 8/11/2009 | 0.508         | 0.738         | 2.1                          | 2.1                          | 15.4                          | 15.6                          |
|       | 9/15/2009 | 0.738         | 0.909         | 0.4                          | 0.4                          | 15.9                          | 15.9                          |
| PB2D  | 8/11/2009 | 0.548         | 0.646         | 2.2                          | 2.2                          | 14.5                          | 14.2                          |
|       | 9/15/2009 | 0.738         | 0.842         | 0.5                          | 0.5                          | 15.2                          | 15.3                          |
|       |           | 0.842         | 0.738         | 0.4                          | 0.4                          | 15.3                          | 15.3                          |
|       |           | 0.738         | 0.601         | 0.4                          | 0.4                          | 15.3                          | 15.4                          |
|       |           | <b>0.601</b>  | <b>0.508</b>  | <b>0.4</b>                   | <b>1.8</b>                   | <b>15.3</b>                   | <b>14.7</b>                   |
|       |           | <b>0.508</b>  | <b>0.639</b>  | <b>1.8</b>                   | <b>0.2</b>                   | <b>14.7</b>                   | <b>15.3</b>                   |
| PB3I  | 8/13/2009 | <b>0.545</b>  | <b>0.738</b>  | <b>5.7</b>                   | <b>3.2</b>                   | <b>11.2</b>                   | <b>12.6</b>                   |
|       |           | 0.738         | 0.954         | 3.1                          | 3.1                          | 13.7                          | 13.7                          |
|       | 9/15/2009 | 0.698         | 0.842         | 1.8                          | 1.8                          | 15.7                          | 15.6                          |
| PC1   | 9/14/2009 | 0.646         | 0.762         | 0.0                          | 0.0                          | 21.9                          | 21.9                          |
|       |           | 0.762         | 0.646         | 0.0                          | 0.0                          | 22.1                          | 22.1                          |
| WB1S  | 8/13/2009 | 0.738         | 0.909         | 6.5                          | 6.5                          | 15.3                          | 15.2                          |
| WB3S  | 8/13/2009 | 0.658         | 0.909         | 5.8                          | 5.8                          | 11.7                          | 11.8                          |
| WC1S  | 8/13/2009 | <b>0.646</b>  | <b>0.808</b>  | <b>3.7</b>                   | <b>3.1</b>                   | <b>11.7</b>                   | <b>12.2</b>                   |

SLPM-standard liters per minute

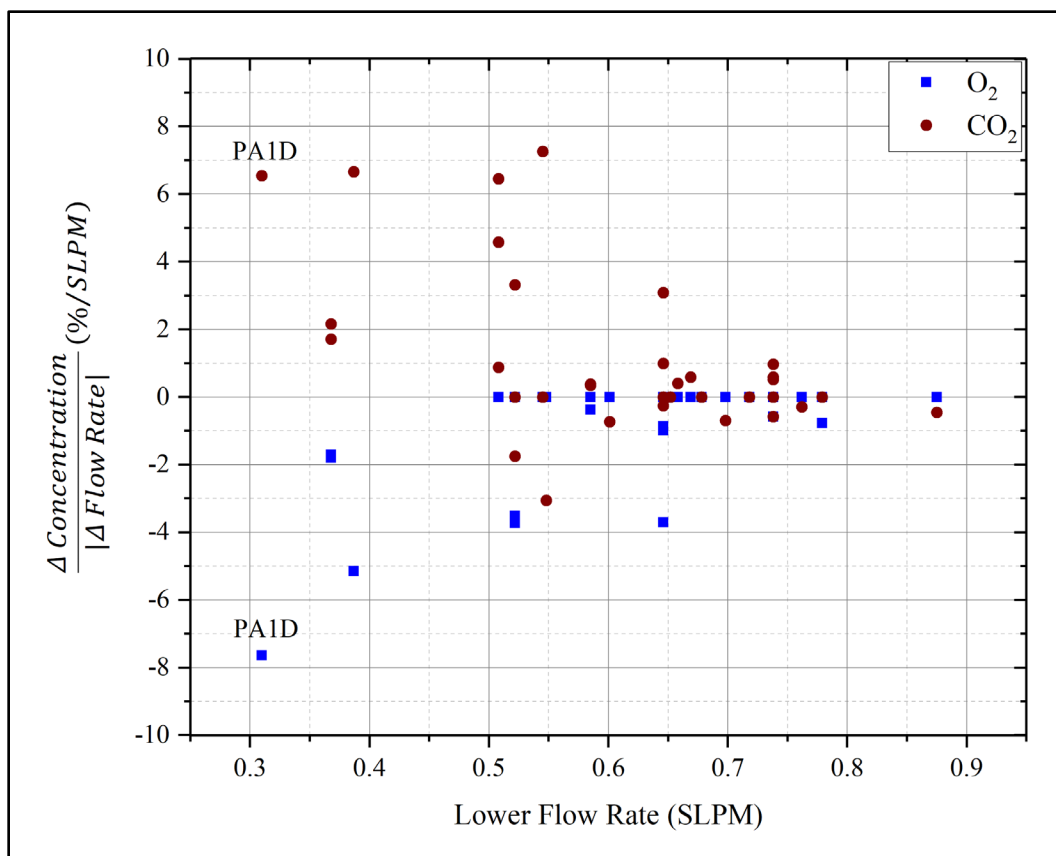


**Figure 25.** The magnitude of change of  $O_2$  and  $CO_2$  concentration with change in flow rate. Data points for PA1D are illustrated on the plot.

However, there was a negative bias in field measurement of  $O_2$  as evidenced by most data points falling below the 1:1 line (**Figure 26**) and through use of the nonparametric Wilcoxon Sign Rank Test (one-tailed test) ( $P < 0.0001$ ) for paired data. There was a positive bias in field measurement of  $CO_2$  as evidenced by most points being above the 1:1 line and through use of the nonparametric Wilcoxon Sign Rank Test (one-tailed test) ( $P = 0.0044$ ) for paired data.

It is possible that the negative bias observed for field  $O_2$  measurement was due to higher flow rates during purging (0.738 to 1.073 SLPM) relative to flow rates during instrument calibration (0.5 SLPM) and observed decrease in  $O_2$  concentration with flow rate. Similarly, it is possible that the positive bias observed for field measurement of  $CO_2$  was due to higher flow rates during purging compared to that for instrument calibration.

### 3.5 Results of Equipment Blanks

Concentrations of  $O_2$  and  $CO_2$  in travel and equipment blanks using ultra-pure  $N_2$  varied from 0.025 – 0.520% and 0.006 – 0.020%, respectively.  $CH_4$  was detected in one equipment blank at

0.0029% (Table 5). Thus, fixed-laboratory analysis of gases was not impacted by travel and equipment blanks.

**Table 4.** Comparison O<sub>2</sub> and CO<sub>2</sub> concentrations measured using a GEM2000 Plus gas analyzer during purging with fixed-laboratory analysis

| Probe          | Sample Date | Flow Rate (SLPM) | O <sub>2</sub> (%) |       |       | CO <sub>2</sub> (%) |       |       | CH <sub>4</sub> (%) |         |       |
|----------------|-------------|------------------|--------------------|-------|-------|---------------------|-------|-------|---------------------|---------|-------|
|                |             |                  | Field              | Lab   | RPD   | Field               | Lab   | RPD   | Field               | Lab     | RPD   |
| PC1            | 9/28/2010   | 0.954            | 0.0                | 0.031 | ----- | 38.3                | 35.48 | 7.6   | 2.0                 | 2.11    | -5.3  |
| WC1S           | 9/28/2010   | 0.762            | 7.8                | 8.60  | -9.8  | 13.4                | 12.54 | 6.6   | <0.1                | <0.0001 | ----- |
| PB1D           | 9/29/2010   | 0.785            | 6.2                | 7.26  | -     | 19.6                | 17.81 | 9.6   | <0.1                | <0.0001 | ----- |
| PB2D           | 9/29/2010   | 0.909            | 9.3                | 10.32 | -     | 14.0                | 14.00 | 0.0   | <0.1                | <0.0001 | ----- |
| PB2D Field Dup | 9/29/2010   | 0.909            | -----              | 10.33 | ----  | -----               | 14.03 | ----- | -----               | <0.0001 | ----- |
| PA1D           | 9/30/2010   | 0.842            | 14.0               | 14.57 | -4.0  | 10.0                | 9.50  | 5.1   | <0.1                | <0.0001 | ----- |
| PA2D           | 9/30/2010   | 0.800            | 6.8                | 7.03  | -3.3  | 18.4                | 16.71 | 9.6   | <0.1                | <0.0001 | ----- |
| PA2D Field Dup | 9/30/2010   | 0.800            | -----              | 7.02  | ----- | -----               | 16.75 | ----  | -----               | <0.0001 | ----- |
| PA2I           | 9/30/2010   | 0.800            | 11.6               | 12.03 | -3.6  | 11.8                | 11.05 | 6.6   | <0.1                | <0.0001 | ----- |
| PA3D           | 9/30/2010   | 0.738            | 17.2               | 17.91 | -4.0  | 3.9                 | 3.92  | -0.5  | <0.1                | <0.0001 | ----- |
| PA4D           | 9/30/2010   | 1.073            | 17.5               | 17.85 | -2.0  | 4.2                 | 4.10  | 2.4   | <0.1                | <0.0001 | ----- |

Note: The minimum concentration field measurement for O<sub>2</sub> was 0.1% so a comparison at a laboratory reported value of 0.031% is not applicable.

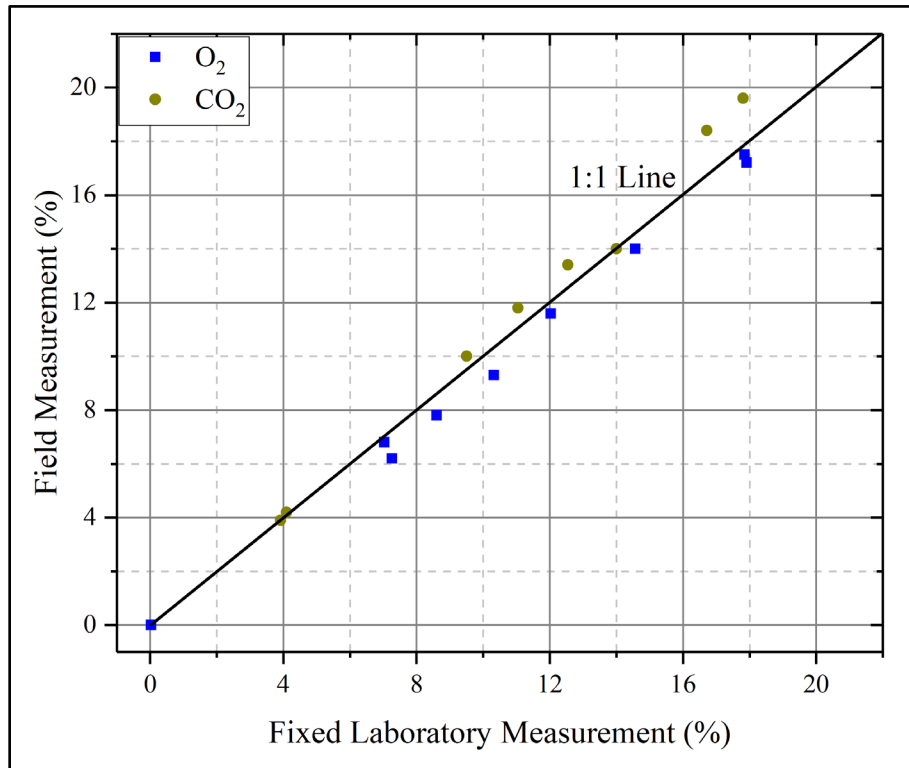


**Figure 26.** Comparison of measured O<sub>2</sub> and CO<sub>2</sub> concentrations using a GEM2000 Plus gas analyzer and fixed-laboratory analysis.

**Table 5.** Analytical Results of Travel and Equipment Blanks

| Sample          | Sample Date | O <sub>2</sub> (%) | CO <sub>2</sub> (%) | CH <sub>4</sub> (%) |
|-----------------|-------------|--------------------|---------------------|---------------------|
| Travel Blank    | 9/22/2010   | 0.030              | 0.016               | <0.0001             |
| Equipment Blank | 9/22/2010   | 0.098              | 0.020               | <0.0001             |
| Travel Blank    | 9/23/2010   | 0.054              | 0.009               | <0.0001             |
| Equipment Blank | 9/23/2010   | 0.026              | 0.014               | 0.0029              |
| Travel Blank    | 9/24/2010   | 0.025              | 0.006               | <0.0001             |
| Equipment Blank | 9/24/2010   | 0.032              | 0.015               | <0.0001             |
| Equipment Blank | 9/25/2010   | 0.025              | 0.008               | <0.0001             |
| Travel Blank    | 9/25/2010   | 0.030              | 0.007               | <0.0001             |
| Travel Blank    | 9/28/2010   | 0.021              | 0.008               | <0.0001             |
| Equipment Blank | 9/28/2010   | 0.051              | 0.015               | <0.0001             |
| Travel Blank    | 9/29/2010   | 0.045              | 0.008               | <0.0001             |
| Equipment Blank | 9/29/2010   | 0.030              | 0.014               | <0.0001             |
| Equipment Blank | 4/18/2011   | 0.520              | 0.015               | <0.0001             |
| Equipment Blank | 4/18/2011   | 0.055              | 0.010               | <0.0001             |
| Travel Blank    | 4/18/2011   | 0.060              | 0.010               | <0.0001             |

### 3.6 Results of Shut-in Testing

Well plugs used for 2.54 cm PVC wells were tested for vacuum loss over a 34-hour period. Vacuum dissipated slowly (**Figure 27**). At 90 kPa vacuum (nearly one atmosphere), leakage was less than 1 SCCM and declined to less than 0.01 SCCM below 40 kPa vacuum (**Figure 27**). Thus, 2.54 cm well caps used in this investigation were relatively gas-tight.

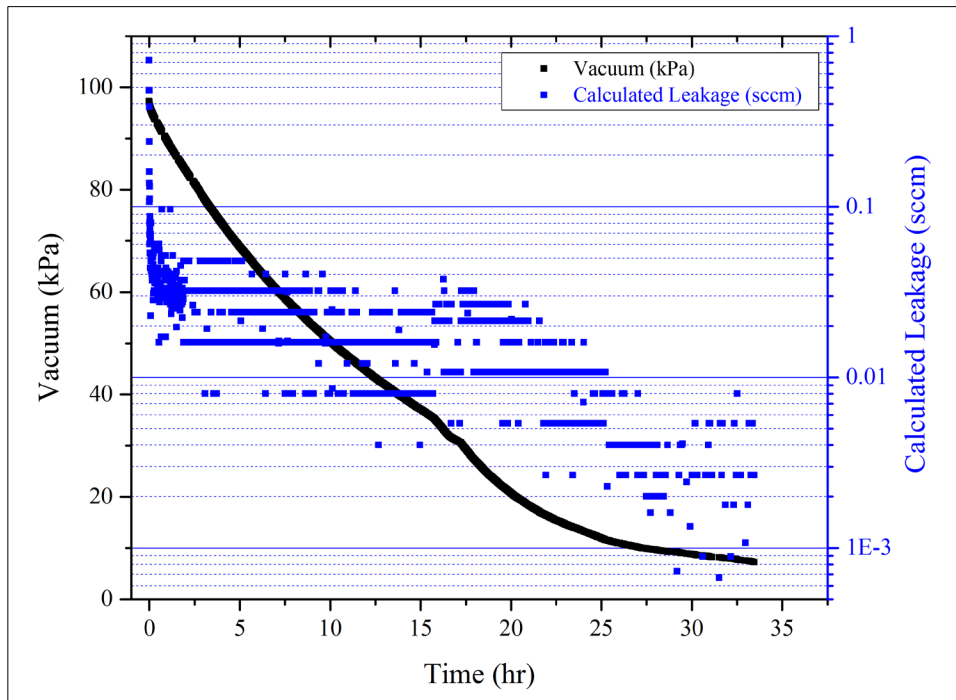


**Figure 27.** Vacuum loss and calculated leakage through vapor well caps

Vacuum testing of chamber fittings and tubing to vapor probes was conducted by periodically opening a toggle valve to atmospheric air to decrease vacuum, as illustrated in **Figure 28**. Even at 95 kPa of vacuum, leakage was < 0.2 SCCM.

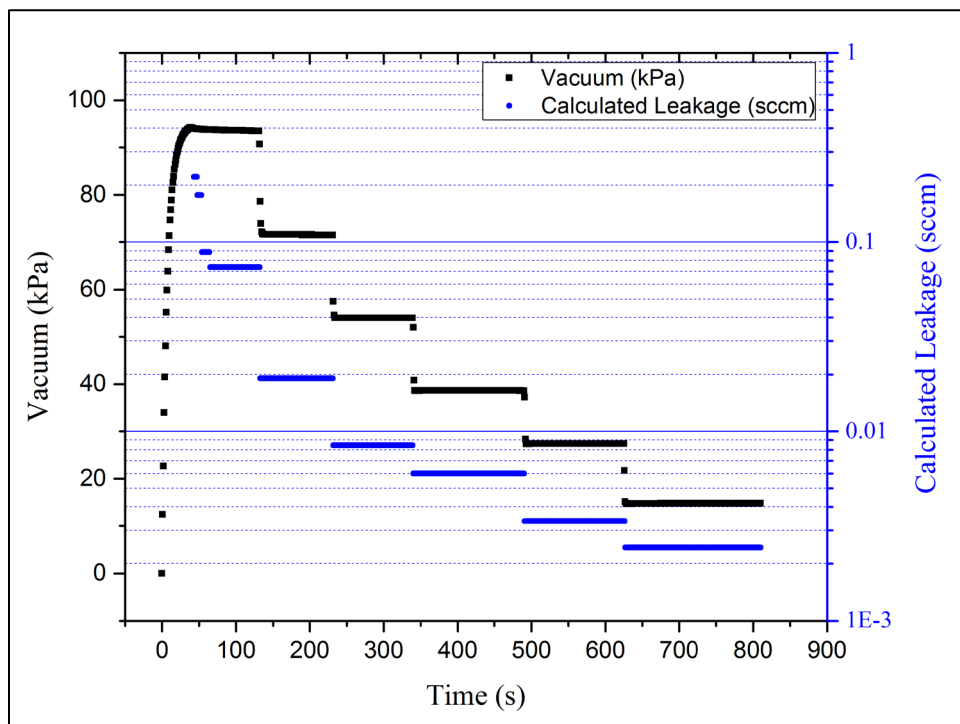


**Figure 28.** Applied vacuum (in steps) and calculated leakage in fittings used for leak chamber construction while testing at WB2S on 8/11/2009

As previously discussed, this procedure was time consuming in the field and was modified to three one-minute shut-in tests at high, medium, and low vacuum. Results of this testing is illustrated in **Figure 29**.

Leakage slightly exceeded the quality control criterion of 1 SCCM in 5 of 140 tests (3.6%) at a maximum flow rate of 1.8 SCCM. When leakage exceeded 1 SCCM, fittings were tightened and shut-in tests at high vacuum were repeated. In one instance, chamber fittings had to be disassembled and individually tested to determine the point of leakage. Given that flow rates used for soil-gas purging and sampling were typically 500 – 1000 SCCM, leakage through chamber fittings and tubing to vapor probes in this investigation was inconsequential.

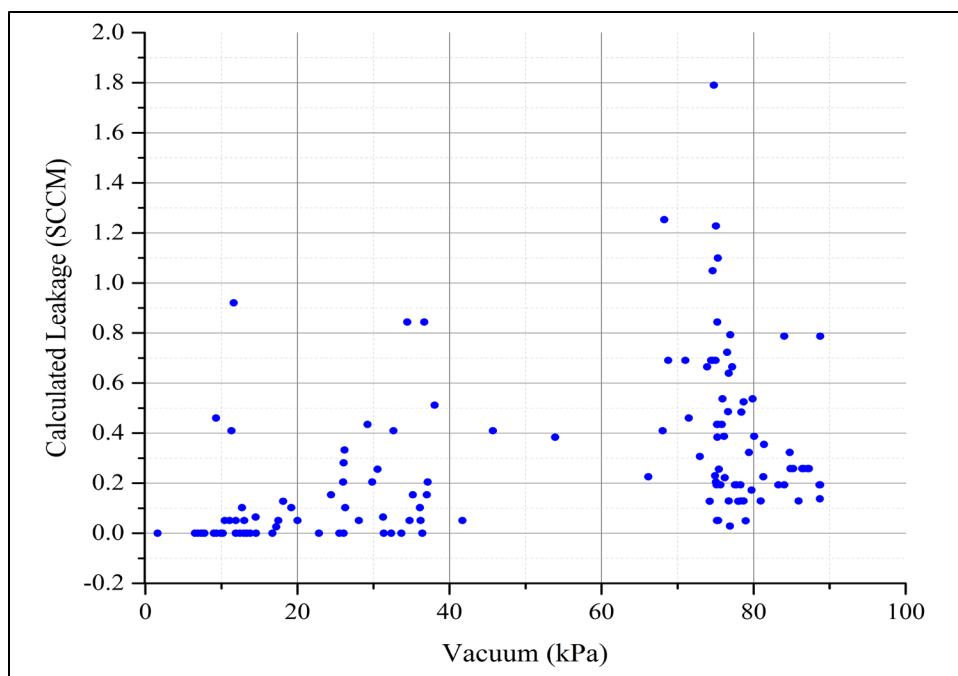


**Figure 29.** Calculated leakage from fittings used for leak chamber construction from one-minute vacuum tests (n=141).

### 3.7 Variation of Tracer Concentration in the Leak Detection Chamber Used for Vapor Probe Clusters

Gas tracer concentration at the point of injection inside the leak detection chamber generally increased rapidly (within tens of seconds) with time. In some cases, gas tracer concentration reached the concentration of injection (10,200 ppmv R-123) and remained constant until gas tracer injection was stopped. In other cases, gas tracer in the chamber did not reach the concentration of injection and was variable likely due to a poor seal between ground surface and the outside of the chamber. In these instances, the maximum concentration of gas tracer inside the chamber and in the soil-gas sampling train was used for leakage calculations.

### 3.8 Results of Leak Testing of Probe and Quick-Connect Compression Fittings

The results of leak testing Swagelok™ quick-connect compression fittings to stainless-steel tubing at Valley Center, KS at 4 (PA3I, PA3D, PA4I, PA4D) of 14 intermediate and deep probes in probe clusters are summarized in **Table 6**. As previously discussed, this type of leak testing is only relevant to intermediate and lower probes in a soil-gas probe cluster since leakage at a surface connection cannot be distinguished from leakage in a borehole. In this investigation,

testing of surface connections for the lowermost probes was often limited by recovery of water during vacuum application.

Leakage through this pathway was only observed at PA3I at 2.1% at a vacuum of only 0.21 kPa (0.84" water). A rapid rise in tracer concentration was detected in the soil-gas train upon introduction of R-123 into the leak detection chamber (**Figure 30**). Leakage at this rate did not impact O<sub>2</sub> and CO<sub>2</sub> concentrations observed during purging. At this probe, connecting compression fittings at the surface prior to insertion into the borehole did not preclude leakage reinforcing the need for this type of leak testing.

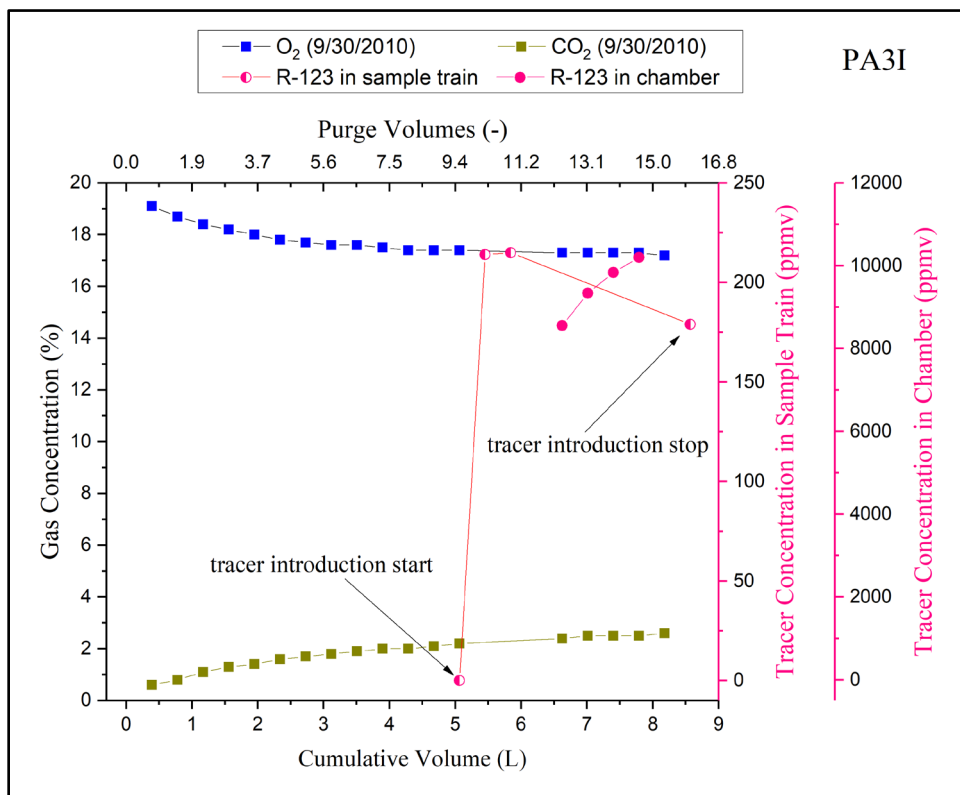


**Figure 30.** Leak testing of probe connection at surface at PA3I. 1 purge volume = 0.534 L.

**Table 6. Results of Leak Testing**

| Leakage Pathway                                 | Date       | Tracer | Tracer Location | Soil-Gas Extraction | Applied Vacuum (kPa) | Maximum Level in Chamber (ppmv) | Level in Sample Bag | Maximum Level in Sample Train (ppmv) | Leakage (%) |
|---|------------|--------|-----------------|---------------------|----------------------|---------------------------------|---------------------|--------------------------------------|-------------|
| <b>Leakage from Surface to Probe Connection</b> |            |        |                 |                     |                      |                                 |                     |                                      |             |
| surface→PA3I                                    | 9/30/2010  | R-123  | surface         | PA3I                | 0.21                 | 10,200                          | -----               | 215                                  | <b>2.1</b>  |
| surface→PA3D                                    | 9/30/2010  | R-123  | surface         | PA3I                | 0.17                 | 10,200                          | -----               | 3.8†                                 | 0           |
| surface→PA4I                                    | 9/30/2010  | R-123  | surface         | PA4I                | 0.16                 | 9,000                           | -----               | 2.9†                                 | 0           |
| surface→PA4D                                    | 9/30/2010  | R-123  | surface         | PA4D                | 0.20                 | 10,200                          | -----               | 6.5†                                 | 0           |
| <b>Leakage from Surface to Upper Probe</b>      |            |        |                 |                     |                      |                                 |                     |                                      |             |
| surface→ PA1S                                   | 8/4/2009   | -----  | no test         | PA1S                | 75                   | -----                           | -----               | low flow                             | -----       |
|   | 9/16/2009  | R-123  | surface         | PA1S                | 16.2                 | 6,778                           | -----               | 10†                                  | 0           |
|   | 11/14/2009 | R-123  | surface         | PA1S                | 16.9                 | 10,200                          | -----               | 4.0†                                 | 0           |
|   | 9/30/2010  | R-123  | surface         | PA1S                | 0.13                 | 10,200                          | -----               | 9,631                                | <b>94.4</b> |
| surface→PA2S                                    | 8/14/2009  | R-123  | surface         | PA2S                | 0.22                 | 3,300                           | -----               | 30                                   | <b>0.9</b>  |
|   | 9/15/2009  | R-123  | surface         | PA2S                | 0.04                 | 8,613                           | -----               | 4.8†                                 | 0           |
|   | 9/30/2010  | R-123  | surface         | PA2S                | 0.25                 | 9632                            | -----               | 0                                    | 0           |
| surface→PA3S                                    | 8/14/2009  | R-123  | surface         | PA3S                | 0.24                 | 3,200                           | -----               | 40                                   | <b>1.3</b>  |
|   | 9/15/2009  | R-123  | surface         | PA3S                | 0.45                 | 8,857                           | -----               | 4.0†                                 | 0           |
|   | 9/30/2010  | R-123  | surface         | PA3S                | 0.40                 | 5,885                           | -----               | 6.0†                                 | 0           |
| surface→PA4S                                    | 8/14/2009  | R-123  | surface         | PA4S                | 0.12                 | 3,418                           | -----               | 36                                   | <b>1.1</b>  |
|   | 9/16/2009  | R-123  | surface         | PA4S                | 0.32                 | 8,356                           | -----               | 17                                   | <b>0.2</b>  |
|   | 9/30/2010  | R-123  | surface         | PA4S                | 0.25                 | 10,200                          | -----               | 3.0†                                 | 0           |
| surface→PB1S                                    | 8/7/2009   | R-123  | surface         | PB1S                | 0.74                 | 10,200                          | -----               | 10                                   | <b>0.1</b>  |
|   | 9/15/2009  | R-123  | surface         | PB1S                | 0.25                 | 7,013                           | -----               | 14                                   | <b>0.2</b>  |
|   | 9/29/2010  | R-123  | surface         | PB1S                | 0.25                 | 6,200                           | -----               | 3.0†                                 | 0           |
| surface→PB2S                                    | 8/11/2009  | R-123  | surface         | PB2S                | 0.99                 | 10,200                          | -----               | 50                                   | <b>0.5</b>  |
|   | 9/15/2009  | R-123  | surface         | PB2S                | 2.12                 | 10,200                          | -----               | 29                                   | <b>0.3</b>  |
|   | 9/29/2010  | R-123  | surface         | PB2S                | 17.4                 | 10,200                          | -----               | 8.2†                                 | 0           |
| surface→PB3S                                    | 8/12/2009  | -----  | -----           | PB3S                | 84.2                 | -----                           | -----               | low flow                             | -----       |
|   | 9/15/2009  | -----  | -----           | PB3S                | 75                   | -----                           | -----               | low flow                             | -----       |
| <b>Leakage from Intermediate to Upper Probe</b> |            |        |                 |                     |                      |                                 |                     |                                      |             |
| PA1I→PA1S                                       | 9/16/2009  | CO     | PA1I            | PA1S                | 16.2                 | -----                           | 20,100              | 11,798                               | <b>58.7</b> |
|   | 9/16/2009  | CO     | PA1I            | PA1S                | 16.2                 | -----                           | 20,100              | 7246                                 | <b>36.0</b> |
|   | 11/14/2009 | CO     | PA1I            | PA1S                | 16.9                 | -----                           | 20,100              | 14,933                               | <b>74.3</b> |
|   | 9/30/2010  | CO     | PA1I            | PA1S                | 0.13                 | -----                           | 1,000               | 0                                    | 0           |
| PA2I→ PA2S                                      | 8/14/2009  | CO     | PA2I            | PA2S                | 0.22                 | -----                           | 20,100              | 3†                                   | 0           |
|   | 9/15/2010  | CO     | PA2I            | PA2S                | 0.04                 | -----                           | 20,100              | 0                                    | 0           |
|   | 9/30/2010  | CO     | PA2I            | PA2S                | 0.25                 | -----                           | 1,000               | 0                                    | 0           |
| PA3I→ PA3S                                      | 8/14/2009  | CO     | PA3I            | PA3S                | 0.24                 | -----                           | 20,100              | 0                                    | 0           |
|   | 9/15/2009  | CO     | PA3I            | PA3S                | 0.45                 | -----                           | 20,100              | 1†                                   | 0           |
|   | 9/30/2010  | CO     | PA3I            | PA3S                | 0.40                 | -----                           | 1,000               | 0                                    | 0           |
| PA4I→ PA4S                                      | 8/14/2009  | CO     | PA4I            | PA4S                | 0.12                 | -----                           | 20,100              | 0                                    | 0           |
|   | 9/16/2009  | -----  | -----           | -----               | -----                | -----                           | -----               | No test                              | -----       |
|   | 9/30/2010  | CO     | PA4I            | PA4S                | 0.25                 | -----                           | 1,000               | 0                                    | 0           |
| PB1I→PB1S                                       | 8/7/2009   | CO     | PB1I            | PB1S                | 0.74                 | -----                           | 20,100              | 4†                                   | 0           |
|   | 9/15/2009  | CO     | PB1I            | PB1S                | 0.25                 | -----                           | 20,100              | 0                                    | 0           |
|   | 9/29/2010  | CO     | PB1I            | PB1S                | 0.25                 | -----                           | 1,000               | 20                                   | <b>2.0</b>  |
| PB2I→PB2S                                       | 8/11/2009  | CO     | PB2I            | PB2S                | 0.99                 | -----                           | -----               | ++                                   | -----       |
|   | 9/15/2009  | CO     | PB2I            | PB2S                | 2.12                 | -----                           | -----               | ++                                   | -----       |
|   | 9/29/2010  | CO     | PB2I            | PB2S                | 17.4                 | -----                           | 1,000               | 0                                    | 0           |
| PA1S→PA1I                                       | 8/5/2009   | R-123  | PA1S            | PA1I                | 0.20                 | -----                           | -----               | †                                    | -----       |

| Leakage Pathway                                 | Date       | Tracer | Tracer Location | Soil-Gas Extraction | Applied Vacuum (kPa) | Maximum Level in Chamber (ppmv) | Level in Sample Bag | Maximum Level in Sample Train (ppmv) | Leakage (%) |
|---|------------|--------|-----------------|---------------------|----------------------|---------------------------------|---------------------|--------------------------------------|-------------|
| <b>Leakage from Intermediate to Lower Probe</b> |            |        |                 |                     |                      |                                 |                     |                                      |             |
| PA1I→PA1D                                       | 9/16/2009  | CO     | PA1I            | PA1D                | 2.22                 | ----                            | 20,100              | 112                                  | <b>0.6</b>  |
|   | 11/14/2009 | CO     | PA1I            | PA1D                | 0.46                 | ----                            | ----                | ‡                                    | ----        |
|   | 9/30/2010  | CO     | PA1I            | PA1D                | 0.41                 | ----                            | 1,000               | 0                                    | 0           |
| PA2I→PA2D                                       | 8/14/2009  | ----   | ----            | PA2D                | ----                 | ----                            | ----                | water                                | ----        |
|   | 9/15/2009  | ----   | ----            | PA2D                | ----                 | ----                            | ----                | water                                | ----        |
|   | 9/30/2010  | CO     | PA2I            | PA2D                | 0.17                 | ----                            | 1,000               | 0                                    | 0           |
| PA3I→PA3D                                       | 8/14/2009  | CO     | PA3I            | PA3D                | 0.11                 | ----                            | 20,100              | 1†                                   | 0           |
|   | 9/15/2009  | CO     | PA3I            | PA3D                | 0.50                 | ----                            | 20,100              | 9†                                   | 0           |
|   | 9/30/2010  | CO     | PA3I            | PA3D                | 0.17                 | ----                            | 1,000               | 0                                    | 0           |
| PA4I→PA4D                                       | 8/14/2009  | CO     | PA4I            | PA4D                | 0.14                 | ----                            | 20,100              | 5†                                   | 0           |
|   | 9/16/2009  | ----   | PA4I            | PA4D                | ----                 | ----                            | ----                | ----                                 | water       |
|   | 9/30/2010  | CO     | PA4I            | PA4D                | 0.20                 | ----                            | 1,000               | 0                                    | 0           |
| PB1I→PB1D                                       | 8/7/2009   | CO     | PB1I            | PB1D                | 0.19                 | ----                            | 20,100              | 4†                                   | 0           |
|   | 9/15/2009  | CO     | PB1I            | PB1D                | 0.20                 | ----                            | 20,100              | 0                                    | 0           |
|   | 9/29/2010  | CO     | PB1I            | PB1D                | 0.20                 | ----                            | 1,000               | 0                                    | 0           |
| PB2I→PB2D                                       | 8/11/2009  | CO     | PB2I            | PB2D                | 0.37                 | ----                            | ----                | ‡                                    | ----        |
|   | 9/29/2010  | CO     | PB2I            | PB2D                | 0.22                 | ----                            | 1,000               | 0                                    | 0           |
| PB3I→PB3D                                       | 8/13/2009  | ----   | ----            | PB3D                | ----                 | ----                            | ----                | ----                                 | water       |
|   | 9/15/2009  | ----   | ----            | PB3D                | ----                 | ----                            | ----                | ----                                 | water       |
| <b>Leakage from Lower to Intermediate Probe</b> |            |        |                 |                     |                      |                                 |                     |                                      |             |
| PA1D→PA1I                                       | 8/5/2009   | CO     | PA1D            | PA1I                | 0.20                 | ----                            | ----                | ‡                                    | ----        |
| PB2D→PB2I                                       | 9/15/2009  | CO     | PB2D            | PB2I                | 0.15                 | ----                            | 20,100              | 0                                    | 0           |
| <b>Leakage from Surface to Monitoring Well</b>  |            |        |                 |                     |                      |                                 |                     |                                      |             |
| surface→WA1S                                    | 8/5/2009   | R-123  | surface         | WA1S                | 0.30                 | not recorded                    | ----                | 0                                    | 0           |
| surface→WB1S                                    | 8/13/2009  | R-123  | surface         | WB2S                | 0.07                 | 7,700                           | ----                | 60                                   | <b>0.8</b>  |
| surface→WB2S                                    | 8/11/2009  | R-123  | Surface         | WB2S                | 2.06                 | not recorded                    | ----                | 0                                    | 0           |
|   | 9/15/2009  | R-123  | ----            | ----                | ----                 | not recorded                    | ----                | water                                | ----        |
| surface→WB2S                                    | 8/11/2009  | R-123  | surface         | WB2S                | 2.06                 | not recorded                    | ----                | ‡                                    | ----        |
|   | 9/15/2009  | -----  | ----            | WB2S                | 24.9                 | recorded                        | ----                | low flow                             | ----        |
| surface→WB3S                                    | 8/13/2009  | R-123  | surface         | WB3S                | 2.74                 | 10,200                          | ----                | 26                                   | <b>0.3</b>  |
|   | 9/15/2009  | ----   | ----            | WB3S                | ----                 | ----                            | ----                | water                                | ----        |
| surface→PC1                                     | 8/12/2009  | R-123  | surface         | PC1                 | 0.12                 | 9,430                           | ----                | 0                                    | 0           |
|   | 9/14/2009  | R-123  | surface         | PC1                 | 0.19                 | 8,696                           | ----                | 227                                  | <b>2.6</b>  |
|   | 9/28/2010  | R-123  | surface         | PC1                 | 0.19                 | 10,200                          | ----                | 144                                  | <b>1.4</b>  |
| surface→WC1S                                    | 8/13/2009  | R-123  | surface         | WC1S                | 1.57                 | 10,200                          | ----                | 9†                                   | 0           |
| surface→WC2S                                    | 8/13/2009  | ----   | ----            | WC2S                | ----                 | -----                           | ----                | water                                | ----        |

† - reading due to elevated background or instrument drift

‡ - readings not recorded or not properly recorded and hence not used

### 3.9 Results of Leak Testing Between Surface and Upper Probe in Probe Clusters

Leakage between the surface and an upper probe was tested 18 times at 6 probes (**Table 6**). Leak testing could not be conducted at one probe due to low flow or low gas permeability. Low concentrations (<10 ppmv) of tracer compound were detected in the soil-gas sampling train during 8 leak tests. However, these levels were similar to instrument drift and hence detection

was not considered leakage. Tracer concentrations between 10 – 50 ppmv resulted in quantification of leakage between 0.1 – 1.3% in 8 leak tests at 5 upper probes.

Significant leakage (94.4%) only occurred at PA1S in September 2010 (**Table 6**). Tracer concentration in the soil-gas sampling train exhibited a breakthrough curve (**Figure 31**) characteristic (tailing of concentration) of preferential or bypass gas flow in porous media (Popovičova and Brusseau 1998).

Gas tracer concentration was measured only once in the chamber during leak testing to enable continuous measurement of tracer concentrations in the soil-gas sampling train. Since O<sub>2</sub> and CO<sub>2</sub> gas concentrations were only measured at the beginning and end of leak testing, the impact of the tracer gas mixture on O<sub>2</sub> and CO<sub>2</sub> concentration profiles in the soil-gas train could not be evaluated. Introduction of argon from the tracer mixture would be expected to decrease O<sub>2</sub> and CO<sub>2</sub> concentrations in extracted soil gas.

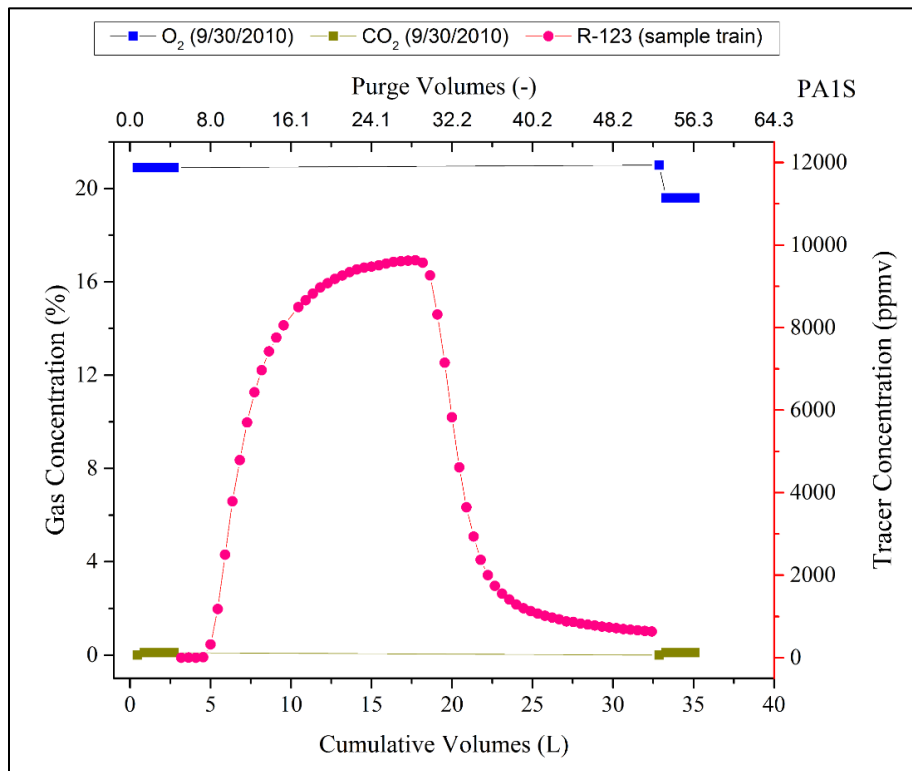


**Figure 31.** Testing of leakage from the surface at PA1S on 9/30/2010. Tracer mixture containing R-123 introduced at 3.6 L. Concentration of R-123 in chamber measured at 10,200 ppmv at 9.5 L of soil-gas extraction. 1 purge volume = 0.622 L

During two previous tests in September and November 2009, leakage was detected between the upper and the intermediate probe, PAII, but not from the surface to the upper probe indicating that a leakage pathway from the surface developed sometime after November 2009. This result indicates absence of leak detection in a previous soil-gas sampling event does not preclude development of leak pathways prior to later soil-gas sampling events.

### 3.10 Results of Leak Testing Between Upper and Intermediate Probes in Probe Clusters

Tracer was introduced into an intermediate probe with soil-gas extraction in the upper probe to test leakage between an intermediate probe and an upper probe 19 times at 7 probe clusters (**Table 6**). Results of 3 tests were not properly recorded and were discarded. The results of leak testing between PA1S and PA1I in September 2009 are illustrated in **Figure 32**.

Prior to testing leakage between PA1S and PA1I, leakage from the surface to PA1S was tested by injection of 10,200 ppmv R-123 in argon in a leak detection chamber. The maximum concentration of R-123 observed in the chamber was 6778 ppmv. Background readings of R-123 in the H25-IR were approximately 6 ppmv which rose to 10 ppmv during testing likely indicating instrument noise rather than leakage. During purging at 0.72 SLPM at 16.2 kPa (65 inches water) vacuum, an anomalous pattern of steadily increasing O<sub>2</sub> (to 4.4%) and CO<sub>2</sub> (to 12.9%) concentrations was observed (**Figure 32a**). A vacuum level of 0.70 kPa (2.8 inches of water) was observed at PA1I during this period indicating pneumatic communication between PA1S and PA1I.

Approximately 27 minutes after ending R-123 tracer testing, a gas tracer mixture containing 2.0% (20,100 ppmv) CO and 98% air (2.0% CO, 77.5% N<sub>2</sub>, 20.5% O<sub>2</sub> gas mixture) was passively introduced into PA1I and the probe was purged again. The concentration of O<sub>2</sub> in PA1S increased from 8.5 to 19.3% while the concentration of CO<sub>2</sub> decreased from 12.1% to 3.9% (**Figure 32b**) as a result of high O<sub>2</sub> and no CO<sub>2</sub> in the CO gas tracer mixture entering PA1I and migrating to PA1S. The experiment was prematurely ended prior to stabilization of tracer and gas concentrations. It is likely that O<sub>2</sub> would have continued to increase and CO<sub>2</sub> would have continued to decrease somewhat had the experiment continued. Tracer gas concentration reached a maximum of 11,800 ppmv indicating leakage at 59% leakage (**Figure 32b**). Change in CO<sub>2</sub> concentration indicated a similar magnitude of leakage at 68%.

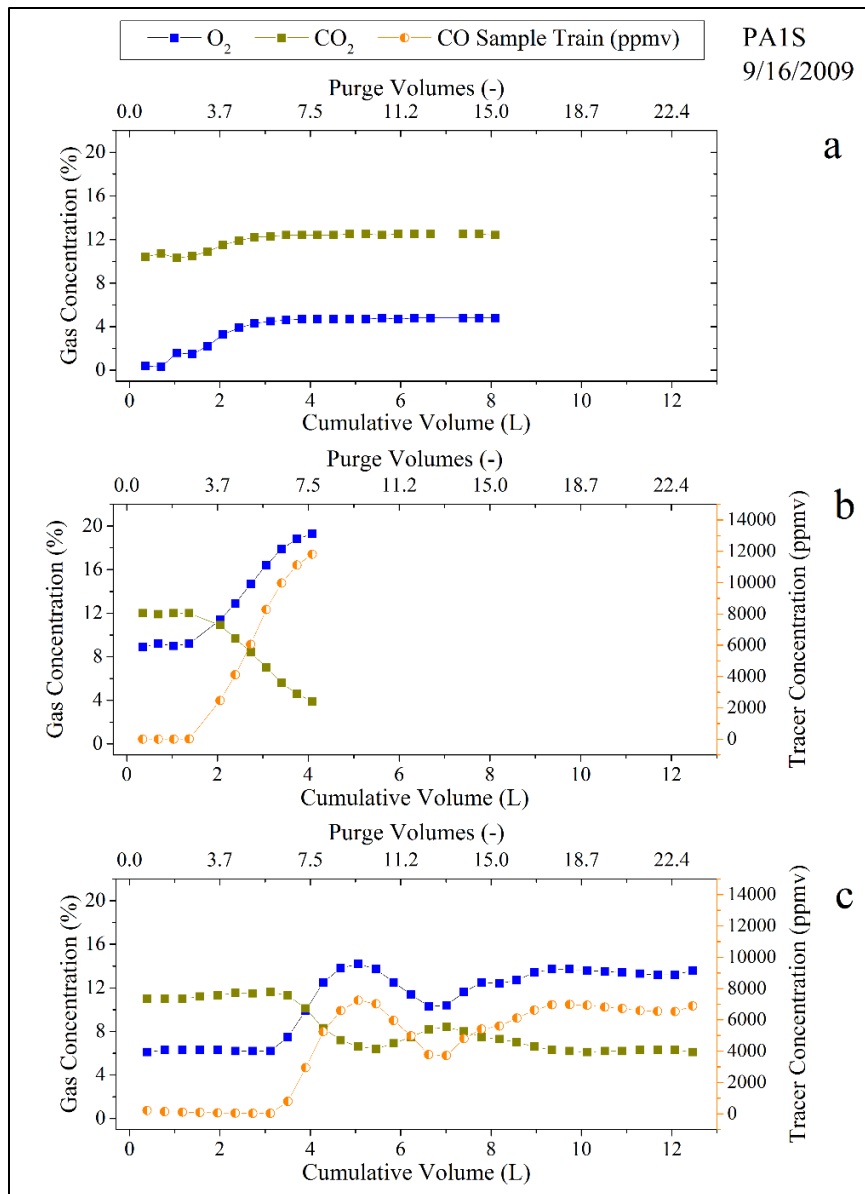


**Figure 32.** Results of leak testing between PA1S and PA1I on 9/16/2009 - soil-gas extraction from PA1S, 1 purge volume = 0.534 L: (a) Introduction of R-123 in chamber at the surface – no leakage from the surface observed, (b) introduction of 20,100 ppmv CO in PA1I, (c) repeat testing of (b).

Leak testing was then repeated. This time, tracer concentration increased to only 7246 ppmv (36% leakage) before decreasing to 3719 ppmv and then increasing to 6,933 ppmv (**Figure 32c**) indicating uneven flow of the gas tracer from the 5-liter Flex-Foil™ gas sampling bag. O<sub>2</sub> and CO<sub>2</sub> concentrations increased and decreased respectively with increasing tracer concentration demonstrating the effect of tracer concentration on measured O<sub>2</sub> and CO<sub>2</sub> concentrations.

Leakage during this test could also be calculated at 40% based on decreased CO<sub>2</sub> concentration.

It is unclear why gas flow from the sampling bag was variable. However, testing was conducted on a windy day necessitating holding of the gas sampling bag. This may have induced some contraction or pressurization of the gas sampling bag resulting in increased flow from the sampling bag. While tests indicated substantial gas communication between PA1S and PA1I, there was significant variation in estimates of leakage.

Leak testing was then conducted in November 2009. Similar to September 2009, leakage from the surface to PA1S was tested by injecting an R-123 gas tracer mixture in a leak detection chamber while purging at 0.74 SLPM and 16.9 kPa (68 inches of water) vacuum at PA1S. R-123 concentration in the chamber reached the injected concentration of 10,200 ppmv but was not detected in the soil-gas sampling train indicating no leakage. A vacuum level of 0.85 kPa (3.4 inches water) was observed at PA1I.

Unlike testing in September 2009, O<sub>2</sub> and CO<sub>2</sub> concentration decreased and increased, respectively during purging prior to introduction of tracer into PA1I (**Figure 33**).

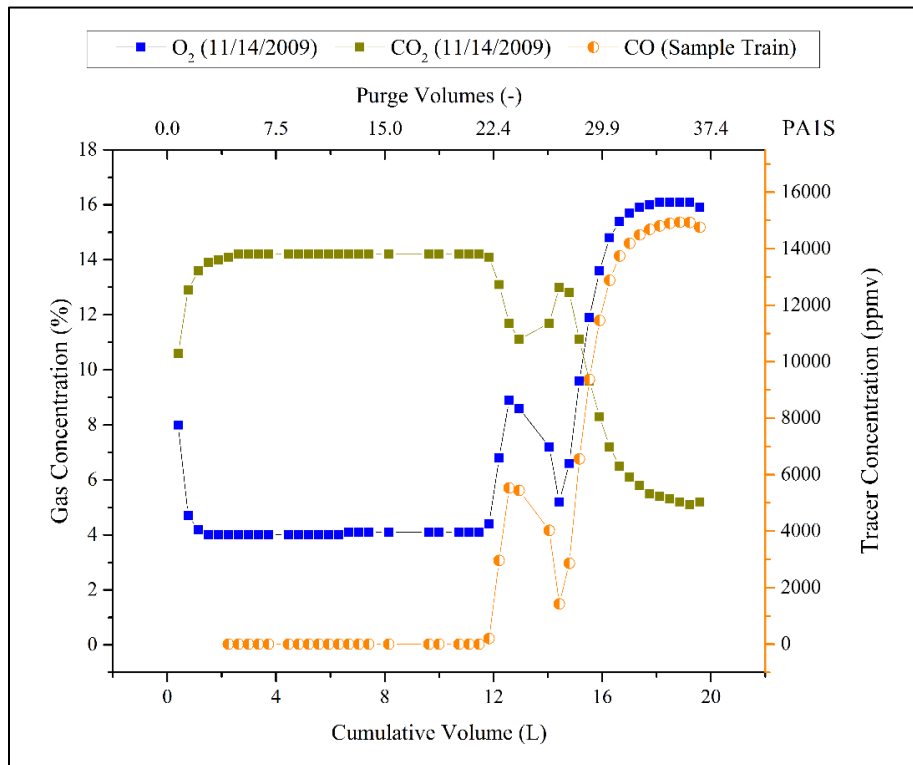


**Figure 33.** Leak testing between PA1S and PA1I on 11/14/2009. Soil-gas extraction from PA1S at 0.74 SLPM and 16.9 kPa vacuum. CO introduced in PA1I at 20,100 ppmv. 1 purge volume = 0.534 L.

However, similar to testing in September 2009, O<sub>2</sub> and CO<sub>2</sub> concentrations increased and decreased, respectively, in unison with increasing tracer concentration (**Figure 33**). Estimated leakage using the CO gas tracer mixture and decline in CO<sub>2</sub> concentration was 74% and 64%, respectively.

In September 2010, leakage from the surface to PA1S was tested by injecting an R-123 gas tracer mixture in a leak detection chamber while purging at 0.91 SLPM and 0.15 kPa (0.61 inches water) vacuum at PA1S. This vacuum level was significantly lower than previous soil-gas sampling events. As previously discussed, leakage from the surface was estimated at 94%. When a CO (1,000 ppmv) and air mixture was introduced into PA1I, no leakage from PA1I to PA1S was detected. Thus, in September and November 2009, most gas flow from PA1S came from the intermediate probe PA1I until a leakage pathway from PA1S to the surface developed after which nearly all gas flow came from the surface.

### 3.11 Results of Leak Testing Between an Intermediate and Lower Probe in a Probe Cluster

When a CO gas tracer mixture was introduced in an intermediate probe with soil-gas extraction in the lower probe to test leakage between an intermediate and lower probe, no leakage was observed in 10 tests at 5 intermediate-lower probe combinations (**Table 6**). Minor leakage (0.6%) was observed during one test at PA1I – PA1D. Testing could not be conducted 3 times due to entry of water as a result of vacuum application. A CO gas tracer mixture was also introduced in a lower probe with soil-gas extraction in an intermediate probe twice to test leakage. One test indicated no leakage. In the other test, data was not properly recorded to interpret results.

### 3.12 Results of Leak Testing Between the Surface and Sandpack of Monitoring Wells

Leakage between the surface and a screened interval in monitoring wells was tested 8 times at 6 monitoring wells (**Table 6**). Improper recording of test results precluded evaluation of leakage during one test. Upwelling of water and low gas flow precluded measurement of leakage during 3 and 1 tests, respectively. Leakage was observed at three monitoring wells at 0.8% (WB1S), 0.3% at WB3S, and 1.4 – 2.6% (PC1).

At PC1, R-123 tracer concentration in the soil-gas sampling train was somewhat erratic but increased throughout soil-gas extraction (**Figure 34**). Methane was detected during purging at this well due to a leak in a natural gas line within 1 meter of the monitoring well.

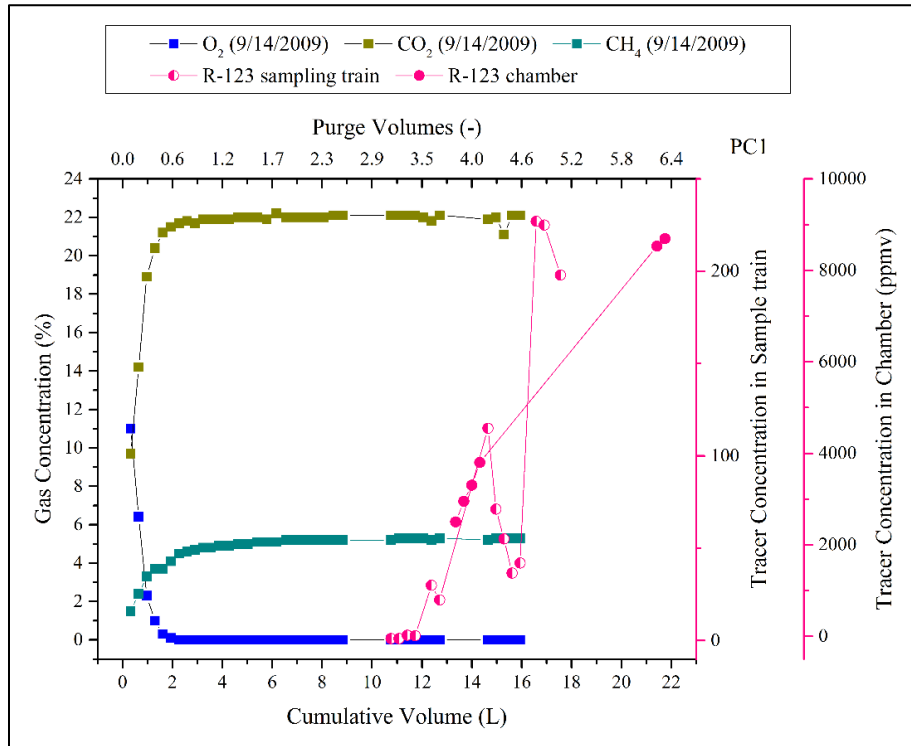


**Figure 34.** Results of leak testing at PC1 on 9/14/2009. 1 purge volume = 3.46 L

### 3.13 Development of a Heuristic Model of Leakage

A heuristic model, illustrated in **Figure 35**, can be used to provide a conceptual model to improve understanding of leakage in a borehole during soil-gas sampling. The length of the concrete and/or bentonite seal is denoted as ‘L’ [L]. Only vertical flow is allowed down a compromised borehole having an integrated gas permeability of  $k_1$  [ $L^2$ ]. In reality, radial gas flow will occur into the borehole above the screened interval in addition to vertical flow from the surface. Since gas flow in cracks is not simulated, the integrated permeability of the borehole incorporates the presence of cracks and openings in and around an essentially impermeable matrix of concrete and bentonite.

Only radial flow is allowed to a screened interval in a homogeneous (no discrete continuous or discontinuous layers) isotropic (radial permeability = vertical permeability) media having a gas permeability of ‘ $k_2$ ’ [ $L^2$ ]. The length of the screened interval is denoted as ‘b’ [L]. The radius of

the borehole is denoted as ‘ $r_1$ ’ [L] while the radius from the center of a borehole to an outer boundary at atmospheric pressure is denoted as  $r_2$  [L]. Atmospheric pressure ‘ $P_{atm}$ ’ [ML<sup>-1</sup>T<sup>-2</sup>] is present at the top of the borehole and at  $r_2$ . Applied vacuum at absolute pressure ‘ $P_{well}$ ’ [ML<sup>-1</sup>T<sup>-2</sup>] is present at  $r_1$  throughout the screened interval.

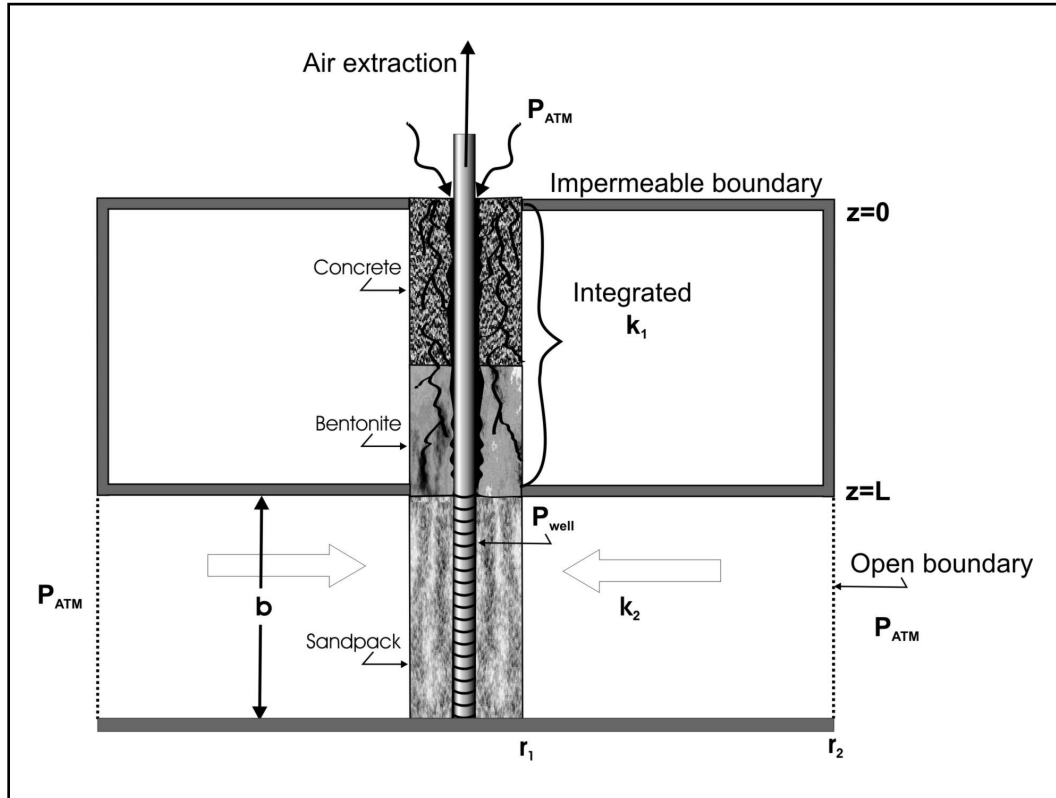


**Figure 35.** Schematic of heuristic model used to evaluate leakage.

The governing equation for one-dimensional homogeneous isothermal steady-state compressible gas flow neglecting slippage and buoyancy is:

$$\frac{d}{dz} \left( \frac{d\phi}{dz} \right) = 0 \quad (26)$$

where

$\phi$  = pressure squared [ML<sup>-1</sup>T<sup>-2</sup>]<sup>2</sup> and

$z$  [L] is the vertical coordinate (positive downward).

When subject to the boundary conditions:

$$\phi(0) = \phi_{\text{atm}} \quad \text{and} \quad \phi(L) = \phi_{\text{well}},$$

Darcy's Law can be used to express vertical volumetric flux ( $Q_z$ ) at  $z = L$  as:

$$Q_z = \pi r_1^2 \frac{k_1}{2\mu P_{\text{well}}} \left( \frac{\phi_{\text{atm}} - \phi_{\text{well}}}{L} \right) \quad (27)$$

where

$\phi_{\text{atm}}$  = atmospheric pressure squared at  $z = 0$  (surface) and

$\phi_{\text{well}}$  = pressure squared at the well at  $z = L$  (depth of sandpack or screened interval), and

$\mu$  = viscosity of gas [ $\text{ML}^{-1}\text{T}^{-1}$ ].

The governing equation for radial homogeneous isothermal steady-state compressible gas flow is:

$$\frac{d}{dr} \left( r \frac{d\phi}{dr} \right) = 0 \quad (28)$$

where  $r$  is the radial coordinate (positive away from well). When subject to boundary conditions:

$$\phi(r_1) = \phi_{\text{well}} \quad \text{and} \quad \phi(r_2) = \phi_{\text{atm}}$$

Darcy's Law can be used to express volumetric radial flux ( $Q_r$ ) at  $r = r_w$  as:

$$Q_r = \frac{\pi b k_2}{\mu P_{\text{well}}} \frac{(\phi_{\text{atm}} - \phi_{\text{well}})}{\ln(r_2 / r_1)}. \quad (29)$$

Leakage ( $\xi$ ) is a non-dimensional term defined as flow through the leakage pathway divided by total flow

$$\xi = \frac{Q_z}{Q_z + Q_r}. \quad (30)$$

After cancelling units,

$$\xi = \frac{1}{1 + \alpha(k_2/k_1)} \quad (31)$$

where  $\alpha$  is a dimensionless coefficient defined as:

$$\alpha = \frac{2bL}{r_1^2 \ln(r_2/r_1)} \quad (32)$$

The dimensionless coefficient  $\alpha$  is a combination of geometric parameters. For a given borehole radius, as the length of the bentonite seal increases,  $\alpha$  increases, thus, leakage decreases. Given relatively large values of the length of a bentonite seal and length of a screened interval compared to the radius of a borehole and logarithmic ratio of propagated vacuum, values of  $\alpha$  will always be greater than one. Hence, when  $k_2/k_1$  or the ratio of radial permeability in the sampled formation is greater than 100X, leakage will be less than 1.0% regardless of  $\alpha$ . Thus, detection of leakage is less likely when a probe is screened in high permeability media such as sand and more likely when a probe is screened in low permeability media such as silt or clay as one would expect. Thus, leak testing is of considerable importance when collecting soil-gas samples from lower permeability media.

### 3.14 Simulation of Shallow Leak Testing with Vertical Pathways

Gas flow simulations were conducted to illustrate difficulty in discerning leakage down a borehole from leakage due to atmospheric recharge when soil-gas sampling is shallow (e.g., < 0.5 m) and desiccation cracks or vertical pathways are present in soil.

Gas flow simulations were conducted using SAIRFLOW (DiGiulio and Varadhan 2001). Two scenarios were considered. In the first scenario, gas is extracted at 0.900 SLPM from soil having a radial gas permeability ( $k_r$ ) of  $1.4e-07 \text{ cm}^2$  under isotropic conditions or a ratio of radial to vertical gas permeability ( $k_r/k_z$ ) = 1.0, and a gas filled porosity of 0.01. In the second scenario, radial permeability remains the same but preferential pathways are simulated by inducing anisotropic conditions where  $k_r/k_z = 0.1$  (vertical gas permeability 10X radial permeability), and a gas filled porosity of 0.05 (reduced from previous simulation to increase gas velocity through soil cracks). The results of simulation are illustrated in **Figure 36**.

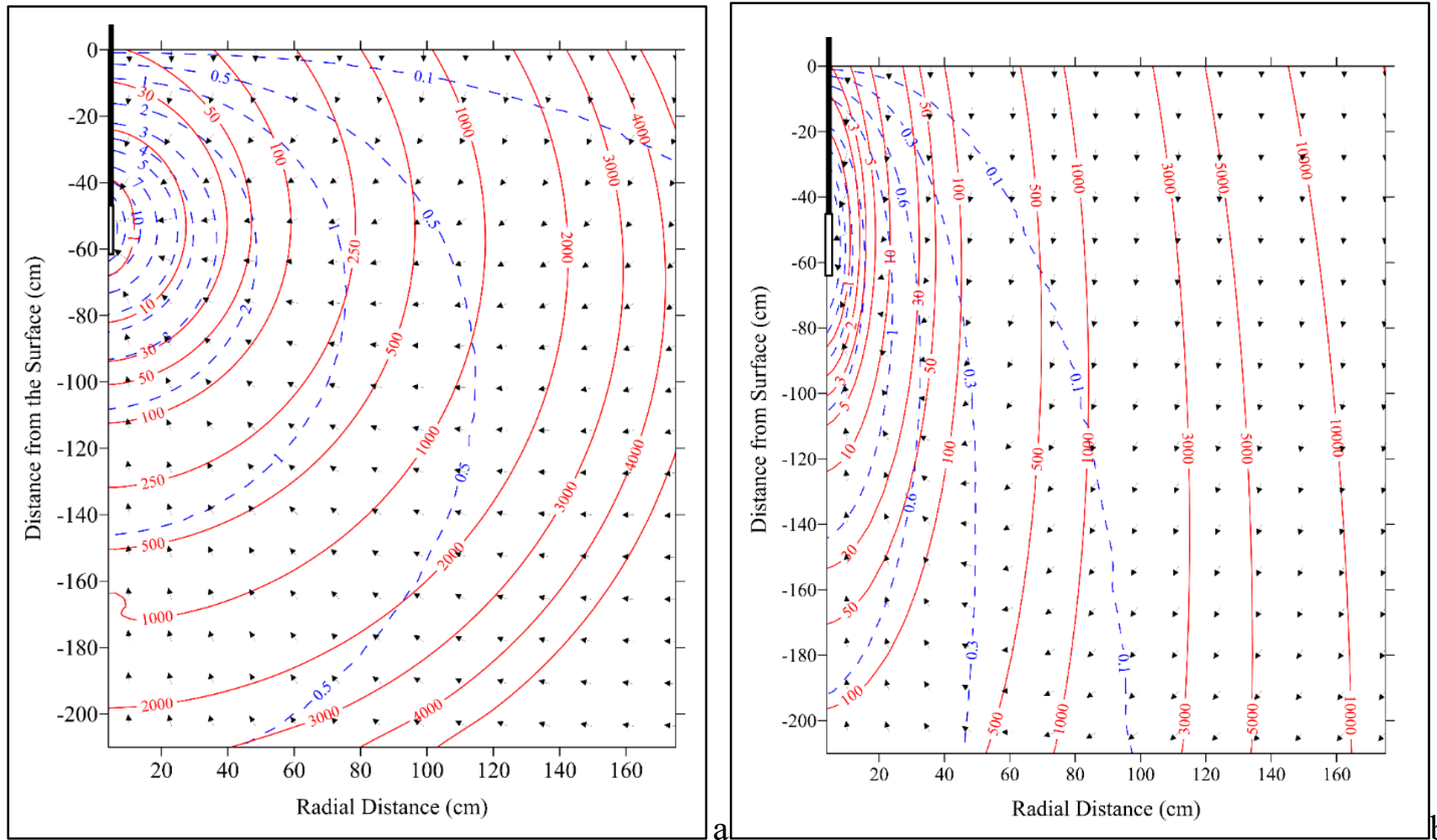


**Figure 36.** Simulation of gas flow at 0.900 SLPM to a screen interval between 0.46 – 0.60 m with a well diameter of 2.5 cm. Blue dashed lines are vacuum (Pa), red solid lines are travel time to the probe (min), arrows denote velocity (cm/s), (a) gas porosity = 0.1,  $k_r/k_z = 1.0$ ,  $k_r = 1.4e-07 \text{ cm}^2$ ; (b) gas porosity = 0.05,  $k_r/k_z = 0.1$ ,  $k_r = 1.4e-07 \text{ cm}^2$ .

Under isotropic conditions, it takes approximately 50 minutes for a gas tracer to enter the soil-gas sampling train (**Figure 36a**). Thus, in the absence of leakage down the borehole, deep desiccation cracks or preferential vertical downward gas flow, gas tracer should not be detected at this depth (leakage should be detected in minutes). However, under anisotropic conditions, gas tracer arrives in the soil-gas sampling train within only 3 minutes (the time period in which leakage testing was performed in this investigation) (**Figure 36b**).

In the latter scenario, leakage preferential pathways (cracks) through soil cannot be differentiated from leakage between the borehole and well casing. In this situation, leak testing could be conducted with and without a surface seal (e.g., bentonite and water) to differentiate atmospheric recharge through cracks from leakage down the borehole.

Shallow (e.g., < 5 ft or 1.5 meter) soil-gas sampling is generally discouraged in guidance documents to support vapor intrusion investigation (Atlantic Partnership in Risk-Based Corrective Action Implementation 2006, American Petroleum Institute 2005, British Columbia Ministry of Environment 2006, Canadian Council of Ministers of the Environment 2008, Electric Power Research Institute 2005, Interstate Technology & Regulatory Council 2007, Missouri Department of Natural Resources 2013, New Jersey Department of Environmental Protection 2005, Ontario Ministry of Environment 2007) due to concern of an increased likelihood of leakage down a borehole, atmospheric recharge during sampling, and expectation of lower soil-gas concentration compared to concentration at greater depth. However, the presence of shallow bedrock or cobbles sometimes necessitates collection of shallow soil-gas samples. In this case, a surface seal may be useful during soil-gas sample collection.

### 3.15 Estimation of Vacuum Loss in Tubing and Fittings

Determination of vacuum loss in tubing and fittings at the surface was necessary to determine vacuum at the sandpack or Geoprobe tip for gas permeability estimation. Vacuum loss in surface fittings varied from 10 to 40 Pa at 0.2 to 1.0 SLPM (**Figure 37**). A non-linear equation ( $R^2 = 0.998$ ) that was used to estimate vacuum loss as function of flow fit the dataset well (**Figure 37**). In soils having lower gas permeability, vacuum loss due to surface fittings and tubing was minor compared to induced vacuum during gas extraction (**Table 7, Figures 38a, b**) indicating little potential for error in estimation of gas permeability due to uncertainty in vacuum loss from

surface fittings and tubing. However, there were several instances in higher permeability soils where vacuum induced by soils was equivalent to or less than vacuum induced by fittings and tubing (**Figure 38c**). A situation in which measured vacuum at the surface is mostly due to fittings and tubing is undesirable. In these instances, there is increased potential for error in estimating gas permeability.

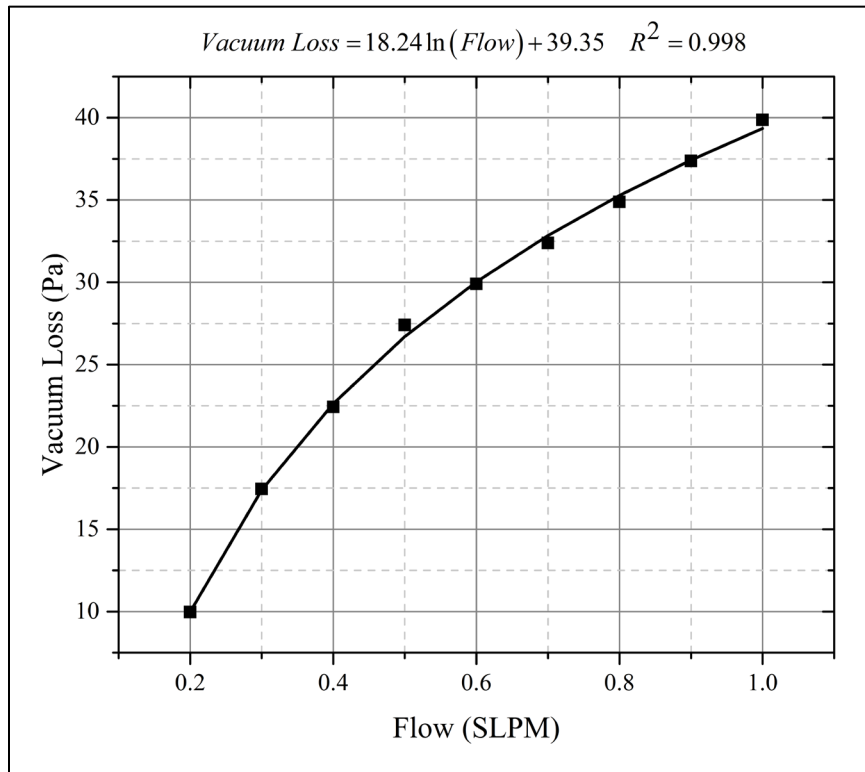


**Figure 37.** Vacuum loss (Pa) as a function of flow (SLPM) at the surface due to fittings associated with the leak detection chamber

In soil-gas probe clusters where dedicated stainless-steel tubing is used for probe construction, potential error associated with gas permeability estimation in higher permeability soils due to both tubing and surface fittings could be eliminated by inserting small diameter tubes to measure vacuum and pressure next to screened intervals used for gas extraction or injection. Thus, in a soil-gas probe cluster having 3 screened intervals, 6 tubes would have to be set and sealed in the borehole. An alternative and more practical approach is to simply use larger diameter tubing.

**Table 7.** Input parameters and results of gas permeability estimation

| Probe | Date       | Atmospheric Pressure (Pa) | Radius Sandpack (cm) | Diameter Tubing (cm) | Lower Permeability Layer (m) | Top Sandpack (m) | Base Sandpack (m) | Water Depth (m) | Flow (SLPM) | Reynolds Number | Vacuum at Surface (Pa) | Estimated Vacuum Loss Fittings (Pa) | Estimated Vacuum Loss Tubing (Pa) | Estimated Vacuum at Sandpack (Pa) | Ratio of Sandpack to Borehole Radius | kr for Prolate Spheriod Solution (cm2) | kr for Axisymmetric Solution (cm2) | Ratio Axisymmetric to Prolate Spheriod | Soil Description               |
|-------|------------|---------------------------|----------------------|----------------------|------------------------------|------------------|-------------------|-----------------|-------------|-----------------|------------------------|-------------------------------------|-----------------------------------|-----------------------------------|--------------------------------------|--|------------------------------------|--|--------------------------------|
| PA1S  | 9/16/2009  | 101300                    | 3.81                 | 0.62                 | 0.00                         | 1.37             | 1.62              | 4.66            | 0.718       | 174             | 17440                  | 33.31                               | 12.45                             | 17394                             | 6.4                                  | 1.74E-10                               | 1.89E-10                           | 1.09                                   | black plastic clay             |
| PA1S  | 9/16/2009  | 101300                    | 3.81                 | 0.62                 | 0.00                         | 1.37             | 1.62              | 4.66            | 0.779       | 189             | 14949                  | 34.79                               | 13.12                             | 14901                             | 6.4                                  | 2.18E-10                               | 2.37E-10                           | 1.09                                   | black plastic clay             |
| PA1S  | 11/14/2009 | 101300                    | 3.81                 | 0.62                 | 0.00                         | 1.37             | 1.62              | 4.66            | 0.738       | 179             | 16942                  | 33.81                               | 12.72                             | 16895                             | 6.4                                  | 1.84E-10                               | 2.00E-10                           | 1.09                                   | black plastic clay             |
| PA1S  | 9/30/2010  | 101300                    | 3.81                 | 0.62                 | 0.00                         | 1.37             | 1.62              | 4.66            | 0.909       | 221             | 130                    | 37.61                               | 13.07                             | 79                                | 6.4                                  | 4.45E-08                               | 4.84E-08                           | 1.09                                   | black plastic clay             |
| PA1I  | 8/5/2009   | 101300                    | 3.81                 | 0.62                 | 2.13                         | 2.74             | 3.20              | 4.66            | 0.705       | 171             | 187                    | 32.97                               | 20.09                             | 134                               | 12.0                                 | 1.45E-08                               | 1.84E-08                           | 1.27                                   | friable brown clay             |
| PA1I  | 9/16/2009  | 101300                    | 3.81                 | 0.62                 | 2.13                         | 2.74             | 3.20              | 4.66            | 0.718       | 174             | 872                    | 33.31                               | 20.60                             | 818                               | 12.0                                 | 2.43E-09                               | 2.71E-09                           | 1.12                                   | friable brown clay             |
| PA1I  | 9/16/2009  | 101300                    | 3.81                 | 0.62                 | 2.13                         | 2.74             | 3.20              | 4.66            | 0.909       | 221             | 1046                   | 37.61                               | 26.12                             | 983                               | 12.0                                 | 2.56E-09                               | 3.12E-09                           | 1.22                                   | friable brown clay             |
| PA1I  | 11/4/2009  | 101300                    | 3.81                 | 0.62                 | 2.13                         | 2.74             | 3.20              | 4.66            | 0.909       | 221             | 1320                   | 37.61                               | 26.19                             | 1257                              | 12.0                                 | 2.00E-09                               | 2.22E-09                           | 1.11                                   | friable brown clay             |
| PA1I  | 9/30/2010  | 101300                    | 3.81                 | 0.62                 | 2.13                         | 2.74             | 3.20              | 4.66            | 0.886       | 215             | 668                    | 37.14                               | 25.36                             | 605                               | 12.0                                 | 4.04E-09                               | 5.00E-09                           | 1.24                                   | friable brown clay             |
| PA1D  | 8/5/2009   | 101300                    | 3.81                 | 0.62                 | 2.13                         | 4.27             | 4.66              | 4.66            | 0.646       | 157             | 174                    | 31.38                               | 26.82                             | 116                               | 10.4                                 | 1.67E-08                               | 2.31E-08                           | 1.39                                   | medium-grained sand            |
| PA1D  | 9/16/2009  | 101300                    | 3.81                 | 0.62                 | 2.13                         | 4.27             | 4.66              | 4.66            | 0.738       | 179             | 897                    | 33.81                               | 30.86                             | 832                               | 10.4                                 | 2.67E-09                               | 3.51E-09                           | 1.32                                   | medium-grained sand            |
| PA1D  | 9/16/2009  | 101300                    | 3.81                 | 0.62                 | 2.13                         | 4.27             | 4.66              | 4.66            | 0.931       | 226             | 1221                   | 38.05                               | 39.05                             | 1144                              | 10.4                                 | 2.45E-09                               | 3.23E-09                           | 1.32                                   | medium-grained sand            |
| PA1D  | 11/14/2009 | 101300                    | 3.81                 | 0.62                 | 2.13                         | 4.27             | 4.66              | 4.66            | 0.931       | 226             | 473                    | 38.05                               | 38.76                             | 397                               | 10.4                                 | 7.04E-09                               | 9.54E-09                           | 1.35                                   | medium-grained sand            |
| PA1D  | 9/30/2010  | 101300                    | 3.81                 | 0.62                 | 2.13                         | 4.27             | 4.66              | 4.66            | 0.842       | 204             | 414                    | 36.21                               | 35.03                             | 342                               | 10.4                                 | 7.38E-09                               | 1.00E-08                           | 1.36                                   | medium-grained sand            |
| WA1S  | 8/5/2009   | 101300                    | 3.81                 | 5.08                 | 2.13                         | 3.96             | 4.66              | 4.66            | 0.864       | 25              | 299                    | 36.68                               | 0.01                              | 262                               | 18.4                                 | 6.94E-09                               | 9.30E-09                           | 1.34                                   | medium-grained sand            |
| PA2S  | 8/14/2009  | 101300                    | 3.81                 | 0.62                 | 1.52                         | 2.35             | 2.65              | 4.66            | 0.886       | 215             | 224                    | 37.14                               | 20.92                             | 166                               | 8.0                                  | 1.84E-08                               | 2.13E-08                           | 1.15                                   | friable brown clay             |
| PA2S  | 9/15/2009  | 101300                    | 3.81                 | 0.62                 | 1.52                         | 2.35             | 2.65              | 4.66            | 0.738       | 179             | 249                    | 33.81                               | 17.43                             | 198                               | 8.0                                  | 1.29E-08                               | 1.48E-08                           | 1.15                                   | friable brown clay             |
| PA2S  | 9/30/2010  | 101300                    | 3.81                 | 0.62                 | 1.52                         | 2.35             | 2.65              | 4.66            | 0.842       | 204             | 249                    | 36.21                               | 19.89                             | 193                               | 8.0                                  | 1.51E-08                               | 1.75E-08                           | 1.16                                   | friable brown clay             |
| PA2I  | 8/14/2009  | 101300                    | 3.81                 | 0.62                 | 1.52                         | 3.14             | 3.81              | 4.66            | 0.842       | 204             | 224                    | 36.21                               | 28.57                             | 159                               | 17.6                                 | 1.15E-08                               | 1.36E-08                           | 1.19                                   | fine- to medium-grained sand   |
| PA2I  | 9/15/2009  | 101300                    | 3.81                 | 0.62                 | 1.52                         | 3.14             | 3.81              | 4.66            | 0.738       | 179             | 224                    | 33.81                               | 25.04                             | 165                               | 17.6                                 | 9.68E-09                               | 1.14E-08                           | 1.18                                   | fine- to medium-grained sand   |
| PA2I  | 9/30/2009  | 101300                    | 3.81                 | 0.62                 | 1.52                         | 3.14             | 3.81              | 4.66            | 0.800       | 194             | 174                    | 35.28                               | 27.13                             | 112                               | 17.6                                 | 1.55E-08                               | 1.86E-08                           | 1.20                                   | fine- to medium-grained sand   |
| PA2D  | 9/30/2009  | 101300                    | 3.81                 | 0.62                 | 1.52                         | 4.36             | 4.66              | 4.66            | 0.800       | 194             | 174                    | 35.28                               | 33.21                             | 106                               | 8.0                                  | 2.61E-08                               | 3.61E-08                           | 1.38                                   | coarse-grained sand            |
| PA3S  | 8/14/2009  | 101300                    | 3.81                 | 0.62                 | 2.44                         | 2.56             | 2.87              | 4.66            | 0.779       | 189             | 237                    | 34.79                               | 19.88                             | 182                               | 8.0                                  | 1.48E-08                               | 1.92E-08                           | 1.30                                   | friable brown clay             |
| PA3S  | 9/15/2009  | 101300                    | 3.81                 | 0.62                 | 2.44                         | 2.56             | 2.87              | 4.66            | 0.909       | 221             | 461                    | 37.61                               | 23.25                             | 400                               | 8.0                                  | 7.87E-09                               | 1.00E-08                           | 1.27                                   | friable brown clay             |
| PA3S  | 9/15/2009  | 101300                    | 3.81                 | 0.62                 | 2.44                         | 2.56             | 2.87              | 4.66            | 0.738       | 179             | 399                    | 33.81                               | 18.86                             | 346                               | 8.0                                  | 7.39E-09                               | 9.40E-09                           | 1.27                                   | friable brown clay             |
| PA3S  | 9/15/2009  | 101300                    | 3.81                 | 0.62                 | 2.44                         | 2.56             | 2.87              | 4.66            | 0.909       | 221             | 448                    | 37.61                               | 23.25                             | 388                               | 8.0                                  | 8.12E-09                               | 1.04E-08                           | 1.28                                   | friable brown clay             |
| PA3S  | 9/30/2010  | 101300                    | 3.81                 | 0.62                 | 2.44                         | 2.56             | 2.87              | 4.66            | 0.800       | 194             | 349                    | 35.28                               | 20.44                             | 293                               | 8.0                                  | 9.45E-09                               | 1.04E-08                           | 1.10                                   | friable brown clay             |
| PA3I  | 8/14/2009  | 101300                    | 3.81                 | 0.62                 | 2.44                         | 3.35             | 3.66              | 4.66            | 0.909       | 221             | 548                    | 37.61                               | 29.71                             | 481                               | 8.0                                  | 6.55E-09                               | 7.73E-09                           | 1.18                                   | fine- to medium-grained sand   |
| PA3I  | 9/15/2009  | 101300                    | 3.81                 | 0.62                 | 2.44                         | 3.35             | 3.66              | 4.66            | 0.909       | 221             | 399                    | 37.61                               | 29.66                             | 331                               | 8.0                                  | 9.50E-09                               | 1.13E-08                           | 1.19                                   | fine- to medium-grained sand   |
| PA3I  | 9/30/2010  | 101300                    | 3.81                 | 0.62                 | 2.44                         | 3.35             | 3.66              | 4.66            | 0.779       | 189             | 209                    | 34.79                               | 25.37                             | 149                               | 8.0                                  | 1.81E-08                               | 2.19E-08                           | 1.21                                   | fine- to medium-grained sand   |
| PA3D  | 8/14/2009  | 101300                    | 3.81                 | 0.62                 | 2.44                         | 4.27             | 4.66              | 4.66            | 0.821       | 199             | 132                    | 35.75                               | 34.07                             | 62                                | 10.4                                 | 3.95E-08                               | 5.67E-08                           | 1.43                                   | coarse-grained sand            |
| PA3D  | 9/15/2009  | 101300                    | 3.81                 | 0.62                 | 2.44                         | 4.27             | 4.66              | 4.66            | 0.738       | 179             | 473                    | 33.81                               | 30.73                             | 409                               | 10.4                                 | 5.42E-09                               | 7.35E-09                           | 1.36                                   | coarse-grained sand            |
| PA3D  | 9/15/2009  | 101300                    | 3.81                 | 0.62                 | 2.44                         | 4.27             | 4.66              | 4.66            | 0.909       | 221             | 498                    | 37.61                               | 37.85                             | 423                               | 10.4                                 | 6.45E-09                               | 8.82E-09                           | 1.37                                   | coarse-grained sand            |
| PA3D  | 9/30/2010  | 101300                    | 3.81                 | 0.62                 | 2.44                         | 4.27             | 4.66              | 4.66            | 0.738       | 179             | 149                    | 33.81                               | 30.63                             | 85                                | 10.4                                 | 2.60E-08                               | 3.68E-08                           | 1.42                                   | coarse-grained sand            |
| PA4S  | 8/14/2009  | 101300                    | 3.81                 | 0.62                 | 1.22                         | 1.98             | 2.29              | 4.66            | 0.909       | 221             | 80                     | 37.61                               | 18.48                             | 24                                | 8.0                                  | 1.33E-07                               | 1.57E-07                           | 1.18                                   | fine-grained sand              |
| PA4S  | 9/16/2009  | 101300                    | 3.81                 | 0.62                 | 1.22                         | 1.98             | 2.29              | 4.66            | 0.909       | 221             | 299                    | 37.61                               | 18.52                             | 243                               | 8.0                                  | 1.30E-08                               | 1.46E-08                           | 1.13                                   | fine-grained sand              |
| PA4I  | 8/14/2009  | 101300                    | 3.81                 | 0.62                 | 1.22                         | 2.77             | 3.08              | 4.66            | 0.842       | 204             | 87                     | 36.21                               | 23.05                             | 28                                | 8.0                                  | 1.04E-07                               | 1.21E-07                           | 1.16                                   | medium-grained sand            |
| PA4I  | 9/16/2009  | 101300                    | 3.81                 | 0.62                 | 1.22                         | 2.77             | 3.08              | 4.66            | 0.909       | 221             | 174                    | 37.61                               | 24.91                             | 112                               | 8.0                                  | 2.81E-08                               | 3.18E-08                           | 1.13                                   | medium-grained sand            |
| PA4I  | 9/30/2010  | 101300                    | 3.81                 | 0.62                 | 1.22                         | 2.77             | 3.08              | 4.66            | 0.954       | 232             | 162                    | 38.49                               | 26.14                             | 97                                | 8.0                                  | 3.39E-08                               | 3.86E-08                           | 1.14                                   | medium-grained sand            |
| PA4D  | 8/14/2009  | 101300                    | 3.81                 | 0.62                 | 1.22                         | 3.57             | 3.87              | 4.66            | 0.842       | 204             | 137                    | 36.21                               | 29.00                             | 72                                | 8.0                                  | 4.05E-08                               | 4.76E-08                           | 1.17                                   | coarse-grained sand            |
| PA4D  | 9/30/2010  | 101300                    | 3.81                 | 0.62                 | 1.22                         | 3.57             | 3.87              | 4.66            | 1.073       | 260             | 199                    | 40.64                               | 36.98                             | 122                               | 8.0                                  | 3.05E-08                               | 3.55E-08                           | 1.16                                   | coarse-grained sand            |
| PB1S  | 9/15/2009  | 101300                    | 3.81                 | 0.62                 | 1.83                         | 2.35             | 2.65              | 4.66            | 0.762       | 185             | 249                    | 34.39                               | 18.00                             | 197                               | 8.0                                  | 1.34E-08                               | 1.60E-08                           | 1.19                                   | sandy clay, friable brown clay |
| PB1S  | 9/15/2009  | 101300                    | 3.81                 | 0.62                 | 1.83                         | 2.35             | 2.65              | 4.66            | 0.622       | 151             | 194                    | 30.69                               | 14.69                             | 149                               | 8.0                                  | 1.44E-08                               | 1.72E-08                           | 1.19                                   | sandy clay, friable brown clay |
| PB1S  | 9/15/2009  | 101300                    | 3.81                 | 0.62                 | 1.83                         | 2.35             | 2.65              | 4.66            | 0.522       | 127             | 145                    | 27.49                               | 12.32                             | 105                               | 8.0                                  | 1.72E-08                               | 2.07E-08                           | 1.20                                   | sandy clay, friable brown clay |

| Probe | Date      | Atmospheric Pressure (Pa) | Radius Sandpack (cm) | Diameter Tubing (cm) | Lower Permeability Layer (m) | Top Sandpack (m) | Base Sandpack (m) | Water Depth (m) | Flow (SLPM) | Reynolds Number | Vacuum at Surface (Pa) | Estimated Vacuum Loss Fittings (Pa) | Estimated Vacuum Loss Tubing (Pa) | Estimated Vacuum at Sandpack (Pa) | Ratio of Sandpack to Borehole Radius | kr for Prolate Spheroid Solution (cm <sup>2</sup> ) | kr for Axisymmetric Solution (cm <sup>2</sup> ) | Ratio Axisymmetric to Prolate Spheroid | Soil Description                |
|-------|-----------|---------------------------|----------------------|----------------------|------------------------------|------------------|-------------------|-----------------|-------------|-----------------|------------------------|-------------------------------------|-----------------------------------|-----------------------------------|--------------------------------------|---|---|--|---------------------------------|
| PB1S  | 11/3/2009 | 101300                    | 3.81                 | 0.62                 | 1.83                         | 2.35             | 2.65              | 4.66            | 0.808       | 196             | 429                    | 35.46                               | 19.12                             | 374                               | 8.0                                  | 7.48E-09  | 8.80E-09  | 1.18                                   | sandy clay, friable brown clay  |
| PB1S  | 9/29/2010 | 101300                    | 3.81                 | 0.62                 | 1.83                         | 2.35             | 2.65              | 4.66            | 0.652       | 158             | 274                    | 31.55                               | 15.41                             | 227                               | 8.0                                  | 9.93E-09  | 1.18E-08  | 1.19                                   | sandy clay, friable brown clay  |
| PB1I  | 8/7/2009  | 101300                    | 3.81                 | 0.62                 | 1.83                         | 3.14             | 3.44              | 4.66            | 0.522       | 127             | 75                     | 27.49                               | 15.99                             | 31                                | 8.0                                  | 5.77E-08  | 6.88E-08  | 1.19                                   | fine-grained sand               |
| PB1I  | 8/7/2009  | 101300                    | 3.81                 | 0.62                 | 1.83                         | 3.14             | 3.44              | 4.66            | 0.762       | 185             | 112                    | 34.39                               | 23.35                             | 54                                | 8.0                                  | 4.84E-08  | 5.73E-08  | 1.18                                   | fine-grained sand               |
| PB1I  | 8/7/2009  | 101300                    | 3.81                 | 0.62                 | 1.83                         | 3.14             | 3.44              | 4.66            | 1.096       | 266             | 159                    | 41.02                               | 33.60                             | 85                                | 8.0                                  | 4.47E-08  | 5.29E-08  | 1.18                                   | fine-grained sand               |
| PB1I  | 9/15/2009 | 101300                    | 3.81                 | 0.62                 | 1.83                         | 3.14             | 3.44              | 4.66            | 0.747       | 181             | 149                    | 34.03                               | 22.90                             | 93                                | 8.0                                  | 2.79E-08  | 3.27E-08  | 1.17                                   | fine-grained sand               |
| PB1I  | 11/3/2009 | 101300                    | 3.81                 | 0.62                 | 1.83                         | 3.14             | 3.44              | 4.66            | 0.762       | 185             | 329                    | 34.39                               | 23.40                             | 271                               | 8.0                                  | 9.73E-09  | 1.11E-08  | 1.14                                   | fine-grained sand               |
| PB1I  | 9/29/2010 | 101300                    | 3.81                 | 0.62                 | 1.83                         | 3.14             | 3.44              | 4.66            | 0.739       | 179             | 187                    | 33.83                               | 22.66                             | 130                               | 8.0                                  | 1.96E-08  | 2.27E-08  | 1.16                                   | fine-grained sand               |
| PB1D  | 8/7/2009  | 101300                    | 3.81                 | 0.62                 | 1.83                         | 3.96             | 4.66              | 4.66            | 1.096       | 266             | 194                    | 41.02                               | 45.50                             | 108                               | 18.4                                 | 2.14E-08  | 2.92E-08  | 1.36                                   | fine-grained sand               |
| PB1D  | 8/7/2009  | 101300                    | 3.81                 | 0.62                 | 1.83                         | 3.96             | 4.66              | 4.66            | 0.875       | 212             | 142                    | 36.91                               | 36.31                             | 69                                | 18.4                                 | 2.68E-08  | 3.68E-08  | 1.37                                   | fine-grained sand               |
| PB1D  | 8/7/2009  | 101300                    | 3.81                 | 0.62                 | 1.83                         | 3.96             | 4.66              | 4.66            | 0.646       | 157             | 120                    | 31.38                               | 26.80                             | 61                                | 18.4                                 | 2.21E-08  | 3.03E-08  | 1.37                                   | fine-grained sand               |
| PB1D  | 8/7/2009  | 101300                    | 3.81                 | 0.62                 | 1.83                         | 3.96             | 4.66              | 4.66            | 0.522       | 127             | 90                     | 27.49                               | 21.65                             | 41                                | 18.4                                 | 2.71E-08  | 3.71E-08  | 1.37                                   | fine-grained sand               |
| PB1D  | 9/15/2009 | 101300                    | 3.81                 | 0.62                 | 1.83                         | 3.96             | 4.66              | 4.66            | 0.716       | 174             | 199                    | 33.26                               | 29.73                             | 136                               | 18.4                                 | 1.11E-08  | 1.48E-08  | 1.34                                   | fine-grained sand               |
| PB1D  | 11/3/2009 | 101300                    | 3.81                 | 0.62                 | 1.83                         | 3.96             | 4.66              | 4.66            | 0.785       | 191             | 391                    | 34.93                               | 32.66                             | 324                               | 18.4                                 | 5.11E-09  | 6.64E-09  | 1.30                                   | fine-grained sand               |
| PB1D  | 9/29/2010 | 101300                    | 3.81                 | 0.62                 | 1.83                         | 3.96             | 4.66              | 4.66            | 0.785       | 191             | 199                    | 34.93                               | 32.59                             | 132                               | 18.4                                 | 1.25E-08  | 1.68E-08  | 1.34                                   | fine-grained sand               |
| WB1S  | 8/13/2009 | 101300                    | 2.86                 | 5.08                 | 1.83                         | 4.66             | 4.72              | 4.72            | 0.738       | 22              | 75                     | 33.81                               | 0.01                              | 41                                | 2.1                                  | 1.14E-07  | 2.29E-07  | 2.02                                   | medium-grained sand             |
| PB2S  | 9/15/2009 | 101300                    | 3.81                 | 0.62                 | 1.68                         | 2.07             | 2.38              | 4.66            | 0.909       | 221             | 2143                   | 37.61                               | 19.62                             | 2085                              | 8.0                                  | 1.52E-09  | 1.74E-09  | 1.14                                   | sandy clay                      |
| PB2S  | 9/15/2009 | 101300                    | 3.81                 | 0.62                 | 1.68                         | 2.07             | 2.38              | 4.66            | 0.639       | 155             | 1644                   | 31.18                               | 13.72                             | 1599                              | 8.0                                  | 1.39E-09  | 1.58E-09  | 1.14                                   | sandy clay                      |
| PB2S  | 9/29/2010 | 101300                    | 3.81                 | 0.62                 | 1.68                         | 2.07             | 2.38              | 4.66            | 0.909       | 221             | 17216                  | 37.61                               | 23.14                             | 17155                             | 8.0                                  | 2.00E-10  | 2.16E-10  | 1.08                                   | sandy clay                      |
| PB2I  | 8/11/2009 | 101300                    | 3.81                 | 0.62                 | 1.68                         | 2.87             | 3.17              | 4.66            | 0.779       | 189             | 100                    | 34.79                               | 21.97                             | 43                                | 8.0                                  | 6.28E-08  | 7.35E-08  | 1.17                                   | fine-grained sand               |
| PB2I  | 9/15/2009 | 101300                    | 3.81                 | 0.62                 | 1.68                         | 2.87             | 3.17              | 4.66            | 0.738       | 179             | 135                    | 33.81                               | 20.82                             | 80                                | 8.0                                  | 3.19E-08  | 3.78E-08  | 1.18                                   | fine-grained sand               |
| PB2I  | 9/15/2009 | 101300                    | 3.81                 | 0.62                 | 1.68                         | 2.87             | 3.17              | 4.66            | 0.909       | 221             | 149                    | 37.61                               | 25.64                             | 86                                | 8.0                                  | 3.64E-08  | 4.33E-08  | 1.19                                   | fine-grained sand               |
| PB2I  | 9/19/2010 | 101300                    | 3.81                 | 0.62                 | 1.68                         | 2.87             | 3.17              | 4.66            | 0.909       | 221             | 159                    | 37.61                               | 25.65                             | 96                                | 8.0                                  | 3.27E-08  | 3.87E-08  | 1.18                                   | fine-grained sand               |
| PB2D  | 9/15/2009 | 101300                    | 3.81                 | 0.62                 | 1.68                         | 3.66             | 4.66              | 4.66            | 0.842       | 204             | 159                    | 36.21                               | 34.95                             | 88                                | 26.4                                 | 1.57E-08  | 2.12E-08  | 1.35                                   | clayey sand, sandy clay         |
| PB2D  | 9/15/2009 | 101300                    | 3.81                 | 0.62                 | 1.68                         | 3.66             | 4.66              | 4.66            | 0.620       | 150             | 159                    | 30.63                               | 25.73                             | 103                               | 26.4                                 | 9.92E-09  | 1.31E-08  | 1.32                                   | clayey sand, sandy clay         |
| PB2D  | 9/15/2009 | 101300                    | 3.81                 | 0.62                 | 1.68                         | 3.66             | 4.66              | 4.66            | 0.508       | 123             | 159                    | 27.00                               | 21.09                             | 111                               | 26.4                                 | 7.52E-09  | 9.83E-09  | 1.31                                   | clayey sand, sandy clay         |
| PB2D  | 9/19/2010 | 101300                    | 3.81                 | 0.62                 | 1.68                         | 3.66             | 4.66              | 4.66            | 0.909       | 221             | 159                    | 37.61                               | 37.73                             | 84                                | 26.4                                 | 1.78E-08  | 2.41E-08  | 1.35                                   | friable brown clay              |
| WB2S  | 8/11/2009 | 101300                    | 2.86                 | 5.08                 | 1.68                         | 3.51             | 4.36              | 4.36            | 0.597       | 18              | 1251                   | 29.94                               | 0.01                              | 1221                              | 29.9                                 | 9.92E-10  | 1.03E-09  | 1.04                                   | fine sand, plastic brown clay   |
| WB2S  | 8/11/2009 | 101300                    | 2.86                 | 5.08                 | 1.68                         | 3.51             | 4.36              | 4.36            | 0.808       | 24              | 1684                   | 35.46                               | 0.01                              | 1649                              | 29.9                                 | 9.96E-10  | 1.04E-09  | 1.04                                   | fine sand, plastic brown clay   |
| WB2S  | 8/11/2009 | 101300                    | 2.86                 | 5.08                 | 1.68                         | 3.51             | 4.36              | 4.36            | 1.074       | 32              | 2058                   | 40.65                               | 0.01                              | 2017                              | 29.9                                 | 1.08E-09  | 1.13E-09  | 1.04                                   | fine sand, plastic brown clay   |
| PB3I  | 8/13/2009 | 101300                    | 3.81                 | 0.62                 | 1.37                         | 2.56             | 2.87              | 3.84            | 0.545       | 132             | 125                    | 28.28                               | 13.89                             | 82                                | 8.0                                  | 2.29E-08  | 2.56E-08  | 1.12                                   | brown clay to fine-grained sand |
| PB3I  | 8/13/2009 | 101300                    | 3.81                 | 0.62                 | 1.37                         | 2.56             | 2.87              | 3.84            | 0.738       | 179             | 194                    | 33.81                               | 18.83                             | 142                               | 8.0                                  | 1.80E-08  | 2.00E-08  | 1.11                                   | brown clay to fine-grained sand |
| PB3I  | 8/13/2009 | 101300                    | 3.81                 | 0.62                 | 1.37                         | 2.56             | 2.87              | 3.84            | 0.954       | 232             | 214                    | 38.49                               | 24.34                             | 151                               | 8.0                                  | 2.18E-08  | 2.44E-08  | 1.12                                   | brown clay to fine-grained sand |
| PB3I  | 9/15/2009 | 101300                    | 3.81                 | 0.62                 | 1.37                         | 2.56             | 2.87              | 3.84            | 0.718       | 174             | 1570                   | 33.31                               | 18.57                             | 1518                              | 8.0                                  | 1.65E-09  | 1.72E-09  | 1.04                                   | brown clay to fine-grained sand |
| PB3I  | 9/15/2009 | 101300                    | 3.81                 | 0.62                 | 1.37                         | 2.56             | 2.87              | 3.84            | 0.582       | 141             | 1196                   | 29.48                               | 15.00                             | 1151                              | 8.0                                  | 1.76E-09  | 1.84E-09  | 1.05                                   | brown clay to fine-grained sand |
| WB3S  | 8/13/2009 | 101300                    | 3.81                 | 5.08                 | 1.37                         | 2.90             | 3.84              | 3.84            | 0.738       | 22              | 2043                   | 33.81                               | 0.01                              | 2009                              | 24.8                                 | 6.39E-10  | 7.07E-10  | 1.11                                   | fine- to medium-grained sand    |
| WB3S  | 8/13/2009 | 101300                    | 3.81                 | 5.08                 | 1.37                         | 2.90             | 3.84              | 3.84            | 0.909       | 27              | 2716                   | 37.61                               | 0.01                              | 2678                              | 24.8                                 | 5.92E-10  | 6.55E-10  | 1.11                                   | fine- to medium-grained sand    |
| PC1   | 8/12/2009 | 101300                    | 3.81                 | 5.08                 | 2.44                         | 2.59             | 4.42              | 5.18            | 0.853       | 25              | 125                    | 36.45                               | 0.01                              | 88                                | 48.0                                 | 1.04E-08  | 1.39E-08  | 1.34                                   | friable brown clay              |
| PC1   | 9/14/2009 | 101300                    | 3.81                 | 5.08                 | 2.44                         | 2.59             | 4.42              | 5.18            | 0.646       | 19              | 137                    | 31.38                               | 0.01                              | 106                               | 48.0                                 | 6.56E-09  | 8.56E-09  | 1.30                                   | friable brown clay              |
| PC1   | 9/14/2009 | 101300                    | 3.81                 | 5.08                 | 2.44                         | 2.59             | 4.42              | 5.18            | 0.762       | 22              | 187                    | 34.39                               | 0.01                              | 152                               | 48.0                                 | 5.36E-09  | 7.41E-09  | 1.38                                   | friable brown clay              |
| PC1   | 11/3/2009 | 101300                    | 3.81                 | 5.08                 | 2.44                         | 2.59             | 4.42              | 5.18            | 0.716       | 21              | 169                    | 33.26                               | 0.01                              | 136                               | 48.0                                 | 5.64E-09  | 7.87E-09  | 1.39                                   | friable brown clay              |
| PC2   | 8/12/2009 | 101300                    | 2.86                 | 5.08                 | 2.44                         | 3.20             | 4.88              | 5.18            | 0.740       | 22              | 872                    | 33.86                               | 0.01                              | 838                               | 58.7                                 | 1.09E-09  | 1.32E-09  | 1.21                                   | friable brown clay              |
| WC1S  | 8/13/2009 | 101300                    | 3.81                 | 5.08                 | 0.00                         | 3.14             | 4.36              | 4.36            | 0.646       | 19              | 1121                   | 31.38                               | 0.01                              | 1090                              | 32.0                                 | 8.58E-10  | 9.51E-10  | 1.11                                   | plastic clay, wet sandy clay    |
| WC1S  | 8/13/2009 | 101300                    | 3.81                 | 5.08                 | 0.00                         | 3.14             | 4.36              | 4.36            | 0.900       | 27              | 1562                   | 37.43                               | 0.01                              | 1525                              | 32.0                                 | 8.57E-10  | 9.61E-10  | 1.12                                   | plastic clay, wet sandy clay    |

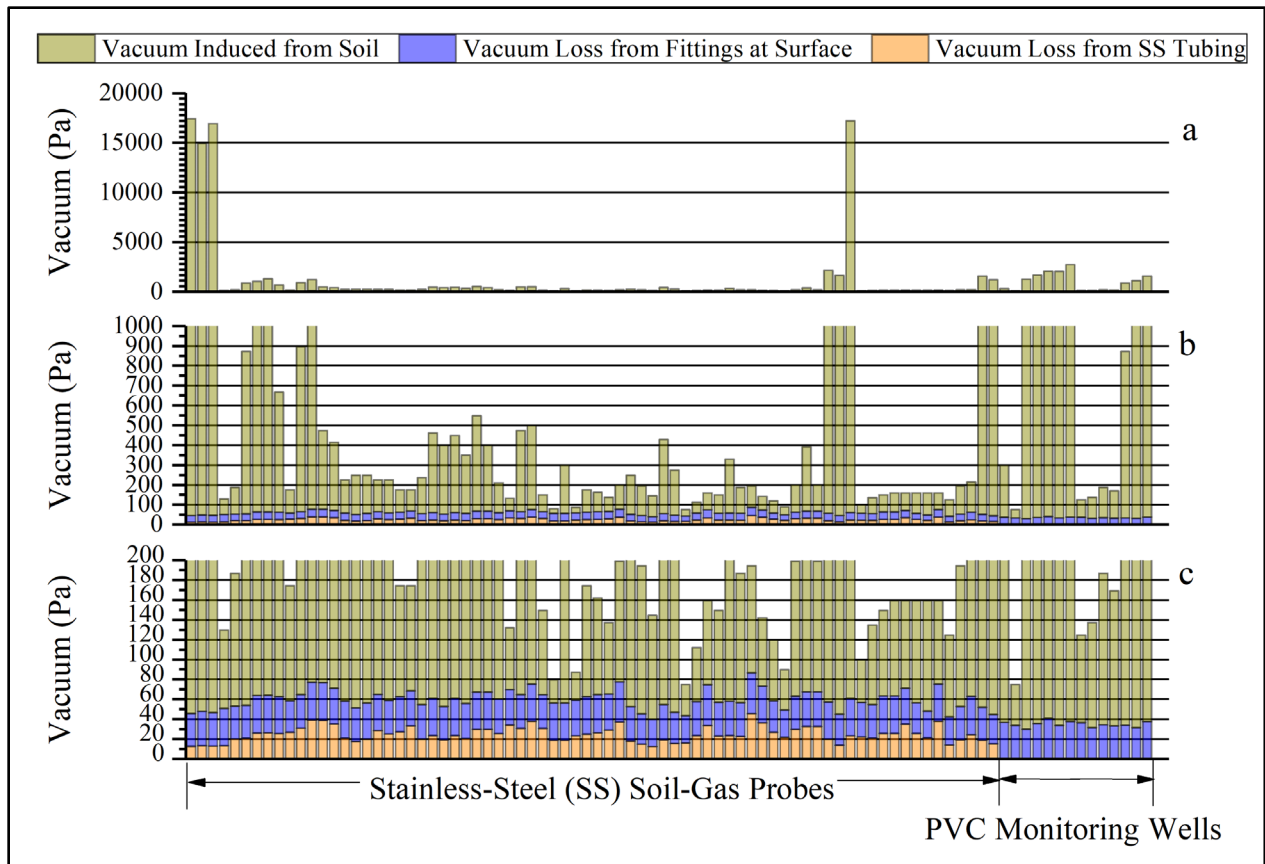


**Figure 38.** Stacked column plot of vacuum induced from soil, fittings at the surface and subsurface tubing during gas permeability testing. Plots illustrated at 3 scales to facilitate comparison of vacuum loss from frictional headloss and soil: (a) scale from 0 to 20,000 Pa, (b) scale from 0 to 1000 Pa, (c) scale from 0 to 200 Pa

Theoretical vacuum or pressure loss as a function of tube length and flow rate were evaluated for 4 internal diameters for tubing or pipe commonly used for soil-gas probe construction and for two direct-push systems – 0.635 cm ID LDPE tubing for the Geoprobe Post-Run-Tubing (PRT) system and 1.59 cm ID steel drive pipe used for the Geoprobe Soil-Gas Cap (SGC) system (**Figure 39**).

Estimated vacuum loss in 0.158 cm ID x 0.318 cm OD (1/8 inch) stainless-steel tubing (not used in this investigation) was excessive, exceeding 1,000 Pa at a flow rate of only 0.1 SLPM and 10,000 Pa at a flow rate of 1 SLPM in tubing lengths of 5, 10, and 15 m (**Figure 39a**). Hence, 0.158 cm ID tubing should not be used for soil-gas probe construction if gas permeability testing is desirable.

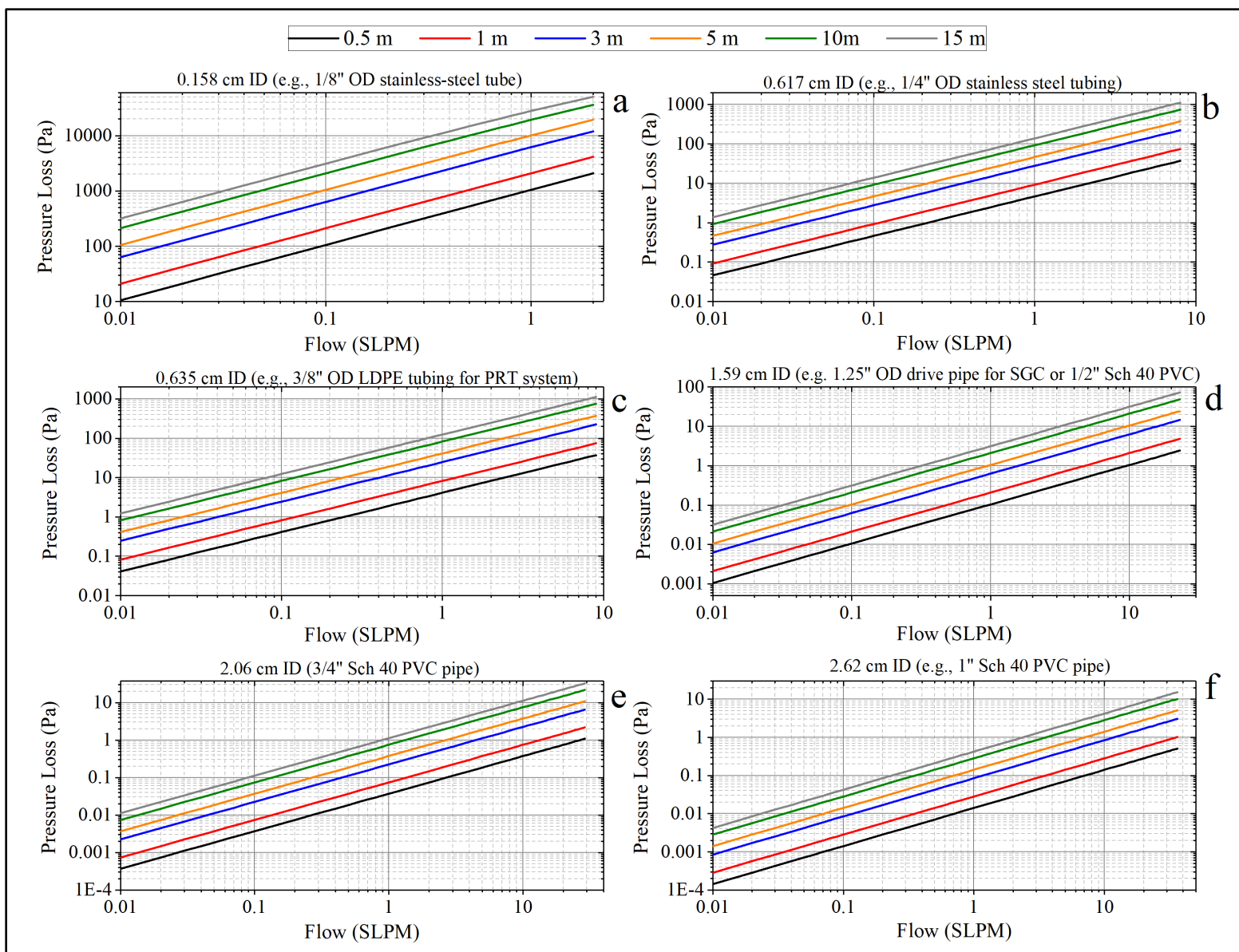


**Figure 39.** Pressure loss as a function of internal diameter of tubing and flow rate.

Estimated vacuum loss in 0.617 cm ID x 0.535 cm OD (¼ inch) stainless-steel tubing used for soil-gas probe cluster construction in this investigation and 0.635 cm ID x 0.953 cm OD (3/8 inch) LDPE tubing used for the PRT direct-push soil-gas sampling were similar with length of tubing and flow rate (**Figures 39b, 39c**). Estimated vacuum loss approached or exceeded 100 Pa at 1.0 SLPM at tubing lengths of 10 – 15 m. Thus, use of tubing of having these internal diameters is undesirable for gas permeability testing at depths exceeding 10 meters which was not the case in this investigation.

Estimated vacuum loss was insignificant regardless of depth at flow rates used for soil-gas sampling (<1 SLPM) for 1.59 cm ID x 3.18 cm OD (1.25 inch) steel drive pipe used for the SGC system or 1.53 cm ID x 2.04 cm OD (½ inch schedule 40 PVC pipe) (**Figure 39d**). Hence, if a direct-push system is to be used for soil-gas sampling and gas permeability estimation is desirable, the SGC system is preferable over the PRT system and ½ inch schedule 40 PVC pipe is preferable for deeper soil gas probes.

Estimated vacuum loss for 2.05 cm ID x 2.67 cm OD (¾ inch schedule 40) PVC pipe was also insignificant regardless of depth at flow rates used for soil-gas sampling (**Figure 39e**). Hence, this is also an option for probe construction at depths exceeding 5 or 10 m if gas permeability testing is desirable. Finally, estimated vacuum loss in 2.62 cm ID x 3.34 cm OD (1 inch schedule 40) PVC pipe was insignificant at flow rates exceeding 10 SLPM. This diameter pipe is often used for combined groundwater sampling and soil-gas sampling across the water table as was done in this investigation.

Recommended internal diameters of probes vary from 1/8 to 1 inch (Interstate Technology & Regulatory Council 2007), 1/8 to ¼ inch (Missouri Department of Natural Resources 2013), ¼ – ¾ inch (British Columbia Ministry of Environment 2011), ¼ to 1 inch (Atlantic Partnership in Risk-Based Corrective Action Implementation 2006, American Petroleum Institute 2005), ¼ to 2 inch (Electric Power Research Institute 2005, Canadian Council of Ministers of the Environment 2008).

### 3.16 Comparison of Prolate-Spheroidal and Axisymmetric-Cylindrical Domains for Permeability Estimation

Estimates of radial gas permeability using the equation for an axisymmetric-cylindrical domain were consistently higher than estimates of radial gas permeability using the modified equation for a prolate-spheroidal domain by a factor of 1.04 to 2.02 (mean=1.22, median=1.19, n=88) (Table 7). Nearly all points lie above the 1:1 line in a comparison of the two equations used for estimation of radial gas permeability (Figure 40). The one data point, circled in blue in Figure 40 appears to be an outlier due to  $L/r_w$  ratio  $> 5$  when using the modified equation for a prolate-spheroidal domain.

The reason for a consistent but slight positive bias in use of the equation for an axisymmetric-cylindrical domain compared to the equation for a prolate-spheroidal domain is unclear. Though, the equation for an axisymmetric-cylindrical domain more accurately represents the geometry of the sandpack and boundary conditions. However, this difference in estimation is minor compared to orders of magnitude variation of radial gas permeability in various soil types.

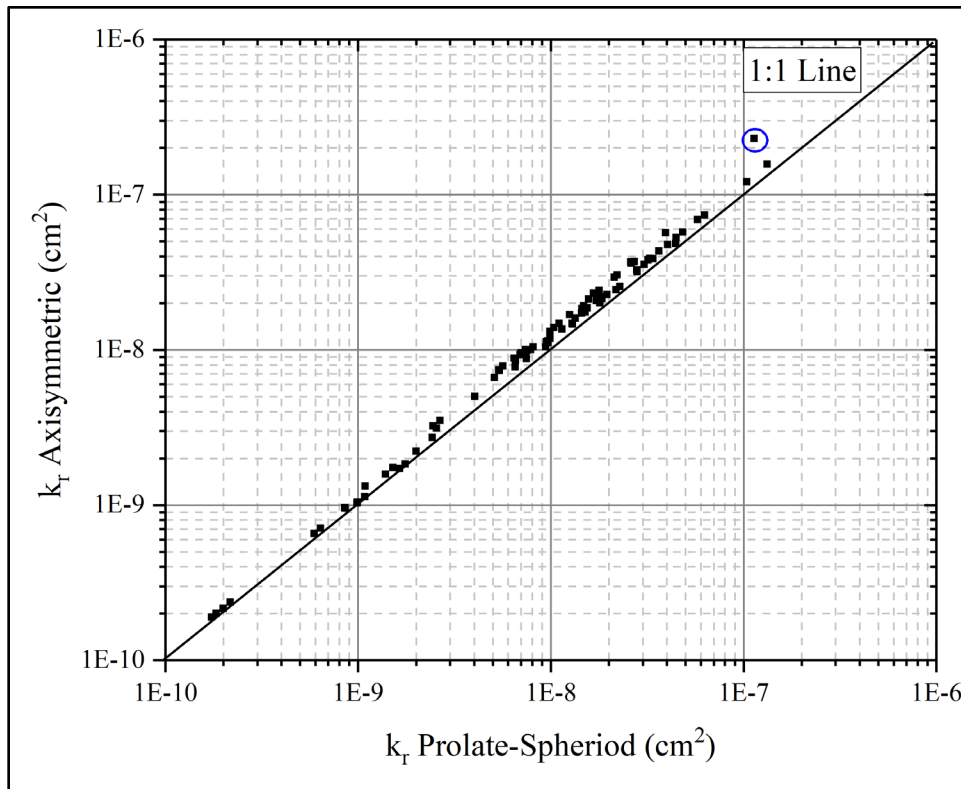


**Figure 40.** Comparison of radial permeability estimation (n=121) using equations for a prolate-spheroidal domain and a radial axisymmetric cylindrical domain. The  $L/r_w$  value for the blue-circled data point was 2.1

Comparison of radial gas permeability estimation using the equation for an axisymmetric-cylindrical domain conducted during the same time period at two different flow rates at PA1S, PA1I, PA1D, PA3D, PB2S, PB2I, PB2D, WB3S, PC1, and WC1S indicated random variability between a factor of 1.01 to 1.33 (**Table 7**). Comparison of radial gas permeability estimation using the equation for an axisymmetric-cylindrical domain at three different flows at PA3S, PB1S, PB1I, WB2S, and PB3I indicated random variability between a factor of 1.05 to 1.63 (**Table 7**). Comparison of radial gas permeability estimation using the equation for an axisymmetric-cylindrical domain at 4 flow rates at PB1D indicated random variability at a factor of 1.27 (**Table 7**). Thus, random variation in use of the equation for axisymmetric cylindrical domain was of similar magnitude to the positive bias observed for estimation of radial gas permeability using the use of the equation for axisymmetric cylindrical domain compared to the equation for a modified prolate-spheroidal domain with the latter equation much easier to solve (hand calculation or EXCEL spreadsheet) compared to the former (e.g., Fortran program).

### 3.17 Evaluation of Temporal Variability in Gas Permeability Estimation

Use of dedicated vapor probes enables evaluation of temporal variability in gas permeability. Temporal variability in radial gas permeability estimation was relatively minor ( $< 3X$ ) at some probes (e.g., PA2S, PA2I, PA3S, PA3I, PA4S, PA4D, WB2S) and moderate (3 to 10X) at other probes (e.g., PA1I, PA1D, PA3D, PA4S, PA4I, PB1I, PB1D, PB2S (**Table 7, Figure 41**)). The cause of temporal variability was not investigated but at locations of minor and moderate variation, it is possible that wetting fronts near the surface decreased permeability for shallow probes and a rising water table decreased permeability in deeper probes due to upward capillary imbibition.

Temporal variability was substantial ( $>10X$ ) at PA1S, and PB3I (**Table 1, Figures 41**). At PA1S, a 242X increase in gas permeability between 11/14/2009 and 9/30/2010 was due to development of a leakage pathway from the surface as evident during leak testing during these dates.

### 3.18 Results of Transient Gas Permeability Estimation

Transient gas permeability estimation was conducted at monitoring wells used for both soil-gas and groundwater sampling -WB3S and WC1S. The 5 best fits, with near equal error estimates, of

radial permeability, the ratio of radial to vertical permeability, gas-filled porosity, and borehole storage are illustrated in **Figure 42**.

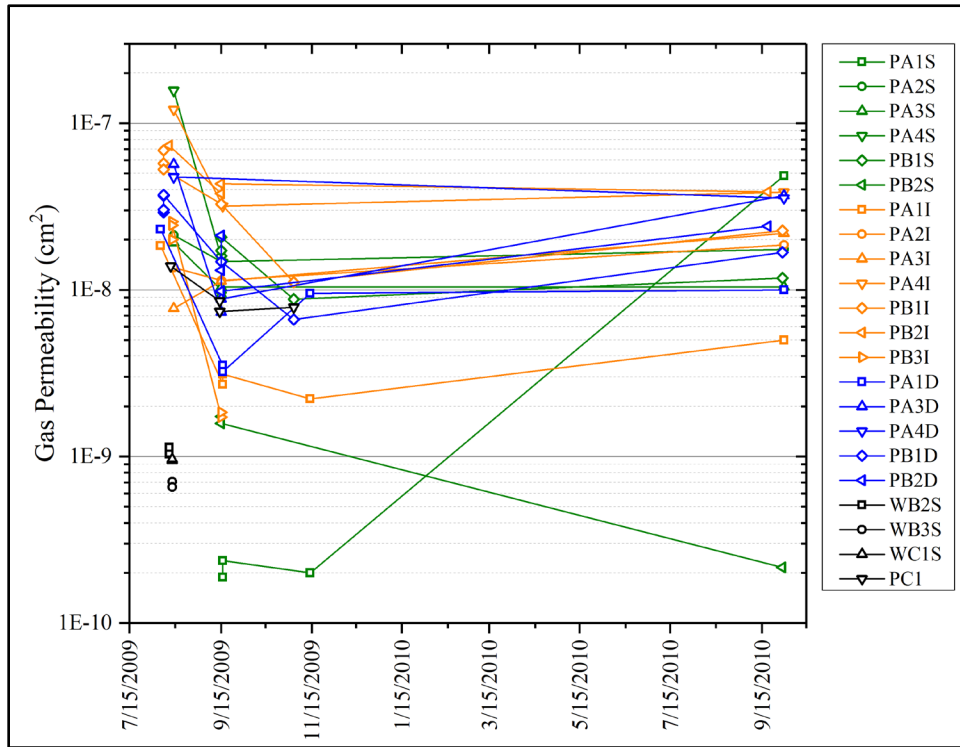


**Figure 41.** Temporal variability in gas permeability estimation at dedicated vapor probes. Green, orange, and blue colors indicate probes at shallow, intermediate, and deeper depths in probe clusters at two residential areas (A, B). Probes in black indicate 1” PVC wells screened across the water table at two residential areas (B, C).

At WB3S, estimates of radial permeability varied from  $1.95e-10 \text{ cm}^2$  to  $2.44e-10 \text{ cm}^2$  (**Figure 42a**) slightly lower than the steady-state estimate of  $7.07e-10 \text{ cm}^2$ . Estimates of gas-filled porosity showed little variation from 1.0 to 2.4% in soils described as fine-grained sand. Estimates of borehole storage varied from  $2075 \text{ cm}^3$  to  $2469 \text{ cm}^3$  equivalent to gas-filled porosity in sandpacks from 12% to 21%. Since most borehole storage volume is associated with the gas-filled porosity of a sandpack, borehole storage cannot be directly calculated prior to transient gas permeability estimation.

At WC1S, estimates of radial permeability varied from  $7.30e-10 \text{ cm}^2$  to  $8.81e-10 \text{ cm}^2$  (**Figure 42b**), slightly lower than the steady-state estimate of  $9.61e-10 \text{ cm}^2$ . Estimates of gas-filled porosity showed moderate variation from 1.4 to 6.0% in soils described as brown clay and sandy

clay. Estimates of borehole storage varied from 2773 cm<sup>3</sup> to 3673 cm<sup>3</sup> equivalent to gas-filled porosity in sandpicks from 11% to 20%.

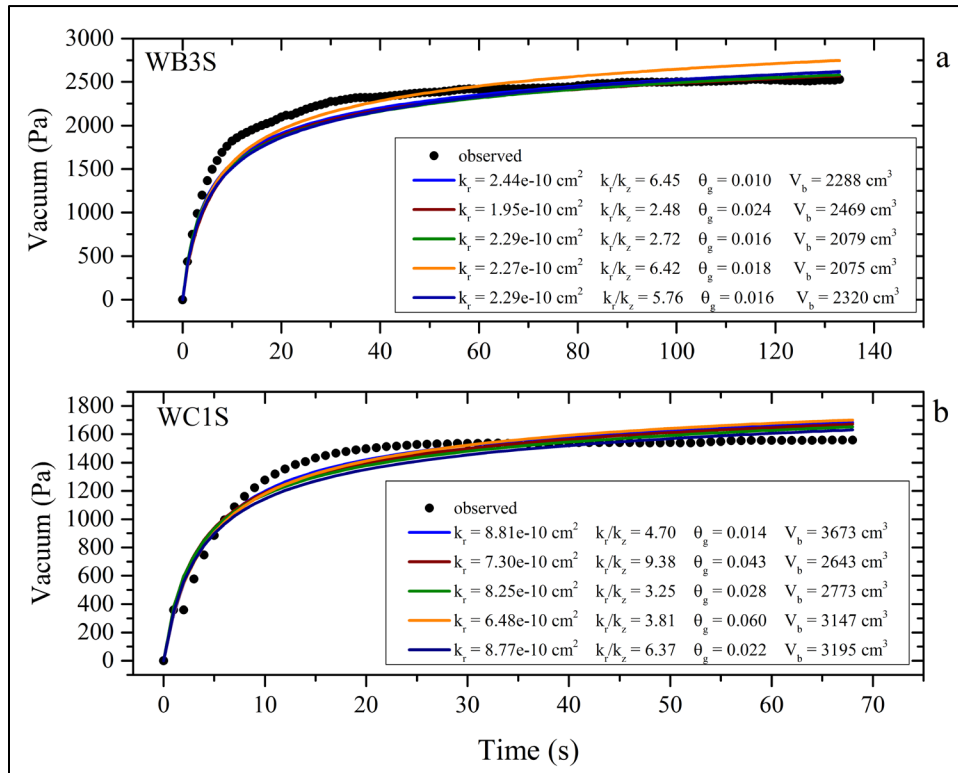


**Figure 42.** Transient gas permeability estimation at (a) WB3s and (b) WC1S August 2009:  $k_r$  = radial permeability (cm<sup>2</sup>),  $k_r/k_z$  = ratio of radial to vertical gas permeability (-),  $\theta_g$  = gas filled porosity (-),  $V_b$  = borehole storage (cm<sup>3</sup>).

Despite the use of 4 fitting parameters during transient gas permeability testing, fit to observed vacuum at both monitoring wells was fairly poor as evident from visual examination. Fitting of transient pressure data was insensitive to ratios of radial to vertical permeability (anisotropy) but sensitive to estimates of gas-filled porosity and borehole storage volume.

### 3.19 Stabilization of O<sub>2</sub> and CO<sub>2</sub> Concentrations During Purging

During this investigation, purging experiments were conducted to determine the number of volumes required for stabilization ( $\pm 0.1\%$  random variation) of O<sub>2</sub> and CO<sub>2</sub> concentrations in vapor probes, monitoring wells, and soil-gas wells as affected by equilibration time (time since soil-gas probe, monitoring well, or soil-gas well completion or setting of bentonite seal) and one or more previous purging events.

At monitoring well WB1S, stabilization appeared to occur after approximately 2 purge volumes (**Figure 43a**). During installation, the borehole was open for 16 hours and purged 149 hours after completion (placement of a bentonite seal). At WB2S, stabilization appeared to occur after approximately 4 purge volumes. During installation, this borehole was open for 3 hours and purged 94.5 hours after completion (**Figure 43b**). At WB3S, stabilization appeared to occur after approximately 2 purge volumes. During installation, this borehole was open for 5 hours and purged 47 hours after completion (**Figure 43c**).

The effect of a subsequent purge event on stabilization of O<sub>2</sub>, CO<sub>2</sub>, and CH<sub>4</sub> concentrations is illustrated in monitoring well PC1 (**Figure 44**). This monitoring well was located within a meter of a natural gas distribution line entering the residence.

Purging on 8/12/2009 commenced only 2 hours after soil-gas well installation resulting in little time for soil-gas equilibration in the sandpack. Initial O<sub>2</sub> and CO<sub>2</sub> concentrations resembled atmospheric concentrations. Stabilization of O<sub>2</sub>, CO<sub>2</sub>, and CH<sub>4</sub> required approximately 4 purge volumes (**Figure 44**). Stabilization of O<sub>2</sub>, CO<sub>2</sub>, and CH<sub>4</sub> during subsequent purging events was achieved in less than 1 purge volume due to increased equilibration time and previous removal of atmospheric air associated with well installation. Significant temporal variability in gas concentration, especially for CO<sub>2</sub> during the 9/20/2010 purging event, occurred in this monitoring well.

At soil-gas probe cluster PB1, purging was conducted from 19 to 22 hours after probe construction. Stabilization of O<sub>2</sub> and CO<sub>2</sub> concentrations in the upper probe, PB1S, required in excess of 16 purge volumes during the first purge event (**Figure 45a**). Resolution of O<sub>2</sub> and CO<sub>2</sub> concentrations with purge volumes in the intermediate probe, PB1I, (**Figure 45b**) and the lower probe, PB1D, (**Figure 45c**) was poor, but stabilization of O<sub>2</sub> and CO<sub>2</sub> concentrations appear to have occurred in less than 4 purge volumes. However, similar to monitoring well PC1, during subsequent purge events stabilization of O<sub>2</sub> and CO<sub>2</sub> concentrations occurred in all probes in less than 2 purge volumes.

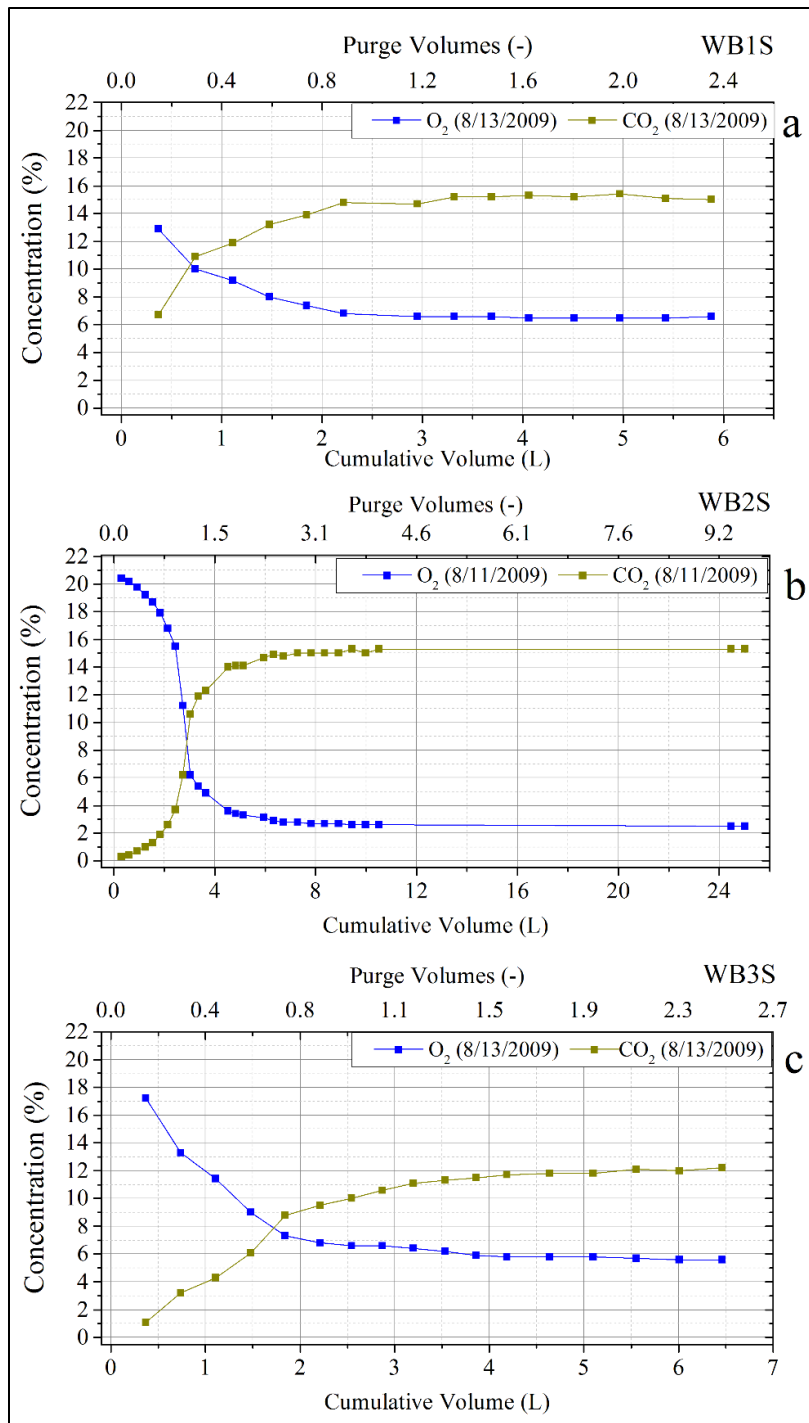


**Figure 43.** Purge test results monitoring wells. (a) WB1S installed 8/6/2009, open borehole 16 hours, closed borehole 149 hours prior to purging, 1 purge volume = 2.46 L. (b) WB2S installed 8/7/2009, open borehole 3 hours, closed borehole 94.5 hours before purging, 1 purge volume = 2.62 L, (c) WB3S installed 8/11/2009, open borehole 5 hours, closed borehole 47 hours before purging, 1 purge volume = 2.64 L.

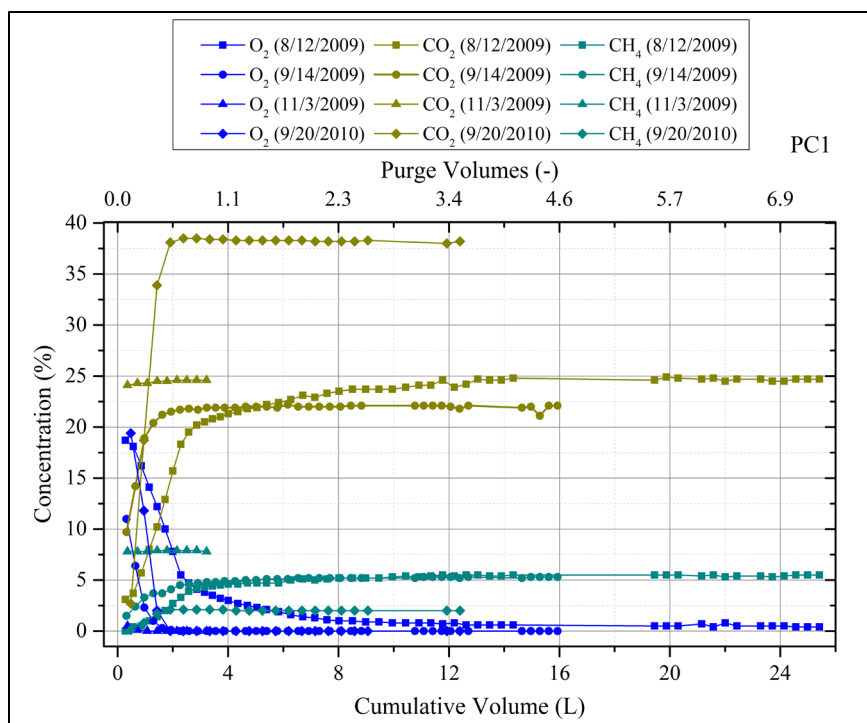


**Figure 44.** Purge testing at PC1 at Valley Center, KS completed on 8/12/2009, open borehole 2.5 hours, closed borehole 2 hours prior to purging. 1 purge volume ~ 3.46 L.

At soil-gas probe cluster PB2, purging was conducted 94 hours after probe construction. Similar to probe cluster PB1, stabilization of O<sub>2</sub> and CO<sub>2</sub> concentrations in the upper probe, PB2S, during the first purge event required almost 10 purge volumes (**Figure 46a**). However, less than 2 purge volumes were required at the intermediate probe, PB2I, (**Figure 46b**) and at the lower probe, PB2D, (**Figure 46c**) during initial purging. During subsequent purge events, stabilization of O<sub>2</sub> and CO<sub>2</sub> concentrations was achieved in 2 or fewer purge volumes for all probes (**Figures 46a, 46b, 46c**).

At soil-gas probe cluster PA4, purging was conducted from 208-209 hours after probe construction. Even after an extensive equilibration time, similar to PB1S and PB2S, stabilization of O<sub>2</sub> and CO<sub>2</sub> concentrations required extraction of almost 4 purge volumes during the first purge event in the upper probe PA4S (**Figure 47a**).

However, less than 2 purge volumes were required for stabilization during initial purging at the intermediate probe, PA4I, (**Figure 47b**) and lower probe, PA4D, (**Figure 47c**). It is unclear why upper probes of some soil-gas probe clusters require greater initial purging for stabilization of O<sub>2</sub>

and CO<sub>2</sub> concentrations. During subsequent purge events, stabilization of O<sub>2</sub> and CO<sub>2</sub> concentrations required 2 or less purge volumes in all probes (**Figures 47a, 47b, 47c**).

At soil-gas probe cluster PA2, initial purging was conducted from 207-211 hours after probe construction. Stabilization of O<sub>2</sub> and CO<sub>2</sub> concentrations during the first purge event required less than 2 purge volumes at the upper probe, PA2S, (**Figure 48a**), the intermediate probe, PA2I, (**Figure 48b**), and the lower probe, PA2D, (**Figure 48c**). Stabilization of O<sub>2</sub> and CO<sub>2</sub> concentrations also occurred in less than 2 purge volumes during subsequent purging events (**Figures 48a, 48b, 48c**).

At soil-gas probe cluster PA3, initial purging was conducted 208-209 hours after probe construction. During initial purging on 8/14/2009 and subsequent purging on 9/15/2009, stabilization of O<sub>2</sub> and CO<sub>2</sub> concentrations was attained in less than 3 purge volumes in all probes (**Figures 49a, 49b, 49c**). However, a significant change in O<sub>2</sub> and CO<sub>2</sub> soil-gas concentrations resulted in the need to remove 10 purge volumes at PA3I to achieve stable concentrations of O<sub>2</sub> and CO<sub>2</sub> on 9/30/2010.

### 3.20 Purging Simulations

O<sub>2</sub> and CO<sub>2</sub> concentrations in the soil-gas sampling train were simulated as a function of purge volume and initial concentrations of O<sub>2</sub> and CO<sub>2</sub> concentration in soil-gas probes and monitoring wells for soil-gas O<sub>2</sub> and CO<sub>2</sub> concentrations of 0% and 21%, respectively, with and without leakage (**Figure 50**).

In the absence of leakage, when gas concentrations in the soil-gas well or probe are equivalent to soil-gas concentration in soil, no purging is required to achieve steady-state O<sub>2</sub> and CO<sub>2</sub> concentrations (**Figure 50a**). However, as demonstrated in this investigation, this is never the case during initial purging since tubing at the surface is exposed to the atmosphere prior to use in a soil-gas sampling train; and in the case of monitoring wells and vapor probe clusters, the borehole was open to the atmosphere during construction.

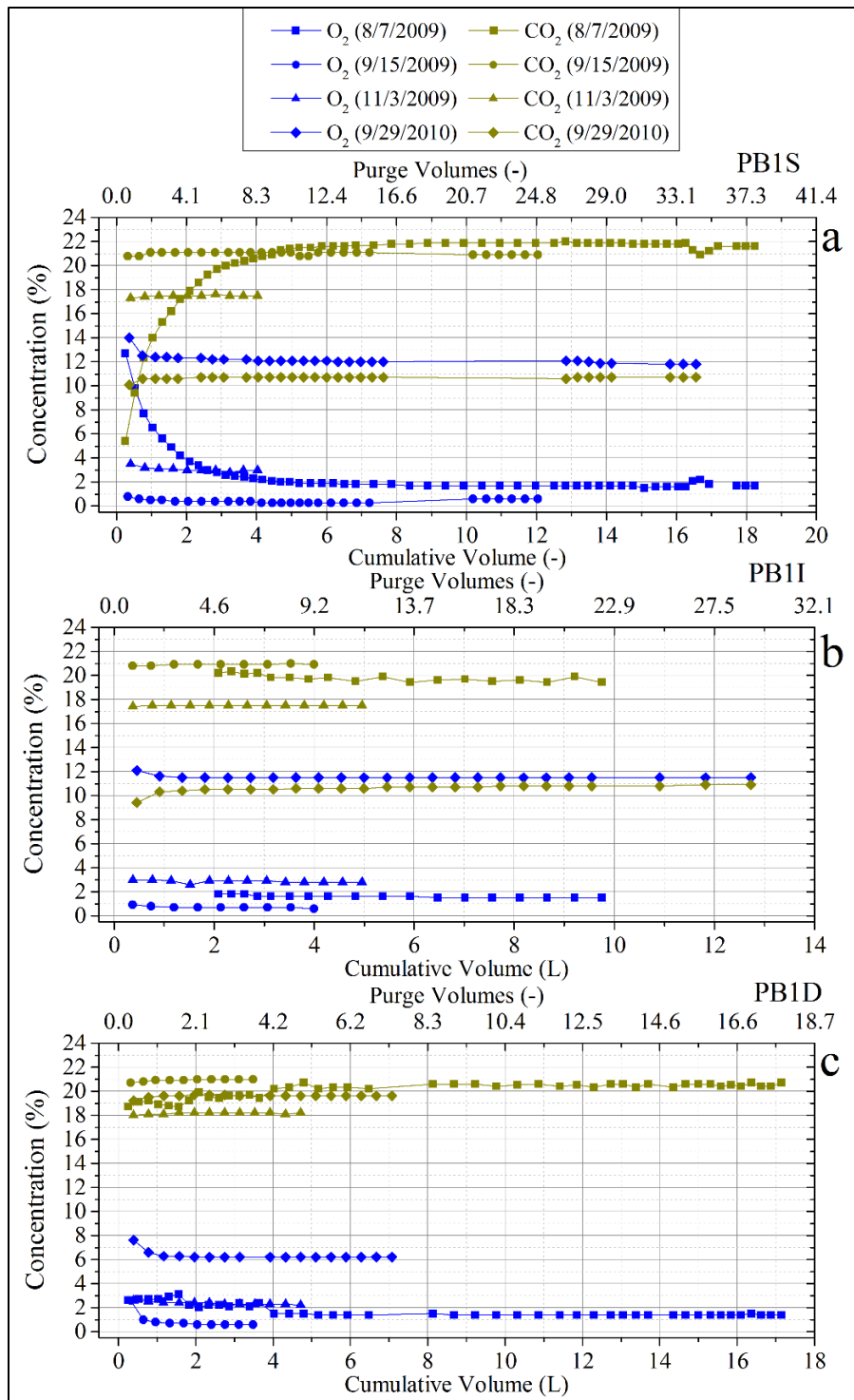


**Figure 45.** Purge test results at soil-gas probe cluster PB1 installed on 8/6/2009. Open borehole time = 3.5 hr. Closed borehole time on 8/7/2009 prior to purging = 19.1, 21.8, and 21.3 hours at PB1S, PB1I, and PB1D, respectively. 1 purge volume = ~ 0.45, 0.52, and 0.93 L at PB1S, PB1I, and PB1D, respectively. O<sub>2</sub> and CO<sub>2</sub> measurements for PB1D affected by variation of flow rate on 8/7/2009.

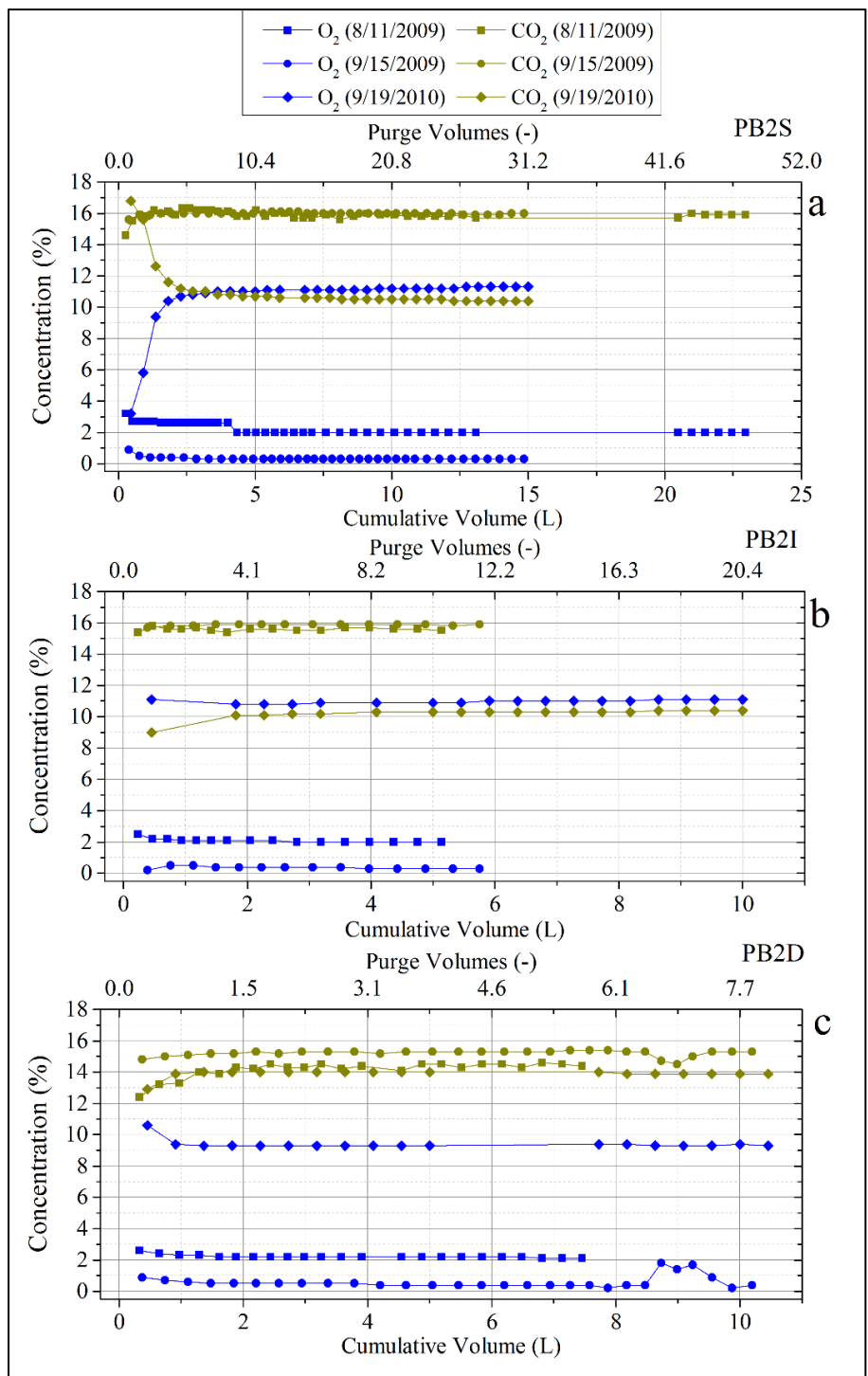


**Figure 46.** Purge test results at soil-gas probe cluster PB2 installed on 8/6/2009. Open borehole time = 4.5 hr. Closed borehole time on 8/7/2009 prior to purging = 93.5, 94.5, and 94.0 hours at PB1S, PB1I, and PB1D, respectively. 1 purge volume = ~ 0.44, 0.46, and 1.27 L at PB2S, PB2I, and PB2D, respectively. O<sub>2</sub> and CO<sub>2</sub> measurements for PB2S and PB2D impacted by flowrate on 8/11/2009 and 9/19/2010, respectively.

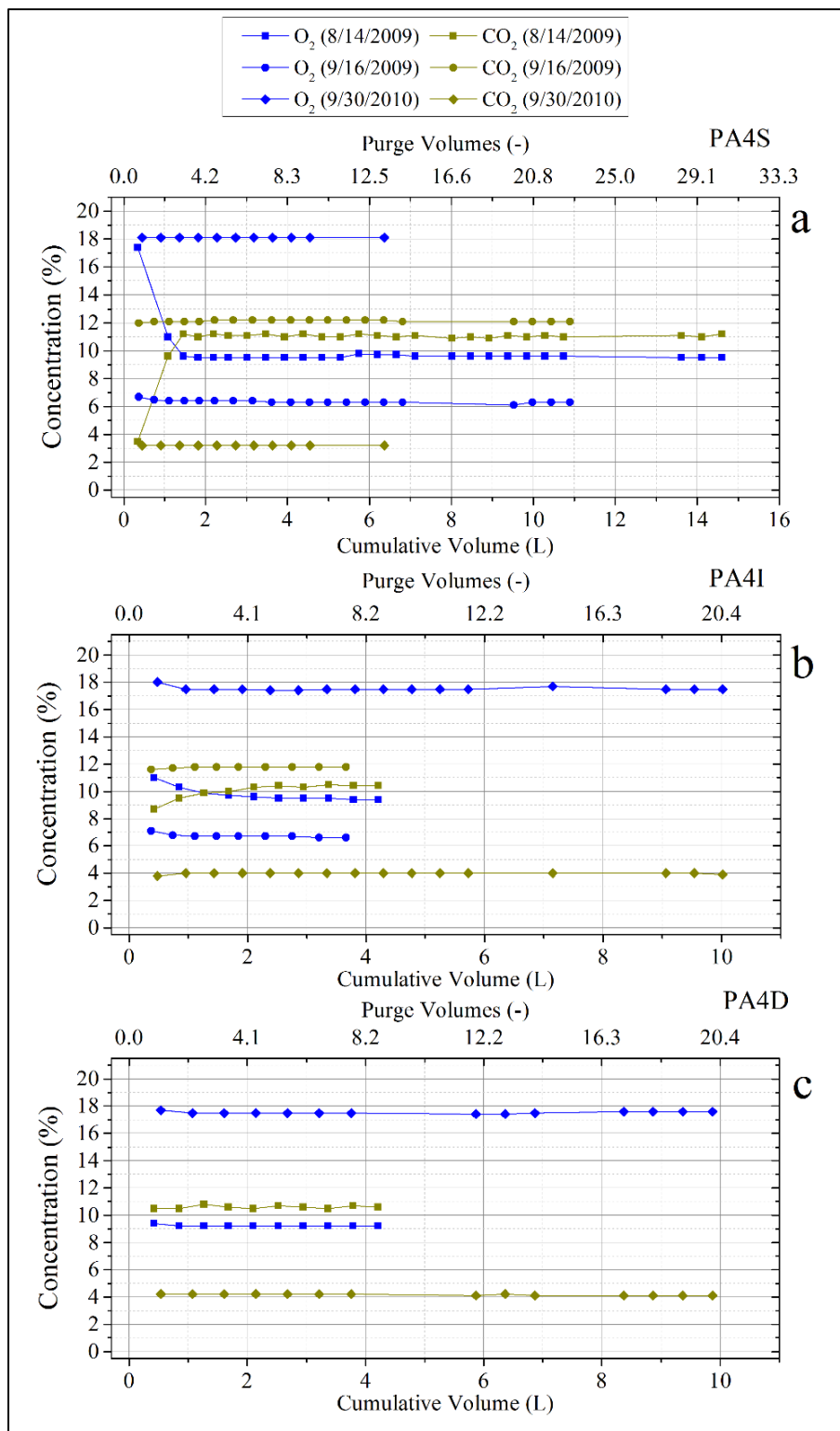


**Figure 47.** Purge test results at soil-gas probe cluster PA4 installed on 8/5/2009. Open borehole time = 5.7 hr. Closed borehole time prior to initial purging = 208, 209, and 209 hours at PA4S, PA4I, and PA4D, respectively. 1 purge volume = ~ 0.44, 0.45, and 0.52 L at PA3S, PA3I, and PA3D, respectively.

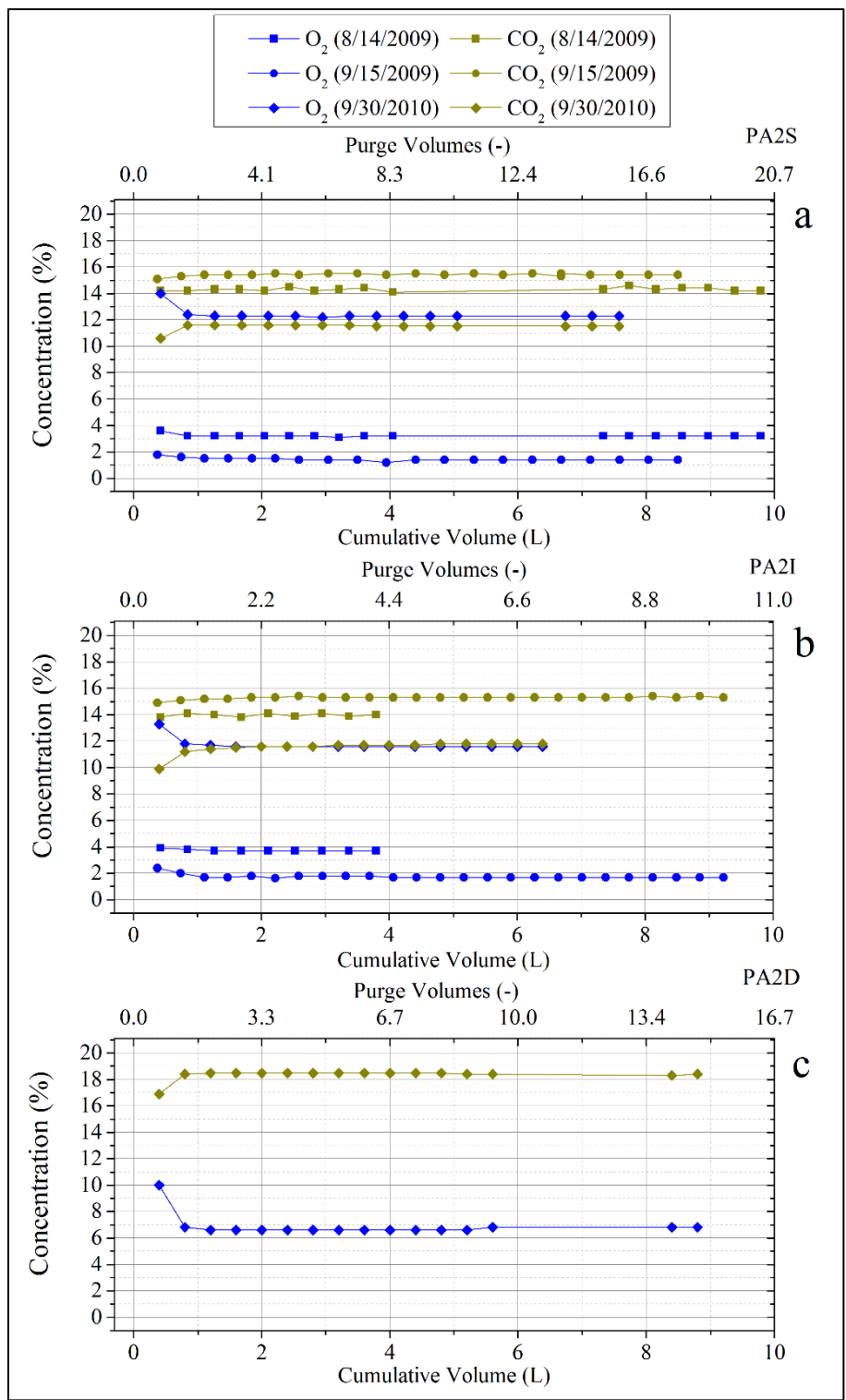


**Figure 48.** Purge test results at soil-gas probe cluster PA2 installed on 8/4/2009. Open borehole time = 23 hr. Closed borehole time prior to initial purging = 207, 208, and 211 hours at PA2S, PA2I, and PA2D, respectively. 1 purge volume = ~ 0.28, 0.91, and 0.62 L at PA2S, PA2I, and PA2D, respectively. PA2D was water-filled during the first two purge events.

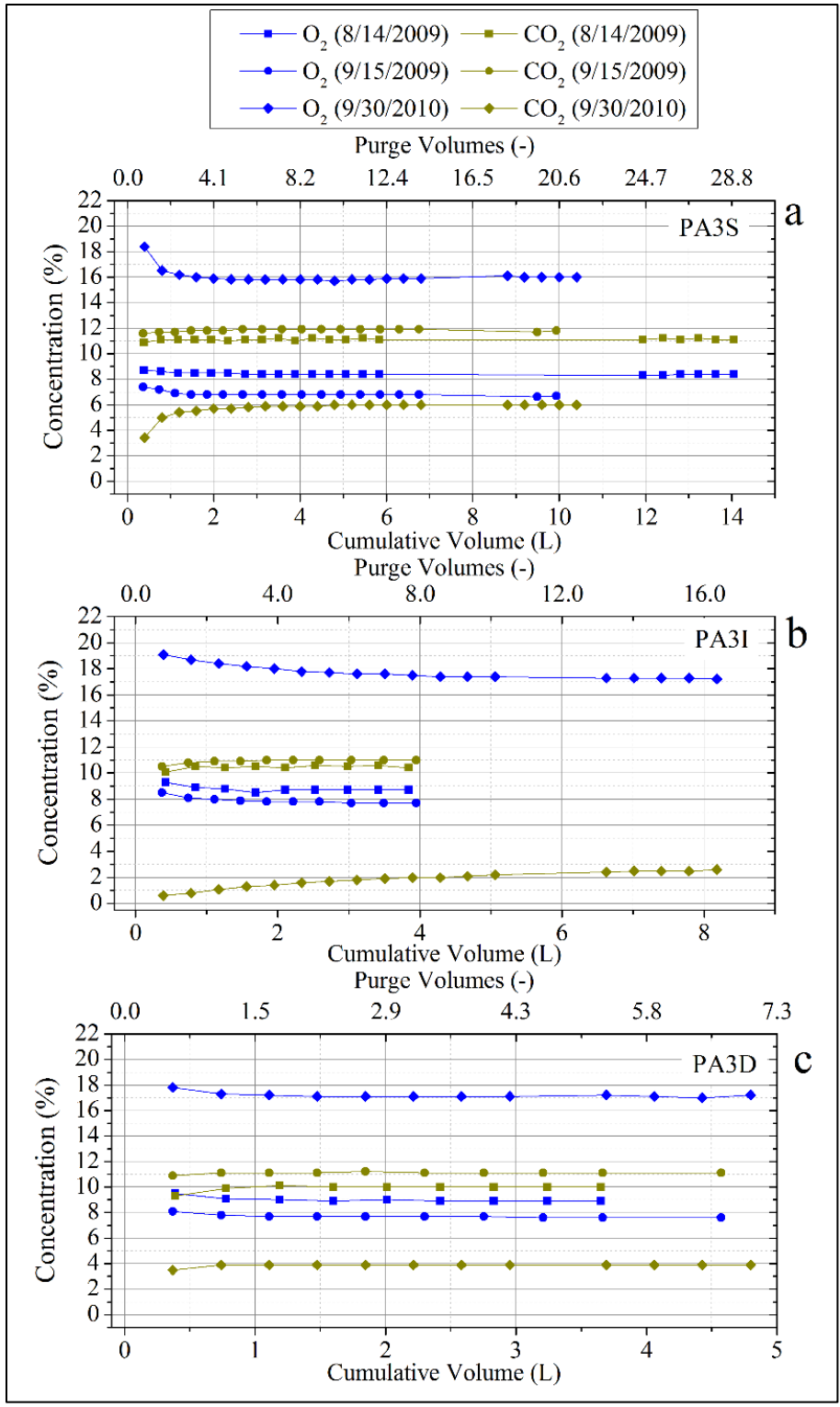


**Figure 49.** Purge test results at soil-gas probe cluster PA3 installed on 8/5/2009. Open borehole time = 8.2 hr. Closed borehole time prior to purging = 208.2, 208.8, and 209.0 hours at PA3S, PA3I, and PA3D, respectively. 1 purge volume = ~ 0.45, 0.47, and 0.58 L at PA3S, PA3I, and PA3D, respectively.

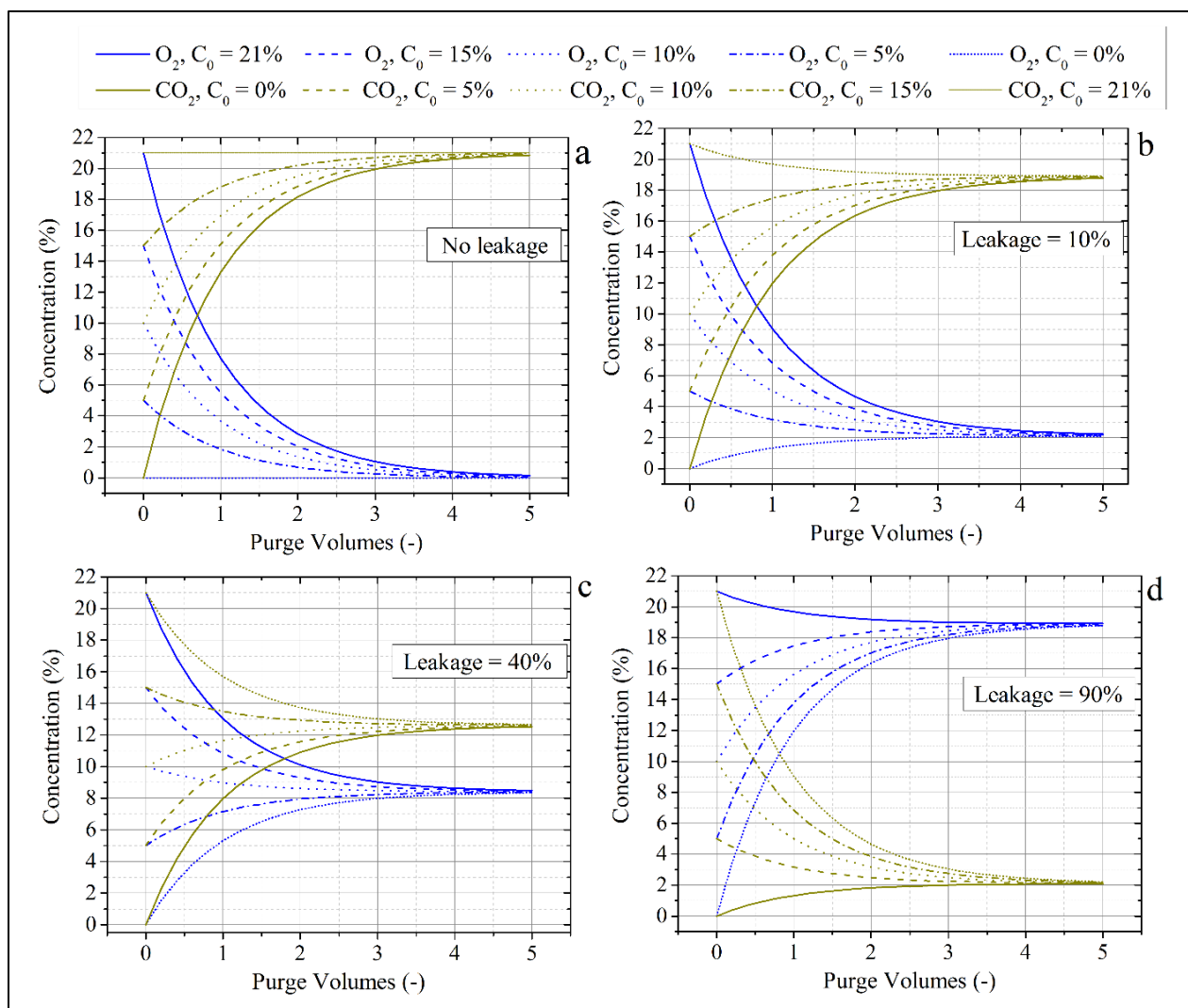


**Figure 50.** Hypothetical purging scenarios for O<sub>2</sub> and CO<sub>2</sub> concentrations in soil-gas at 0% and 21%, respectively, and initial soil-gas concentrations in soil-gas probes for O<sub>2</sub> and CO<sub>2</sub> at 21%, 15%, 10%, 5%, and 0% for (a) no leakage, (b) 10% leakage, (c) 40% leakage, and (d) 90% leakage.

In the worst-case scenario where O<sub>2</sub> and CO<sub>2</sub> concentrations in the probe are 21% and 0%, respectively, 4.6 purge volumes are necessary to be within 1% of soil-gas concentration (**Figure 50a**). Approximately 1.7, 2.3, 2.7, and 3.0 purge volumes are necessary to be within 5% of soil-gas concentration when gas concentrations in the probe are initially within 71, 48, 24, and 0% of soil-gas concentrations. Hence, as generally demonstrated in this investigation, fewer purge volumes are required for stabilization of O<sub>2</sub> and CO<sub>2</sub> concentrations in probes or monitoring wells that have been previously purged.

Recommended purge volumes vary from a specification of 3 purge volumes (Alberta Government 2007, British Columbia Ministry of Environment 2011, Health Canada 2007, New

Jersey Department of Environmental Protection 2005) to 3 to 4 purge volumes (Interstate Technology & Regulatory Council 2007), to 3 – 5 purge volumes (Atlantic Partnership in Risk-Based Corrective Action Implementation 2006, City Chlor France 2013, Electric Power Research Institute 2005, Interstate Technology & Regulatory Council 2007, Missouri Department of Natural Resources 2013). Thus, in the absence of air injection during well or probe installation, a 3 to 5 purge volume requirement prior to soil-gas sampling generally appears reasonable.

However, in several instances in this investigation, greater than 5 purge volumes was required for stabilization of O<sub>2</sub> and CO<sub>2</sub> concentrations. Based on simulation results, this must be the result of disequilibrium in soils or conditions outside the wellbore as a result of probe or well construction or a changing concentration profile outside the borehole. Hence, purge testing as performed in this investigation is necessary to evaluate O<sub>2</sub> and CO<sub>2</sub> concentration stabilization prior to sample collection.

However, there is a requirement in a number of guidance documents relevant to soil-gas sampling (e.g., Electric Power Research Institute 2005, Interstate Technology & Regulatory Council 2007, Missouri Department of Natural Resources 2013, New Jersey Department of Environmental Protection 2005, British Columbia Ministry of Environment 2011, Ontario Ministry of Environment 2007, American Petroleum Institute 2005, Alberta Government 2007, Health Canada 2007) not to exceed 0.2 SLPM during purging or sampling which precludes the use of portable gas analyzers to evaluate gas concentration during purging as was performed in this investigation. Given the results of this investigation, there is a need to reconsider this requirement.

Leakage does not appear to affect time for O<sub>2</sub> and CO<sub>2</sub> stabilization (**Figures 50a, 50b, 50c, 50d**). However, leakage dramatically affects O<sub>2</sub> and CO<sub>2</sub> concentration profiles (**Figures 50b, 50c, 50d**). It is often assumed that leakage is indicated by increasing O<sub>2</sub> and decreasing CO<sub>2</sub> during purging (e.g., Canadian Council of Ministers of Environment, 2008). This assumption appears to be generally valid. However, a corollary assumption that a decrease in O<sub>2</sub> concentration and an increase in CO<sub>2</sub> concentration during purging indicates little or leakage is not valid. A decrease in O<sub>2</sub> concentration and an increase in CO<sub>2</sub> concentration could be observed even at 90% leakage (**Figures 50d**) when the initial O<sub>2</sub> concentration in a vapor probe

is 21% and the initial CO<sub>2</sub> concentration is 0%. There are numerous initial O<sub>2</sub> and CO<sub>2</sub> concentration conditions in which a decrease in O<sub>2</sub> concentration and an increase in CO<sub>2</sub> concentration could be observed at lesser values of leakage (**Figures 50b, 50c**).

There has been some discussion in the literature on the potential impact of purge volume on sample results. In a comparison of “macro-purging” (1 purge volume = 24.6 ml) using the Geoprobe PRT system, and a drive rod system having a 0.254 mm (0.01 in) internal diameter stainless-steel tube for “micro-purging” (1 purge volume = 1.2 ml), Schumacher et al. (2009) found that micro-purging resulted in measurement of higher vapor concentrations (by a factor of 2 to 27X) of cis-1,2-dichloroethene, trichloroethene, tetrachloroethene, toluene, ethylbenzene, m,p-xylene, and o-xylene. Schumacher et al. (2009) state that purging should be minimized to ensure collection of soil-gas from the immediate vicinity of a soil-gas probe.

In contrast however, DiGiulio et al. (2006) compared vapor concentrations of cis-1,2-dichloroethene, 1,1-dichloroethene, 1,1,1-trichloroethane, and trichloroethene during extraction of 0.5 to 102.5 liters of gas from vapor probes and found no change after removal of the first purge volume (1 purge volume = ~ 1 liter). McAlary et al. (2010) state that “high purge volume” (up to 100,000 L) sampling is more appropriate in determining an integrated concentration (in this case sub-slab) over a wide area for risk assessment purposes to support vapor intrusion investigations.

It would appear that the volume of soil-gas extraction during purging is dependent upon a desired integrated volume for concentration profiling. For instance, extraction of 100,000 L of soil-gas would not be appropriate for soil-gas sampling near the surface in the absence of an upper low permeability (slab) boundary and when profiling over short vertical distance in direct-push systems is desirable. If gas permeability testing is conducted, then gas flow modeling could be conducted to determine a desired integrated volume of soil around a probe for soil-gas sampling as illustrated in **Figure 36**.

## Summary

The purpose of this investigation was to improve quality assurance/quality control protocols related to soil-gas sampling, especially those associated with leak, purge, and gas permeability testing and use of portable gas analyzers to support these activities. Leak detection chambers were designed to enable simultaneous leak, purge, and gas permeability testing prior to soil-gas sample collection. Multiple tracers were deployed in probe clusters to discern leakage between screened intervals rather than just from the surface as is typically done. The following is a brief summary of findings separated in 4 areas: portable gas analyzers, shut-in and leak testing, gas permeability testing, and purge testing.

### Portable Gas Analyzers

Portable gas analyzers used in this investigation included: (1) the Landtec GEM 2000 Plus equipped with electrochemical (EC) cells for measurement of oxygen (O<sub>2</sub>), carbon monoxide (CO), and hydrogen sulfide (H<sub>2</sub>S) and infrared (IR) cells for measurement of methane (CH<sub>4</sub>) and CO<sub>2</sub>; (2) the Bacharach H25-IR equipped with an IR cell for measurement of 1,1-dichloro-2,2,2-trifluoroethane (R-123), a gas tracer; and (3) the Thermo Scientific TVA-1000B equipped with a flame ionization detector (FID) and a photoionization detector (PID) (10.6 electron volt lamp).

Portable gas analyzers were calibrated at the beginning of a workday using gas standards. Calibration was checked (bump tests) throughout the workday using gas standards at concentrations of calibration and at other concentrations. During bump testing of the GEM2000 Plus portable gas analyzer, there was a significant number of measurements outside the stipulated QC criterion of  $\pm 1\%$  for O<sub>2</sub> and  $\pm 0.3\%$  for CH<sub>4</sub> at 2.5% necessitating frequent recalibration. While reasons for exceedance of the QC criterion are unknown, this observation reinforces the need for frequent bump tests throughout a workday. Depending on use of measurements from portable gas analyzers, it may be desirable to conduct bump tests prior to and after soil-gas measurement at individual probes.

In many instances, the stipulated QC criterion was achieved but a minor negative or positive bias was observed. In two cases, O<sub>2</sub> measurement at 20.9% with calibration at 4.0% and CO<sub>2</sub> measurement at 20.0% with calibration at 5.0%, a significant negative bias was observed. In the latter case, the quality control criterion of  $\pm 3.0\%$  was attained for 6 of 6 measurements.

Depending on use of measurements, the presence of bias in portable gas analyzers may impact decision making and could be of importance when comparing field measurements with fixed laboratory results.

A comparison of gas measurement at concentrations of calibration and at other concentrations in standard gases provided mixed results. For example, measurement of CO<sub>2</sub> using the GEM 2000 Plus portable gas analyzer at 20.0% with calibration at 20.0% improved measurement compared to measurement of CO<sub>2</sub> at 20.0% with calibration at 5.0%. However, calibration of CO<sub>2</sub> at 5.0% did not improve measurement at 5.0% compared to calibration at 20.0% and 35.0%. Thus, in this investigation, the benefit of using calibration standards with concentrations close to expected concentrations of measurement was not apparent.

Since portable gas analyzers were used in the soil-gas sampling train, the impact of flow rate on gas measurement was investigated using two methods. The first method of evaluation involved restricting flow rate of gas standards from SKC 5-liter (L) Flex-Foil™ gas sampling bags using gas standards for the FID, PID, and R-123. There was a slight increase in R-123 measurement with flow using the H25IR. However, there was a strong increase in FID response but little apparent change in response in PID response with increased flow using the TVA 1000B. Thus, FID measurements must be corrected for flow when volatile hydrocarbons are present in soil gas. This finding should be of importance at other locations where a portable FID is used for soil-gas hydrocarbon measurement.

The second method of evaluating restriction of flow on the portable gas analyzer (GEM 2000 Plus) measurement was to restrict flow in the actual soil-gas sampling train. CO<sub>2</sub> concentrations increased with flow rate while O<sub>2</sub> concentration decreased with flow rate. The rate of change of O<sub>2</sub> and CO<sub>2</sub> concentration was greatest at lower flow rates. At flow rates above approximately 0.65 standard liters per minute (SLPM) there was little impact on O<sub>2</sub> and CO<sub>2</sub> measurement. Thus, in this investigation, a minimum flow rate of 0.65 SLPM was necessary for use of the GEM2000 Plus portable gas analyzer in the soil-gas sampling train. If in-line portable gas analyzers are used to evaluate stabilization of gas concentrations prior to soil-gas sample collection, flow testing is necessary to evaluate the potential effect of flow rate on instrument readings.

Measurements of O<sub>2</sub> and CO<sub>2</sub> using the GEM2000 Plus portable gas analyzer at flow rates in excess of 0.65 SLPM were compared with fixed-laboratory analyses. There was a slight negative bias in field measurement of O<sub>2</sub> and a slight positive bias in field measurement of CO<sub>2</sub> compared to fixed-laboratory measurement. However, this bias was within the stipulated quality control criterion for both gases.

### Shut-In and Leak Testing

In this investigation, 2.54 cm (1”) rubber well plugs with brass quick-connect fittings were used for sampling 2.54 cm internal diameter (ID) PVC monitoring wells. At 90 kPa vacuum (~390 inches of water vacuum or nearly one atmosphere), leakage was less than 1 SCCM and declined to less than 0.01 SCCM below 40 kPa vacuum. Vacuum during soil-gas sampling was typically less than 0.5 kPa and the flow rate during purging and sampling was typically between 900 – 1000 SCCM. Thus, leakage from well plugs was virtually nonexistent and required no modification for use.

The leak detection chamber and sampling train used in this investigation had numerous fittings. To enable rapid leak testing in the field, shut-in testing was conducted in three one-minute tests at high, medium, and low vacuum. Fittings were tested prior to each purge and sampling event. Leakage exceeded 1 SCCM in only 5 out of 141 tests. When leakage exceeded 1 SCCM, fittings were tightened and shut-in tests at high vacuum (e.g. 90 kPa) were repeated until leakage was below 1 SCCM. Thus, leakage through fittings used for the leak detection chamber and soil-gas sampling train were inconsequential in this investigation. Given adequate shut-in testing, use of a fairly complicated soil-gas sampling train with numerous fittings, as was the case in this investigation, should not be a limiting factor for soil-gas sampling.

Unlike fittings used for a leak detection chamber for a soil-gas sampling train, compression fittings on soil vapor probes, O-rings on PVC pipe, and bentonite in the borehole generally cannot be modified above a vapor probe, soil-gas well, or monitoring well installation. Thus, a leak detection chamber and gas tracers must be used to evaluate leakage in the borehole.

Helium (He) is invariably used in chambers for leak detection. However, He is a buoyant gas necessitating the presence of sufficient vacuum in a leakage pathway to a screened interval to

overcome buoyancy. In this investigation, gas mixture containing tracers were formulated to have gas densities similar to expected soil-gas gas densities to eliminate the potential for negative bias in leak detection. A tracer gas mixture containing 1% R-123 and 99% argon (Ar) was typically used for chamber application. A tracer gas mixture containing 1 – 2% CO in air was typically used for passive introduction into 5-L Flex-Foil™ gas sampling bags.

Leakage between stainless-steel tubing and Swagelok™ stainless-steel quick-connect compression fittings attached to tubing was evaluated at 4 probe cluster locations. This type of leak testing is relevant only to quick-connect fittings for intermediate and lower probes in a soil-gas probe cluster since leakage through the quick-connect fitting at the upper probe cannot be distinguished from leakage down the borehole as a result of a poor bentonite seal. Leakage was detected at one location at 2.1%. Detection of leakage was unexpected since quick-connect compression fittings were carefully tightened to stainless-steel tubing prior to deployment in boreholes since working space in boreholes was limited.

Leakage down the annular bentonite seal between the surface and the screened interval of the upper probe was tested 15 times at 6 probe clusters. Leakage occurred during a sampling event to some degree at all 6 upper probes tested. In 5 upper probes, maximum leakage varied from 0.1% to 1.3%. Leakage in excess of this range (94.4%) occurred at one probe (PA1S). During two previous tests in September and November 2009, leakage was detected from the intermediate probe, PA1I, but not from the surface indicating that a leakage pathway from the surface developed sometime after November 2009. This result indicates that the absence of leak detection in a previous soil-gas sampling event does not preclude the development of leak pathways prior to later soil-gas sampling events. Hence, depending on intended use of data, leak testing prior to every soil-gas sampling event should be considered.

Leakage between screened intervals of upper and intermediate probes was tested 19 times at 7 probe clusters. Leakage (2.0%) was detected on one occasion at probe cluster PB1. At probe cluster PA1, there was an anomalous pattern of increasing O<sub>2</sub> concentration during purging at the upper probe, PA1S, prior to introduction of tracer at the intermediate probe, PA1I. After passive introduction of a tracer mixture containing 2.1% CO and 97.9% air at PA1I, O<sub>2</sub> concentration increased and CO<sub>2</sub> concentration decreased in PA1S as a result of tracer gas containing O<sub>2</sub> entering the sample train. Leakage between PA1S and PA1I was estimated at

58.7%. To evaluate reproducibility, leak testing was repeated with leakage measured at 36.0%. Thus, while both tests indicated significant leakage, there was considerable variability between results. Leak testing was repeated two months later with leakage estimated at 74.3%.

Tracer was introduced in an intermediate probe with soil-gas extraction in the lower probe to test leakage between an intermediate and lower probe. No leakage was observed in 10 tests at 5 intermediate-lower probe combinations. Leakage (0.6%) was observed during one test at PAII – PA1D. Thus, the ability to evaluate leakage between probes in a probe cluster by extracting soil-gas from one probe while passively introducing tracer in an overlying or underlying probe was demonstrated in this investigation. This procedure could be applicable to probe cluster configurations elsewhere.

Leakage between the surface and an unsaturated portion of a screened interval in monitoring wells was tested 8 times at 6 monitoring wells with leakage at 0.8% and 2.6% observed at two monitoring wells. With the exception of testing at PA1S, these rates of leakage were not lower than those associated with probe clusters. Probe clusters provide an economic means, especially in consolidated media, to repeatedly sample soil-gas over multiple intervals.

While common in stray gas and soil-atmosphere greenhouse gas exchange investigations, shallow (< 1 m) soil-gas sampling is generally discouraged at vapor intrusion investigations due to concern regarding entry of atmospheric air during sampling. However, when consolidated media or cobbles are at or near the surface, direct-push sampling below 1 m is often infeasible.

Gas flow simulations were conducted to determine whether leakage down a borehole could be distinguished from atmospheric recharge in soil having preferential vertical pathways (e.g., desiccation cracks). In a simulation assuming isotropic (radial permeability = vertical permeability) conditions, travel time of atmospheric air to a probe far exceeds a typical time of leak testing (minutes). However, when anisotropic conditions were simulated (vertical permeability = 10X radial permeability at the same radial permeability), gas tracer arrived in the soil-gas sampling train in less than 3 minutes – the time in which leakage was observed. These results indicate that sealing of the surface using bentonite or some other means in the vicinity of a vapor probe should be considered during leak testing when soil-gas sampling is shallow (e.g. < 1 m) to distinguish leakage from atmospheric recharge.

A heuristic model was developed to provide a conceptual model of leakage in a borehole during soil-gas sampling. For a given borehole radius, as the length of the bentonite seal increases, leakage decreases. When the ratio of radial permeability in the sampled formation to vertical permeability of a borehole sealant is greater than 100X, leakage will be less than 1.0% regardless of geometric factors. Thus, leakage is less likely when a probe is screened in high permeability media such as sand and more likely when a probe is screened in low permeability media such as silt or clay, as one would expect. Thus, leak testing is of considerable importance when collecting soil-gas samples from lower permeability media.

### Gas Permeability Testing

During soil-gas sampling, measurement of gas flow and vacuum occur at the same location or probe similar to slug testing performed in groundwater investigations. Since vacuum measurement at the surface is not equivalent to vacuum in the screened interval due to frictional headloss, vacuum loss in tubing or well casing must be estimated in addition to vacuum loss in fittings at the surface used for the leak detection chamber and soil-gas sampling train. In this investigation, a non-linear equation was used to estimate vacuum loss as function of flow rate in surface fittings using data from a field experiment conducted with the leak detection chamber and surface fittings. Vacuum loss varied from 10 to 40 Pa at flow rates from 0.2 to 1.0 SLPM. Vacuum loss in straight tubing and pipe was estimated using theoretical equations for laminar flow which was maintained during all gas permeability determinations.

In general, vacuum loss due to surface fittings, tubing, and pipe was relatively minor compared to high induced vacuum in lower permeability soils. However, in higher permeability soils, there were several instances using 0.617 cm internal diameter (ID) x 0.535 cm (1/4 inch) outside diameter (OD) stainless-steel tubing where vacuum induced by soils was equivalent to or less than vacuum induced by fittings and tubing. In this situation, a general conclusion can be drawn that when soils are of relatively high permeability, quantification of gas permeability is constrained by potential error in estimation of vacuum loss from surface fittings and tubing.

To aid future gas permeability estimation efforts for others, theoretical vacuum or pressure loss as a function of tube length and flow rate were evaluated for 6 internal diameters for tubing or pipe commonly used for soil-gas probe construction. In small diameter tubing such as 0.158 cm

ID x 0.318 cm OD (1/8" OD) stainless-steel tubing, expected vacuum loss during testing would be excessive and hence is not suitable for gas permeability testing.

Estimated vacuum loss in 0.617 cm ID stainless-steel tubing used for soil-gas probe cluster construction and 0.635 cm ID LDPE tubing used for the Geoprobe PRT direct-push soil-gas sampling exceeded 100 Pa at 1.0 SLPM at tubing lengths of 10 – 15 m. Thus, use of tubing with comparable small internal diameters is undesirable for gas permeability testing at depths exceeding 10 meters.

Estimated vacuum loss was insignificant regardless of depth at flow rates used for soil-gas sampling (<1 SLPM) for 1.59 cm ID steel drive pipe used for the Geoprobe soil-gas cap sampling system or for 1.53 cm ID (1/2" schedule 40 PVC pipe). Hence, the SGC system is preferable over the PRT system and 1/2" and larger schedule 40 PVC pipe is preferable for deeper soil gas probes for gas permeability estimation.

The pseudo-steady-state radial gas flow equation is typically used for gas permeability estimation to support active soil-gas sampling. Since vacuum propagates to infinity in a closed radial domain, use of this equation necessitates stipulation of a pressure boundary at some arbitrary distance from a vapor probe. To overcome this limitation, the California Environmental Protection Agency recommends use of a modified equation for a prolate-spheroidal domain. Estimates of radial permeability using this relatively simple algebraic equation were compared with use of a more geometrically correct, but computationally more difficult (requiring use of a Fortran code) solution for an axisymmetric-cylindrical domain. Estimates of radial permeability using the modified equation for a prolate-spheroidal domain were consistently lower than the latter by a factor of 1.03 to 1.43 compared to estimates of radial permeability using a solution in an axisymmetric-cylindrical domain. The reason for a slight negative bias in permeability estimation is unclear.

Comparison of gas permeability measurements conducted during the same time period at two and three different flow rates indicated random variability between a factor of 1.01 to 1.63. Thus, random variation in radial gas permeability estimation was greater than variability due to the choice of model for gas permeability estimation. Also, the difference in use of equations for permeability estimation is minor when considering variation in orders of magnitude in

permeability of various soil types. Hence, use of the modified equation for a prolate-spheroidal domain to estimate radial permeability is appropriate for reporting gas permeability where required. However, use of more sophisticated analytical solutions is necessary for gas flow simulation and particle tracking or time of travel to a screened interval during purging.

Temporal variability in gas permeability estimation was relatively minor ( $< 3X$ ) to modest ( $3X$  to  $10X$ ) at most probes. However, temporal variability was substantial ( $>10X$ ) at some probes. The presence of lower permeability at two monitoring wells allowed transient gas permeability testing. Transient gas permeability was estimated using an analytical solution for an axisymmetric-cylindrical domain incorporating the effect of borehole storage. This solution enables the use of 4 fitting parameters (radial permeability, the ratio of radial to vertical permeability or anisotropy, gas-filled porosity, and borehole storage). Estimates of borehole storage were constrained by realistic estimates of gas-filled porosity in sandpacks (e.g., 10 – 40%). Estimates of radial permeability were constrained by steady-state gas permeability estimation. Curve fitting was relatively insensitive to anisotropy. Curve fitting however was very sensitive to formation gas-filled porosity estimation which was relatively low (e.g., 1 – 9%) as would be expected in lower permeability media. Gas-filled porosity is an important parameter in particle tracking or estimation of time of travel during gas flow simulation. Thus, if gas flow simulations in lower permeability media are desirable to support active soil-gas sampling, transient gas permeability estimation should be considered.

### Purging

Vapor probes, soil-gas wells, and monitoring wells are typically purged prior to soil-gas sample collection. The often-stated purpose of purging is to remove atmospheric air remaining in the borehole after probe or well installation. Recommended initial (after probe installation) purge volumes vary from 2 to 5 internal volumes (including the gas-filled porosity of sandpacks). In some instances, fixed gases (typically  $O_2$  and  $CO_2$ ) are monitored to evaluate attainment of stabilization.

During this investigation, purging experiments were conducted to determine the number of purge volumes required for stabilization ( $\pm 0.1\%$  random variation on a portable gas analyzer) of  $O_2$  and  $CO_2$  concentrations in vapor probes and monitoring wells as affected by equilibration time

(time since soil-gas probe, monitoring well, or soil-gas well completion or setting of bentonite seal). Purging simulations were conducted using a mass-balance mixing model to compare observed versus expected results.

Extraction of 2 to 4 purge volumes was typically required for stabilization of O<sub>2</sub> and CO<sub>2</sub> concentrations during the first purge event regardless of time of purging (0.3 – 211 hours) after probe or monitoring well installation. However, the rate of change in O<sub>2</sub> and CO<sub>2</sub> concentration appeared more rapid in probes having lesser equilibration time, especially in probes with low O<sub>2</sub> and high CO<sub>2</sub> concentrations (i.e. distinct contrast with atmospheric air). During subsequent purge events, stabilization O<sub>2</sub> and CO<sub>2</sub> concentrations was often achieved in less than 1 purge volume. These observations were consistent with purging simulations.

In some instances in soil-gas probe clusters, in excess of 10 purge volumes was required for stabilization of O<sub>2</sub> and CO<sub>2</sub> concentrations during the first purge event in the upper probe while only 2 to 4 purge volumes were required for stabilization of O<sub>2</sub> and CO<sub>2</sub> concentrations in intermediate and lower probes. The reason for this anomalous behavior was unclear. However, based on simulation results, gas removal in excess of 10 purge volumes indicates a perturbation of O<sub>2</sub> or CO<sub>2</sub> concentration outside the borehole either naturally present or induced during probe installation. For instance, at one probe in a soil-gas probe cluster, a significant change in soil-gas concentration over two sampling periods resulted in the need for purging in excess of 10 purge volumes for stabilization O<sub>2</sub> and CO<sub>2</sub> concentrations.

Finally, it is often assumed that leakage is indicated by increasing O<sub>2</sub> and decreasing CO<sub>2</sub> during purging. This assumption appears to be generally valid. However, a corollary assumption that a decrease in O<sub>2</sub> concentration and an increase in CO<sub>2</sub> concentration during purging indicates little leakage is not valid. Simulations conducted here indicate that a decrease in O<sub>2</sub> concentration and an increase in CO<sub>2</sub> concentration could be observed even at 90% leakage when the initial O<sub>2</sub> concentration in a vapor probe is 21% and the initial CO<sub>2</sub> concentration is 0%. There are numerous initial O<sub>2</sub> and CO<sub>2</sub> concentration conditions in which a decrease in O<sub>2</sub> concentration and an increase in CO<sub>2</sub> concentration could be observed at lesser values of leakage.

## References

Aelion, M.C.; Shaw, J.N.; Ray, R.P.; Widdowson, M.A.; Reeves, H.W. Simplified methods for monitoring petroleum-contaminated ground water and soil vapor. *Journal of Soil Contamination* **1996**, 5(3), 225-241.

Alaska Department of Environmental Conservation Division of Spill Prevention and Response, Contaminated Sites Program. *Vapor Intrusion Guidance for Contaminated Sites*, October **2012**

Alpers, C.N.; Dettman, D.L.; Lohmann, K.C.; Brabec, D. Stable isotopes of carbon dioxide in soil gas over massive sulfide mineralization at Crandon, Wisconsin. *Journal of Geochemical Exploration* **1990**, 38, 69-86.

Alberta Government. *Preliminary Draft Report on Development of Tier 2 Site Specific Remediation Objectives for Soil Vapour in Alberta*, July **2007**.

American Petroleum Institute. *Collecting and Interpreting Soil Gas Samples from the Vadose Zone: A Practical Strategy for Assessing the Subsurface Vapor-to-Indoor Air Migration Pathway at Petroleum Hydrocarbon Sites*. Publication Number 4741. **2005**. Available at <http://www.api.org/ehs/groundwater/lnapl/upload/4741final111805.pdf>

American Society for Testing and Materials. *Standard Practice for Active Soil Gas Sampling in the Vadose Zone for Vapor Intrusion Investigations*, D7663-12, April **2012**

Amos, R.T.; Mayer, K.U.; Bekins, B.A.; Delin, G.N.; Williams, R.L. Use of dissolved and vapor-phase gases to investigate methanogenic degradation of petroleum hydrocarbon contamination in the subsurface. *Water Resources Research* **2005**, 41, 1-15.

Annunziatellis, A.; Beaubien, S.E.; Bigi, S.; Ciotoli, G.; Coltella, M.; Lombardi, S. Gas migration along fault systems and through the vadose zone in the Latera caldera (central Italy): Implications for CO<sub>2</sub> geological storage. *International Journal of Greenhouse Gas Control* **2008**, 2, 353-372.

Atlantic Partnership in Risk-Based Corrective Action Implementation. *Atlantic Risk-Based Corrective Action for Petroleum Impacted Sites in Atlantic Canada. Guidance for Soil Vapour and Indoor Air Monitoring Assessments*, July **2006**.

Atlantic Richfield Company – A BP Affiliated Company, *Recommended Practices Manual for Making Decisions About Vapor Intrusion*, Prepared by: Bart Eklund, URS Corporation, Austin, TX and Victor J. Kremesec, Jr., Atlantic Richfield Co., Warrenville, IL, September **2006**.

Arizona Department of Environmental Quality. *Soil Vapor Sampling Guidance*, Revised May 19, **2011**

Azzaro, R., S. Branca, S. Giammanco, S. Gurrieri, R. Rasa, and M. Valenza. New evidence for the form and extent of the Pernicana Fault System (Mt. Etna) from structural and soil-gas surveying. *Journal of Volcanology and Geochemical Research* **1998**, 84:143-152.

Bacharach H25-IR Infrared Refrigerant Gas Leak Detector, Instruction 3015-4342 Operation & Maintenance, Rev. 1 – January **2006**, 621 Hunt Valley Circle, New Kensington, PA 15068

Baehr, A.L.; Hult, M.F. Evaluation of unsaturated zone air permeability through pneumatic tests, *Water Resources Research* **1991**, 27(10), 2605-2617.

Baehr, A.L.; Joss, C.J. An updated model of induced airflow in the unsaturated zone, *Water Resources Research* **1995**, 31(2), 417-421.

Banikowski, J.E.; Kaczmar, S.W.; Hunt, J.F. Field Validation of helium as a tracer gas during soil vapor sample collection. *Soil & Sediment Contamination* **2009**, 18, 243-263.

Barber, C.; Davis, G.B.; Briegel, D.; Ward, J.K. Factors controlling the concentration of methane and other volatiles in groundwater and soil-gas around a waste site. *Journal of Contaminant Hydrology* **1990**, 5, 155-169.

Bassett, R.L.; Neuman, S.P.; Rasmussen, T.C.; Guzman, A.; Davidson, G.R.; Lohrstorfer, C.F. *Validation Studies for Assessing Unsaturated Flow and Transport through Fractured Rock*. NUREG/CR-6203. Prepared for Division of Regulatory Applications, Office of Nuclear Regulatory Research, U.S. Nuclear Regulatory Commission, Washington, D.C., **1994**.

Bateson, L.; Vellico, M.; Beaubien, S.E.; Pearce, J.M.; Annunziatellis, A.; Ciotoli, G.; Coren, F.; Lombardi, S.; Marsh, S. The application of remote-sensing techniques to monitor CO<sub>2</sub>-storage sites for surface leakage: Method development and testing at Latera (Italy) where naturally produced CO<sub>2</sub> is leaking to the atmosphere. *International Journal of Greenhouse Gas Control* **2008**, 2, 388-400.

Baubron, J.C., A. Rigo, and J.P. Toutain. Soil gas profiles as a tool to characterize active tectonic areas: The Jaut Pass example (Pyrenees, France). *Earth and Planetary Science Letters* **2002**, 196:69-81.

Beaubien, S.E.; Ciotoli, G.; Coombs, P.; Dictor, M.C.; Krüger, M.; Lombardi, S., Pearce, J.M.; West, J.M. the impact of a naturally occurring CO<sub>2</sub> gas vent on the shallow ecosystem and soil chemistry of a Mediterranean pasture (Latera, Italy). *International Journal of Greenhouse Gas Control* **2008**, 2, 373-387.

Beaubien, S.E.; Jones, D.g.; Gal, f.; Barkwith, A.K.A.P.; Braibant, G.; Baubron, J.-C.; Ciotoli, G.; Graziani, s.; Lister, T.R.; Lombardi, S.; Michel, K.; Quattrocchi, f.; Strutt, M.H. Monitoring of near-surface gas geochemistry at the Weyburn, Canada, CO<sub>2</sub>-EOR site, 2001-2011. *International Journal of Greenhouse Gas Control* **2013**, 16S, S236-S262.

Bouchard, D.; Hunkeler, D.; Höhener, P. Carbon isotope fractionation during aerobic biodegradation on n-alkanes and aromatic compounds in unsaturated sand. *Organic Geochemistry* **2008**, 39, 23-33.

British Columbia Ministry of Environment. *Guidance on Site Characterization for Evaluation of Soil Vapour Intrusion into Buildings*, Prepared by Golder Associates Ltd, May 2011 **2011**.

California Environmental Protection Agency, Department of Toxic Substances Control, Los Angeles Regional Water Quality Control Board, San Francisco Regional Water Quality Control Board, *Advisory Soil Gas Investigations*, April **2012**.

California Environmental Protection Agency, Department of Toxic Substances Control, *Guidance for the Evaluation and Mitigation of Subsurface Vapor Intrusion to Indoor Air* (Vapor Intrusion Guidance), October **2011**.

Canadian Council of Ministers of the Environment. *Final Scoping Assessment of Soil Vapour Monitoring Protocols for Evaluating Subsurface Vapor Intrusion into Indoor Air*, PN 1427. Prepared by Geosyntec Consultants, **2009**.

Carrigan, C.R.; Heinle, R.A.; Hudson, G.B.; Nitao, J.J.; Zucca, J.J. Trace gas emissions on geological faults as indicators of underground nuclear testing. *Nature* **1996**, 382, 528-531.

Cho, J.S.; DiGiulio, D.C.; Pneumatic pumping test for soil vacuum extraction. *Environmental Progress* **1992**, 11(3), 228-233.

Ciotoli, G., Guerra M.; Lombardi, S.; Vittori, E. Soil gas survey for tracing seismogenic faults: A case study the Fucino basin (central Italy). *Journal of Geophysical Research* **1998**, 103(B10), 781-783.

Ciotoli, G., Etiope, G.; Guerra, M.; Lombardi, S. The detection of concealed faults in the Ofanto basin using the correlation between soil-gas fracture surveys. *Tectonophysics* **1999**, 299(3-4), 321-332.

Ciotoli, G., Lombardi, S.; Morandi, S.; Zarlenga, F. A multidisciplinary statistical approach to study the relationships between helium leakage and neotectonic activity in a gas province: The Vasto basin, Abruzzo-Molise (central Italy). *The American Association of Petroleum Geologists Bulletin* **2004**, 88(3), 355-372.

Ciotoli, G., Etiope, G.; Guerra, M.; Lombardi, S.; Duddridge, G.A.; Grainger, P. Migration of gas injected into a fault in low permeability ground. *Quarterly Journal of Engineering Geology and Hydrogeology* **2005**, 38, 305-320.

Ciotoli, G., S. Lombardi, A. Annunziatellis. Geostatistical analysis of soil gas data in a high seismic intermontane basin: The Fucino Plain, central Italy. *Journal of Geophysical Research* **2007**, 112(B05407), doi:10.1029/2005JB004044.

City Chlor (France). *Soil-Gas Monitoring: Soil-Gas Well Designs and Soil-Gas Sampling Techniques*, INERIS reference: DRC-13-114341-03542A, April **2013**

Colorado Department of Labor and Employment, Division of Oil and Public Safety, Remediation section (Colorado). *Petroleum Hydrocarbon Vapor Intrusion Guidance Document*, December 11, **2007**

D'Alessandro, W.D.; Parello, F. Soil gas prospection of He, <sup>222</sup>Rn, and CO<sub>2</sub>: Vulcano Porto area, Aeolian Islands, Italy. *Applied Geochemistry* **1997**, 12, 213-224.

Deyo, B.G.; Robbins, G.A.; Binkhorst, G.K. 1993. Use of oxygen and carbon dioxide detectors to screen soil gas for subsurface contamination. *Ground Water* **1993**, 31(4), 598 - 604.

DiGiulio, D.C. A conceptual understanding of leakage during soil-gas sampling. 17th Annual Association for Environmental Health and Sciences (AEHS) Meeting Workshop on Soil-Gas

Sample Collection and Analysis San Diego, CA March 21 – 22, **2007a**.  
[https://iavi.rti.org/attachments/WorkshopsAndConferences/12\\_DiGiulio\\_Hartman\\_Leakage.pdf](https://iavi.rti.org/attachments/WorkshopsAndConferences/12_DiGiulio_Hartman_Leakage.pdf)

DiGiulio, D.C. Evaluating vapor equilibration and purging on soil-gas sampling. In 17th Annual Association for Environmental Health and Sciences (AEHS) Meeting Workshop on Soil-Gas Sample Collection and Analysis San Diego, CA March 21 – 22, **2007b**.  
[https://iavi.rti.org/attachments/WorkshopsAndConferences/10\\_DiGiulio\\_Vapor\\_Equilibration\\_and\\_Purging.pdf](https://iavi.rti.org/attachments/WorkshopsAndConferences/10_DiGiulio_Vapor_Equilibration_and_Purging.pdf)

DiGiulio, D.C. EPA Studies identify techniques for critical leak testing prior to soil-vapor sampling. *Technology News and Trends*, September 2009,  
<https://clu-in.org/products/newsletters/tnandt/view.cfm?issue=0909.cfm>

DiGiulio, D.C., and R. Varadhan. Steady-state, field-scale gas permeability estimation and pore-gas velocity calculation in a domain open to the atmosphere, *Remediation*, **2000**, 10(4), 13-25.

DiGiulio, D.C.; Varadhan, R. *Development of Recommendations and Methods to Support Assessment of Soil Venting Performance and Closure*. United States Environmental Protection Agency, Office of Research and Development, National Risk Management Research Laboratory, Ada, OK, EPA/600/R-01/070, September, **2001a**

DiGiulio, D.C. and R. Varadhan. Limitations of ROI testing for venting design: Description of an alternative approach based on attainment of critical pore-gas velocities in contaminated media, *Ground Water Monitoring and Remediation*, **2001b**.

DiGiulio, D.C., C. Paul, R. Cody, R. Willey, S. Clifford, P. Kahn, R. Mosley, A. Lee, and K. Christensen. *Assessment of Vapor Intrusion in Homes near the Raymark Superfund Site Using Basement and Sub-Slab Air Samples*. EPA/600/R-05/147, U.S. Environmental Protection Agency, Office of Research and Development, National Risk Management Research Laboratory, **2006a**.

DiGiulio, D.C., C. Paul, B. Scroggins, R. Cody, R. Willey, S. Clifford, R. Mosley, A. Lee, K. Christensen, and R. Costa. *Comparison of Geoprobe PRT, AMS GVP soil-gas sampling systems with dedicated vapor probes in sandy soils at the Raymark Superfund Site*. EPA/600/R-06/11, U.S. Environmental Protection Agency, Office of Research and Development, National Risk Management Research Laboratory, **2006b**.

Electric Power Research Institute. *Reference Handbook for the Site-Specific Assessment of Subsurface Vapor Intrusion to Indoor Air*, EPRI Document #1008492, Palo Alto, CA, March **2005**.

Environment Protection Authority Victoria. Transpacific Waste Management P/L Fraser Road Landfill s53V Environmental Audit - Risk of Harm from Methane Generation, November, **2009**

Falta, R.W. A program for analyzing transient and steady-state soil gas pump tests. *Groundwater* **1996**, 34(4), 750-755

Fountain, J.C.; Jacobi, R.D.; Detection of buried faults and fractures using soil gas analysis. *Environmental and Engineering Geoscience* **2000**, 6(3), 201-208.

Fridman, A.I. Application of naturally occurring gases as geochemical pathfinders in prospecting for endogenous deposits. *Journal of Geochemical Exploration* **1990**, 38(1-2):1-11.

Geoprobe. PRT Active Sampling. Accessed on 8/30/2016 at <http://geoprobe.com/prt-active-sampling>

Guzman, A.; Lohrstorfer, C. Appendix B: Zero Permeability Test Field Operating Procedure. In Validation Studies for Assessing Unsaturated Flow and Transport through Fractured Rock. NUREG/CR-6203. Prepared by R.L. Bassett, S.P. Neuman, T.C. Rasmussen, A. Guzman, G.R. Davidson, C.F. Lohrstorfer. Prepared for Division of Regulatory Applications, Office of Nuclear Regulatory Research, U.S. Nuclear Regulatory Commission, Washington, D.C., **1994**

Hartman, B. How to collect reliable soil-gas data for risk-based applications, Part 1: Active Soil-Gas Method. *LUST Line Bulletin* **2002**, 42, 17-22.

Hartman, B. How to collect reliable soil-gas data for risk-based applications – Specifically vapor Intrusion, Part 3 – Answers to Frequently Asked Questions. *LUST Line Bulletin* **2004**, 48, 12-17.

Hartman, B. How to collect reliable soil-gas data for risk-based applications - Specifically vapor Intrusion, Part 4 - Updates on Soil-gas collection and analytical procedures. *LUST Line Bulletin* **2007**, 53, 14-19.

Hawaii Department of Health (Hawaii). *Technical Guidance Manual for the Implementation of the Hawai'i State Contingency Plan, Section 7, Soil Vapor and Indoor Air Sampling Guidance*, February **2014**

Hayes, H., Benton, D.J.; Khan, N. The Impact of Sampling Media on Soil Gas Measurements. Proc. Of AWMA Vapor Intrusion – The Next Great Environmental Challenge – An Update, September 13-15, 2006. Los Angeles, CA.

Health Canada. *Draft Guidance Manual for Environmental Site Characterization in Support of Health Risk Assessment*, May **2007**.

Henderson, R.E. Portable gas detectors used in confined space and other industrial atmospheric monitoring programs. In Safety and Health in Confined Spaces, McManus, Neil, Lewis Publishers, Boca Raton, FL, 1999.

Hers, I.; Li, L.; Hannam, S. Evaluation of soil gas sampling and analysis techniques at a former petrochemical plant site. *Environmental Technology* **2004**, 25, 847-860.

Illinois Environmental Protection Agency. Soil Gas Sampling Protocol, June, **2013**, <http://www.epa.illinois.gov/topics/cleanup-programs/taco/vapor-intrusion/soil-gas-sampling-protocol/index>

Interstate Technology & Regulatory Council. Vapor Intrusion Pathway: A Practical Guideline, January **2007**, <http://www.itrcweb.org/documents/vi-1.pdf>

Interstate Technology & Regulatory Council. *Petroleum Vapor Intrusion: Fundamentals of Screening, Investigation, and Management. PVI-1*. Interstate Technology & Regulatory Council, Washington, D.C. Petroleum Vapor Intrusion Team. 2014, [www.itrcweb.org/PetroleumVI-Guidance](http://www.itrcweb.org/PetroleumVI-Guidance).

- Jewell, K.P.; Wilson, J.T. A new screening method for methane in soil gas using existing groundwater monitoring wells. *Ground Water Monitoring & Remediation* **2011**, 31(3), 82-94.
- Johnson, P.C.; Stanley, C.C.; Kembrowski, M.W.; Byers, D.L.; Colthart, J.D. A practical approach to the design, operation, and monitoring of in-situ soil venting systems. *Ground Water Monitoring and Remediation* **1990**, 10(2), 159–178.
- Jones, V.T. and R.J. Drozd. Predictions of oil and gas potential by near-surface geochemistry. *The American Association of Petroleum Geologists Bulletin* **1983**, 67(6):932-952.
- Joss, C.J.; Baehr, A.L. *Documentation of AIR2D, A computer Program to Simulate Two-Dimensional Axisymmetric Airflow in the Unsaturated Zone*, U.S. Geological Survey Open-File Report 97-588, West Trenton, NJ **1997**.
- Kansas Department of Health and Environment. *Standard Operating Procedure - BER-37 – Collection of Soil Vapor Samples for Analysis of Volatile Organic Compounds*. January 1, **2011**.
- Kerfoot, H.B. Is soil-gas an effective means of tracking contaminant plumes in ground water? What are the limitations of the technology currently employed? *Ground Water Monitoring and Remediation* **1988**, 8(2), 54-57.
- King, C.Y., B.S. King, W.C. Evans, and W. Zang. 1996. Spatial radon anomalies on active faults in California. *Applied Geochemistry*, 11:497-510.
- Landtec GEM2000 and GEM2000 Plus Gas Analyzer & Extraction Monitor Operation Manual for Serial Numbers 10000 and Up (2007), Landtec North America, 850 S. Via Lata, Suite 112, Colton, CA 92324
- Lewicki, J.L. and S.L. Brantley. 2000. CO<sub>2</sub> degassing along the San Andreas fault, Parkfield, California. *Geophysical Research Letters*, 27(1):5-8.
- Lewicki, J.L., W.C. Evans, G.E. Hilley, M.L. Sorey, J. Rogie, and S.L. Brantley. 2003. Shallow soil CO<sub>2</sub> flow along the San Andreas and Calaveras Faults, California. *Journal of Geophysical Research*, 108(B4):2187, doi:10.1029/2002JB002141.
- Li, D.X.; Lundegard, P.D. Evaluation of subsurface oxygen sensors for remediation monitoring. *Ground Water Monitoring and Remediation* **1996**, Winter, 106–111.
- Maine Bureau of Remediation and Waste Management. *Protocol for Collecting Soil Gas Samples*. Standard Operating Procedure: RWM-DR-026, Feb 2, 2009
- Marrin, D.L. Soil-gas sampling and misinterpretation, *Ground Water Monitoring and Remediation* **1988**, 8(2), 51-54
- Marrin, D.L.; Kerfoot. H.B. Soil-gas surveying techniques. *Environmental Science and Technology* **1988**, 22(7), 740-745.
- McAlary, T.A., Nicholson, P.; Groenevelt, H.; Bertrand, D.M. A case study of soil-gas sampling in silt and clay-rich (low-permeability) soils. *Ground Water Monitoring & Remediation* **2009**, 29(1), 144-152.

McAlary, T.A.; Nicholson, P.; Yik, L.K.; Bertrand, D.; Thrupp, G. High purge volume sampling – A new paradigm for subslab soil gas monitoring. *Ground Water Monitoring and Remediation* **2010**, 30(2), 73-85.

Michigan Department of Environmental Quality, Remediation and Redevelopment Division. *Guidance Document for the Vapor Intrusion Pathway*, May **2013**

Minnesota Pollution Control Agency, Remediation Division. *Vapor Intrusion Technical Support Document*, August 2010.

Missouri Department of Natural Resources. *Missouri Risk-Based Corrective Action Process for Petroleum Storage Tanks, Appendix C, Evaluation of the Vapor Intrusion Pathway*, October **2013**.

Montana Department of Environmental Quality. *Montana Vapor Intrusion Guide*, April 22, **2011**

New Hampshire Department of Environmental Services. *Vapor Intrusion Guidance*, July 5, **2011**

New Jersey Department of Environmental Protection. *NJDEP Vapor Intrusion Guidance*, October **2005**.

New York State Department of Health, Center for Environmental Health, Bureau of Environmental Exposure Investigation. *Guidance for Evaluating Soil Vapor Intrusion in the State of New York*, October **2006**.

Nyquist, J.E.; Wilson, D.L.; Norman, L.A.; Gammage, R.B. Decreased sensitivity of photoionization detector total organic vapor detectors in the presence of methane. *American Industrial Hygiene Association*, **1990**, 51, 326-330.

Ohio Environmental Protection Agency, Division of Drinking and Ground Waters. Technical Guidance Manual for Ground Water Investigations, Chapter 11, Soil Gas Monitoring for Site Characterization, **August 2008**.

Ontario Ministry of Environment. Draft Report. Technical Guidance Document. Soil Vapour at Contaminated Sites, Behavior, Assessment and Monitoring, September 2007.

Oregon Department of Environmental Quality. *Environmental Cleanup Program. Guidance for Assessing and Remediating Vapor Intrusion in Buildings*, March 25, **2010**

Patterson, B.M.; Davis, G.B. An in situ device to measure oxygen in the vadose zone and in ground water: Laboratory testing and field evaluation. *Ground Water Monitoring and Remediation*, **2008**, 28(2), 68-74.

Perina, T.; Lee, T-C. Steady-state soil vapor extraction from a pressure-controlled or flow controlled well, *Ground Water Monitoring and Remediation*, **2005** 25(3), 63-72.

Popovičova, J.; Brusseau, M.L. Contaminant mass transfer during gas-phase transport in unsaturated porous media. *Water Resources Research*, **1998** 34(1), 83-92.

Robbins, G.A.; Deyo, B.G.; Temple, M.R.; Stuart, J.D.; Lacy, M.J. Soil-gas surveying for subsurface gasoline contamination using total organic vapor detection instruments, Part I. Theory

and laboratory experimentation. *Ground Water Monitoring and Remediation*, **1990a**, 10(3), 122-131.

Robbins, G.A.; Deyo, B.G.; Temple, M.R.; Stuart, J.D.; Lacy, M.J. Soil-gas surveying for subsurface gasoline contamination using total organic vapor detection instruments, Part II. Field experimentation. *Ground Water Monitoring and Remediation*, **1990b**, 10(4), 110-117.

Robbins, G.A.; McAninch, B.E.; Gavas, F.M.; Ellis, P.M. An evaluation of soil-gas surveying for H<sub>2</sub>S for locating subsurface hydrocarbon contamination, *Ground Water Monitoring and Remediation*, **1995**, Winter, 124-132.

RSKSOP-313v1 - *Standard Operating Procedure, Determination of R-123 using the H25-IR Infrared Refrigerant Gas Leak Detector*, U.S. Environmental Protection Agency, Office of Research and Development, National Risk Management Research Laboratory, Groundwater and Ecosystems Restoration Division, Ada, OK

RSKSOP-314v1 - *Standard Operating Procedure, Determination of Fixed Gases using the GEM2000 and GEM2000 Plus Gas Analyzers & Extraction Monitors*, U.S. Environmental Protection Agency, Office of Research and Development, National Risk Management Research Laboratory, Groundwater and Ecosystems Restoration Division, Ada, OK

RSKSOP-320v0 - *Standard Operating Procedure, Determination of Organic and Inorganic Vapors Using the TVA-1000B Toxic Vapor Analyzer*, U.S. Environmental Protection Agency, Office of Research and Development, National Risk Management Research Laboratory, Groundwater and Ecosystems Restoration Division, Ada, OK, May 2010.

Schumacher, B.A.; Zimmerman, J.H.; Sibert, C.R.; Varner, K.E.; Riddick, L.A. Macro- and micro-purge soil-gas sampling methods for the collection of contaminant vapors. *Ground Water Monitoring and Remediation*, **2009**, 29(1), 138-143.

Schumacher, B.A.; Zimmerman, J.H.; Elliot, R.J.; Swanson, G.R. The effect of equilibration time and tubing material on soil gas measurements. *Soil and Sediment Contamination*, **2016**, 25(2), 151-163.

Senum, G.I. quenching or enhancement of the response of the photoionization detector. *Journal of Chromatography A*, **1981**, 205, 413-418.

Shan, C.; Falta, R.W.; Javandel, I. Analytical solutions for steady state gas flow to a soil vapor extraction well, *Water Resources Research*, **1992**, 28(4), 1105-1120.

Thermo Electric Corporation - TVA-1000B Toxic Vapor Analyzer, Instruction Manual, P/N BK3500, Environmental Instruments, 27 Forge Parkway, Franklin, MA 02038, Dec 1 2003.

Thompson, C.V.; Goedert, M.G. Field-portable instrumentation for gas and vapor samples. In *Encyclopedia of Analytical Chemistry*, John Wiley & Sons, Ltd. 2009.

U.S. Air Force, Air Force Center for Environmental Excellence (AFCEE). *Addendum One to Test Plan and Technical Protocol for a Field Treatability Test for Bioventing – Using Soil Gas Surveys to Determine Bioventing Feasibility and Natural Attenuation Potential*, February **1994**.

U.S. Air Force, U.S. Navy, and U.S. Army, *Tri-Services Handbook for the Assessment of the Vapor Intrusion Pathway*, Final Draft, IOH-RS-BR-HB-2008-0001, February 15, **2008**

US Army Corps of Engineers (USACE) Engineering and Design EM 1110-1-4001, Soil Vapor Extraction and Bioventing, 3 June 2002.

[http://www.publications.usace.army.mil/Portals/76/Publications/EngineerManuals/EM\\_1110-1-4001.pdf](http://www.publications.usace.army.mil/Portals/76/Publications/EngineerManuals/EM_1110-1-4001.pdf)

United States Department of Defense (DOD), *Vapor Intrusion Handbook*, Prepared by Tri-Service Environmental Assessment Workgroup, January, **2009**.

U.S. Department of the Navy, SSC Pacific. *Review of Best Practices, Knowledge and Data Gaps, and Research Opportunities for the U.S. Department of Navy Vapor Intrusion Focus Areas*, Technical Report 1982, May **2009**.

U.S. Environmental Protection Agency (EPA), *Soil-Gas and Geophysical Techniques for Detection of Subsurface Organic Contamination*, Office of Research and Development, Environmental Monitoring Systems Laboratory, Las Vegas, NV, December, **1987**.

U.S. Environmental Protection Agency (EPA), *Soil Gas Sampling*, Environmental Response Team, SOP# 2042 Rev0.0, June 1, **1996**.

U.S. Environmental Protection Agency (EPA), *Expedited Site Assessment for Storage Tank Sites - A Guide for Regulators*, EPA 510-9-97-001, Office of Solid Waste and Emergency Response, Washington, D.C., March, **1997**.

U.S. Environmental Protection Agency (EPA), *Soil-Gas Measurement*, Office of Research and Development, Environmental Monitoring Systems Laboratory, Las Vegas, NV, March, **2003**.

U.S. Environmental Protection Agency (EPA). *Vertical Distribution of VOCs in Soils from Groundwater to the Surface/Subslab*, Office of Research and Development, National Exposure Research Laboratory, Las Vegas, NV, EPA/600/R-09/073, August **2009**.

U.S. Environmental Protection Agency (EPA). *Technical Guide for Addressing Petroleum Vapor Intrusion at Leaking Underground Storage Tank Sites*, EPA 510-R-15-001, Office of Underground Storage Tanks, Washington, D.C., June, **2015**

Washington District of Columbia, Department of Energy & Environment, Toxic Substances Division, Underground Storage Tanks Branch. *Petroleum Vapor Intrusion Guidance, Appendix C – Collection of Soil Gas Samples Technical Guidance*, March **2016**

Washington State Department of Ecology, Toxics Cleanup Program. *Guidance for Evaluating Soil Vapor Intrusion in Washington State: Investigation and Remedial Action – Appendix C Soil Gas Sampling for VI Assessment*, Revised February **2016**

Wilson, D.J. Soil gas volatile organic compound concentration contours for locating vadose zone nonaqueous phase liquid contamination. *Environmental Monitoring and Assessment*, **1997**, 48, 73-100.

Wilson, J.T.; Jewell, K.; Adair, C.; Paul, C.; Ruybal, C.; DeVaul, G.; Weaver, J.W. Ground Water Issue Paper: *An Approach that Uses the Concentrations of Hydrocarbon Compounds in*

*Soil Gas at the Source of Contamination to Evaluate the Potential for Intrusion of Petroleum Vapors into Buildings (PVI)*. U.S. Environmental Protection Agency, Office of Research and Development, National Risk Management Research Laboratory, Groundwater and Ecosystems Restoration Division, Ada, OK, EPA/600/R-14/318, December 2014

Wisconsin Department of Natural Resources. *Addressing Vapor Intrusion at Remediation & Redevelopment Sites in Wisconsin (RR-800)* Update: July **2012**

Wisconsin Department of Natural Resources. *Sub-Slab Vapor Sampling Procedures*, RR-986 July **2014**

Wong, T.T.; Agar, J.G.; Grefoire, M.Y. Technical rationale and sampling procedures for assessing the effects of subsurface volatile organic contaminants on indoor air quality. In 56<sup>th</sup> Canadian Geotechnical Conference, 4<sup>th</sup> Joint IAHR/CGS Conference, 2003 NAGS Conference, **2003**

ISSUE



PRESORTED STANDARD  
POSTAGE & FEES PAID  
EPA  
PERMIT NO. G-35

Office of Research and Development (8101R)  
Washington, DC 20460

Official Business  
Penalty for Private Use  
\$300